A FLUID INCLUSION AND GEOCHEMICAL INVESTIGATION

OF THE FLUORITE DEPOSITS

OF THE SOUTHERN PENNINE OREFIELD

A Thesis

Submitted for the degree of

DOCTOR OF PHILOSOPHY

in the

FACULTY OF SCIENCE OF THE UNIVERSITY OF LEICESTER

by

PHILIP ATKINSON

B.Sc. (Newcastle upon Tyne)

August 1983

A Fluid Inclusion and Geochemical Investigation of the Fluorite Deposits of the Southern Pennine Orefield
P. Atkinson (1983)

The fluorite deposits of the Southern Pennine Orefield occur in vein fillings and metasomatic replacements.

Primary and secondary fluid inclusions define five discrete phases of fluorite mineralization or remobilization. Homogenization temperature ranges for the five events are; (1) 100-171°C; (2) 62-82°C; (3) 65-99°C; (4) 73-106°C; (5) 66-68°C. Little evidence was found of east-west thermal gradients having operated during any of the events. The inclusion types are further characterized by distinctive melting point ranges of ice, hydrohalite or antarcticite. Major element concentrations of the ore fluids have been determined from cation ratios in inclusion leachates modelled in the ternary system $NaCl-CaCl_2-H_2O$.

High Ca/Na ratios in the type 2, 4 and 5 fluids indicate compositions atypical of present-day high salinity formation waters resident in deep sedimentary basins.

Mineral solubility data has been used to determine limits for trace anion and cation activities. Ranges for oxygen and sulphur fugacity and pH have also been estimated for mineralizing phases 3 and 4.

REE analysis of fluorite and carbonates showed LREE-enriched chondrite normalized patterns with negative cerium and europium anomalies. Total lanthanide abundances are low.

Strontium isotope ratios range from 0.7082 to 0.7101 indicating ore fluid interaction with wall rocks enriched in radiogenic strontium with respect to Visean marine carbonates.

Muscovite, biotite and K-feldspar can be demonstrated to have been unstable in the ore fluids at 100°C and represent potential fluorine source minerals. Dissolution or alteration of aluminium silicates could have produced fluoride release into the brines.

The homogeneity of the inclusion fluids, the uniform REE content of the fluorite and equilibrium mineral textures indicate a non-mixing mechanism of mineralization. An open system, "one pass" model of mineralization with fluorite precipitated as a result of metasomatism of carbonates and possibly limited cooling, and sulphide deposition through pH increase is proposed.

ACKNOWLEDGEMENTS

I would like to thank the following people for helping me with the research project.

Drs A.M. Evans and T.D. Ford for supervising this work and for help in the writing of this thesis.

Dr J.N. Walsh for providing facilities for REE analysis.

Drs M.J. Norry and R. Cliff for help in obtaining the strontium isotope analyses.

Mr N.G. Marsh and Mr R.N. Wilson for help with electron probe microanalysis and X.R.F. analysis.

Mr J. Hedges and Mr C. Cornwell of Laporte Industries for allowing access to the Sallet Hole Mine.

Drs D.A.C. Manning and B.L. Weaver for critically reading parts of this manuscript.

Dr G. Arter for assistance with computer programming.

Miss S. Button for helpful advice on drawing diagrams.

I would also like to thank N.E.R.C. for providing a research assistantship.

List of symbols used in the text

Symbol	Definition
a_i	activity of the ith species
γ_i	individual ion activity coefficient of the ith ion
ΔG	standard Gibbs free energy of reaction
ΔH	standard enthalpy of reaction
I	stoichiometric ionic strength
K	equilibrium constant
K'	molal equilibrium constant
K_s	activity product constant
log	common or base 10 logarithm
M	molarity (moles per litre H_2O)
m	molality (moles of solute per kg H_2O)
m_i	molality of the ith species
P	pressure (atmospheres)
pH	$-\log a_{H^+}$
ppm	parts per million (mg per kg)
R	gas constant (1.99×10^{-3} kcal $mole^{-1}$ deg^{-1})
ΔS	standard entropy of reaction
T	temperature (^{o}C or ^{o}K)
z_i	charge on the ith species

CONTENTS

APPENDICIES

LIST OF PLATES

LIST OF FIGURES

CHAPTER 1

INTRODUCTION

1.1: THE AIMS OF THE RESEARCH PROJECT

The thermometric fluid inclusion study made by Rogers (1977) failed to show any evidence of east-west thermal gradients having produced the generalized mineral zonation of the Southern Pennine Orefield. It was considered that a more detailed fluid inclusion study may reveal even small regional temperature variations which occurred during the mineral events. A detailed fluid inclusion study of the High Rake Deep Rake vein system may also indicate the magnitude of lateral, vertical and horizontal thermal gradients that existed during the hydrothermal events. Paired homogenization and final ice melting temperatures may be expected to indicate whether mineral deposition occurred as the result of fluid mixing or precipitation from a single solution. Chemical analyses of the fluid inclusions can be used to establish limits for various physicochemical conditions of ore-formation.

The potential sources of fluorine may be limited by looking at the stability of various fluorine-bearing mineral phases in the ore fluids. The source of the mineralizing brines can be investigated by using the major element chemistry of the ore fluids and the REE chemistry of fluorite and associated gangue minerals. Strontium isotope

ratios may also be used to indicate whether the calcium in the fluorite is derived from the host rock or whether it has been introduced from an external source. Hydrogeological aspects of mineralization also require some investigation.

In conclusion, theories of ore genesis for the deposits of the Southern Pennine Orefield (Ineson and Ford, 1982) have been numerous and varied and generally the major constraint on genetic models has been the current theory of ore deposition for Mississippi Valley-type ore deposits. The main aim of the project is to place some physical, chemical and hydrological constraints on fluorite deposition and associated sulphide deposition within which a genetic theory may be modelled.

1.2: GEOGRAPHICAL SETTING

The South Pennine Orefield is situated almost entirely in the County of Derbyshire although there is some related mineralization in North Staffordshire. The Orefield is almost entirely hosted in limestone, and forms a high plateau, ranging in altitude from 350-450m. The plateau is gently dissected by valleys but occasional steep sided gorges are present. Much of the area is drained by subsurface water movement and surface streams are limited to areas close to the boundary of the Dinantian limestones with the overlying Namurian shales. The major rivers of the district are the Wye, Derwent, Lathkill, Manifold and Dove. Karst features such as gorges, caves, potholes, sink-holes, dry valleys and scars are common. There are numerous remains of small mine

Figure 1.1: Carboniferous stages and zonal subdivisions.

SERIES	STAGES	CORAL/BRACHIOPOD ZONE	GONIATITE ZONE
WESTPHALIAN	D		
	C		
	B		A
	A		G_2
NAMURIAN	YEADONIAN		G_1
	MARSDENIAN		R_2
	KINDERSCOUTIAN		R_1
	ALPORTIAN		H_2
	CHOKIERIAN		H_1
	ARNSBERGIAN		E_2
	PENDELIAN		E_1
DINANTIAN	BRIGANTIAN	D_2	P_2
	ASBIAN	D_1	P_1
	HOLKERIAN	S_2	B_2
	ARUNDIAN	C_2S_1	
	CHADIAN	C_1, C_2S_1	
	COURCEYAN	K,Z	

workings in the district which may be used to pick out the lines of the mineral veins. Limestone quarrying also makes a major impact on the scenery of the district, particularly outside the National Park boundaries. Flanking the Orefield on its western and northern edges, Namurian sandstones have weathered to produce a scarp and slope topography. The hardest and thickest beds have produced craggy escarpments known locally as "edges". These Namurian sandstones and shales form the highest hills in the Southern Pennines with Kinderscout, just to the north of the Orefield, rising to a height of 630m.

1.3: STRATIGRAPHY AND DEEP STRUCTURE OF THE OREFIELD

Five hundred metres of Dinantian limestones are exposed in the area, but at no place is the base of the series seen. Two boreholes have penetrated the sub-Carboniferous basement. The Woodale borehole reaches early Viséan or late Tournasian (Courceyan) strata which overlies a sequence of altered volcanics, of possibly Pre-Cambrian age (Cope, 1949; Cope, 1973). The stages and the faunal subzones of the Carboniferous series are shown in figure 1.1. Potassium-argon dating of the altered volcanics gives an age range of 200-383ma (Cope 1979) which places the sequence in the Lower Devonian. The large range in ages may be the result of the diffusion of argon into or out of the mineral lattice during hydrothermal alteration and, therefore, the ages are not very meaningful. At Woodale, the total thickness of the Dinantian

rocks penetrated was approximately 300m. Another deep borehole was drilled at Eyam and here, the sub-Carboniferous basement was encountered at 1803m (Dunham, 1973). Therefore, the Dinantian thickens considerably from west to east. Using gravity data Maroof (1976) modelled the depth to sub-Carboniferous basement on three sections across various parts of the Derbyshire Dome. On Maroof's traverse, the thickness of the Dinantian ranged from 130m to 300m in the south and 200m to 500m in the north. The gravity data does not support any suggestion of an underlying granite beneath the dome. The structure of the pre-Carboniferous basement has been modelled from seismic data (Whitcombe and Maguire, 1981). They suggested that the Southern part of the dome is underlain by Charnian-type Pre-Cambrian basement lying at a depth of 2km. They postulate an intervening 1.8km of Devonian and Ordovician sediments separating the Dinantian from the Pre-Cambrian basement. They also suggested that data from the LISPB seismic line (Bamford et al.,1977) indicated similar basement lying 2km below the surface in the vicinity of Buxton.

The main part of the Orefield at outcrop is formed by the Brigantian and Asbian stages of the Dinantian. The greater part of these stages are composed of massive calcarenites, locally with interbedded chert nodules, the latter being particularly common in the upper beds. Reef complexes are common on the northern and western edges of the district with highly fossiliferous calcilutite bioherms (Ford, 1976). Intercalated, highly altered lavas and tuffs are well developed in the Brigantian and Asbian rocks. Intrusive igneous rocks are rare. Although limestones

Figure 1.2

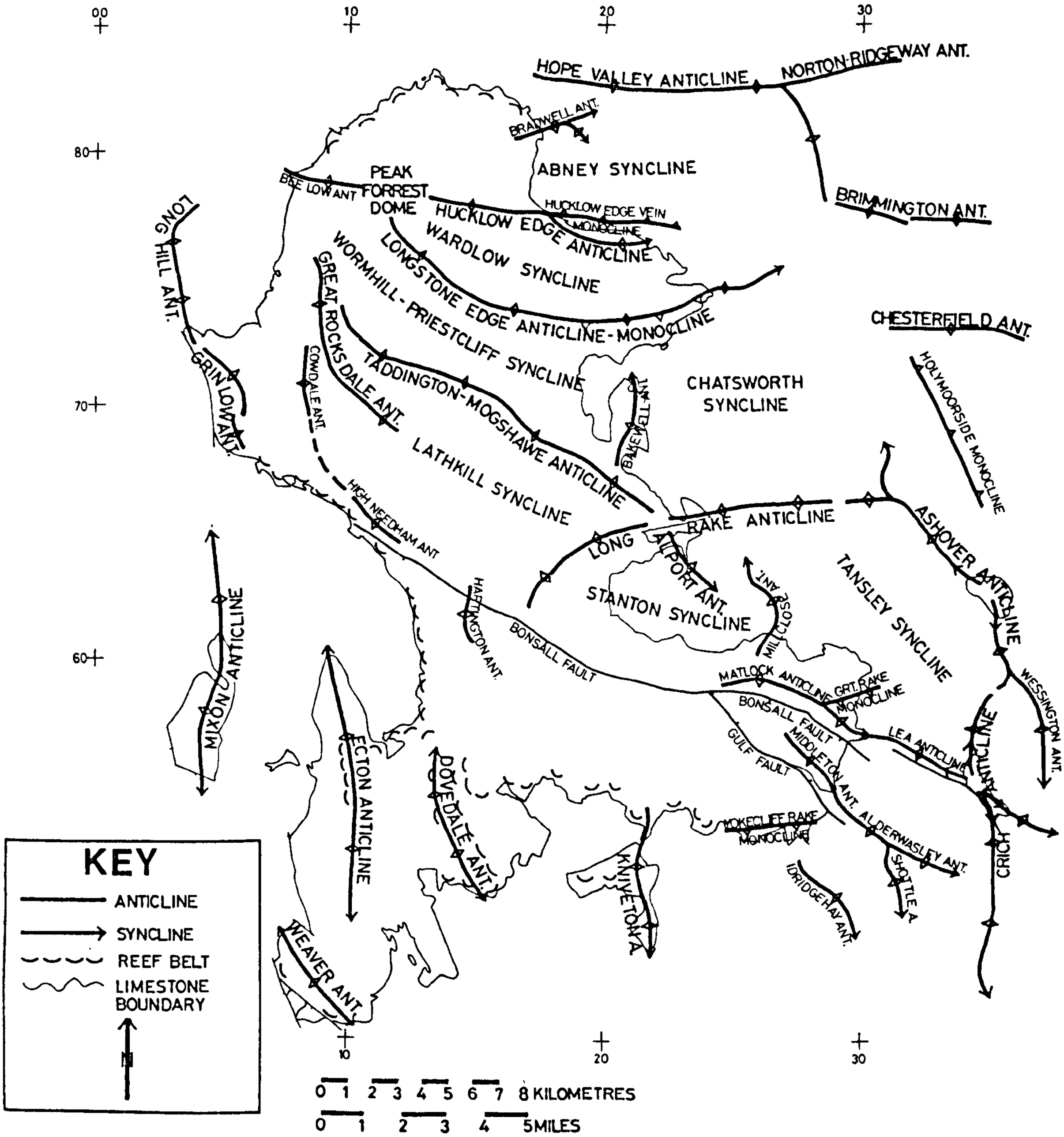

MAIN FOLDS OF THE SOUTH PENNINE OREFIELD

represent the predominant lithology at outcrop, the Eyam borehole showed that a considerable part of the Dinantian succession was composed of dolomite. In the lower part of the Arundian and in the Tournaisian (Courceyan), a sequence (170m) of mudstones with interbedded nodular anhydrite was found.

The Dinantian rocks are overlain by Namurian shales and sandstones. The lowest unit of the Namurian is represented by the Edale Shales which range in thickness from 50-270m and have often been considered to represent an impervious capping to the Dinantian (Firman and Bagshaw , 1974) which precluded the formation of any mineral deposits in the Namurian. Detailed accounts of the stratigraphy of parts of the Orefield have been given by Stevenson and Gaunt (1971), Smith et al., (1967), Worley (1978) and Frost and Smart (1979). A simplified map of the Derbyshire Block and its geological setting are shown in figure 1.2.

1.4: STRUCTURE OF THE OREFIELD

The Derbyshire Dome or Derbyshire block is considered to be a complex interference pattern of folds produced by the intersection of north-south, east-west and north-west to south-east trending folds. The main structural features of the Orefield are shown in figure 1.3, taken from Ford and Ineson (1971). Domes and basins are present as well as saddles and ridges on the major anticlines and synclines. There is a lot of evidence to show that many of the folds were active during sedimentation. If a single horizon is

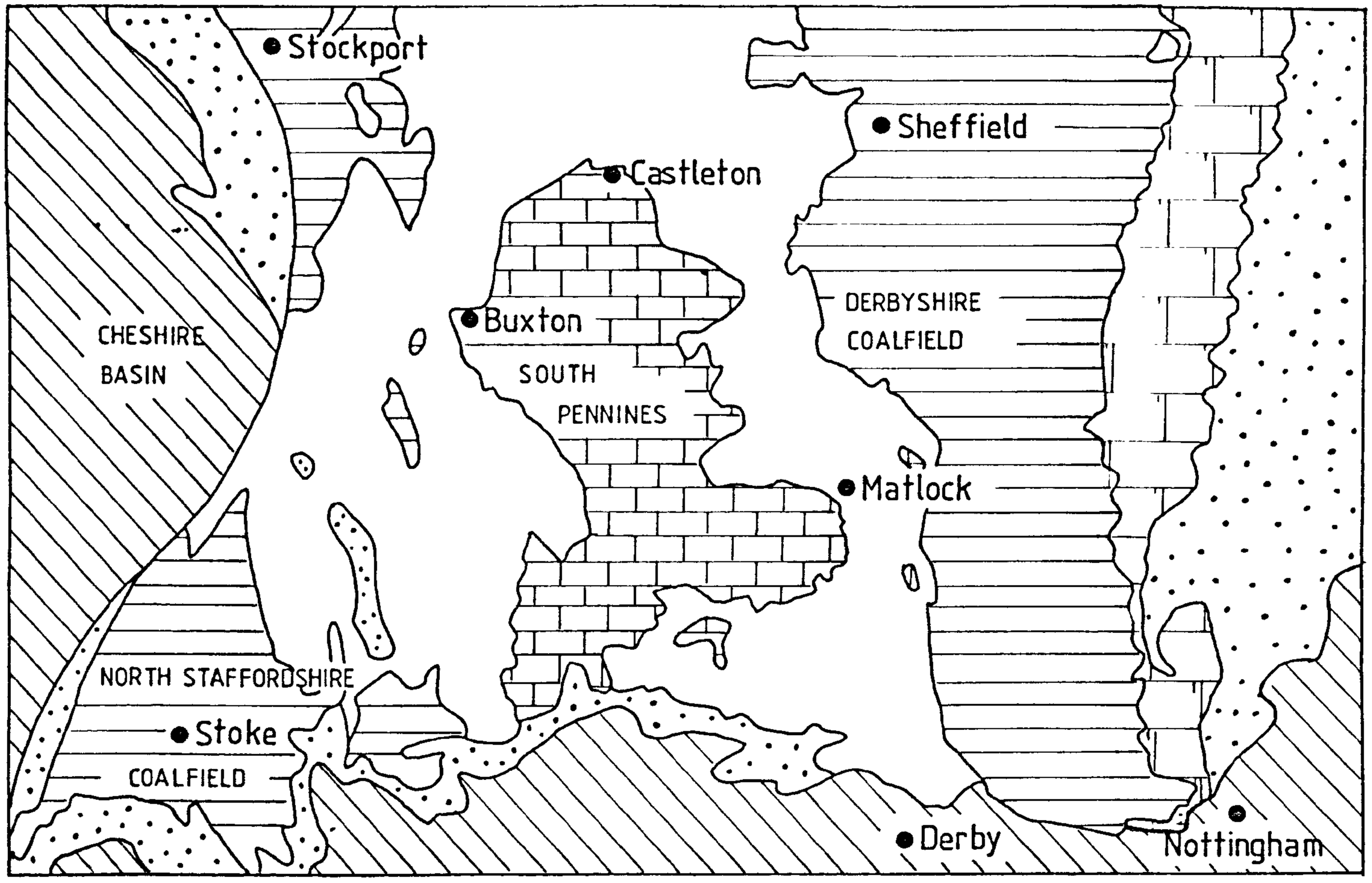

Figure 1.3: A simplified geological map of central northern England.

followed from a syncline to an anticline, a change from deeper to shallower water facies often occurs. Dips are usually low, and generally do not exceed 20°. Faults, particularly in the eastern part of the Dinantian outcrop are often mineralized. The dominant fault trends are north-west to south-east and east-west. The north-west to south-east striking faults usually show a small normal displacement as well as having a component of either sinistral or dextral wrench movement. Most of the NW-SE faults show horizontal slickensiding and are usually vertical. Important fractures of this type are the Bonsall and Gulf faults. The Block as a whole is not bordered by a major fault in the same way as the Alston Block, but the Red Rock fault does downfault the Triassic sediments of the Cheshire Basin against Namurian strata to the west of the Orefield.

1.5: OUTLINE OF THE GEOLOGICAL HISTORY AND PALAEOGEOGRAPHY

Dinantian and Namurian sedimentation was dominated by the presence of tectonically controlled blocks and basins. Two long narrow basins, the Edale and Widmerpool basins adjoin the Orefield on the north-east and south-west sides. The Craven-Bowland basin is the largest basin in the vicinity and formed the eastern border of the Derbyshire Block in Dinantian times (figure 1.4). St Georges land lay to the south of the Widmerpool basin and was not submerged until Asbian times. The large difference between the thickness of the Carboniferous succession in the Woodale Borehole and the

Figure 1.4: Location of blocks and basins in central northern England. Redrawn from Kent (1967).

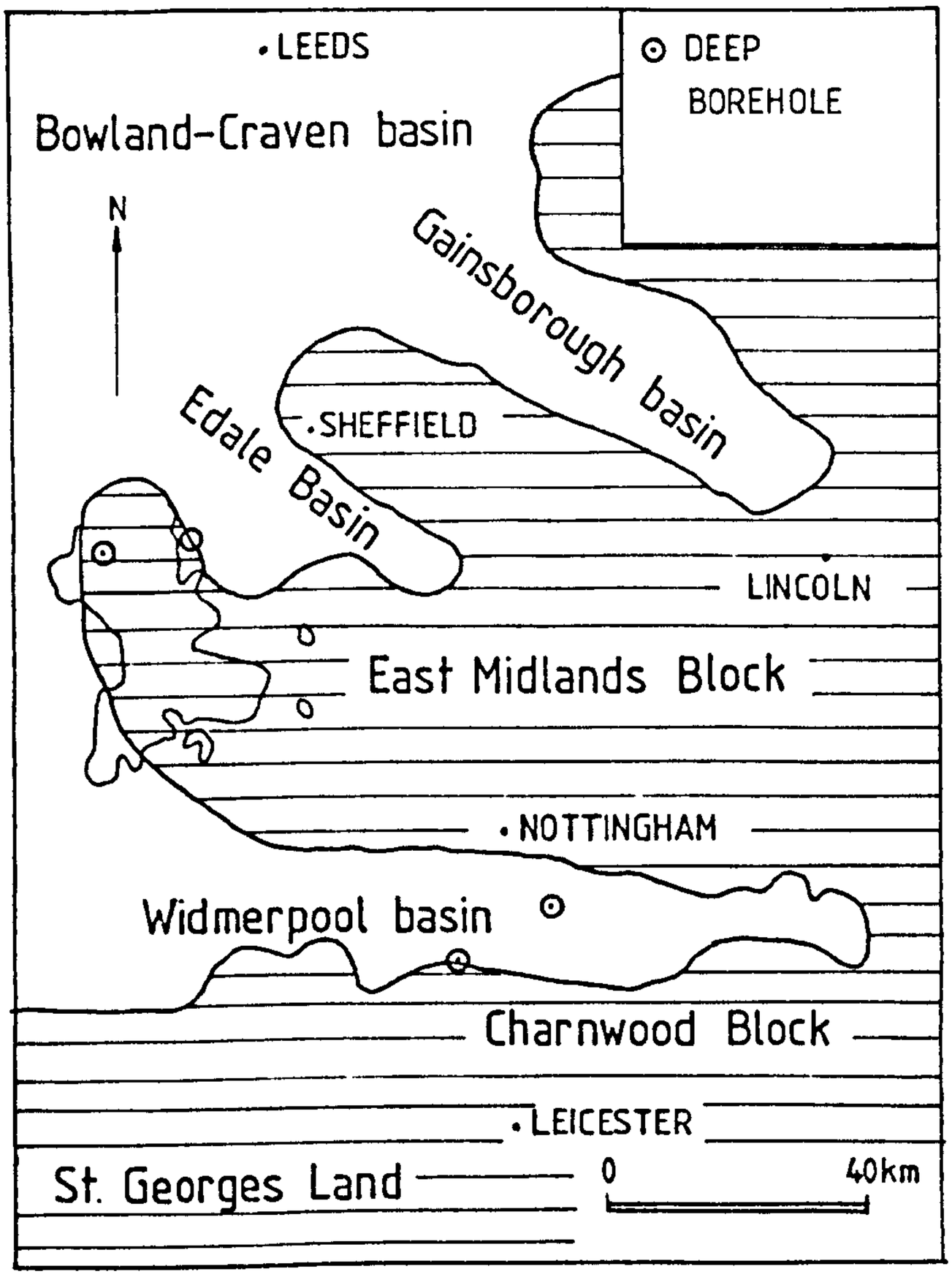

Eyam borehole indicates the effect of block and basin sedimentation in the Dinantian.

Considerable thicknesses of Namurian sediments were deposited in the Central Province of Northern England (See figure 1.5). Feldspathic clastic sequences were derived from the Scottish or Norwegian Caledonides while protoquartzites were supplied from the southern massif. Much of the material was deposited in deep submarine channels on the edges of deltas while other deposits were laid down in braided fluviatile channels (Jones, 1980). In the early part of the Namurian, then sediments of each stage thicken considerably on moving into the basins. The Derbyshire Block itself probably remained relatively free of sediment until in the Arnsbergian and Pendelian as condensed sequences at Hucklow Edge and Wardlow Mires indicate (Ramsbottom, 1967). Deposition in the Kinderscoutian was more uniform and by the Marsdenian stage the Derbyshire Block had little effect on deposition of sediment. The isopachytes (figure 1.5) for the Roaches Grit (R_2) show that the deepest part of the trough occupied by the delta partly overlies the Derbyshire Block itself (Jones, 1980). Isopachytes for the Namurian (figure 1.5) series (Ramsbottom, 1967) show that the thickest sediments lie in the Bowland-Craven basin. Further away from the Orefield, thick sequences of sediments accumulated in the Rhenish Basin.

Cyclic sedimentation continued in the Westphalian. There is some evidence of thickening of beds in basinal areas but little evidence that the Derbshire Block influenced sedimentation (Frost and Smart, 1979). The Westphalian series apparently thickens from the south-west to the north-east, or

Figure 1.5.

The thickness of Namurian strata in the vicinity of the Derbyshire Block.

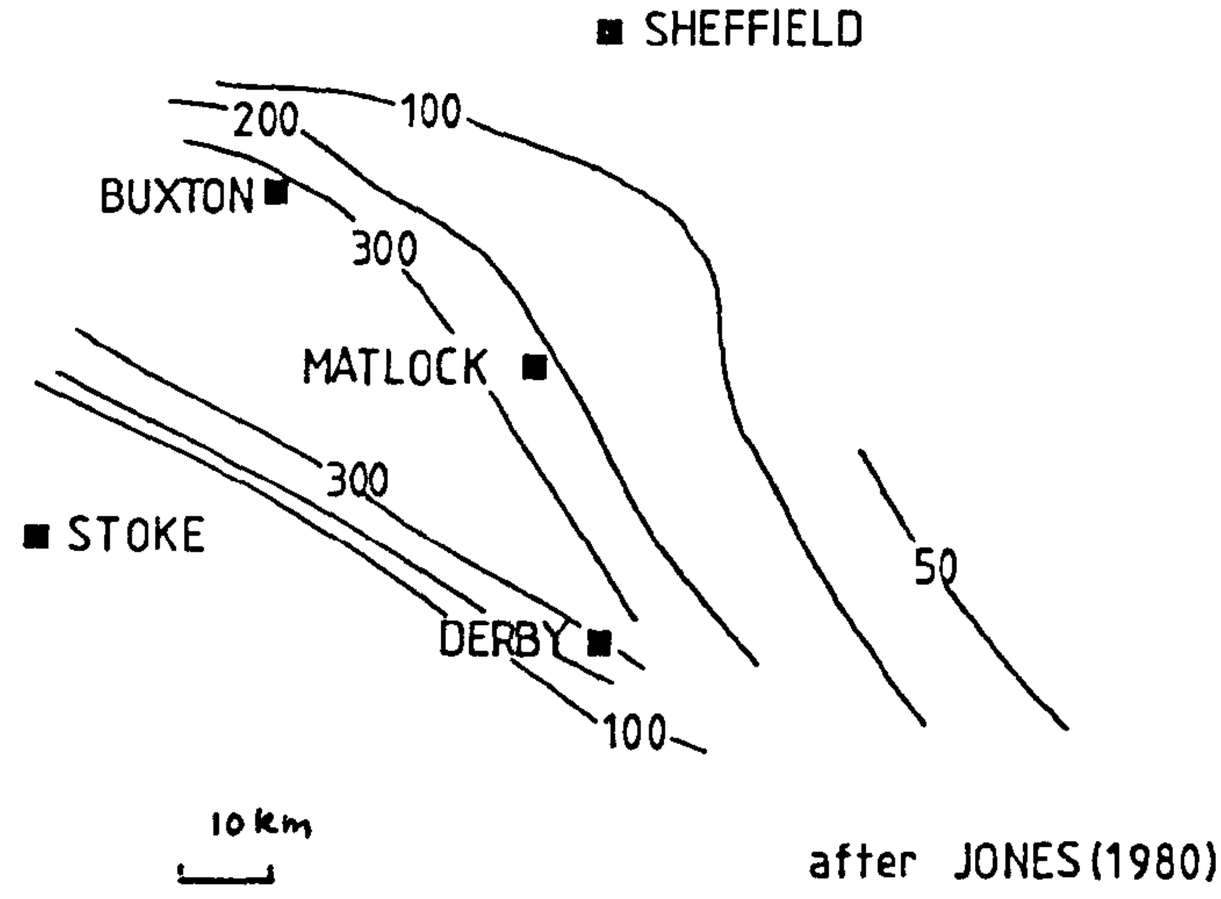

Isopachytes at 305m intervals for the Namurian strata of the Central Province of Northern England

from the Leicestershire Coalfield to the North Derbyshire Coalfield. The Pennine anticline was created at the end of the Carboniferous period, and erosion occurred intermittently in the Permo-Trias and the Tertiary. Thick sedimentary sequences accumulated, particularly in the Cheshire Basin, and in the Severn and North Sea Grabens, in the Mesozoic. There is no evidence that the Derbyshire Block was covered by Permian deposits but the district probably received a covering of Triassic sediments. No more than two hundred metres of mainly Keuper Marl are likely to have been deposited.

1.6: MINERALIZATION

1.6.1: SULPHIDE MINERALS

The most abundant sulphide mineral in the district is galena, with lesser quantities of sphalerite, marcasite, nickel—rich marcasite, pyrite, nickel—rich pyrite, bravoite ($FeNiS_2$) and chalcopyrite. The sulphide mineral paragenesis has been investigated by Ixer and Townley (1979) and they observed a very uniform primary sulphide mineralogy over the entire Orefield. They saw no evidence of systematic variation in the abundance, presence or absence of any sulphide minerals apart from a general increase in the abundance of sulphide minerals within mineral deposits on approaching the eastern margin of the Orefield.

1.6.2: NON-SULPHIDE MINERALS

The gangue minerals are fluorite, calcite, baryte, quartz, dolomite, cerussite and smithsonite. A general paragenetic sequence for the gangue mineral assemblage has been proposed by Firman and Bagshawe (1974). They noted an early phase of columnar or rhombic calcite lining the vein walls in many deposits in the southern part of the Orefield. This is then followed by multiple generations of fluorite and baryte. Brecciation has been observed in this stage (Ineson and Al-kufaishi (197Ø)) along with faulting, suggesting a slow multiphase mineralizing event. Dunham (1952) noted evidence of multiphase fluorite mineralization in the Hucklow Edge Vein. The final stage of mineralization at many localities is the filling of the remaining open vughs in the raplacement and vein deposits by large scalenohedral calcite crystals. Firman and Bagshaw (1974) reported a late stage of quartz mineralization but this is seen in a very few deposits in the field

1.6.3: THE FORM OF THE OREBODIES

Dunham (1952) listed four types of orebody present in the Southern Pennine Orefield. These are: (a) Steep veins developed in part by simple fissure fillings but in some cases opening to considerable widths where limestone replacement has occurred; (b) narrow veins (scrins) formed by the mineralization of the conjugate joints in the limestone; (c) blanket replacement deposits formed by the partial

metasomatism of the wall rock between scrins; (d) irregular vertical or horizontal pipe-like replacement deposits. Numerous transitions between types (b) and (d) occur. Larger veins in the district are sometimes referred to as "rakes". Rakes are continuously mineralized fractures which may continue over considerable distances. Two of the most important examples are the Long Rake and the Hucklow Edge vein systems. Veins may reach thirty metres in width but five to seven metres is more usual. Scrins cannot usually be followed for more than a few hundred metres.

1.6.4: REGIONAL GANGUE MINERAL ZONATION

Wedd and Drabble (1908) were the first workers to report a regional mineral distribution and they proposed a zone of fluorite mineralization lying along the eastern margin of the Orefield. Dunham (1952) modified the boundary of the fluorite zone as did Mueller (1954). Mueller (1954) not only suggested a fluorite zone, subdivided into three subzones based on mineral colouration and inclusion content but also produced baryte and calcite zone boundaries. The western margin of the fluorite zone as given by Mueller (1951), Dunham (1952) and Mueller (1954) are shown in figure 1.6. The fluorite zone boundary changes made by Mueller between 1951 and 1954 is in itself indicative of the poorly defined nature of the zones. It is interesting to note that Mueller's zone is based on 10% fluorite in a deposit while Dunham's zone is based on the commercial limit of 40%. Mueller (1954) went further on to

Figure 1.6: The diagram shows the western boundary of the fluorite zone as drawn by Mueller (1951; 1954) and Dunham (1952). The diagram was taken from Firman and Bagshaw (1974).

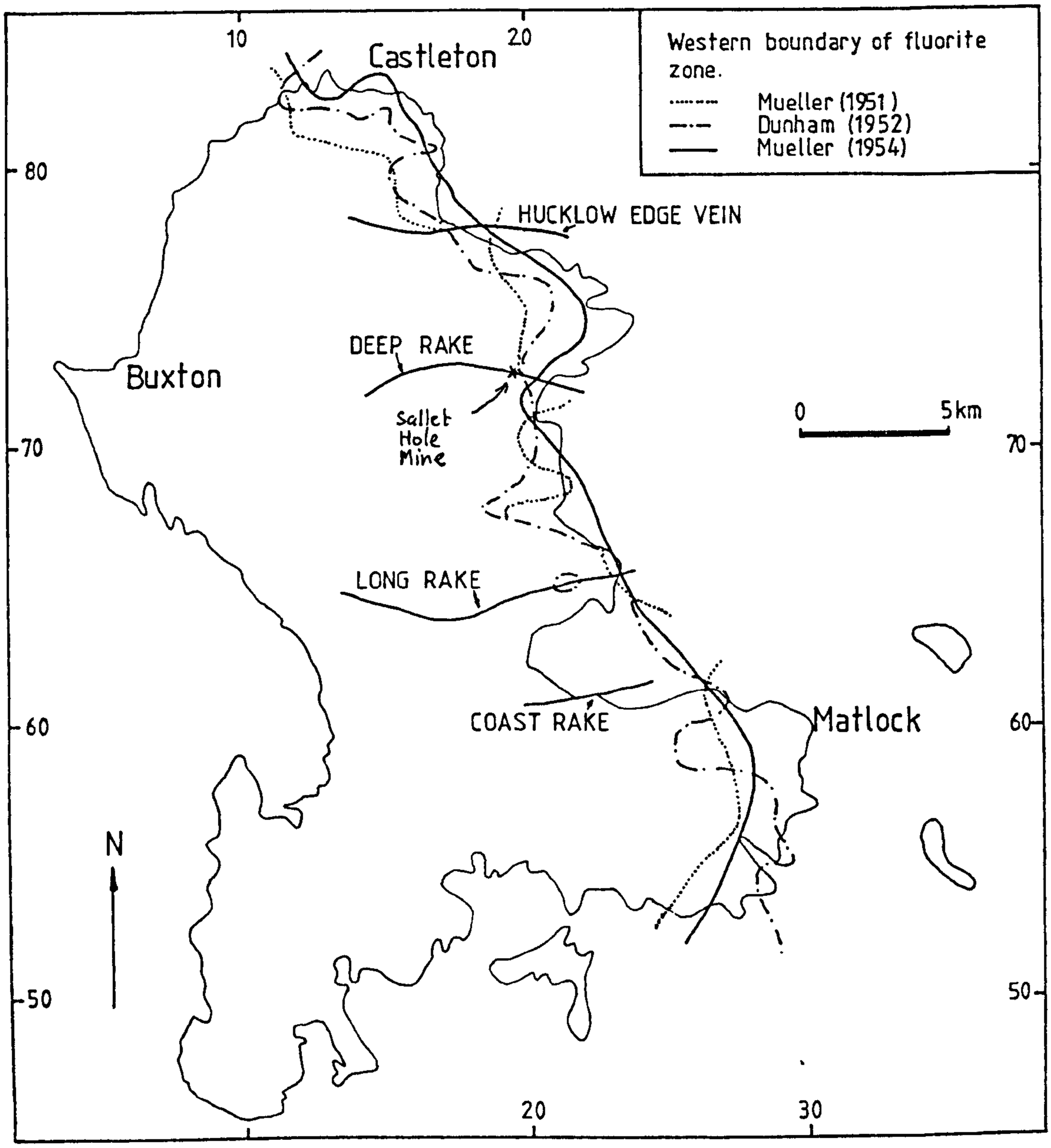

use the colouration of fluorite as an indicator of depositional temperature. He found that by heating purple fluorite to 400°C, the mineral became colourless. Therefore, he suggested that clear or yellow fluorite was deposited at temperatures in excess of 400°C and purple fluorite was deposited below 400°C. This theory gave the supposed mineral zonation a thermal significance. Firman and Bagshaw (1974) have shown that these boundaries are erroneous and they recommended that they should not be used. However, it is still the case that the number of economic fluorite deposits which have been worked or are being worked do lie close to the eastern margin of the Dinantian outcrop.

1.6.5: STRATIGRAPHIC CONTROL ON MINERAL DEPOSITION

It has been suggested by various workers that there is an association between the major mineral deposits of the Orefield and the anticlinal structures present in the Dinantian limestone (Wedd and Drabble (1908), Shirley and Horsfield (1945), Mueller (1954)). Smith et al., (1967) on resurveying the Matlock district only partly confirmed the anticlinal setting of major mineral deposits. Stevenson and Gaunt (1971) produced similar conclusions for the northern part of the Orefield, earlier studied by Shirley and Horsfield (1945), although they did confirm the anticlinal association of Hanging Flat Vein, Middlefield Rake and Crosslow Vein.

Butcher (1976) concluded that many of the major veins and replacements were situated on the crests and flanks of

east-west and north-west to south-east trending anticlines. He sited the Great Rake (Matlock), and Gregory Vein as being good examples. Monoclines also are occasionally found to host ore deposits. Examples are the Coast Rake at Elton and High Rake on Longstone Edge. The Hucklow Edge Vein is also thought to follow a monocline which follows the Southern boundary of the Abney syncline. On the other hand some major veins lie obliquely across major anticlines or simply trend parallel to the dip of tilted beds.

1.6.6: GANGUE MINERAL PARAGENESIS AND DEPTH

Wedd and Drabble (1908) claimed that all the fluorite deposits of the district were confined to the top 180m of limestone and this conclusion has been supported by evidence from various sources. Traill (1939) concluded that although fluorite was an important mineral in the upper levels of the Millclose Mine, calcite was the only gangue mineral in the deeper levels. It is possible, however, that this was wall rock control. Baryte was also found to die out at depth. The Great Rake at Matlock was also found to carry calcite on moving east into the Tansley syncline. Moving west into the Tansley syncline, fluorite was found to die out and be replaced by calcite in the deeper workings of the Gregory Mine (Dunham, 1952). Wedd and Drabble gave the Old End Mine at Crich as another example. In the north of the district Green *et al*. (1887) reported that the Hucklow Edge Vein reaches its greatest thickness below the Namurian shales and was found to thin at depth.

1.6.7: DIRECTION OF FLUID MOVEMENT

The evidence for upward moving solutions as proposed by Schnellman and Willson (1949) is ambiguous. The main evidence comes from the papers of Traill (1939) and Shirley (1949) and comes predominantly from the structures of ore deposits seen at the Millclose Mine. No fluorite has been found in Namurian or Westphalian sediments covering or surrounding the Dinanatian limestones of the Orefield. This is often ascribed to the impermeable nature of the Namurian cover rock. However, in the Northern Pennine Orefield mineral veins have penetrated numerous shale horizons, although significant thinning of the vein often occurs (Dunham, 1948). Small occurrences of baryte, galena and calcite have been found in Namurian rocks in the vicinity of the Orefield (Ineson et al., 1972). At some localities deposits lie on the down dip side of a "feeder", as is seen at Long Rake and replacement bodies may lie on top of lavas, as at Masson Hill (Ixer, 1978). Firman and Bagshawe (1974) concluded that the field relations suggest that the solutions moved both laterally and up dip.

1.6.8: LITHOLOGICAL CONTROLS

The fluorite occurs in both limestones and dolomites, with relatively trivial quantities hosted by lavas and tuffs. Primary porosity does not appear to be an important control

on ore deposition, except in unusual circumstances. Traill (1939) stated that coarse grained light coloured limestones were replaced in preference to dark, fine grained material at the Millclose Mine. Dolomitization produced an increase in secondary porosity and was thought to be the reason why it formed a good host for ore deposits. Quite a number of deposits are situated on the dolomite-limestone boundary. One of the largest deposits of this type is the Masson Hill replacement fluorite body. Firman and Bagshawe (1974) suggested that many of the fluorite replacement deposits hosted in dolomites appear to have been formed by descending ore fluids, as they are usually sited at the lower limestone-dolomite boundary whereas replacments in limestones are generally sited at the upper boundary.

Worley (1978) examined thirty nine ore deposits in the field and concluded that eighty per cent of these occurred in Brigantian shelf or pale facies limestones. Lithological controls included lavas, tuffs, shale partings, prominent bedding planes, stylolitic seams, erosion surfaces, shell beds, chert bands and reef and pseudobrecciated limestones. Worley also noted that few, if any, replacement bodies were sited directly under the Namurian shale cover. The highest coarse, permeable bedding being the host. The porosity of limestones is increased by number of these features, which tend to be more abundant in anticlinal structures. Worley (1978) found little evidence to suggest that the chemical purity of the limestone was an important control on ore deposition.

1.7: PREVIOUS FLUID INCLUSION RESEARCH

Fluid inclusion studies on fluorite from the Southern Pennine Orefield were very limited before the work of Rogers (1977). Roedder (1967a) reported some final ice melting temperatures for fluid inclusions in fluorite from Masson Hill, Bradwell Moor and Treak Cliff Cavern. Roedder (1967b) used material from Derbyshire to demonstrate the behaviour of metastable superheated ice. Smith (1973) published mean homogenization temperatures for two fluorite samples from Ladywash Mine (73.8°C) and the Odin Vein (127.5°C). Rogers (1977) produced mean homogenization temperatures for twenty nine localities and found that the temperature range was 92°C to 154°C. Final ice melting temperatures ranged from -23.4°C to -14.8°C. He noted that hydrocarbons were not particularly common in fluorite from the district. The most recent fluid inclusion research has been done by Moore (1980), who reported homogenization temperatures for inclusions falling in the range 80°C-100°C, confirming the results of Smith (1973). Carbon dioxide/water ratios and D/H ratios were determined using mass spectrometry. δD vaues were found to be very low (-100 to -8‰), in comparison with fluid inclusions in fluorite from the Northern Pennine Orefield (-46 to +8‰). The carbon dioxide/water ratios were found to lie between 0.007 and 0.332 (weight ratios). Transition metal concentrations in the inclusion leachates were determined by atomic absorption although the analytical variation was reported as being very high.

1.8: A SUMMARY OF OTHER GEOCHEMICAL RESEARCH RELATING TO THE MINERAL DEPOSITS OF SOUTHERN PENNINE OREFIELD

Smith (1974) analysed numerous fluorite samples taken from the Ashover and Crich inliers for lanthanum, cerium and yttrium. Concentrations were found to be much lower than those measured in fluorite from the Alston Block. Coomer and Ford (1975) presented lead isotope data for seventeen galena samples from the Orefield. The lead was found to be extremely homogeneous, suggesting that the lead in the galena had had considerable opportunity to mix before deposition occurred. The lead from the Derbyhire Block appears to be more radiogenic than lead from the Alston Block, and they suggested that the trend may be similar to that observed by Heyl et al., (1971), in the Mississippi Valley orefields. Carlon (1978) claimed to have observed uniform changes in the Ba/Sr ratios in baryte on moving west along a number of veins and related this to the ore fluid chemistry and east-west thermal gradients. He also measured strontium concentrations in some fluorite and calcite samples. Robinson and Ineson (1979) made a study of sulphur, carbon and oxygen isotopes in the sulphides, sulphate and carbonate minerals of the Orefield. The $\delta^{34}S$ values ranged from -23 - +7‰ for sulphides. Baryte shows a wide range of values ($\delta^{34}S$ +4 to +23 and $\delta^{18}O$ +9 - 26‰). They suggested that these values are produced by the mixing of sea water sulphate and fresh water sulphate. They suggested a dual source for reduced sulphur, including both the reduction of sea water sulphate and addition of sulphur from kerogens in the limestone. Ineson and Mitchell (1973)

used the potassium-argon method to date clay minerals formed as a result of hydrothermal alteration. Ages produced range from Lower Permian to Late Triassic.

CHAPTER 2

OIL IMMERSION METHODS FOR THE MEASUREMENT OF HOMOGENIZATION AND MELTING TEMPERATURE VALUES IN FLUID INCLUSIONS

2.1 INTRODUCTION

Much of the fluorite found in the district does not readily lend itself to standard thick section preparation techniques. It was considered that measurement of melting points and homogenization temperatures could be better achieved by the use of immersion oils. Rankin and Aldous (1979) have advocated the use of tritolyl phosphate as an immersion agent suitable for freezing studies. The unpleasant nature of the chemical as well as its tendency to vaporize at relatively low temperatures lead to the use of silicone oil as a preferred immersion agent. An important point is whether material collected from vughs and vein wall linings contains inclusions which are representative of those found in the main phase of ore formation. The use of oil immersion allows the more commonly found fragmented and granular material to be studied.

2.2: DATA COLLECTION

A Linkam TH6ØØ temperature programmable heating-freezing

Figure 2.1

Calibration of the Linkam TH 600 heating and freezing stage.

The graph shows a plot of recorded temperature against actual melting temperature for a number of organic compounds, in the temperature range - 90°C to 0°C.
The recorded melting temperature of carbon tetrachloride was ignored when drawing the calibration curve.

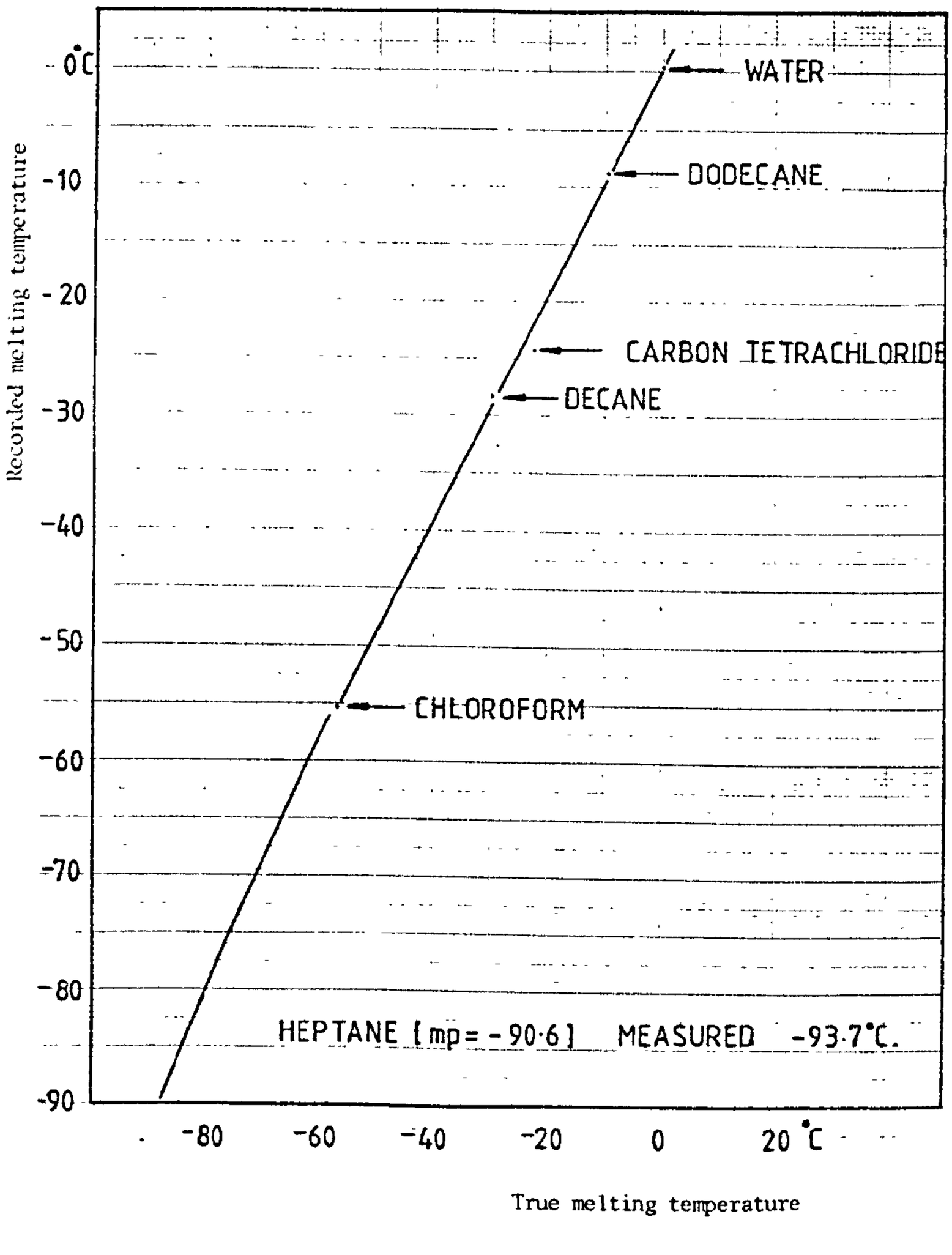

stage (Shepherd, 1981) was used to make microthermometric measurements. The stage was regularly calibrated using the melting points of compounds recommended by Macdonald and Spooner (1981). The compounds were placed between two glass cover slips in order to measure their melting points. Figures 2.1 and 2.2 show the relation between the true temperature of the heating stage and the measured temperature. The latter authors recommended a universal heating rate of $\emptyset.4^{o}C\ min^{-1}$. Such a rate was found to be too slow and a rate of $1^{o}C$ or $2^{o}C$ per minute was used in measuring homogenization temperatures. A slower heating rate of $\emptyset.5^{o}C\ min^{-1}$ was used for determining melting point measurements. In general, only the thermometric properties of one inclusion were measured from a single mineral grain or doubly polished section in order to determine statistically representative sample means. Homogenization temperatures were always measured before melting temperature measurements were made. The increase in the homogenization temperature after freezing was ascribed to the high degree of filling of many of the inclusions which produced stretching of the inclusions on cooling. Lawler and Crawford (1983) recommended that the homogenization temperature of an inclusion should be measured before melting temperature measurements are made. They showed that disappearance of the vapour bubble on freezing is particularly likely to produce stretching of a fluid inclusion in an easily deformed mineral such as fluorite.

Figure 2.2

Calibration of the Linkam TH600 heating and freezing stage

The graph shows a plot of recorded melting temperature against actual melting temperature for a number of organic compounds, in the temperature range 50°C to 200°C

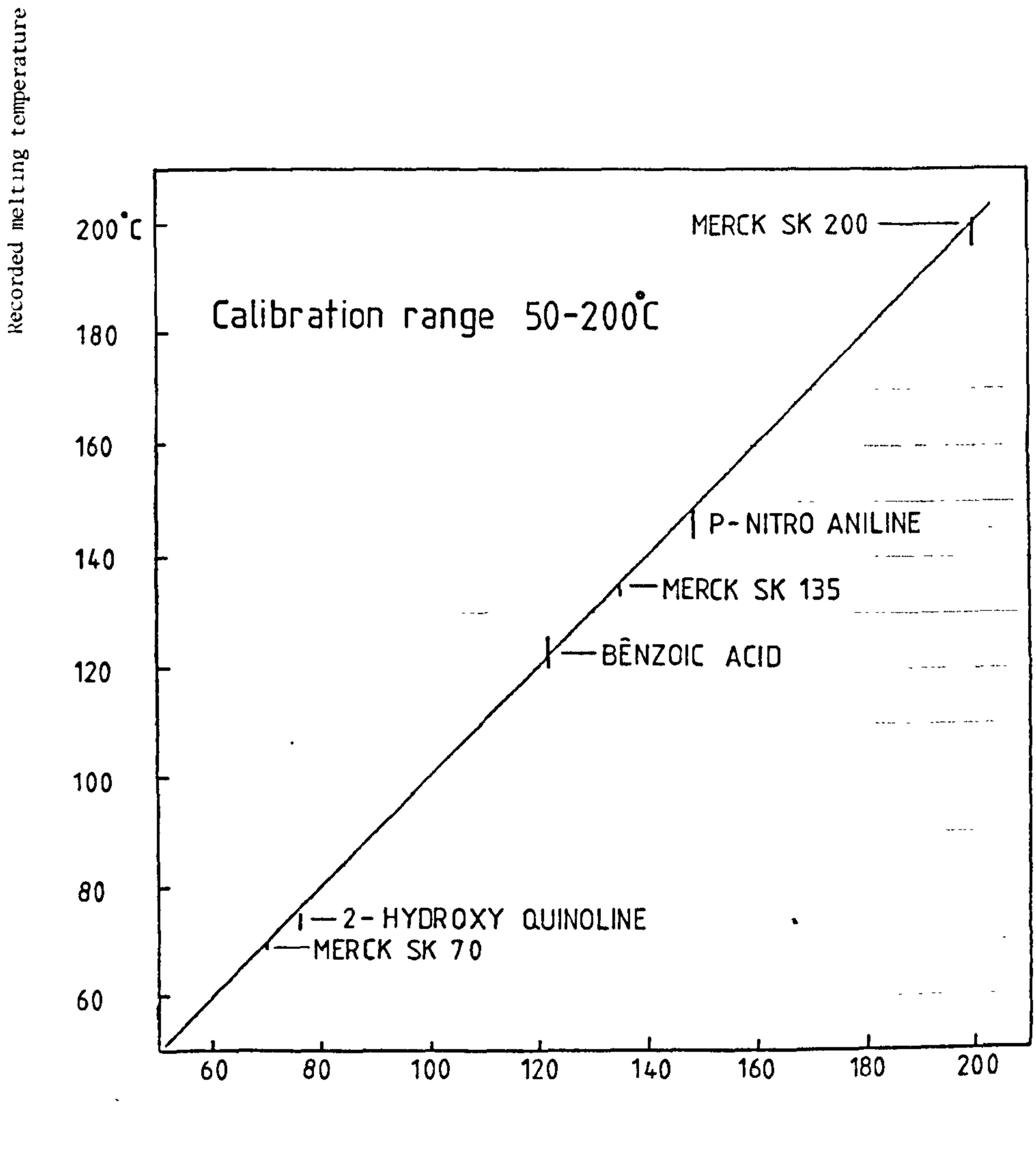

2.3: USE OF SILICONE OIL

Granular or fragmented grains were placed on a 25mm glass cover slip and silicone oil dropped on to the fragments until they were just covered. Dow Corning 200 silicone oil was used which has a refractive index of 1.403 at 25°C, a value which is reasonably close to that of fluorite (1.433-1.435). The oil is colourless, odourless and has a viscosity of $1m^2s^{-1}$. Silicone oil has the disadvantage that it freezes into an aggregate of rounded, slightly opaque globules in the range -50° to -60°C. It does, however, still allow the measurement of first melting, final hydrohalite and ice melting temperatures. The refractive index of the silicone oil increases at lower temperatures and, therefore, the image quality improves for melting temperature measurements. The great advantage of silicone oil over tritolyl phosphate is that it does not undergo significant volatilization at temperatures below 200°C. Therefore, both homogenization and final ice melting temperatures may be measured without moving the sample from the microscope stage. Some vaporization does occur in the temperature range 120° to 200°C and the upper window of the specimen chamber requires cleaning after every second or third run, but image quality is never significantly impared during a single run. Silicone oil also has the advantage over tritolyl phosphate that it has no apparent harmful effects on human tissue.

The persistence of pseudosecondary and secondary inclusions within fractured material suggested that tests for fluid inclusion leakage could be made by looking at

homogenization temperature means obtained from thick sections and similar means obtained from the same sample which had been crushed in the laboratory. Samples were crushed in a pestle and mortar and then sieved. The optimum grain size for oil immersion fell in the range 250μm to 350μm. It was noted that all negative crystal fluid inclusions were destroyed but chains of secondary and pseudosecondary inclusions were still readily recognizable and a visual inspection indicated that these inclusions had not leaked significantly. Four samples were used to test the comparability of homogenization temperatures measured from thick polished sections and crushed grains. Samples were taken from Pictor Pipe (SK1745 8011), Gregory Mine (SK344 6173) and Treak Cliff Cavern (SK136 832) The results of these tests are shown in table 2.1, 2.2, and 2.3. The f-test may be initially applied in order to examine whether a t-test or a non-parametric Mann-Whitney U-test should be used to compare two sample populations. Where an f-test fails at a 5% level of significance, only the result of the Mann-Whitney U-test should be considered.

Chi-square tests indicated that the majority of the sample populations were normally distributed, with the exception of the measurements made on the thick polished sections of fluorite from Gregory Mine. The failure of the test is probably the result of the abnormally low standard deviation and the small sample size. As can be seen from the results of the tests, there is very little difference between the homogenization temperatures measured from polished sections and mineral grains immersed in oil. Most of the populations compared showed indistinguishable distributions

about the mean and similar variances at a 95% confidence level. The sample from the Gregory Mine gave the poorest results, but even in this case sample populations were found not to be dissimilar at a better than 99% confidence level. Differences in homogenization temperature may also have been influenced by the improved thermal conductivity of silicone oil when compared to fluorite and the closer proximity of inclusions in the crushed grains to the thermocouple. A sample from Temple Mine (SK2926 58Ø6) was used to check variation in final ice melting temperatures but as expected, none was found.

TABLE 2.1

COMPARISON OF HOMOGENIZATION TEMPERATURES GAINED FROM INCLUSIONS IN DOUBLE POLISHED THICK SECTIONS AND MINERAL GRAINS IMMERSED IN SILICONE OIL

Sample 1: Yellow fluorite, Pictor Pipe.

	Thick Section (A)	Crushed grains (250-350μm) (B-E)			
Groupings	A	B	C	D	E
No of inclusions examined	1Ø	1Ø	1Ø	1Ø	1Ø
Mean T_H °C	83.1	86.3	85.5	85.4	86.4
σ	5.6	5.6	5.4	4.3	5.8
Median °C	83.7	87.6	84.3	85.1	87.1
χ^2-statistic	1.2	2.Ø	Ø.4	Ø.4	1.2
Test groupings		A-B	A-C	A-D	A-E
t-statistic		-1.29	-Ø.97	-1.Ø3	-1.28
Level of significance		Ø.21	Ø.35	Ø.32	Ø.22
f-statistic		1.67	Ø.94	1.Ø5	1.65
U-statistic		39.5	4Ø.5	33.5	3Ø.5
Level of significance		Ø.15	Ø.45	Ø.49	Ø.23

f-(critical [α = Ø.Ø5]) = 4.41, χ^2-(crit., [α = Ø.Ø5]) = 3.84

TABLE 2.2

COMPARISON OF HOMOGENIZATION TEMPERATURES GAINED FROM INCLUSIONS IN DOUBLE POLISHED THICK SECTIONS AND MINERAL GRAINS IMMERSED IN SILICONE OIL

Sample 2: Purple fluorite, Treak Cliff Cavern.

	Thick section	Crushed grains (250-350μm)
Groupings	A	B
Number of inclusions examined	24	24
Mean T_H	139.1	136.5
Standard deviation	5.6	7.3
Median	139.9	137.5
X^2-statistic	2.Ø	Ø.33
X^2-critical (α = Ø.Ø5) = 3.84		
Test Group	A-B	
T-Statistic	1.36	Significant at α = Ø.18
f-Statistic	1.85	(f-critical(α = Ø.Ø5) = 4.Ø)
U-Statistic	235.Ø	Significant at α = Ø.27

TABLE 2.3

COMPARISON OF HOMOGENIZATION TEMPERATURES GAINED FROM INCLUSIONS IN DOUBLE POLISHED THICK SECTIONS AND MINERAL GRAINS IMMERSED IN SILICONE OIL

Sample 3: Yellow fluorite, Gregory Mine.

	Thick section (A)	Crushed Grains (250-350μm)	
Groupings	A	B	C
No. of inclusions examined	10	10	10
Mean T_H °C	92.2	90.1	89.2
Standard deviation	1.83	1.73	1.55
Median °C	92.2	90.1	89.2
X^2-statistic	8.4	3.6	2.0
X^2-critical (α = 0.05) = 3.84			
Test groupings		A-B	A-C
t-Statistic		2.31	2.68
Significant at		0.03	0.02
f-Statistic		5.33	7.23
f-critical (α = 0.05,) = 4.41, (α = 0.01) = 8.29			
U-statistic		19.5	15.0
Significant at		0.02	0.01

2.4 DISCUSSION AND CONCLUSIONS

The results of the tests clearly indicate that fluid inclusions are not as prone to leakage by mechanical damage as has often been supposed (Roedder, 1976), although the experiments of Roedder and Skinner (1968) did suggest that fluid inclusions were not susceptible to leakage when high pressures were applied to the host minerals. The obvious problem encountered when using mineral grains for fluid inclusion studies is the difficulty in classifying the inclusion into the categories of primary, secondary or pseudosecondary. However, for certain reasons which are very specific to the fluorite deposits of the Southern Pennine Orefield, data obtained from mineral grains is very useful in supplementing information gathered from the study of thick double polished sections. Roedder (1976) argued that the varied paragenetic sequences seen in low temperature Mississippi Valley-type deposits were the result of the large fluctuations in the chemical composition of the ore fluid. However, unless mineral deposition occurs as a result of high degrees of fluid mixing the major element chemistry of the fluid is unlikely to change since dominant cations in the brine are Na^{+} ,Ca^{++}, and K^{+} which cannot be easily removed from the brine in any quantity (Helgeson, 1970). It will be shown in chapter 3 that fluorite mineralization occurred in a series of hydrothermal events, and in each event the ore fluid had a characteristic composition which was maintained over the entire Orefield. Therefore, the recognition of a

characteristic melting sequence in an inclusion of unknown origin enables the inclusion to be classified from the hydrothermal sequence which has been established from other localities by the study of polished thick sections. The position of the fluorite in the hydrothermal sequence may be tentatively recognized by the earliest fluid composition preserved in a fluid inclusion in the mineral sample in question and these inclusions may be classified as primary or pseudosecondary. Therefore, inclusions may be usefully studied in metasomatic replacements and brecciated and fractured deposits and both homogenization and melting temperature measurements collected. A good example of a deposit within the district which is suited to this type of technique is the vein filling of Deep Rake and High Rake in the Sallet Hole Mine which is almost entirely composed of brecciated and granular fluorite.

CHAPTER 3

FLUID INCLUSION STUDIES

3.1: INTRODUCTION

The fluid inclusion study on fluorite from the Orefield carried out by Rogers (1977) did not confirm any consistent east-west homogenization or final ice melting temperature variation which may be expected if the ore fluids had moved from east to west. Secondly, the work of Smith (1973; 1974) and Moore (1980) suggested that the homogenization temperatures reported by Rogers (1977) were erroneously high. The Linkam TH600 heating and freezing stage, used in this study, is both more accurate and precise than the Leitz 1350 heating stage and the freezing stage [similar to that designed by Roedder (1962)] used by Rogers (1977). Homogenization and final ice melting temperature pairs may be measured for each inclusion and the derived data may be used to look for any temperature and salinity variation that occurred during the mineralizing events. Variation in fluid salinity may be useful in ascertaining whether mineral deposition occurred as result of fluid mixing (Zimmerman and Kesler, 1981).

Smith (1974) made a detailed study of the transverse, longitudinal and vertical variation in homogenization temperatures of fluid inclusions in fluorite from the Red Vein and the Groverake Vein in the Northern Pennine Orefield. A similar study of temperature and fluid salinity variation

in inclusions in fluorite from the Deep Rake-High Rake vein system may also be useful in establishing the physicochemical conditions of mineralization. It is also important to ascertain the possible difference between the filling temperature and homogenization temperature. In order to do this, the thickness of strata overlying the host rocks at the time of the mineralization must be estimated.

3.2: ORIGIN OF FLUID INCLUSIONS

Criteria for ascertaining the origin of fluid inclusions have been given by Roedder (1979). These criteria can be used to categorise fluid inclusions into three types, primary, secondary and pseudosecondary. As Roedder states, "None of the criteria are absolute, and many are only suggestive or are applicable to material from certain deposits...". "It is unfortunate but true that many inclusions simply do not permit application of any of the criteria.". This latter statement is very pertinent to the study of fluid inclusions in fluorite from the Southern Pennine Orefield. The recognition of primary, secondary and pseudosecondary fluid inclusions within thick doubly polished sections will be discussed briefly in sections 3.3.1 and 3.3.2.

3.3: CLASSIFICATION OF FLUID INCLUSIONS

3.3.1: PRIMARY INCLUSIONS

Interference in the growth of a crystal may may cause the formation of primary fluid inclusions, by the trapping of the fluid into irregularities on the growing face. Crystals are known to grow as a series of blocks. If the rate of growth of some of the blocks varies, angular re-entrants will occur which may be covered by later material. The gaps between re-entrants will form primary inclusions. Negative crystal or multifaceted inclusions were rarely observed. Although such inclusions are not definitive proof of primary origin, when coupled with the the characteristics of being large, isolated and randomly distributed, they may be taken to be primary. Surface cracks may cause the trapping of primary fluids. A more important mechanism is, however, formation by the capture of a solid particle on to a growing face. Growth will be inhibited on the covered portion while growth on the surrounding face will continue normally. This may either result in the particle being moved perpendicular to the growing face and thus the formation of a string of inclusions or as is more likely, the solid inclusion will be trapped within the crystal and partially surrounded by fluid. Examples of this latter type are observed relatively frequently. However, the categorical interpretation of this type of inclusion as being primary is strongly doubted. This type of inclusion could easily form by the coincidence of a sulphide grain being intersected by a plane of secondary

inclusions.

3.3.2: SECONDARY AND PSEUDOSECONDARY INCLUSIONS

Secondary inclusions are those that form by any process after the crystallization of the host has taken place (Roedder, 1981). Thus if a crystal undergoes brittle deformation, fluids entering fractures may re-cement the mineral and enclose post depositional fluid inclusions. Obviously, the chemical composition and temperature of the fluid need have little in common with the solution from which the mineral was formed. Using paragenetic relationships, the abundance and distribution of fluid inclusions, the sequence of fluids which gave rise to the mineralizing events may be recognized (Chivas and Wilkins, 1977). Overprinting does, however, cause changes in the type and abundance of preserved inclusions (Bloom, 1981).

Pseudosecondary inclusions (Roedder, 1979) represent an intermediate between primary and secondary types. They are most likely formed when fracturing of a growing mineral occurs. There is much evidence to show that faulting took place during and between mineralizing events in the Southern Pennine Orefield (Firman and Bagshaw, 1974). Homogenization temperatures and final ice melting point measurements should be broadly similar but some small variations are almost certain to be observed. The positive identification of pseudosecondary types is often very difficult. It is convenient to assume that inconclusively identified secondary fluid inclusions are pseudosecondary when their heating and

freezing data closely correlates with data derived from primary inclusions (Zimmerman and Kesler, 1981). This assumption can be usefully applied to fluid inclusion studies on fluorite from the Orefield under discussion.

3.4: FLUID INCLUSIONS IN FLUORITE FROM THE SOUTHERN PENNINE OREFIELD: OUTLINE OF FORM AND OCCURRENCE

Seven hydrothermal events are recorded in fluid inclusions in fluorite found in the Southern Pennine Orefield. They can be recognized by a combination of optical and thermometric observations. Unfortunately, positive identification of most of the listed types relies on freezing data alone. This means that unless a thorough thermometric study is carried out, the fluid phases represented in a given sample will not be correctly recognized. On observation of characteristic physical features alone, three or four of the seven types may be tentatively classified.

3.5: FORM AND OCCURRENCE OF FLUID INCLUSION TYPES

3.5.1: TYPE 1 FLUID INCLUSIONS

These are biphase aqueous-vapour inclusions, as are all the other fluid inclusion types listed. They can be readily distinguished from other inclusions by their low degree of filling. Irregularly dispersed, large negative crystal or

multifaceted forms are relatively common in material from Treak Cliff and can be assumed to be primary. One of the cube faces is usually observed to be parallel to a growth face of the host grain, as indicated for example by a band of anomalous colouration. These types of inclusion range in size from 200μm to 20μm. Numerous deviations away from the plain negative crystal shape have been observed and some are illustrated in figure 3.1. Small grains, clustered on the vapour-liquid interface are commonly observed. They may represent detrital fragments, originally suspended in the hydrothermal solution. If this were true, the implication would be that the ore-forming fluid had a substantial velocity. The grains could be composed of resinous hydrocarbons or possibly an inorganic precipitate of some type.

On crushing, the vapour bubble within the inclusion invariably expands. The maximum internal pressure is calculated to be in the range, 21 to 32 atmospheres (The calculation is outlined in the appendicies).

Pseudosecondary fluid inclusions are the most abundant of the type 1 inclusions. Thermometric evidence indicates the inclusions cannot be strictly termed pseudosecondary (Section 3.3.2) but it is almost certain that the solutions present in the type 1 secondary and type 1 primary fluid inclusions were very closely related. The inclusions are small (<20μm) and exhibit spherical, oblate and flattened forms. The smaller inclusions show some variation in the degree of filling, which may be attributed to necking down and metastability. These inclusions lie on surfaces which may be planar, or curved and possibly interrupted by occasional discontinuities

Plate 3.1

Type 1 pseudosecondary fluid inclusions

(a) Planes of inclusions in fluorite from Treak Cliff Cavern can be seen to have cut a horizontal growth face at angles between 40° and 45°. The diagonal bands of colouration may have been introduced at a post-depositional stage.

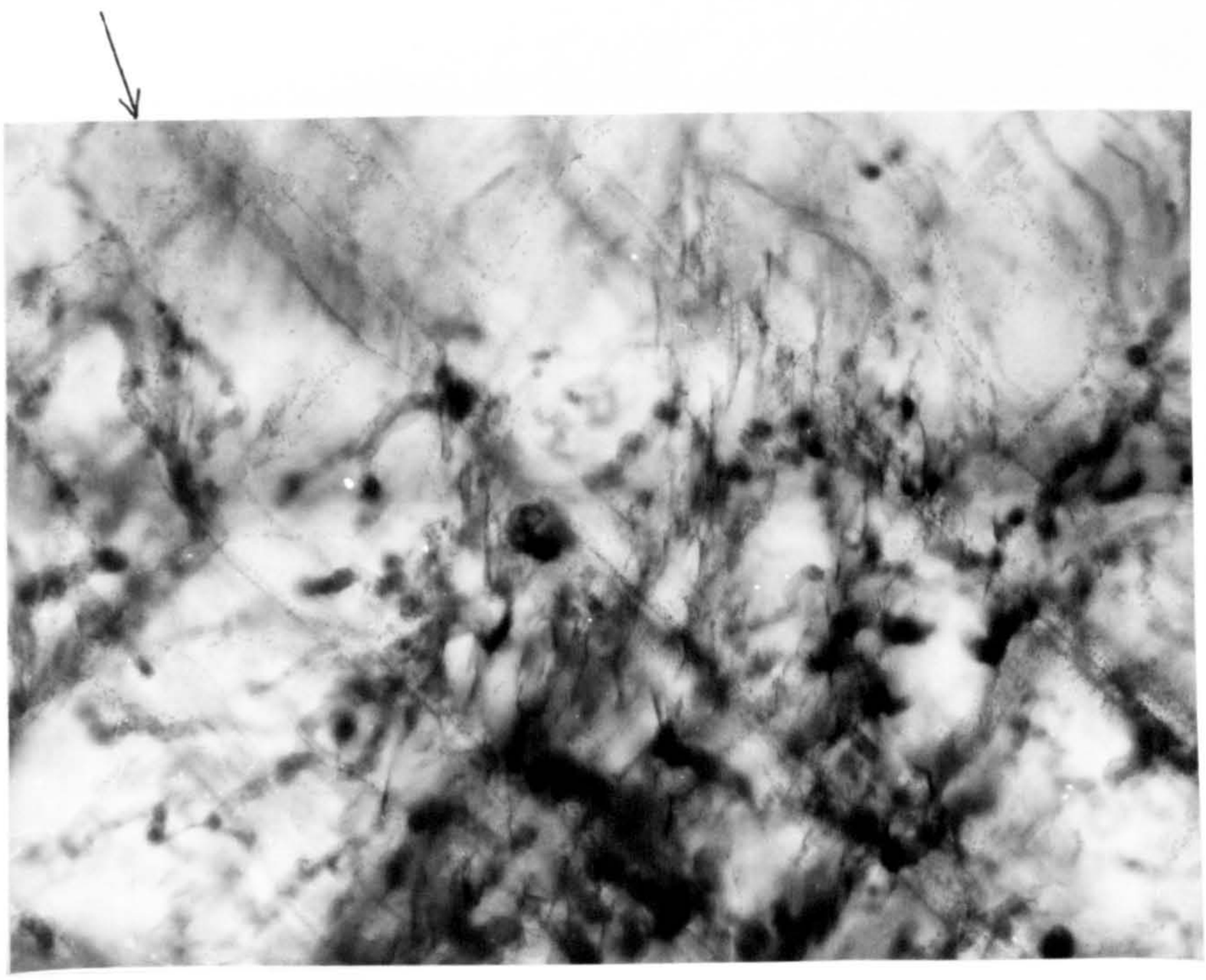

Field width: 2.44mm

(b) An enlargement of part of the photomicrograph shown above illustrates the nature of the inclusion bands.

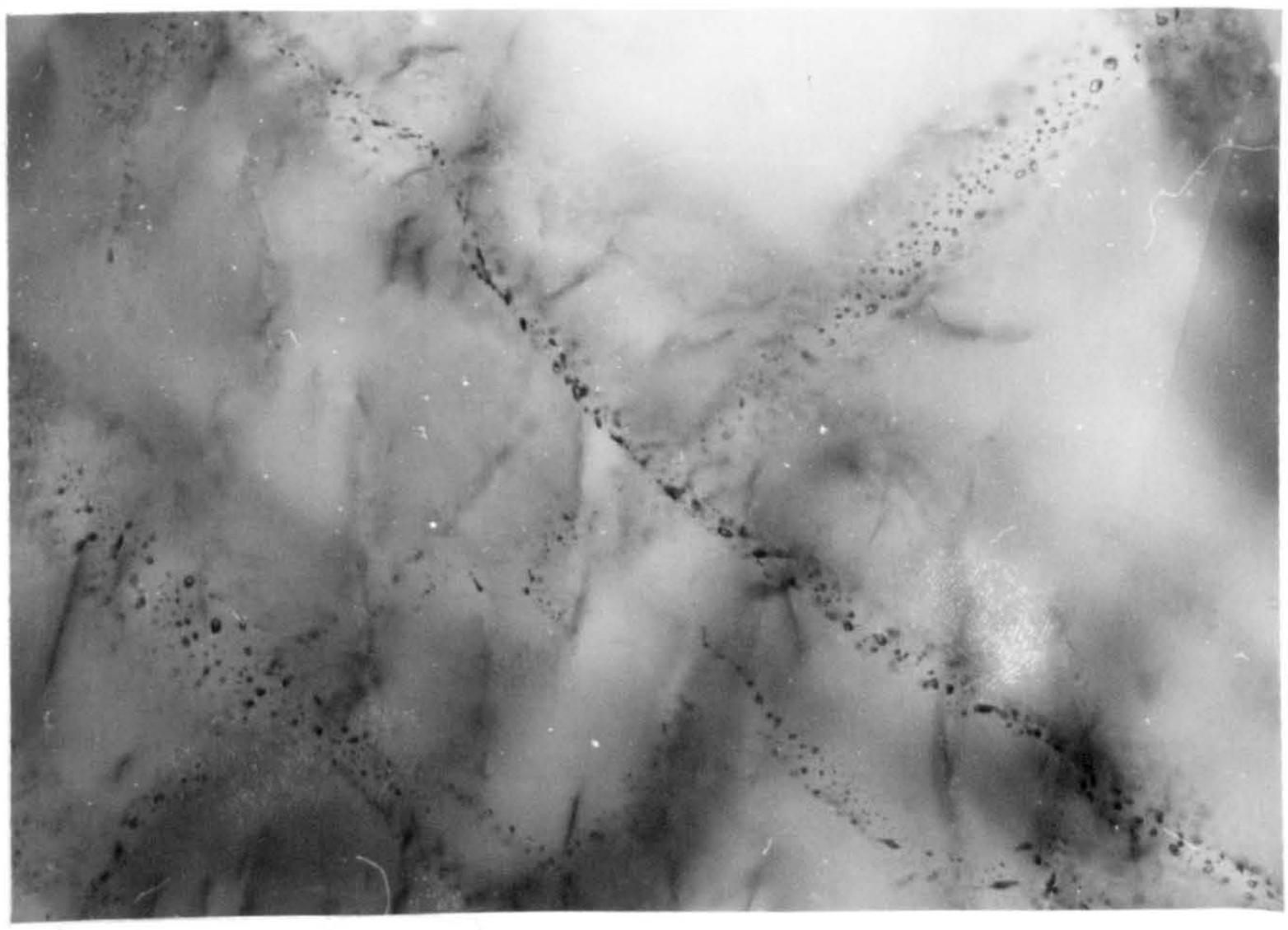

Field width: 820μm

Figure 3.1

Examples of the variation in form of type 1 primary fluid inclusions.

The scale bar represents 0.05mm.

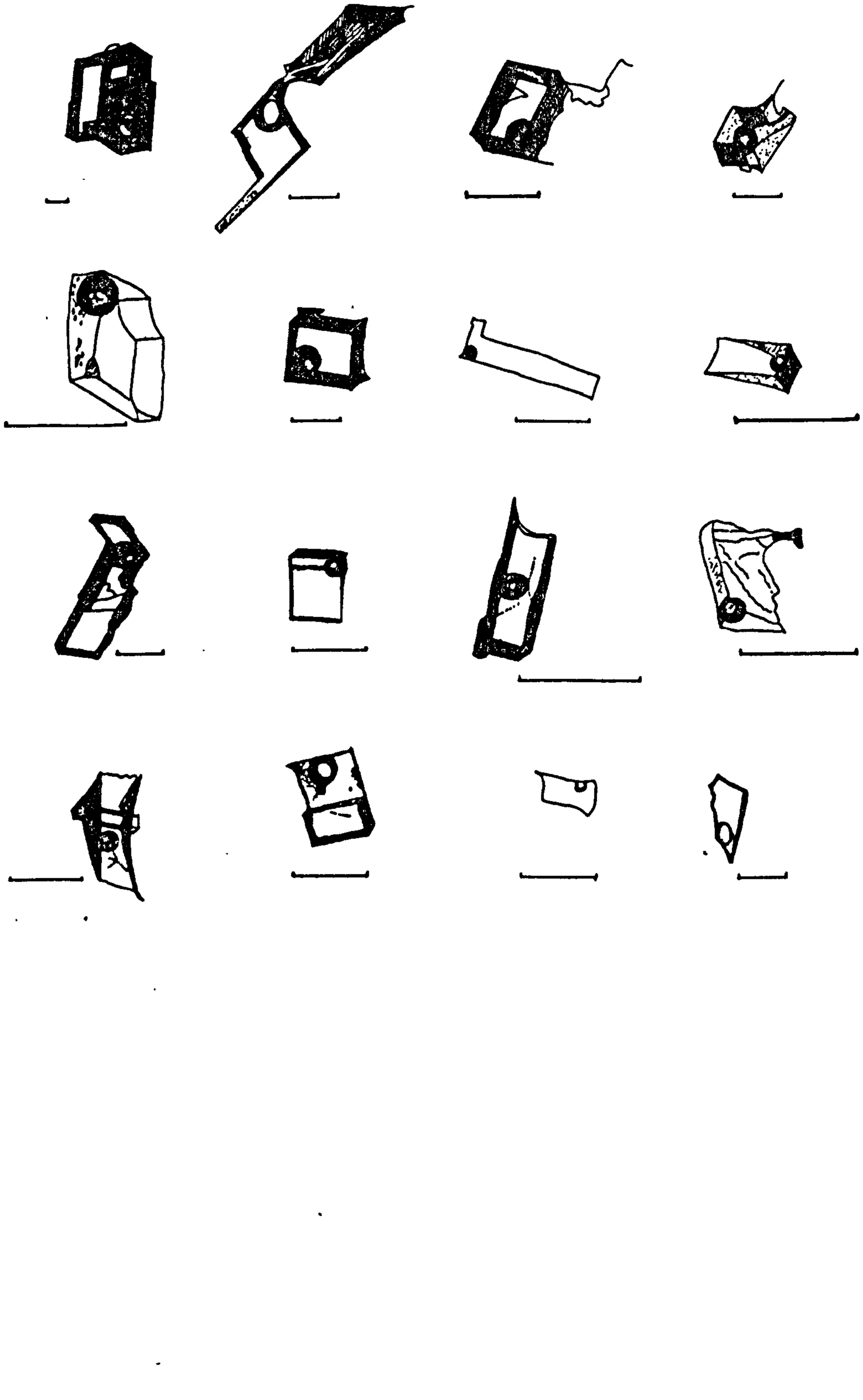

and abrupt terminations. Sometimes these planes of inclusions are associated with bands of colouration and individual inclusions may be outlined by purple rims. The orientation of these planes is strongly controlled by the crystallography of the fluorite. They nearly always intersect the growth face at an angle of 45 degrees, forming a cubic cross-cutting array (plate 3.1).

3.5.2: TYPE 2 FLUID INCLUSIONS

These are biphase aqueous inclusions with occasional daughter halite cubes. The high refractive index of the included fluid optically characterizes this inclusion type. Rogers (1977) noted inclusions containing halite daughter crystals. This inclusion type has a limited distribution in fluorite from the Peak District and primary examples have only been recognized in samples from the Smalldale Pipe and Treak Cliff (plate 3.2). The majority of inclusions are considered to be pseudosecondary, although few could be identified as such using the criteria set down by Roedder (1979). The inclusions range in size from 5µm to 50µm. The optimum size for thermometric measurement lies in the range 10µm to 50µm. The larger inclusions may contain a daughter halite crystal taking the form of a small plain cube.

Quartz crystals are also common within inclusions in fluorite from the Smalldale Pipe. They occur as elongate prisms or small freely-grown double terminated crystals. They are easily observed under crossed polars and show the characteristic straight extinction of quartz. The presence of

Plate 3.2

(a) Irregularly distributed type 2 fluid inclusions in fluorite from the Smalldale Pipe. The inclusions are probably primary.

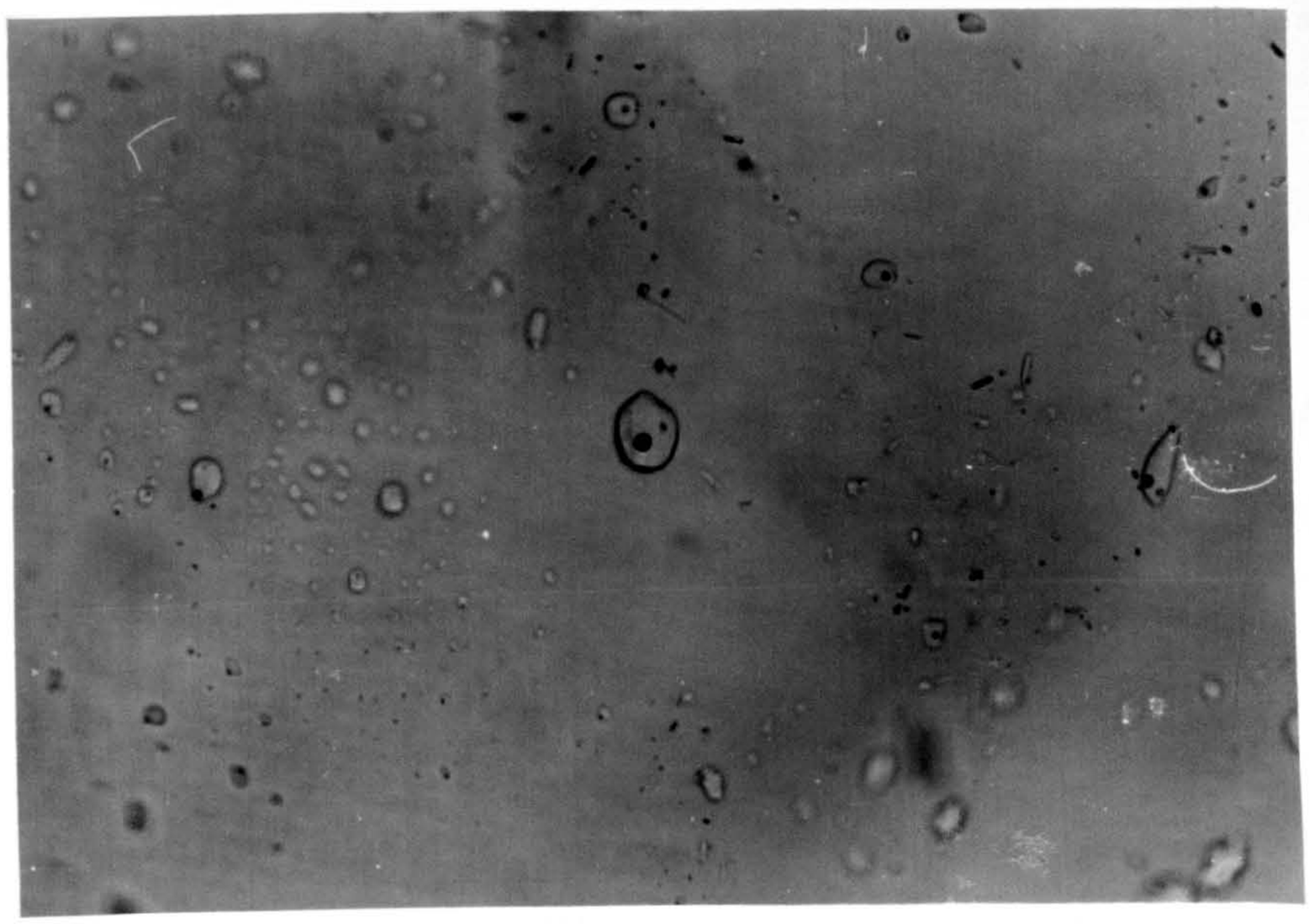

Field width: 650μm

(b)

Elongate, type 7 fluid inclusions in fluorite from the Smalldale Pipe. The inclusions show varied degrees of filling.

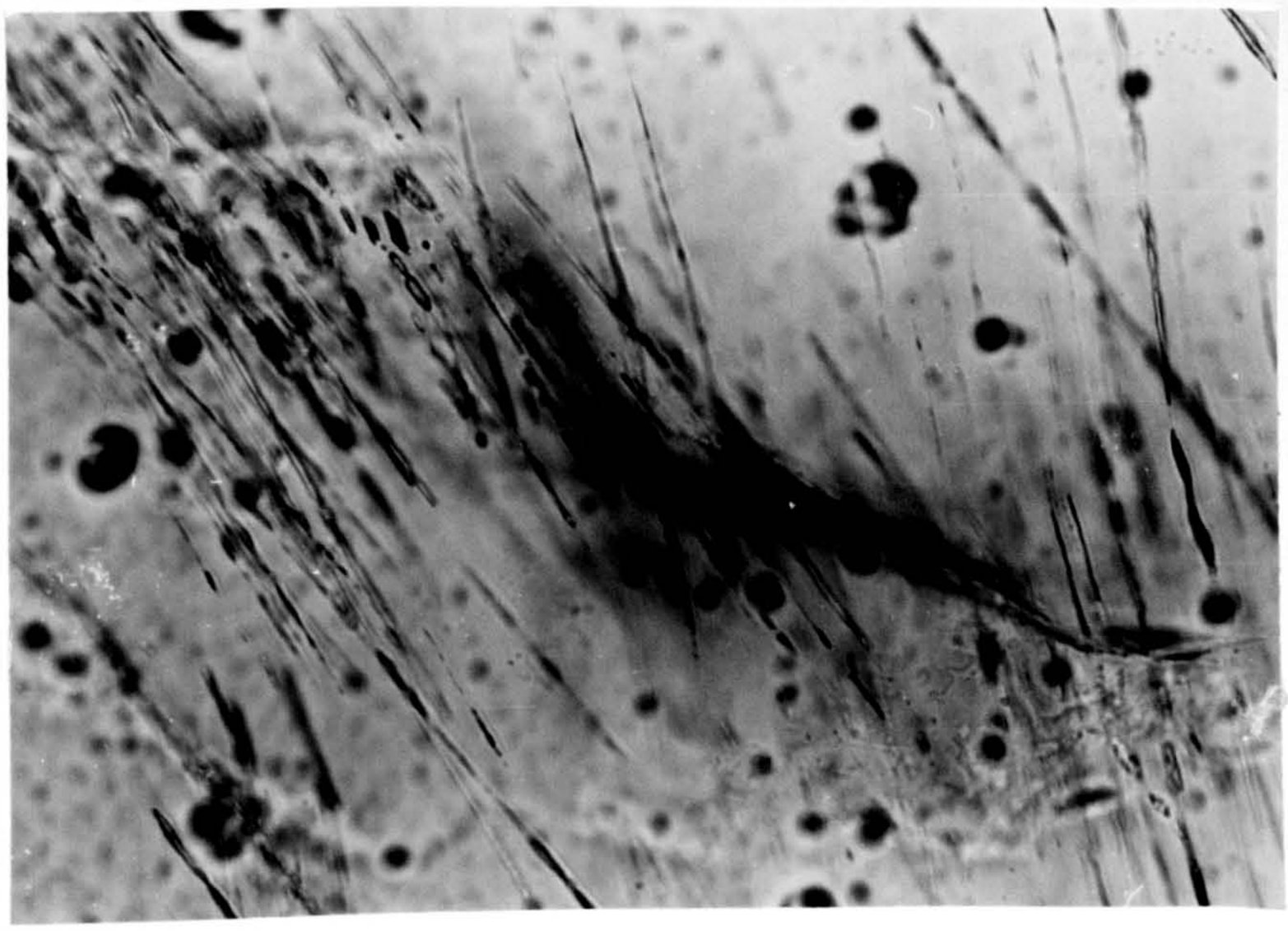

Field width: 500μm

these inclusions presents problems. It is impossible for the quartz to have grown within the inclusion from the inclusion fluid itself. Quartz crystals do occur in both the fluorite and in the fluid inclusions but the number of crystals in a given volume of inclusion free fluorite is much less than the number in a similar volume which contains a plane of fluid inclusions. There appears to be two possibilities. The first is that the quartz was deposited while the fracture was open and the second is that the inclusions formed on a plane which contained quartz initially incorporated into the fluorite on metasomatism of limestone. The fluorite may have preferentially fractured along zones of weakness, created by the presence of quartz inclusions. Any disruptions in the lattice probably represent favourable sites for dissolution to take place. A conclusion which can be drawn is that the solution was not grossly undersaturated with dissolved silica and consequently it is unlikely that the solution had undergone any significant period of residence within a limestone reservoir. Similar quartz inclusions have been observed within inclusion types 3 and 4.

3.5.3: TYPES 3 AND 4 FLUID INCLUSIONS

Both these types are biphase aqueous-vapour inclusions. A very few primary plain cubic inclusions have been observed, indicating that these fluids have been responsible for fluorite deposition. Types 3 and 4 inclusions are commonly poorly shaped and may be flattened or clustered into thin, discontinuous planar or curving trails (plate 3.6). The

larger inclusions are often very irregularly shaped, with both flat and curving walls and lengths of up to 500μm. Variation in the degree of filling suggests coalescence and necking down of some inclusions (plate 3.6). The cubic lattice of fluorite seems to have had little affect in controlling their form. The smaller inclusions are usually flattened and may adopt rounded, subrounded or angular shape. The trails are often very densely packed and the variation in the degree of filling in the particularly closely spaced individuals suggests that necking down has been an important process. Most measurements were made on inclusions in the size range of 5μm to 30μm. These types of inclusion could rarely be classified as pseudosecondary with any degree of certainty. They are, however, the most commonly observed inclusion types within fluorite from the district.

3.5.4: TYPES 5 AND 6 FLUID INCLUSIONS

Most of the remarks pertaining to types 3 and 4 can be applied to types 5 and 6. However, their occurrence is very rare. No primary examples have been observed. The type 5 inclusions contain large quantities of calcium chloride. They have been found in material from Deep Rake, Sallet Hole and in samples from the Treak Cliff Cavern and were associated with type 2 inclusions. Type 6 inclusions are similar to the type 4 inclusions but have a higher final ice melting point. Both types of inclusion could result from the coalescence of the the aforementioned inclusion types during migration.

3.5.5: TYPE 7 FLUID INCLUSION

This type of fluid inclusion occurs as bunches of radiating needle like tubular cavities, frequently arranged perpendicular to the growth face (plate 3.2). Mueller (1954) observed these inclusions in fluorite from the "Bradwell Spar Zone". He described them as elongate, gas inclusions repelled from the edge loci of the cubes. Examination of these inclusions by the author suggests that the "gas" inclusions are probably either completely filled liquid inclusions or fluid inclusions which lost their fluid content as a result of leakage. These inclusions could be produced by rapid growth of the fluorite. However,in general these inclusions occur at the centre of crystal faces and not at cube edges. Considering the growth of a cube in the most simple terms one would expect that the most rapid development should take place on the cube edges. A more probable origin is the is the re-cementation of existing fractures. This, however, does not explain the lack of inclusions at the cube edges.

3.6: THERMOMETRIC STUDIES

The thermometric data discussed in this section is presented in appendix 1. Notes on the methods of data collection used in the thermometric fluid inclusion study have been presented in sections 2.2 and 2.3. Calibration curves for the Linkam TH600 heating-freezing stage are shown in figures 2.1 and 2.2. Short notes on some of the

statistical tests are also given in appendix 1.

3.6.1: TYPE 1 FLUID INCLUSIONS

Samples from nine localities were found to contain type 1 fluid inclusions. The homogenization temperatures of 157 inclusions were measured. The majority of the fluid inclusions examined were pseudosecondary. The histogram (figure 3.2) showing the distribution of homogenization temperatures from a population of 109 measurements suggests that the population is negatively skewed but the calculated coefficient of skewness is 0.086. The maximum and minimum recorded temperatures were 169.9°C and 100.1°C respectively. The mean value for 109 determinations was 136.5°C ±28.6°C. The median value is 138.2°. The range given is evaluated from the standard deviation σ and is stated as $\pm 2\sigma$.

The abundance of primary inclusions in fluorite from Treak Cliff Cavern has permitted a comparison between the homogenization temperatures of primary inclusions and those of associated secondary inclusions. The mean homogenization temperature of 10 primary inclusions was 143.0°C ±20°C, while the mean of 21 pseudosecondary inclusions was 134.2°C ±15°C. Both groups were normally distributed at a 10% level of significance. Therefore, solutions present at the time of deposition were hotter and showed a greater temperature range than late stage fluids present in pseudosecondary inclusions.

Mean homogenization temperatures for the nine localities examined ranged from 157.3°C ±16°C to 119.5°C ±6.2°C. Standard deviations ranged from 4.5 to 15.1. The

Figure 3.2

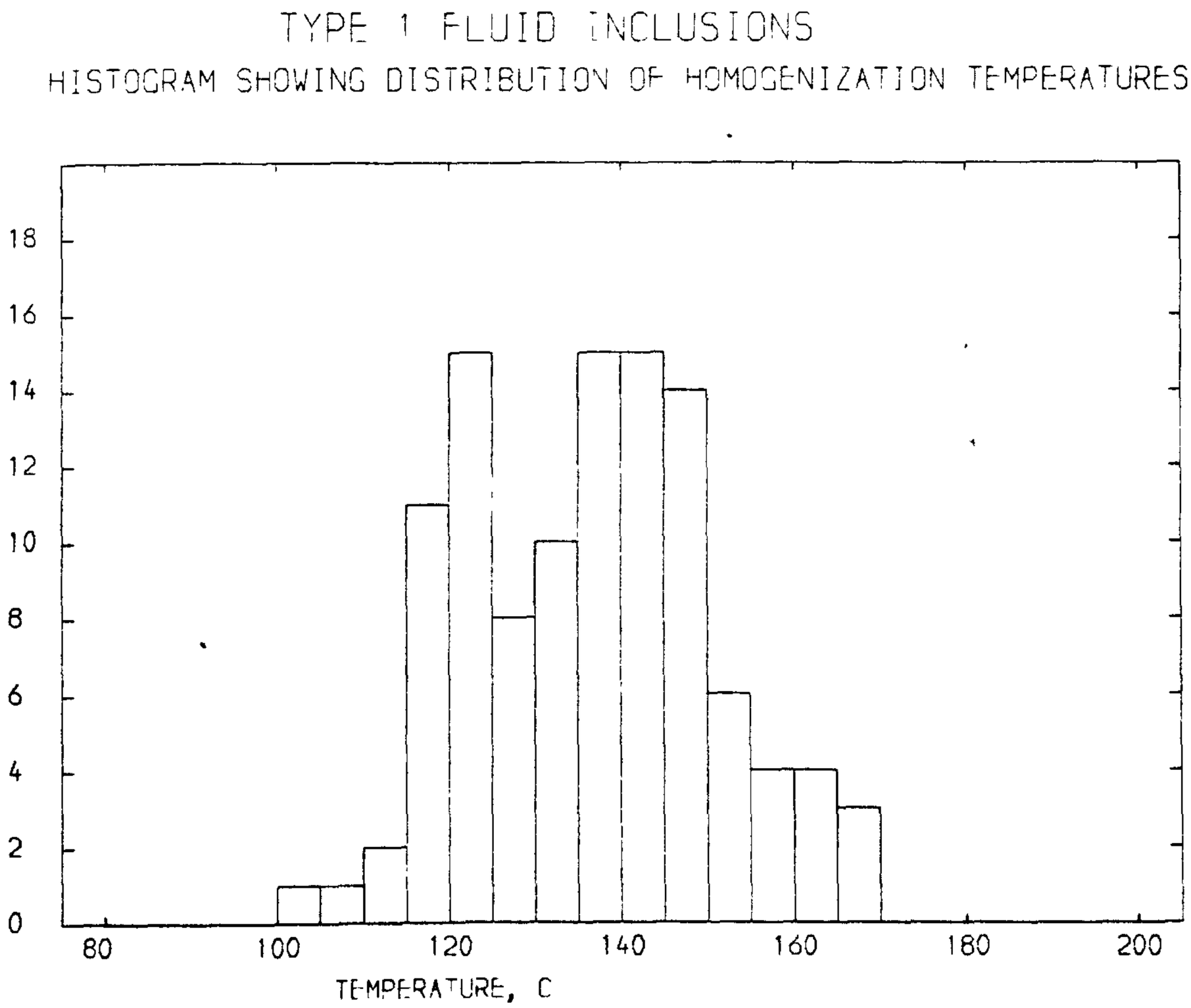
TYPE 1 FLUID INCLUSIONS
HISTOGRAM SHOWING DISTRIBUTION OF HOMOGENIZATION TEMPERATURES
0
2
4
6
8
10
12
14
16
18
80
100
120
140
160
180
200
TEMPERATURE, C
NUMBER OF SAMPLES PLOTTED = 109
INCREMENT = 5.0 DEGREES CELCIUS

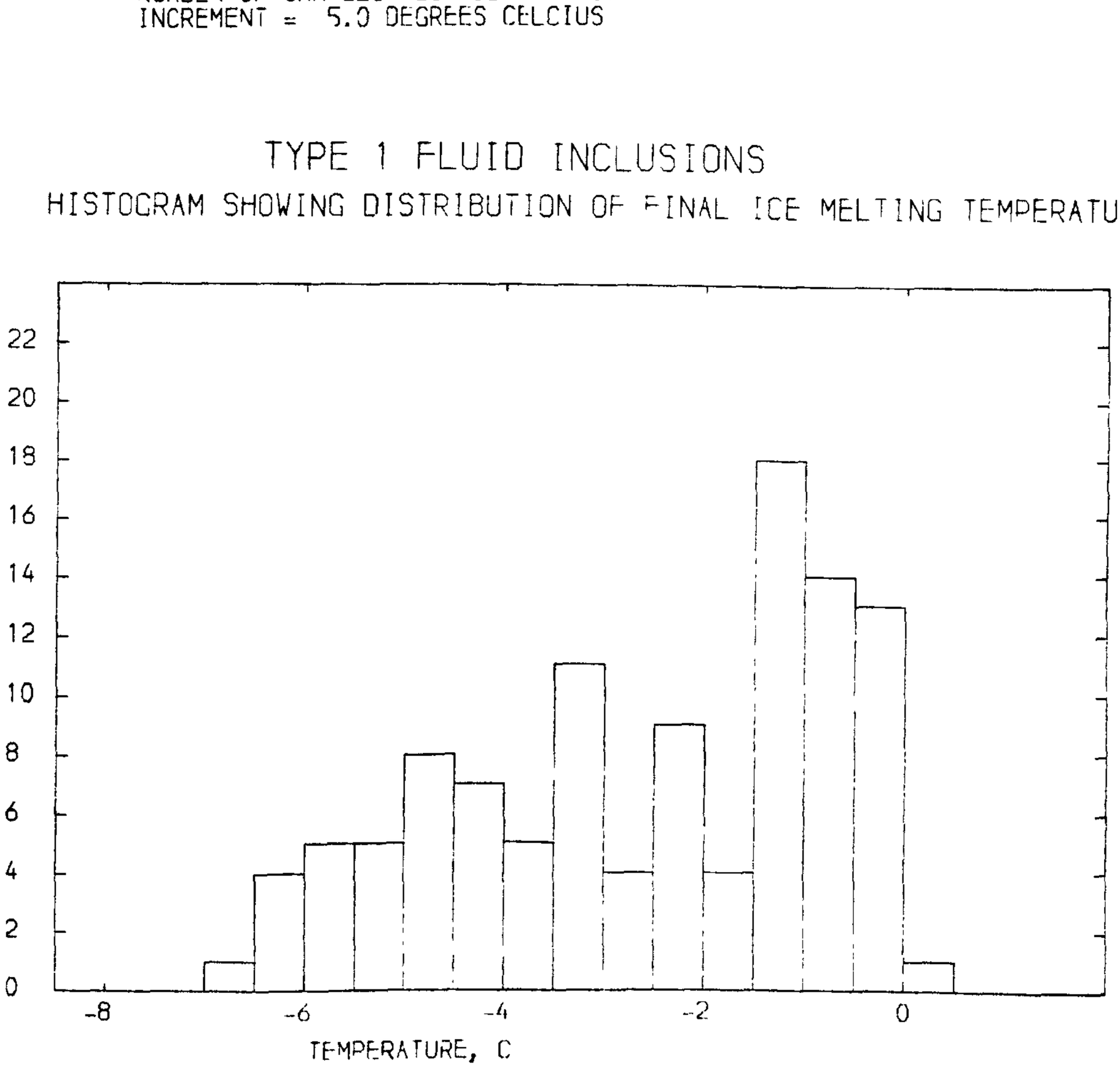
TYPE 1 FLUID INCLUSIONS
HISTOGRAM SHOWING DISTRIBUTION OF FINAL ICE MELTING TEMPERATURES
0
2
4
6
8
10
12
14
16
18
20
22
-8
-6
-4
-2
0
TEMPERATURE, C
NUMBER OF SAMPLES PLOTTED = 109
INCREMENT = 0.5 DEGREES CELCIUS

majority of samples had normally distributed temperatures. No correlation was found to exist between the mean homogenization temperature and the range of measurements observed within a specific sample. This observation suggests that locally increased temperatures were not accompanied by increased fluctuations in temperature.

Melting point determinations were made on 109 fluid inclusions which had previously been heated to obtain their homogenization temperatures. Inclusions are prone to leakage or stretching after freezing so reliable homogenization temperatures must be obtained before cooling (Lawler and Crawford, 1983). Despite the very low salinity of the inclusion fluids, freezing does not usually occur above -30°C. First melting is observed with difficulty. Liquid has been seen to form in the range -40°C to -10°C. Significant melting of ice usually occurs in the range -10°C to -3°C. Roedder (1967b) used fluid inclusions in material from the Southern Pennine Orefield to demonstrate superheated metastable melting of ice. All the melting sequences he noted were seen in inclusions in fluorite from Treak Cliff.

The low temperature behaviour of the type 1 inclusions suggests that melting point determinations can be accounted for by the binary system NaCl-H_2O (figure 3.5), and estimates of salinity and density can be directly estimated from this system (Potter et al., 1978; Crawford, 1981). No solid phases apart from ice were formed on freezing.

The distribution (figure 3.2) of the final ice melting temperatures is negatively skewed (Coefficient of skewness = -0.41). The mean final ice melting temperature for the 109 measurements is -2.6°C $\pm$2.7°C. The maximum and minimum

temperatures recorded were 0.0°C and -6.6°C. The final ice melting temperature of primary and pseudosecondary inclusions were compared. Nine primary inclusions had a mean melting temperature of -0.4°C ±0.5°C while the pseudosecondaries had a mean of 0.9°C ±0.3°C. A t-test indicates that the melting point values are derived from two populations, at a 5% level of significance. As with the homogenization temperatures, the primary inclusions showed the greatest range of temperatures. It is interesting to note at this point that primary inclusions are associated with more saline secondary inclusions. It is often assumed in the literature that primary inclusions are more saline than secondaries (eg Roedder, 1971). When Roedder (1967) examined the "blue john" fluorite from Treak Cliff he suggested that the type 1 inclusions appeared on the outermost rim of the crystals while the interior contained strongly saline inclusions. From cross-cutting relationships between planes of secondary inclusions it can be easily shown that the saline inclusions represent a later phase of mineralization. Therefore, the implicit assumption that dilution occurs from primary to secondary must be treated with great caution.

Figure 3.3 shows a plot of final ice melting temperature against homogenization temperature. The points form a diffuse pattern with little correlation occurring between temperature and salinity. When similar diagrams are plotted for individual samples, some show elongated or linear trends. Examples are fluorite from Moss Rake, Odin Mine, and Dirtlow Rake. A linear trend suggests mixing of two end member solutions. Some regional thermal and salinity variation is also indicated by the skewed distributions of

Figure 3.3

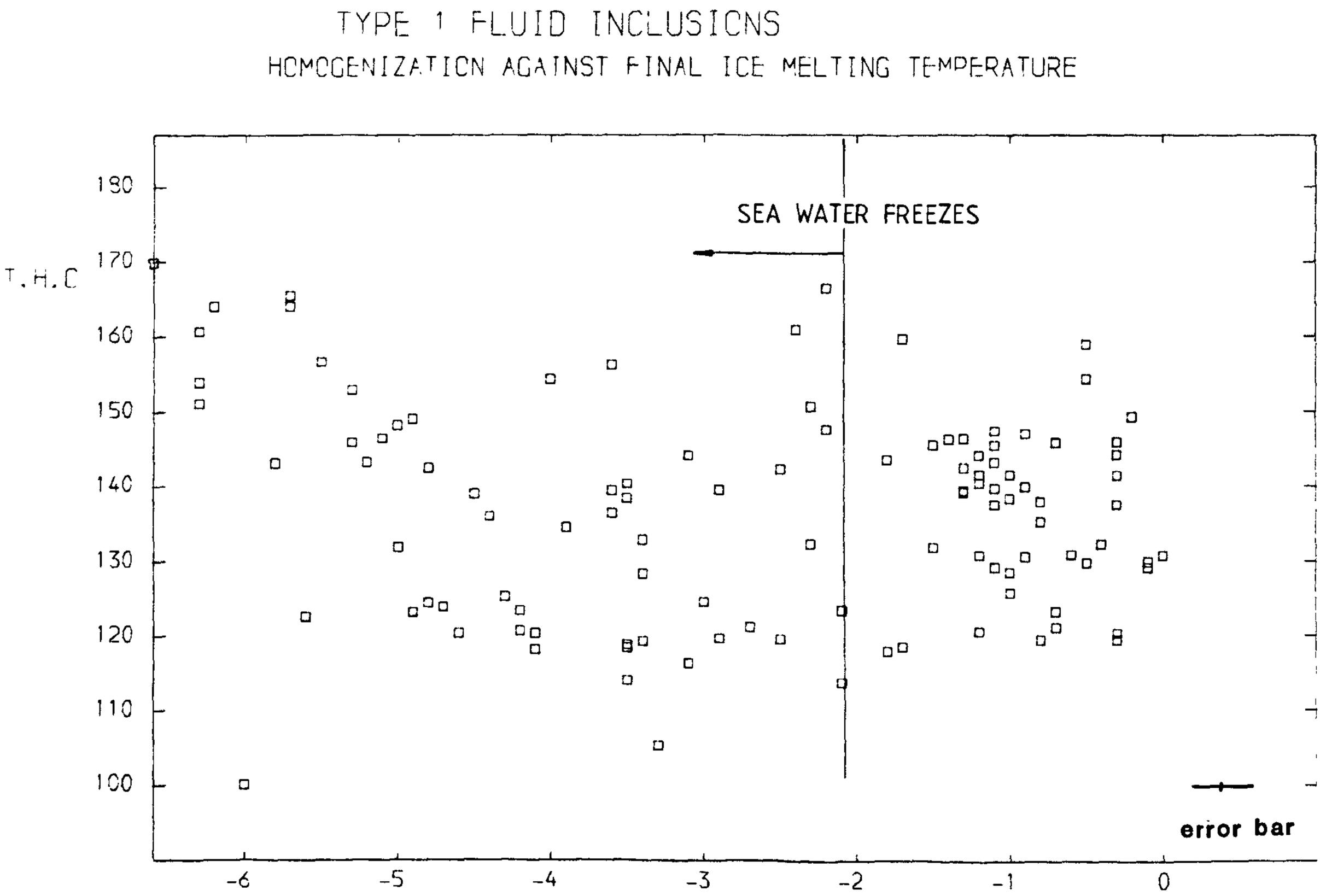

The diagram shows a plot of homogenization temperature against final ice melting temperature for the type 1 fluid inclusions.

the two populations.

3.6.2: TYPE 2 FLUID INCLUSIONS

Mean homogenization temperatures were determined for 45 inclusions and final hydrate melting temperatures for 32. Figure 3.4 shows the distribution of homogenization temperatures. The population is negatively skewed (Skewness = -1.61). This population shows the lowest variance of all the four populations. The mean and range is $75.1^{o}C \pm 6.2^{o}C$. The median of $75.3^{o}C$ suggests a relatively normal distribution. The temperature range observed was $62^{o}C$-$82^{o}C$, therefore, the range overlaps the type 3 and type 4 homogenization temperature limits. Assuming that the pressure correction for inclusion types 2, 3, and 4 are similar, type 2 inclusions were formed in the lowest temperature hydrothermal episode to have formed fluorite. The f-test is unable to distinguish the populations of the four samples taken from Smalldale Quarry, Hope Quarry, Treak Cliff Cavern and Sallet Hole Mine. The uniformity and magnitude of the variances suggests that the mineralization occurred in a geothermally stable environment.

Freezing of type 2 fluid inclusions often proves to be difficult and cooling down to the temperature range $-150^{o}C$ to $-100^{o}C$ is frequently required. Inclusions smaller than 5μm are extremely difficult to freeze. Solidification takes place slowly, with the growth of hexagonal "snowflake" like masses from a nucleus (plate 3.3). Concentrated calcium chloride solutions (30-45 weight %) usually demonstrate similar characteristics on freezing. Concentrated sodium chloride

Plate 3.3

A typical type 2 fluid inclusion melting sequence.

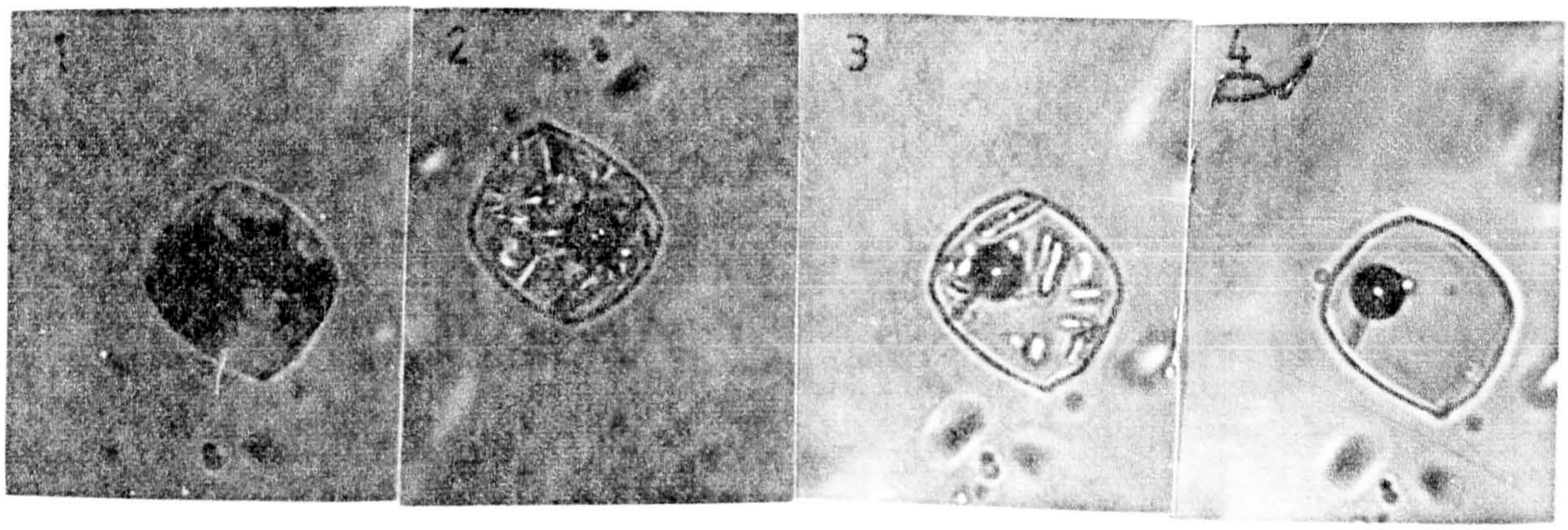

Field width: 60μm.

(1) Solidification of the fluid takes place slowly at -80°C after cooling to -150°C. Note the "snowflake" like growth of antarcticite crystals.

(2) Antarcticite ($CaCl_2.6H_2O$) is the only solid phase present at -24°C.

(3) Elongate, anisotropic crystals can be clearly distinguished at -7.5°C.

(4) Final melting of antarcticite occurs at +6.0°C.

Photomicrograph of antarcticite crystals formed from a concentrated (c40wt%) calcium chloride solution. Some crystals show the expected hexagonal form.

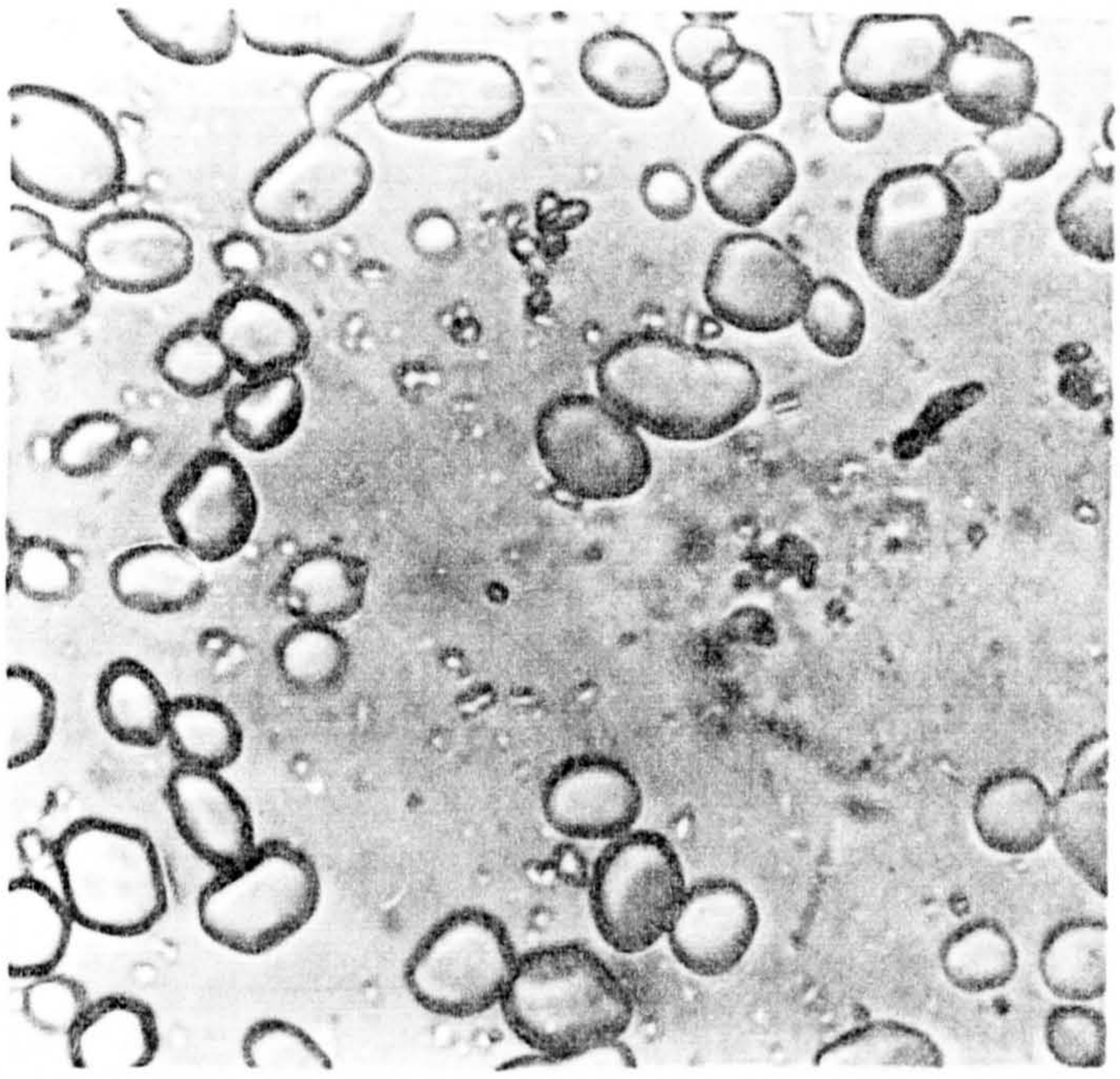

Field width: 300μm.

Figure 3.4

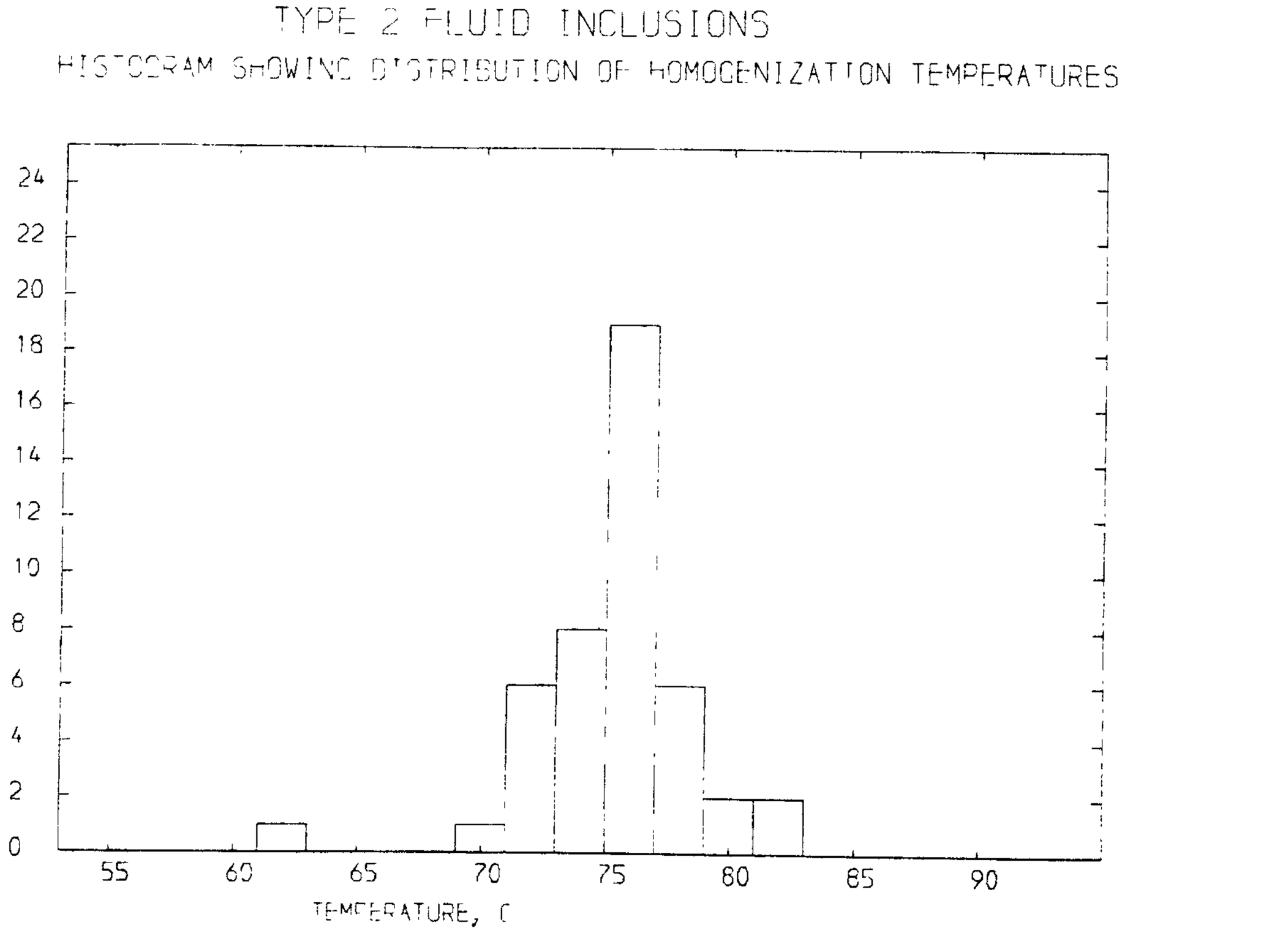
TYPE 2 FLUID INCLUSIONS
HISTOGRAM SHOWING DISTRIBUTION OF HOMOGENIZATION TEMPERATURES
24
22
20
18
16
14
12
10
8
6
4
2
0
55
60
65
70
75
80
85
90
TEMPERATURE, C
NUMBER OF SAMPLES PLOTTED = 45
INCREMENT = 2.5 DEGREES CELCIUS

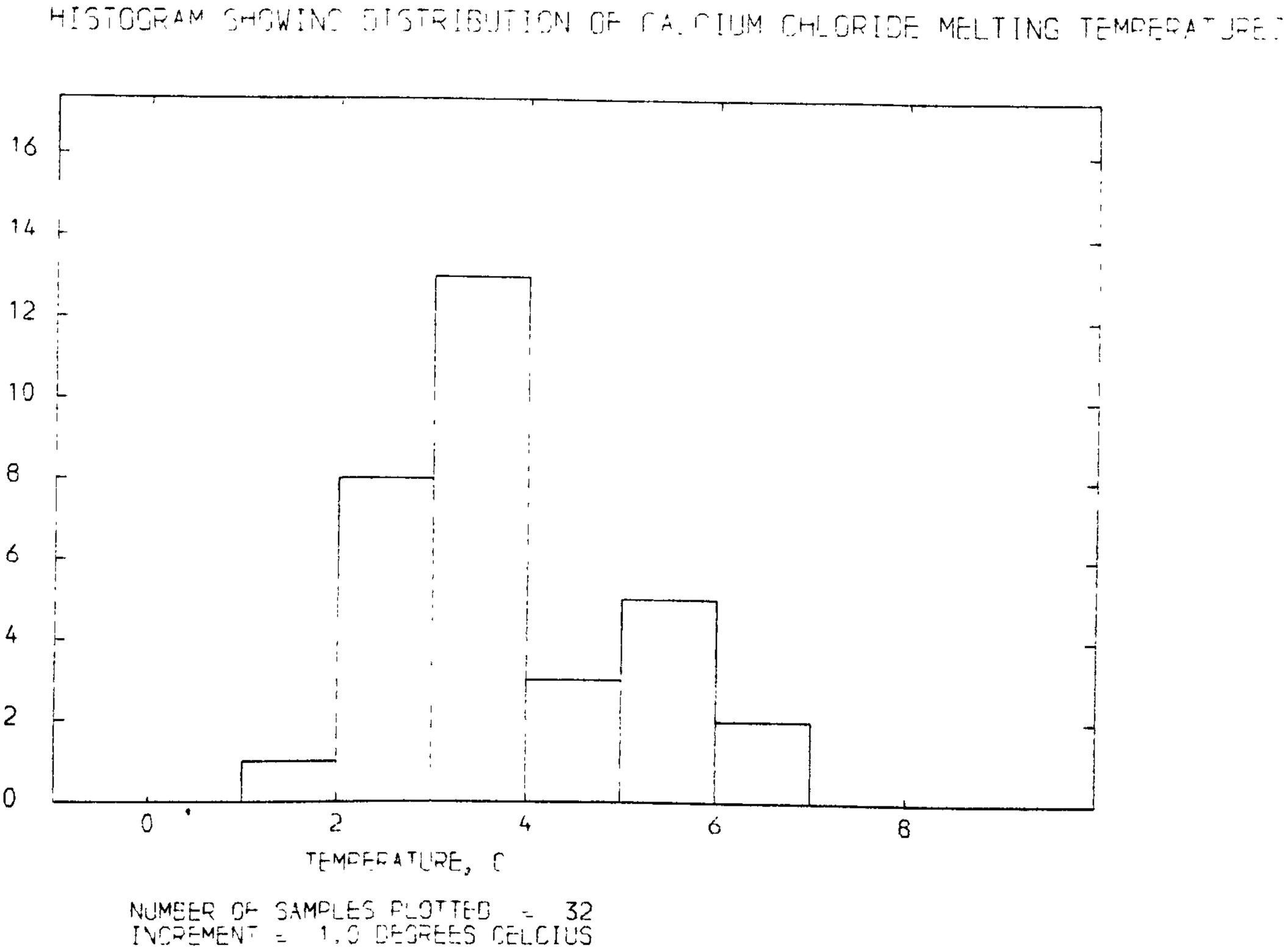
HISTOGRAM SHOWING DISTRIBUTION OF CALCIUM CHLORIDE MELTING TEMPERATURES
16
14
12
10
8
6
4
2
0
0
2
4
6
8
TEMPERATURE, C
NUMBER OF SAMPLES PLOTTED = 32
INCREMENT = 1.0 DEGREES CELCIUS

solutions generally solidify instantaneously and then proceed to recrystallize (Plate 3.4). First melting takes place in the region of -50°C. Anisotropic crystals showing a relatively high relief are usually the only solid phase at -25°C although ice crystals have been observed to form in occasional examples. The positive identification of the phase is problematical. Carbon dioxide clathrate and methane hydrate can be dismissed since no gas bubbles are evolved even on rapid melting. Crushing the inclusion in oil indicates that the internal gas pressure does not exceed 16 atmospheres. Several factors point to the solid being antarcticite ($CaCl_2 .6H_2O$). Firstly, the style of freezing, which has already been mentioned. Secondly, the hydrate always melts above 0.1°C (figure 3.5), although this could be the result of the slowness of the incongruent melting of hydrohalite. A third point is that a concentrated sodium chloride solution usually produces a mass of fine crystals (plate 3.4) of hydrohalite on first melting, usually smaller than those shown in plate 3.4 (Crawford, 1981). Antarcticite crystals are illustrated in plate 3.3. The melting sequence is, therefore, interpreted as first melting at the eutectic E1, with the path progresssing into the antarcticite-liquid field (figure 3.6). Even relatively small concentrations of sodium chloride will produce melting along the antarcticite-hydrohalite cotectic. The occasional observation of daughter halite indicates that the composition lies in or close to the sodium chloride-liquid field at 25°C. Weight percentages of calcium chloride can be estimated from figure 3.7 if only small sodium chloride concentrations are present.

Only a small body of freezing data was gathered for

Plate 3.4

Photomicrographs of hydrohalite

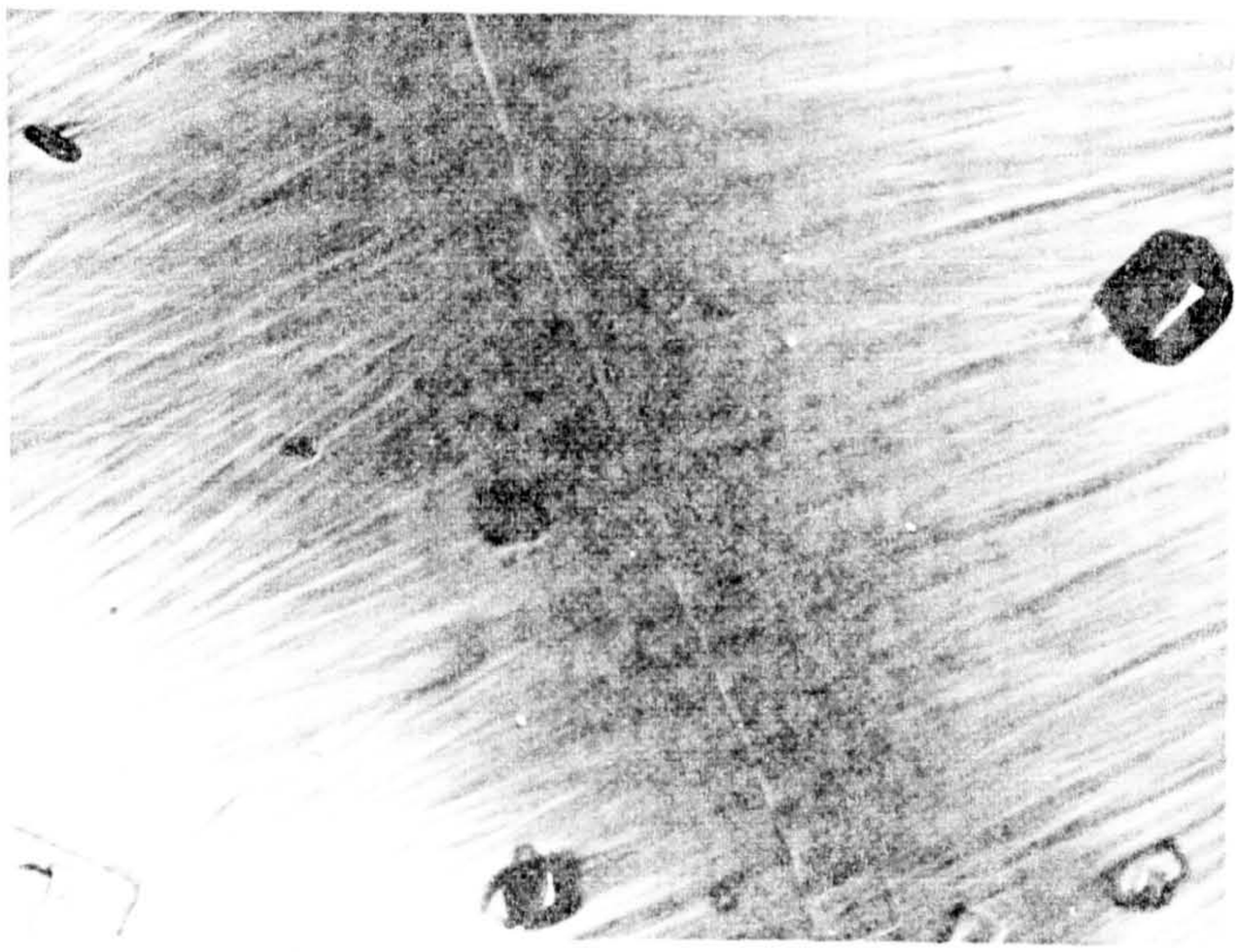

Crystallization of $NaCl.2H_2O$ after freezing at $-50^{\circ}C$.
Field width: 190μm.

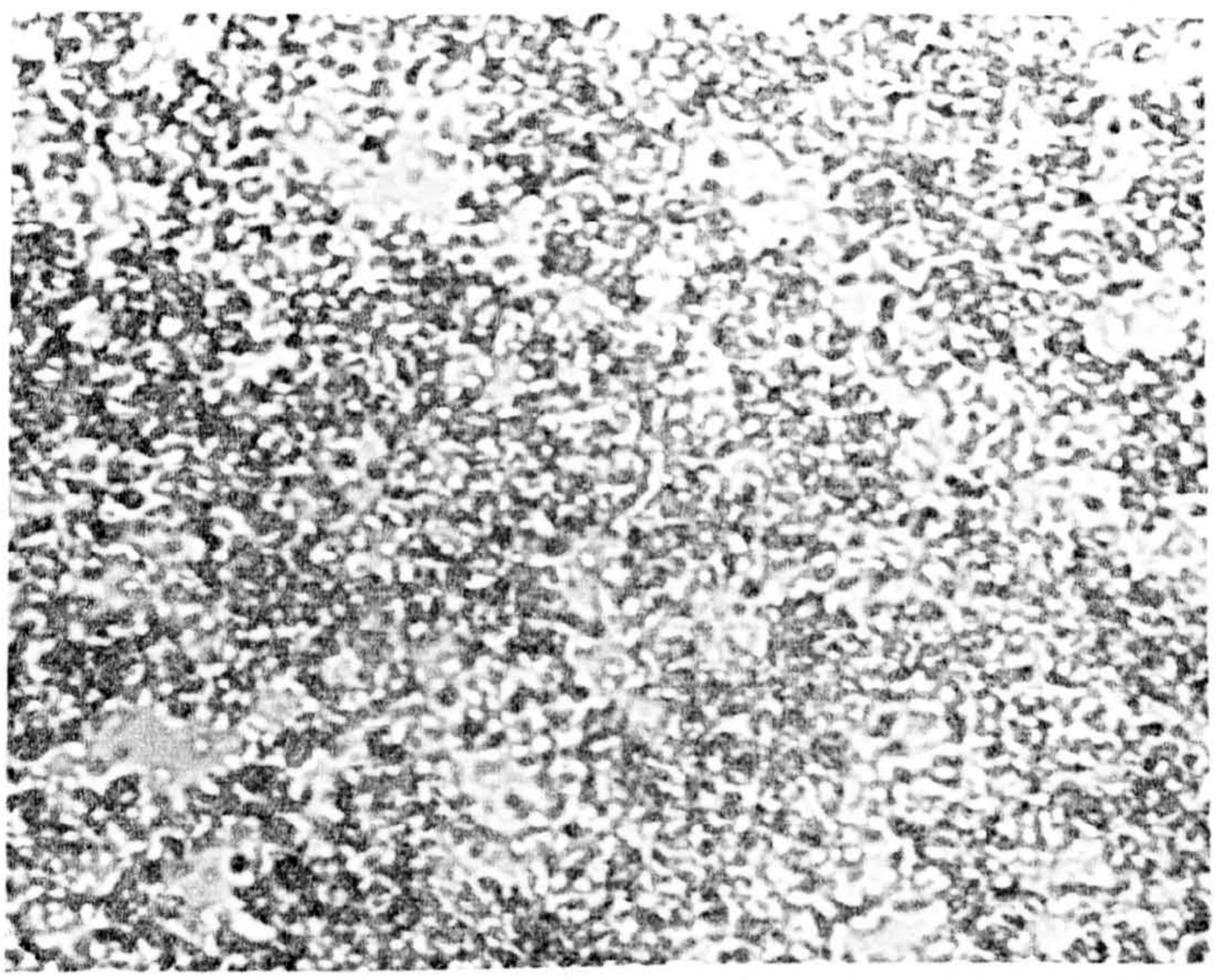

Fine grained hydrohalite formed after first melting at $-20^{\circ}C$
Field width: 140μm

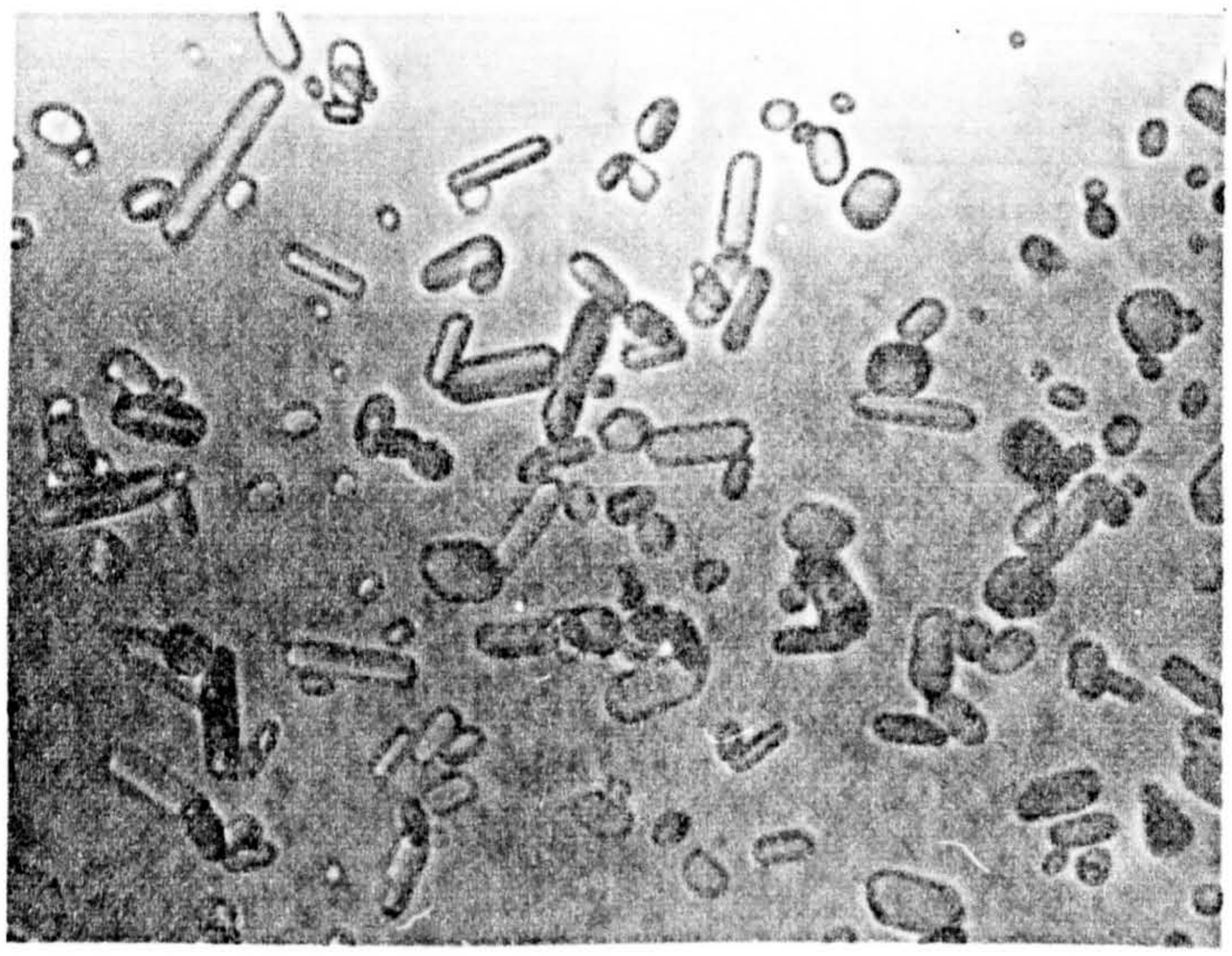

Large monoclinic crystals of hydrohalite at $0^{\circ}C$.
Field width: 108μm.

Figure 3.5

The system $NaCl-H_2O$. The diagram shows the solid phases present in the system as a function of temperature and fluid composition at 1 bar. All phases coexist with vapour. The diagram has been taken from Crawford (1981).

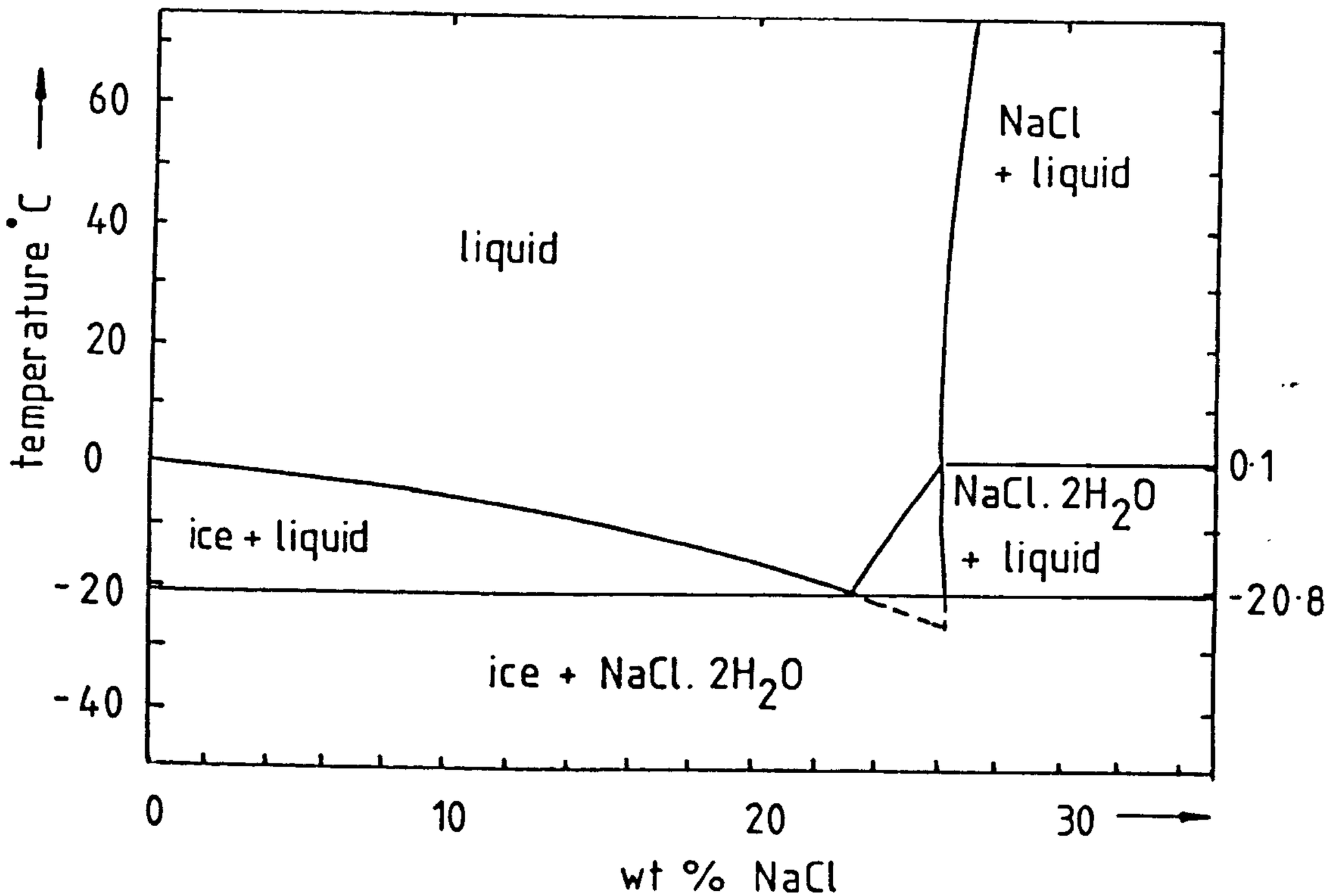

Figure 3.6

The system $NaCl-CaCl_2-H_2O$. Phase boundaries and melting points of solid phase are shown. The diagram has been taken from Konnerup-Madsen (1979).

E1 (eutectic) $-52^{o}C$; P = $-23^{o}C$.

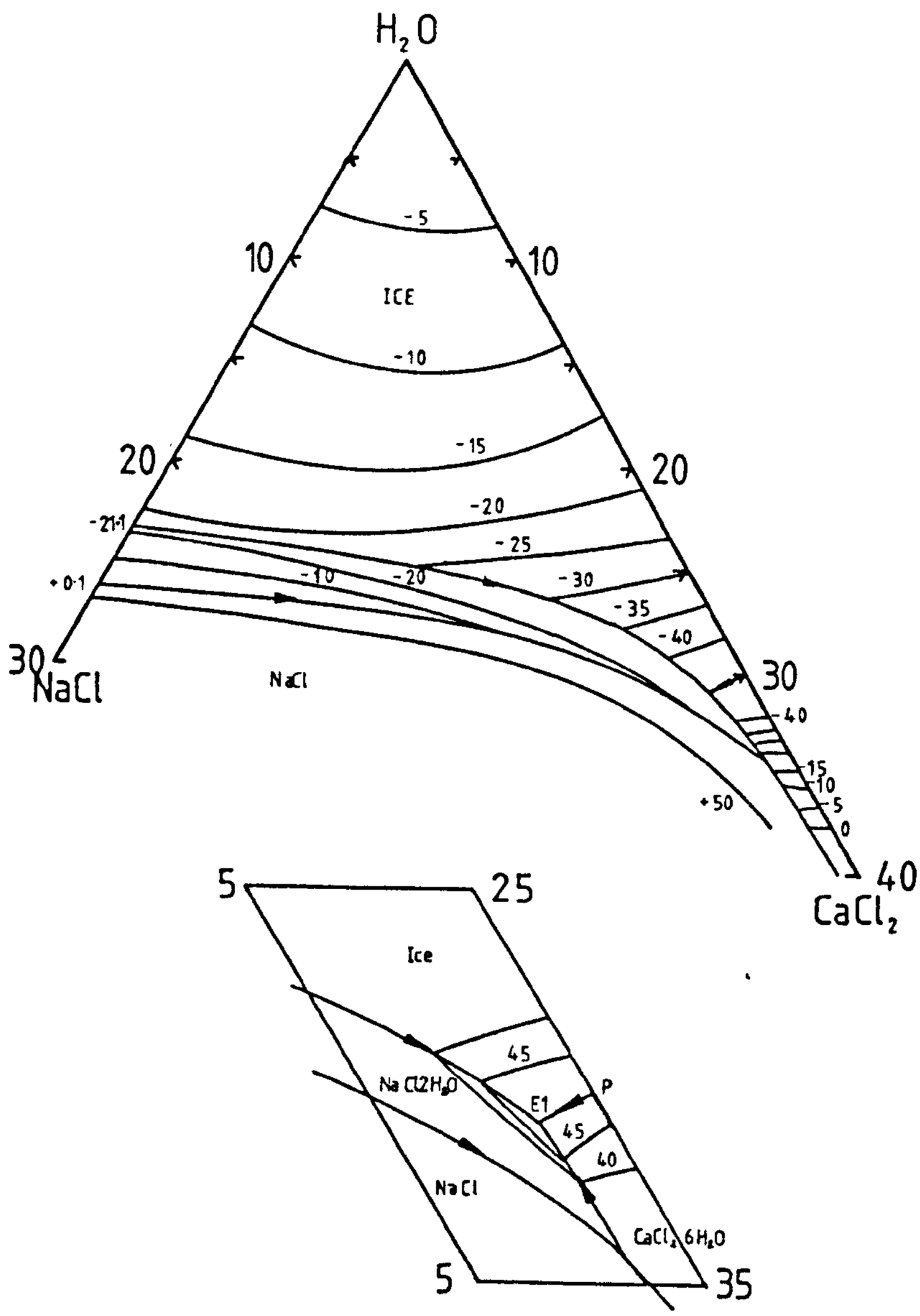

Figure 3.7

The system $CaCl_2$-H_2O at 1 bar, showing the phases present as a function of temperature and composition, with all phases coexisting with a vapour phase. Taken from Crawford (1981).

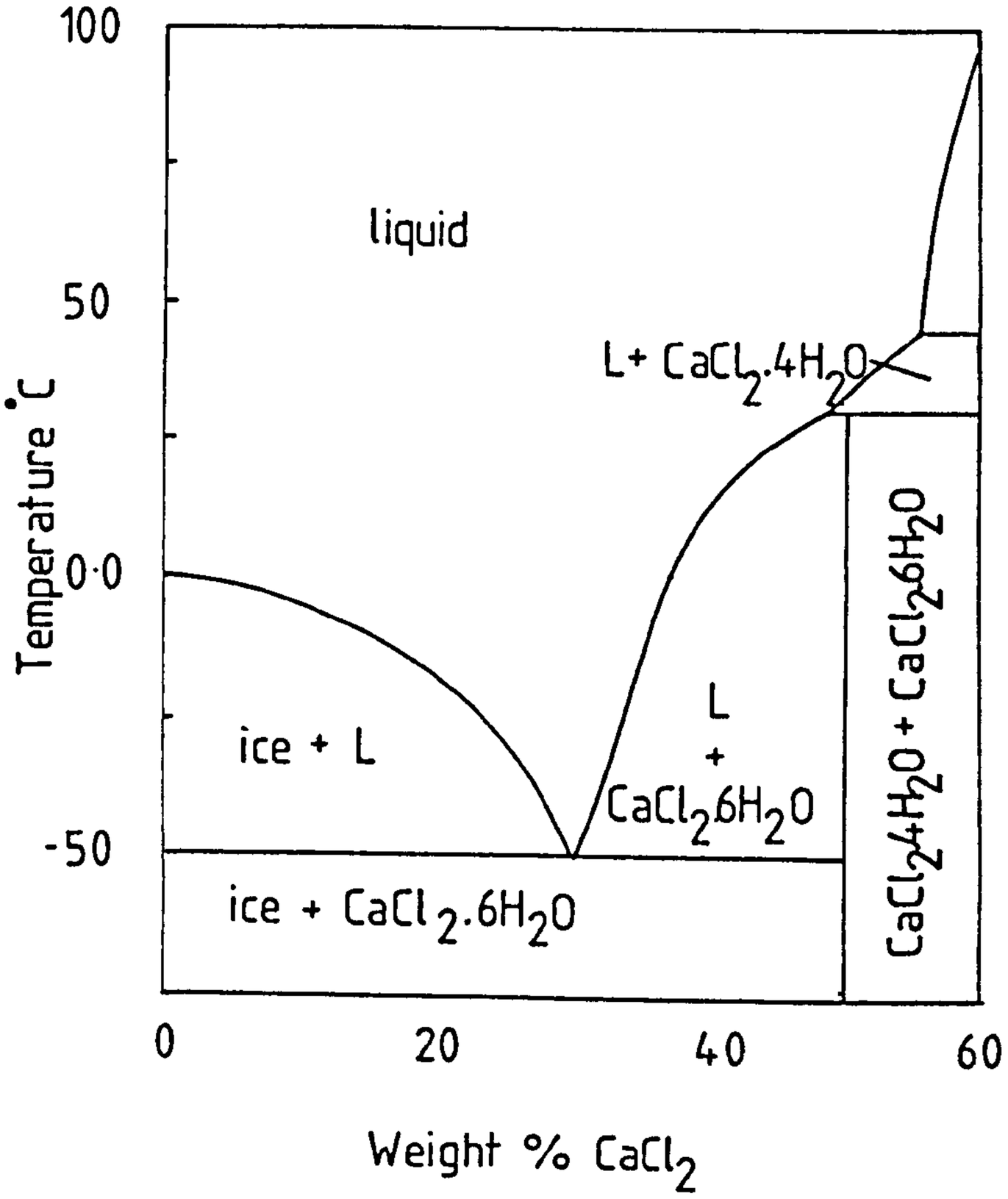

this inclusion type. Antarcticite melting was observed to occur in the range 1.8°C to 6.6°C. The mean and median values are 3.7°C and 3.4°C, and the skewness is Ø.612. The distribution has been plotted in figure 3.4. A f-test indicated the sample means do show some variation, but this could be produced as an effect of the sluggish melting of a hydrated solid, rather than reflecting variation in fluid composition.

3.6.3: TYPE 3 FLUID INCLUSIONS

Mean homogenization temperatures have been obtained for a total of 2Ø samples, excluding Sallet Hole Mine. As noted in section 3.2.1, examples of primary negative crystal inclusions are rare and therefore, all the measurements reported are derived from pseudosecondary or secondary fluid inclusions. Figure 3.8 shows a histogram drawn for a population of 221 homogenization temperature measurements. The distribution is negatively skewed (skewness = -.215). The mean homogenization temperature is 84.1°C $\pm$13.4°C. The median is 84.2°C. The minimum and maximum values determined were 64.9°C and 98.9°C respectively. The highest and lowest mean values for individual samples were 91.6°C and 76.8°C.

The small range in homogenization temperatures for the entire district, and the normal distribution of the population indicates that heat flow was reasonably uniform within the Orefield when mineralization was taking place and that temperature fluctuations occurred but were irregular and not particularly large. It is also interesting to observe

Figure 3.8

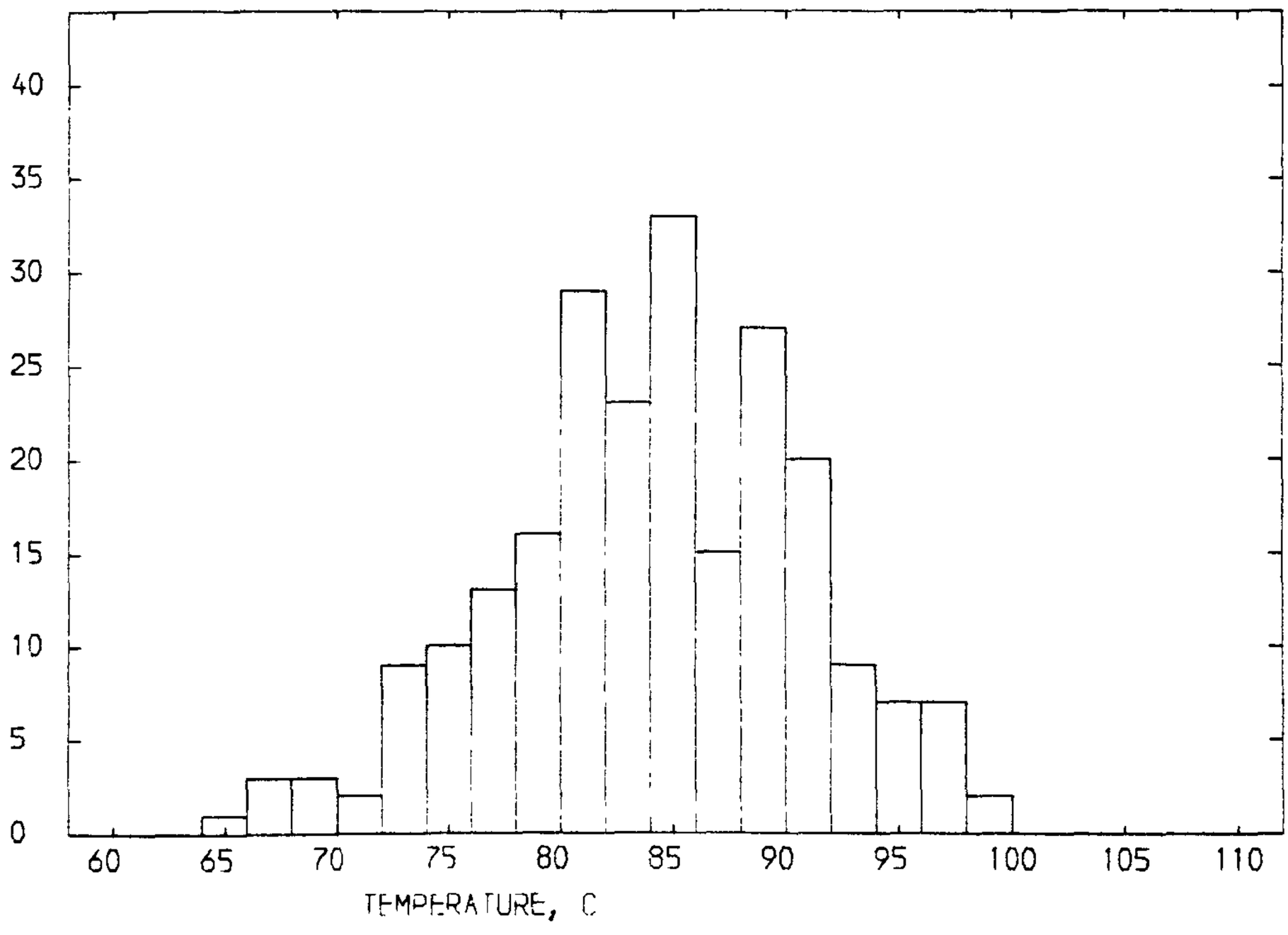
TYPE 3 FLUID INCLUSIONS
HISTOGRAM SHOWING DISTRIBUTION OF HOMOGENIZATION TEMPERATURES
40
35
30
25
20
15
10
5
0
60
65
70
75
80
85
90
95
100
105
110
TEMPERATURE, C
NUMBER OF SAMPLES PLOTTED = 229
INCREMENT = 2.0 DEGREES CELCIUS

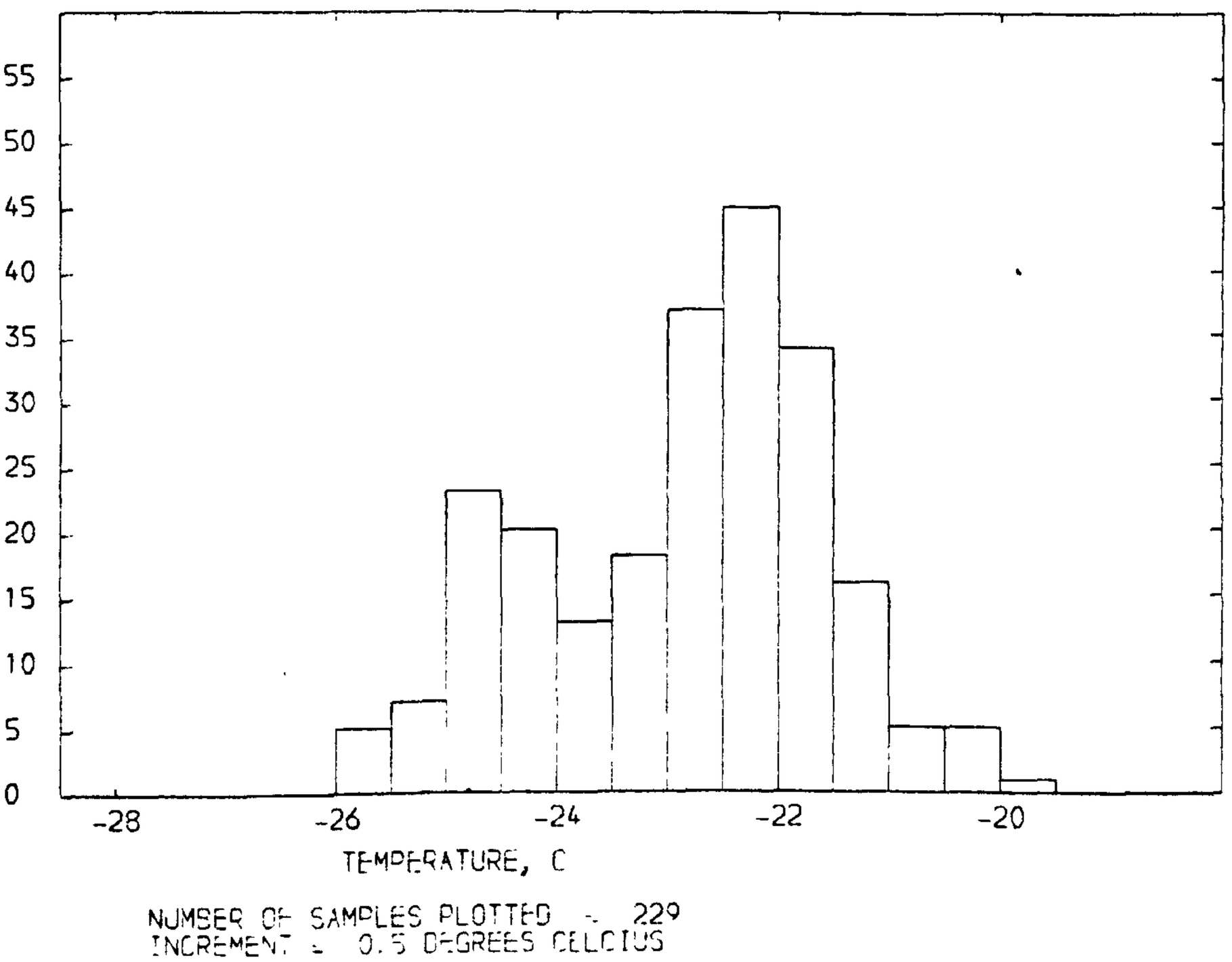
TYPE 3 FLUID INCLUSIONS
HISTOGRAM SHOWING DISTRIBUTION OF FINAL ICE MELTING TEMPERATURES
55
50
45
40
35
30
25
20
15
10
5
0
-28
-26
-24
-22
-20
TEMPERATURE, C
NUMBER OF SAMPLES PLOTTED = 229
INCREMENT = 0.5 DEGREES CELCIUS

that the standard deviation of the entire population is little different from the standard deviation of any individual sample. The standard deviation of individual samples ranged from 2.2^{o} to 10.0^{o}. Of the 20 samples, two were found not to have normally distributed homogenization temperatures at a 5% level of significance. The temperature ranges showed no correlation with mean homogenization temperatures.

Freezing point determinations were made on the fluid inclusions already used for homogenization temperature measurements. The inclusions must be cooled to temperatures in the range, $-65^{o}C$ to $-85^{o}C$ to produce solidification of the brine. If rates of cooling were particularly slow, then solidification may be achieved at higher temperatures. In common with the type 2 inclusions, the inclusion is initially transparent after freezing. However, recrystallization of the solid quickly proceeds and the inclusion assumes an opaque, pale brown colouration. First melting is often difficult to observe. Qualitative analysis indicates that sodium, calcium and magnesium are present within the fluid so the eutectic for the system is approximately $-53^{o}C$. On warming, melting does not take place gradually. Nucleation of the vapour phase often does not occur until the inclusion possesses a high liquid-ice ratio. This point is usually reached at temperatures in excess of $-30^{o}C$. At this stage vapour, liquid, ice and hydrohalite can be identified. Hydrohalite can be recognized by its high refractive index (R.I.= 1.416) and its anisotropy (Crawford, 1981). The hydrohalite almost invariably melts before the ice. The difference may range from a few tenths of a degree to a few degrees. An occasional

example of hydrohalite melting after the ice is probably the result of metastability. The ternary system $NaCl-CaCl_2-H_2O$ (figure 3.6) can be used to trace the melting sequence. Melting progresses from the eutectic E1, along the hydrohalite-ice cotectic until the point is reached where the hydrohalite disappears and the system enters the ice and liquid field. A projection from the 100% H_2O composition on to the point where the melting path moves away from the hydrohalite-ice cotectic, will pass through a point which represents the fluid composition. Using the contours to plot the final ice melting temperature, a $NaCl/CaCl_2$ ratio may be determined for the solution (Crawford, 1981). Some uncertainty exists in using this method since plotting of isotherms on to the cotectic is critical and inaccuracy can lead to significant errors. Secondly, hydrohalite may persist metastably, thus giving an erroneously high ratio. The melting sequence described above is illustrated in plate 3.5. The inclusion shown has leaked and therefore, the degree of filling is lower than is normal.

The distribution of final ice melting temperatures (figure 3.8) for a population of 221 fluid inclusions is slightly negatively skewed (Skewness = -0.32). The mean, median and range of the population is $-22.9^{o}C$, -22.7^{o}, $\pm 2.6^{o}C$. The maximum and minimum final melting temperatures recorded are $-20^{o}C$ and $-26^{o}C$ respectively. Four of the 20 samples tested could not be shown to be normally distributed at a 5% level of significance. Assuming that the samples are representative, one may infer that there is some regional salinity variation. A plot of homogenization temperature against final ice melting temperature yields a diffuse

Plate 3.5

A typical type 3 fluid inclusion melting sequence

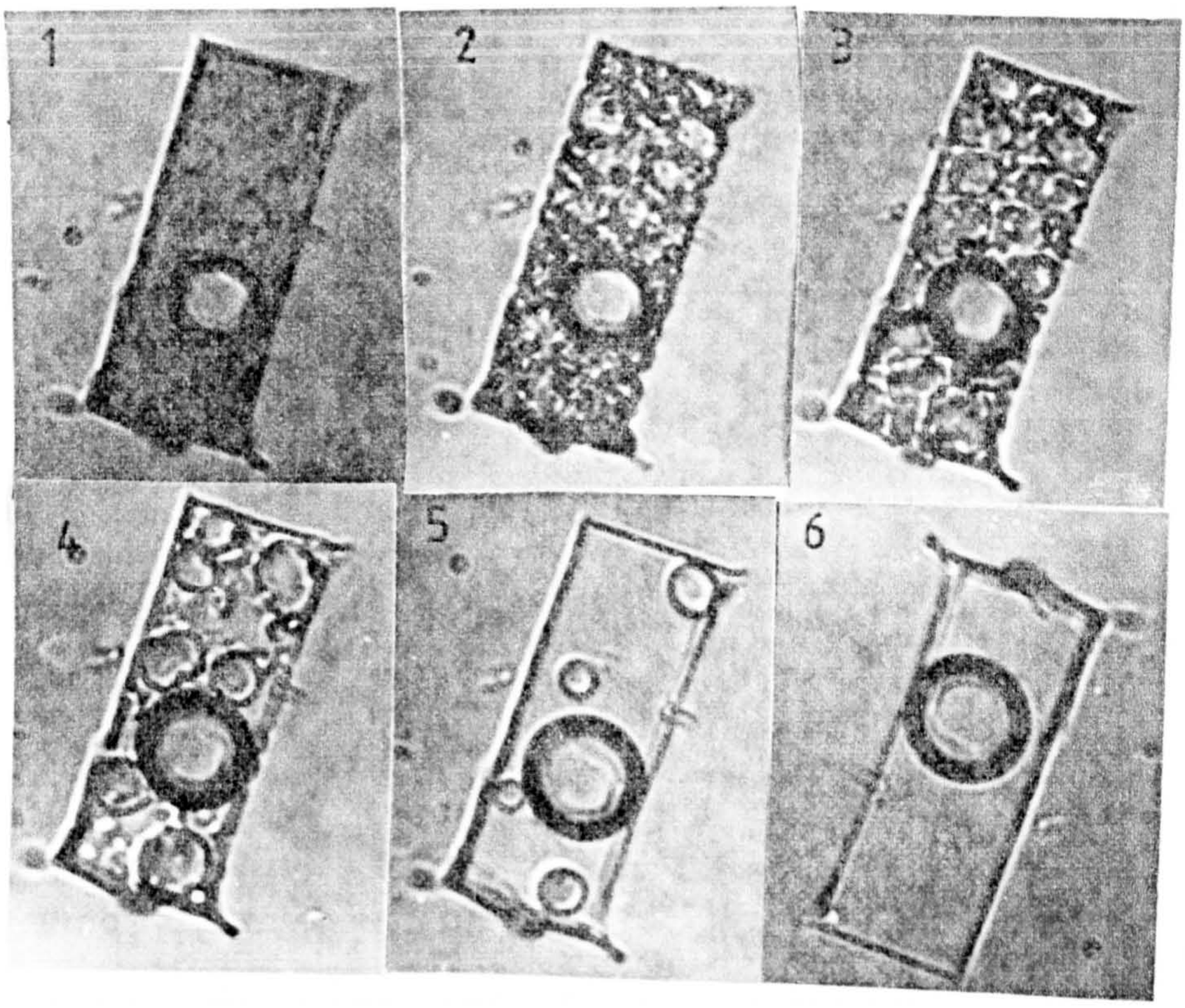

Field width: 60µm.

(1) Recrystallization of the metastable ice formed on initial freezing.

(2) Liquid forming after first melting at -45°C.

(3) Hydohalite and ice present at -30°C.

(4) Large low relief ice crystals with fine grained hydrohalite crystals at -22.3°C.

(5) Final hydrohalite melting at -21.7°C.

(6) Final ice melting at -20°C.

(leakage of the inclusion had occurred as a result of repeated heating and freezing and therefore, the degree of filling is low)

Figure 3.9

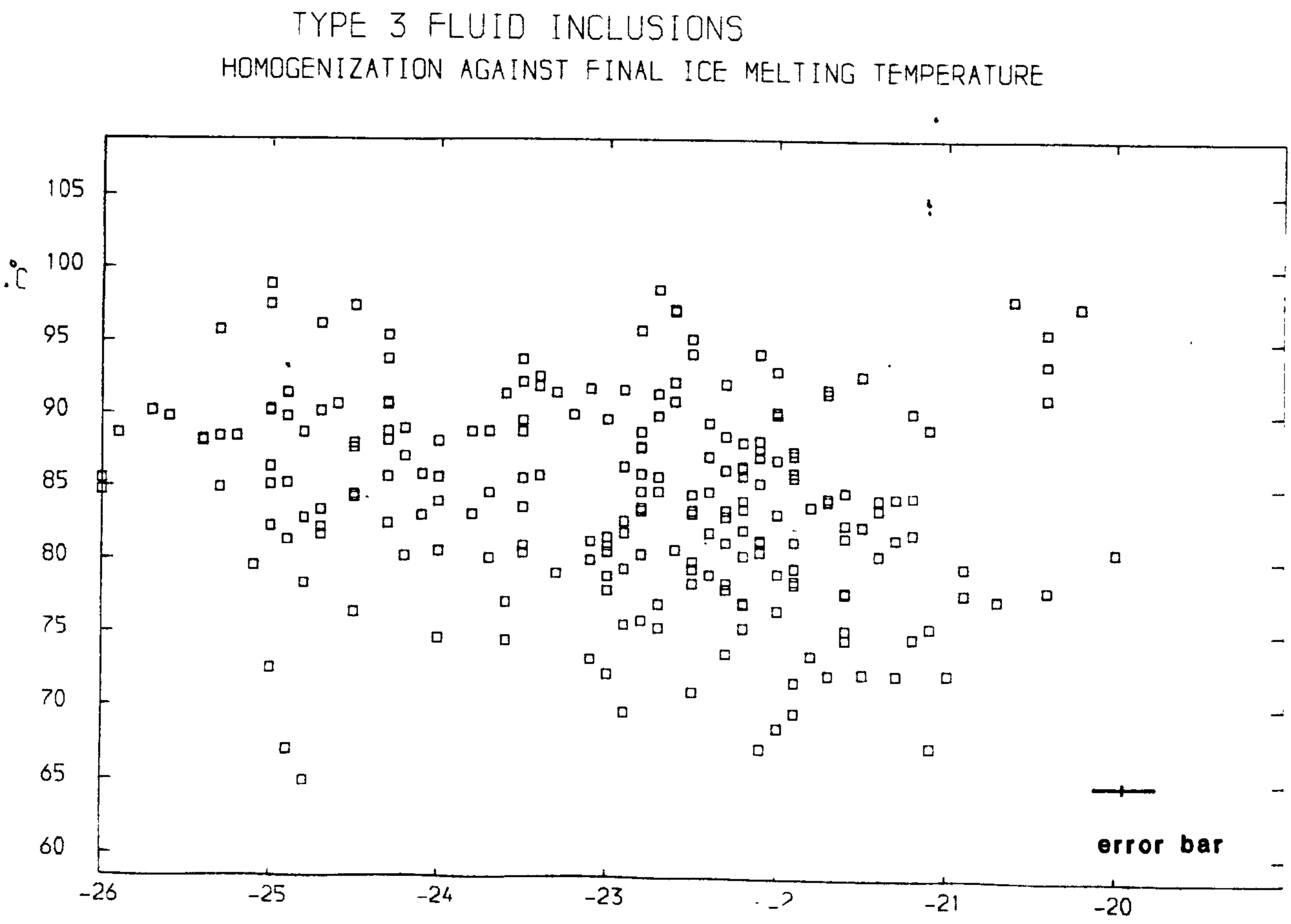

The diagram shows a plot of homogenization temperature against final ice melting temperature for the type 3 ore fluid. The diagram illustrates the lack of any correlation between fluid temperature and salinity.

pattern (figure 3.9) Again temperature appears to have had little control on salinity. Patterns drawn for individual samples show similar distributions, with no evidence for localized mixing.

3.6.4: TYPE 4 FLUID INCLUSIONS

Samples from 20 localities were found to contain sufficient type 4 fluid inclusions to establish representative mean homogenization and final ice melting temperatures. As stated in section 3.2.1, there is a dearth of easily identifiable, negative crystal fluid inclusions.

The shape of the upper histogram of figure 3.10 suggests that the population of 218 measurements is a normal one. However, the population is positively skewed (Skewness = 0.497). The range of values is slightly greater than shown in the type 3 population. The maximum and minimum values are 106^{o}C and 63.4^{o}C respectively. The homogenization temperature median and mean for a the selected population is 84.3^{o} and 84.4^{o}C $\pm$11.2^{o}C. The calculated temperature range for this group is even more restricted than the type 3 range. The standard deviation of the population is not significantly greater than that of any individual sample. Therefore, strong regional temperature variation associated with this phase of mineralization can be dismissed.

Statistical treatment of the 20 samples showed that the there was no correlation between the magnitude of homogenization temperatures and their corresponding ranges. Standard deviations ranged from 1.7^{0} to 6.1^{0}. Nineteen of the twenty

samples were found to be normally distributed at a 5% level of significance.

Freezing point determinations were made for a similar number of fluid inclusions. The inclusions freeze at a higher temperature than the type 3 inclusions, an observation which allows an immediate distinction to be drawn between type 3 and type 4 inclusions. The temperature at which this occurs lies in the range $-55^{o}C$-$65^{o}C$. If the vapour phase fails to renucleate after heating, the freezing temperature may be increased considerably. Again crystallization of the solid which forms initially on freezing, will proceed below the eutectic temperature ($-53^{o}C$).

Variation in the dissolved salt composition of the inclusion fluids is indicated by the differing stages at which the melting path moves into the ice-liquid field. The disappearance of hydrohalite may occur in the range $-40^{o}C$ to $-25^{o}C$. Melting normally takes place at the lower end of the temperature range, suggesting a high $CaCl_2/NaCl$ ratio. Variation in the $CaCl_2/NaCl$ ratio could be produced by variation in brine chemistry or by the mixing of types 3 and 4 inclusion fluids as a result of the processes of necking down and inclusion migration. If changing $CaCl_2/NaCl$ ratios in the brine itself produced this phenomena, it is difficult to explain the remarkably uniform final ice melting temperatures.

The distribution of final ice melting temperatures shown in figure 3.10. The population of final ice melting temperatures is positively skewed (Skewness = 0.049). A mean melting temperature for the population was determined as $-17.5^{o}C$ $\pm 1.8^{o}C$. The median is $-17.5^{o}C$. This range is

Plate 3.6

(a) A planar group of secondary fluid inclusions. Vapour bubbles are often seen to be absent in the smaller fluid inclusions.

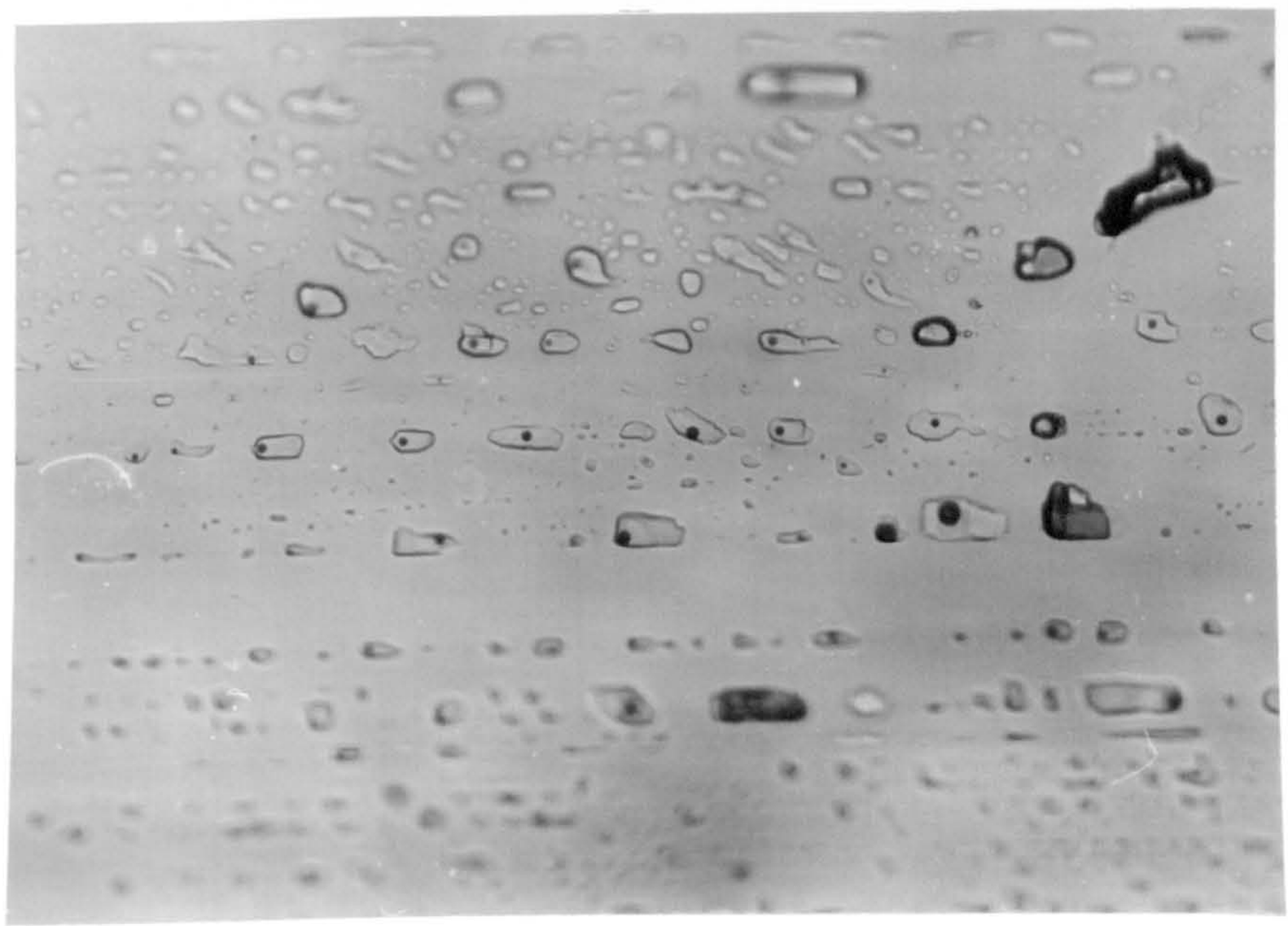

Field width: 510μm

(b) Secondary fluid inclusions showing evidence of the processes of necking down and coalescence. Again, smaller inclusions are usually vapourless

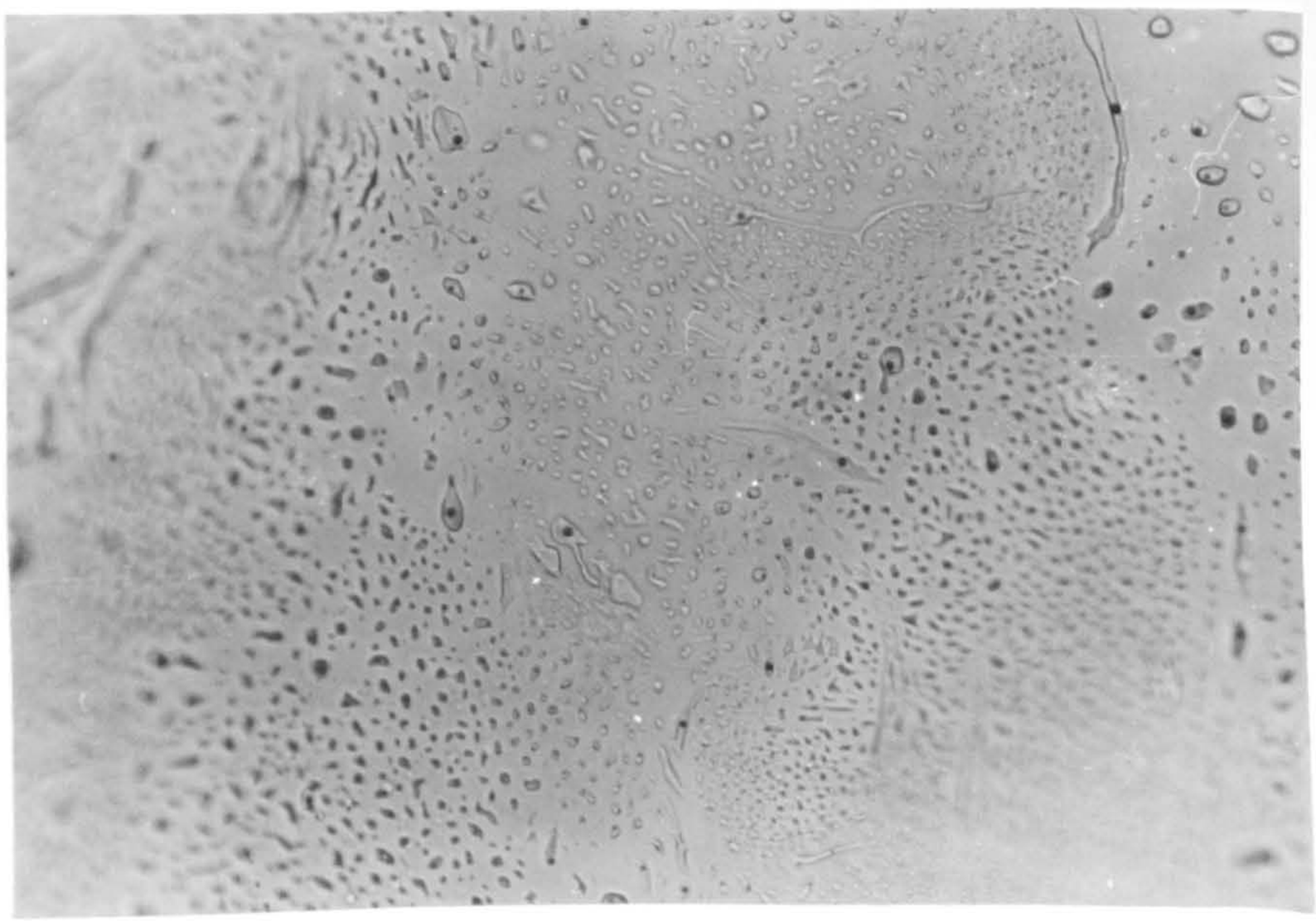

Field width: 800μm

Figure 3.10

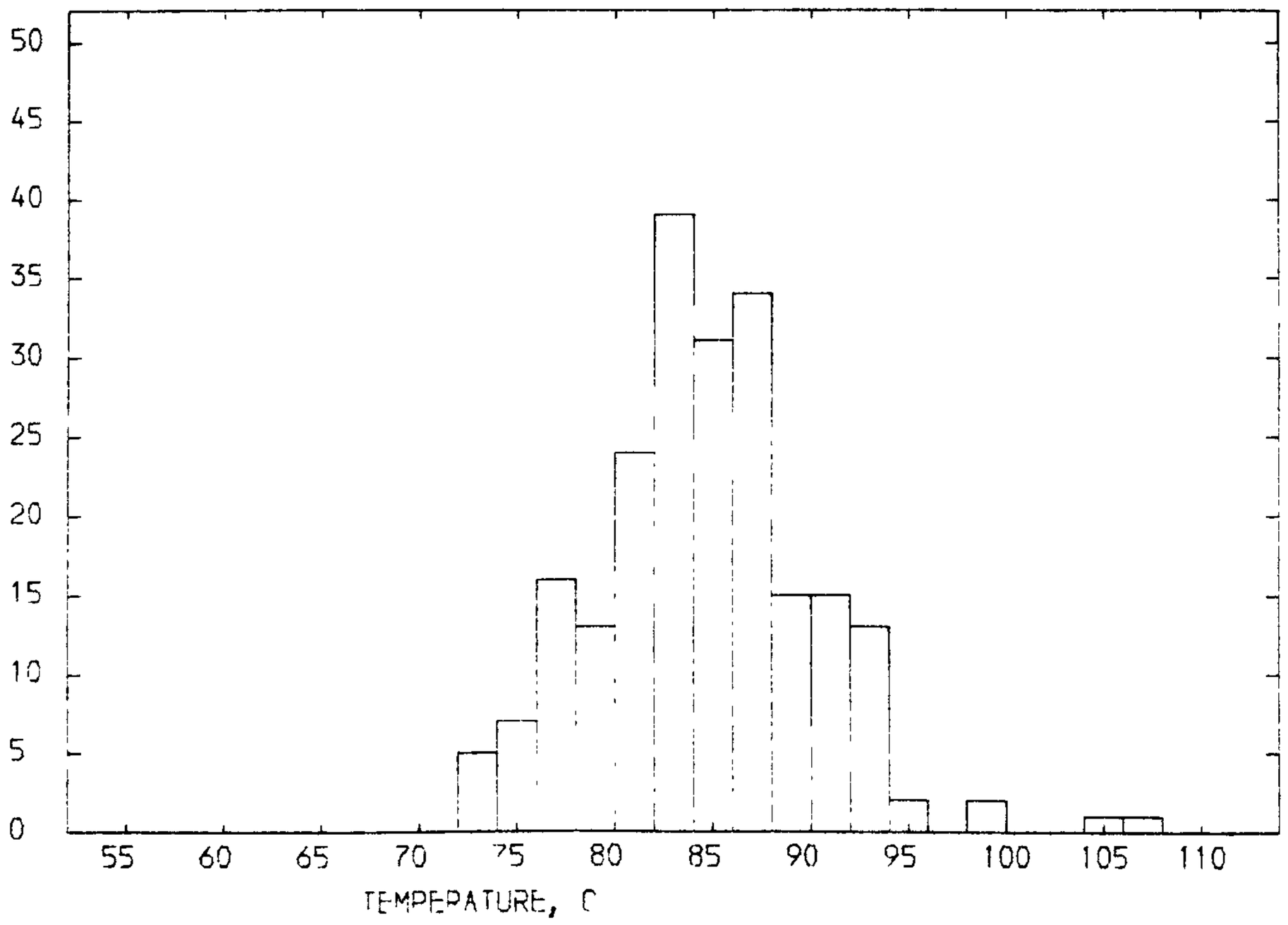
TYPE 4 FLUID INCLUSIONS
HISTOGRAM SHOWING DISTRIBUTION OF HOMOGENIZATION TEMPERATURES
50
45
40
35
30
25
20
15
10
5
0
55
60
65
70
75
80
85
90
95
100
105
110
TEMPERATURE, C
NUMBER OF SAMPLES PLOTTED = 219
INCREMENT = 2.0 DEGREES CELCIUS

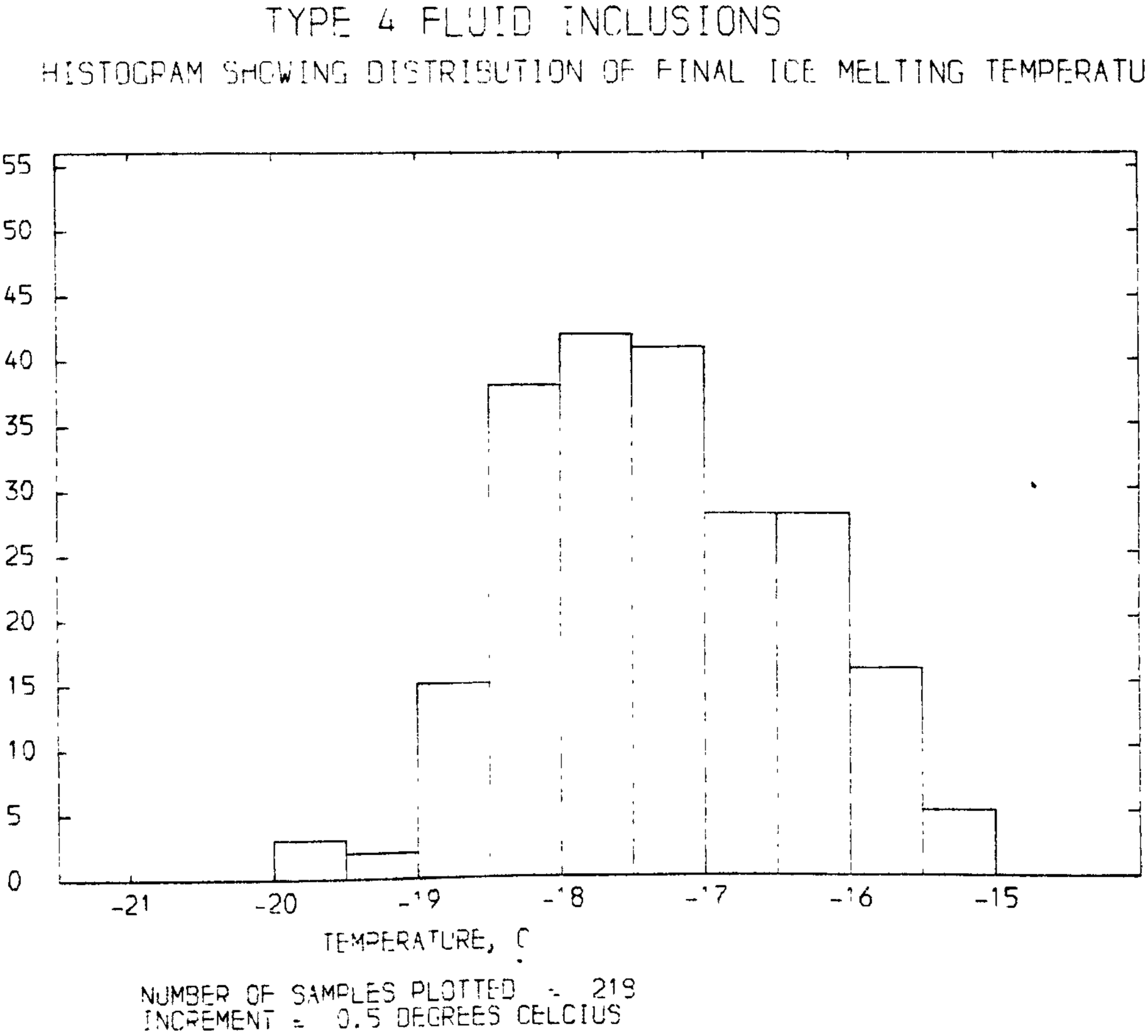
TYPE 4 FLUID INCLUSIONS
HISTOGRAM SHOWING DISTRIBUTION OF FINAL ICE MELTING TEMPERATURES
55
50
45
40
35
30
25
20
15
10
5
0
-21
-20
-19
-18
-17
-16
-15
TEMPERATURE, C
NUMBER OF SAMPLES PLOTTED = 219
INCREMENT = 0.5 DEGREES CELCIUS

significantly less than that determined for the type 3 inclusions. Maximum and minimum final ice melting temperatures were -19.5^{o}C and -15.4^{o}C respectively. The standard deviation of the 2Ø selected samples ranged from Ø.3 to Ø.9. The melting point measurements were all found to be normally distributed at a 5% level of significance. No correlation could be determined between final ice melting temperatures and homogenization temperatures. The diffuse pattern formed on plotting homogenization temperature against final ice melting temperature is shown in figure 3.11.

3.6.5: TYPE 5 FLUID INCLUSIONS

Type 5 fluid inclusions were observed in two samples of fluorite from Treak Cliff Cavern and Deep rake, Sallet Hole Mine. The mean homogenization temperature and final ice melting temperature determined from eight inclusions was 66.3$\pm$4^{o}C and -39.4$\pm$1.8^{o}C respectively for the sample from Sallet Hole Mine and 68.3$\pm$11^{o}C and -38.4$\pm$Ø.2^{o}C for the sample from Treak Cliff. If calcium and sodium chlorides are the major dissolved salts, then their concentration ranges can be estimated as 2.3-2.5m $CaCl_2$ and Ø-Ø.34m NaCl.

Figure 3.11

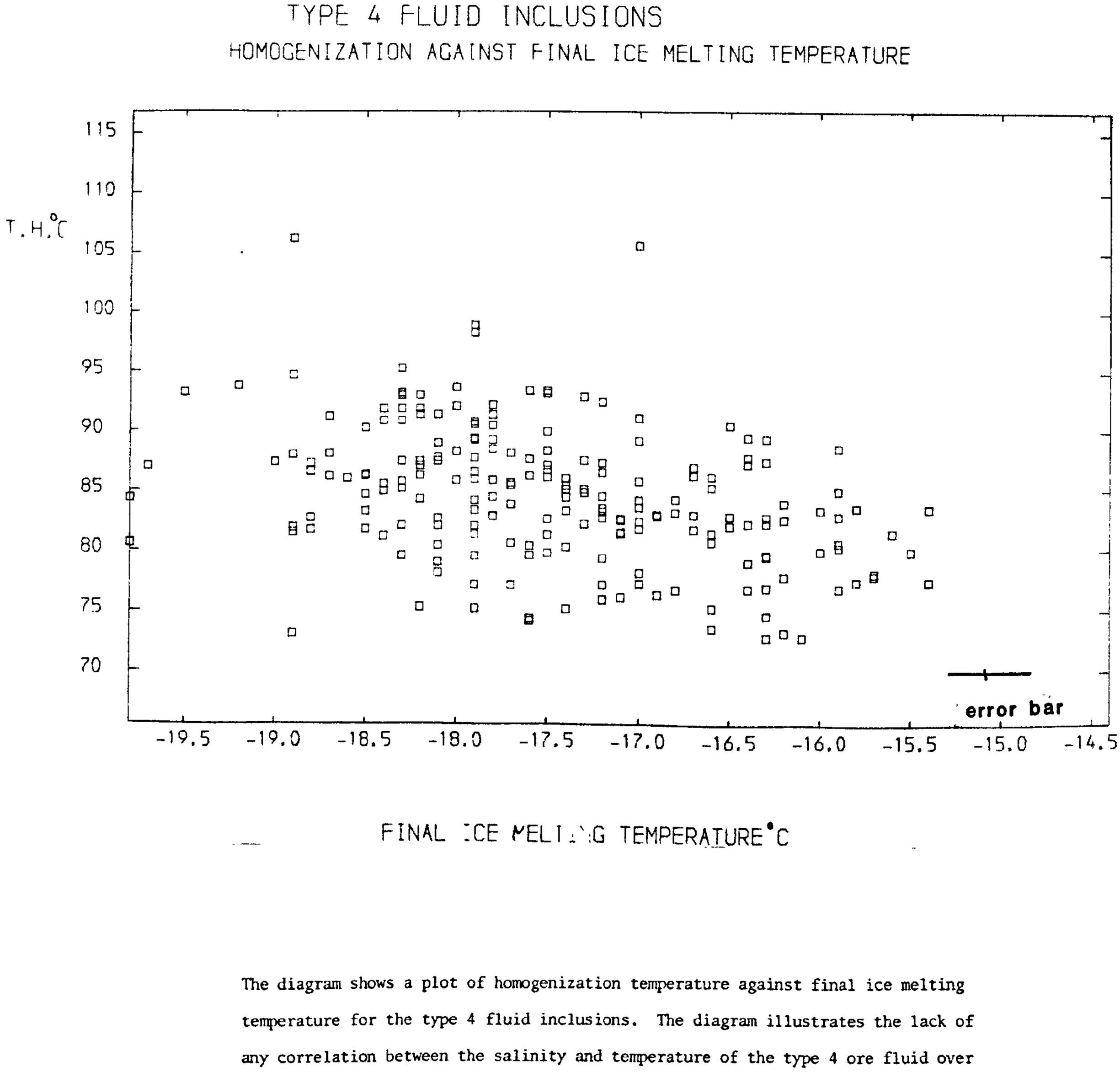

The diagram shows a plot of homogenization temperature against final ice melting temperature for the type 4 fluid inclusions. The diagram illustrates the lack of any correlation between the salinity and temperature of the type 4 ore fluid over the entire orefield.

3.7: THERMOMETRIC STUDY OF THE SALLET HOLE MINE

Sallet Hole Mine is the only extensive working fluorite mine in the district, and as such it makes a useful locality for studying longitudinal, vertical, and transverse thermal gradients that existed during the hydrothermal events as indicated by homogenization temperatures. Salinity variation as represented by changes in the final ice melting temperature was also investigated. One hundred and thirty five paired thermometric measurements were made on samples taken from five slits in the mine. (A slit is a cutting off a level into the vein.) A transverse section of High Rake was sampled in a slit in the western end of the mine and similar sections in Deep Rake on sub-level 1 and on sub-level 2. The distance between the High Rake and Deep Rake sample sites is approximately 900m.

At the slit in High Rake, the vein is 2m wide. The north wall is composed of altered volcanics, downthrown to the south by 4m to 5m. The south wall is composed of fluoritized limestone lying on top of the the volcanics. Plots of homogenization temperature against final ice melting temperature (figure 3.12) for the three samples taken shows a predominance of type 4 inclusions in fluorite from the north wall of the vein. This suggests that either the vein is composed of two generations of fluorite with the later phase 4 material having being deposited on the north wall of the rake or, alternatively, extensive fracturing on the north side of a completely filled vein gave better access to later hydrothermal activity. Hence the greater ease of formation of

secondary fluid inclusions within fluorite. This trend is is also seen in the traverse of Deep Rake (figure 3.13) at slit "B". Two slits were sampled on sub-level 2 and one on sub-level 1. The vein dips vertically and is composed of loosely held fluorite with subordinate baryte between largely unaltered limestone walls. One slit sampled on sub-level 1, lying 26m above sub-level 2 was sampled at the south wall, and 1m and 2.2m into the vein. All the samples were taken from the main vein filling and not from isolated vughs containing large crystals.

3.7.1: TYPE 3 FLUID INCLUSIONS

3.7.1.1: TRANSVERSE VARIATION IN SALINITY AND HOMOGENIZATION TEMPERATURES FOR TYPE 3 FLUID INCLUSIONS

Enough data is available to test transverse variation in filling and last melting temperatures of the type 3 fluid inclusions found in fluorite from the High Rake vein traverse Measured means, standard deviations and medians are given in table 3.1. Comparison of the calculated f-statistic with the critical values given by Davis (1973), suggests that there is no difference in the means of the homogenization and final ice melting temperatures on the vein traverse at a 5% level of significance. Therefore, the composition and temperature of the hydrothermal fluid remained the same across the vein during the formation of the fluid inclusions.

Figure 3.12

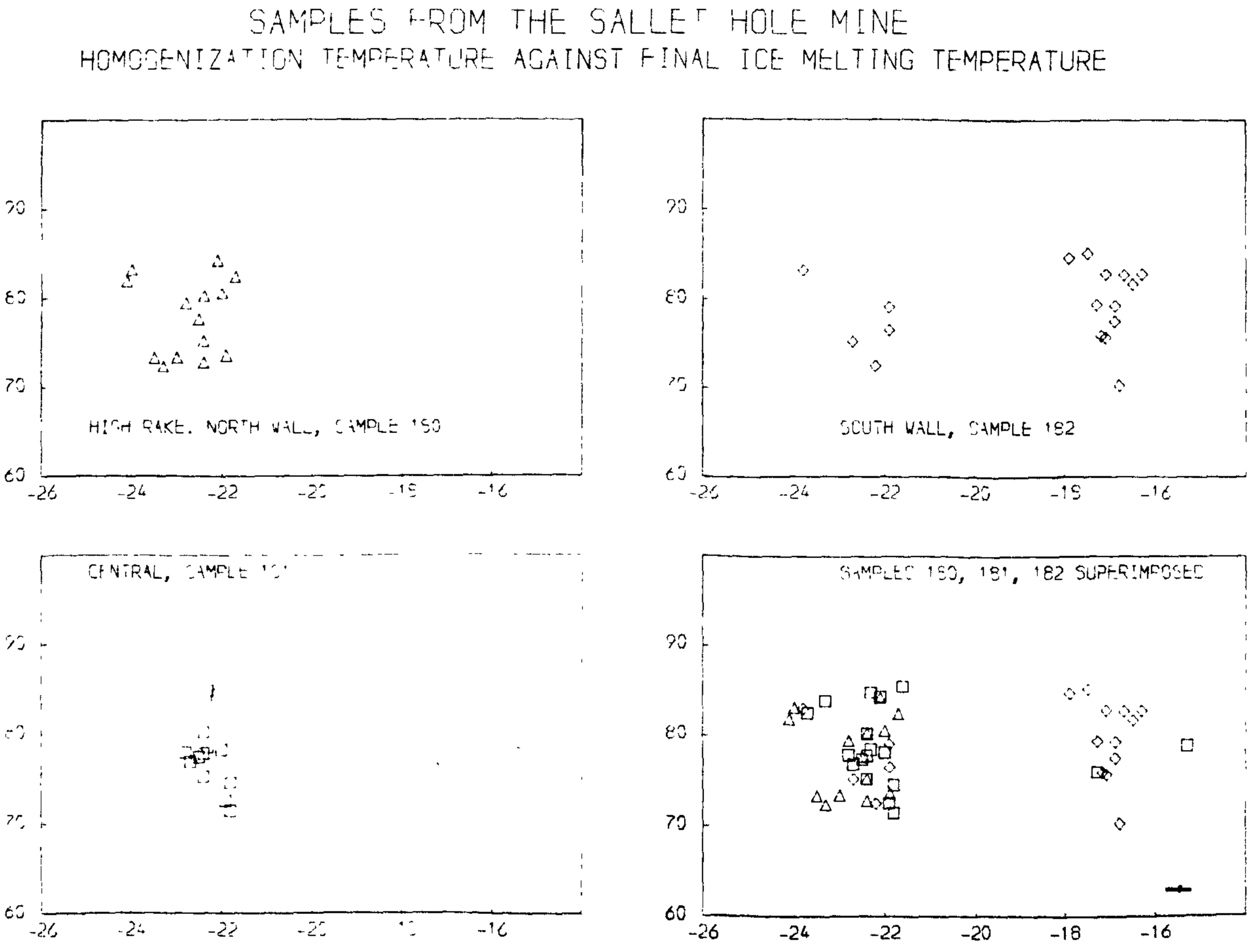

The diagram shows a series of plots of homogenization temperature against final ice melting temperature for three samples of fluorite from a section of the High Rake Vein at the western end of the Sallet Hole Mine.

Figure 3.13

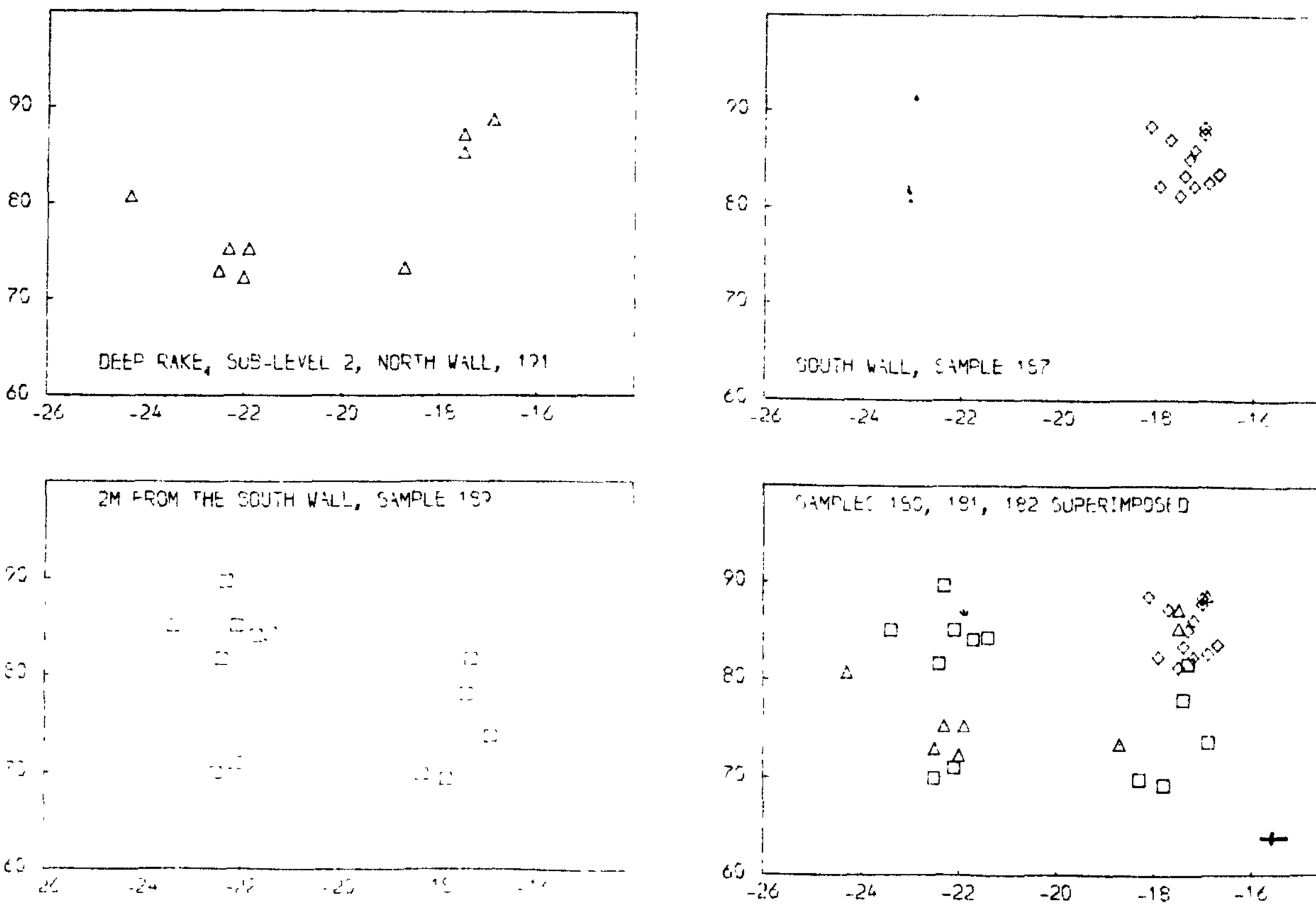

The diagram shows a series of plots of homogenization temperature against final ice melting temperature for three samples of fluorite taken from a traverse of Deep Rake at the northern end of the Sallet Hole Mine.

TABLE 3.1

COMPARISON OF MEANS, MEDIANS AND STANDARD DEVIATIONS OF FILLING AND FINAL ICE MELTING TEMPERATURES OF FLUORITE SAMPLES FROM A TRAVERSE OF HIGH RAKE.

(a) Homogenization temperatures ^{o}C.

	North	Central	South
Number	11	15	5
Mean	78.1	79.Ø	77.3
σ	4.4	4.7	4.1
Median	79.5	77.9	76.5

f-statistic = Ø.31
degrees of freedom among samples = 2
degrees of freedom between replicates = 28

(b) Final ice melting temperatures ^{o}C.

	North	Central	South
Number	11	15	5
Mean	-23.1	-22.9	-22.8
σ	Ø.7	Ø.5	Ø.4
Median	-22.9	-22.9	-22.7

f-statistic = Ø.4Ø

3.7.1.2: LONGITUDINAL VARIATION

The total population of 29 measurements of homogenization temperatures and final ice melting temperatures from fluorite samples from the High Rake slit "A" are compared with a similar population from slit "B" in table 3.2.

TABLE 3.2

COMPARISON OF HOMOGENIZATION AND FINAL ICE MELTING TEMPERATURES IN SAMPLES FROM SLIT "A" AND SLIT "B".

(a) Homogenization temperatures ^{o}C.

	HIGH RAKE "A"	DEEP RAKE "B"
Number	31	8
Mean	78.4	81.4
σ	4.4	7.1
Median	77.9	84.2

f-statistic = 2.23
degrees of freedom among samples = 1
degrees of freedom between replicates = 37

(b) Final ice melting temperatures ^{o}C.

	HIGH RAKE "A"	DEEP RAKE "B"
Number	31	8
Mean	-23.0	-22.9
σ	0.55	0.50
Median	-22.9	-22.8

f-statistic = 0.16

Again, there is little evidence of lateral thermal or salinity variation on the High Rake-Deep Rake vein system of Longstone Edge. The uniformity of the data also suggests a very limited degree of heat loss to the vein walls.

TABLE 3.3

VARIATION IN HOMOGENIZATION AND FINAL ICE MELTING TEMPERATURES IN FLUORITE SAMPLES FROM SLIT "D".

(a) Homogenization temperatures°C.

north wall	0.0m	1.0m	2.0m	3.0m
Number	9	10	10	
Mean	78.5	82.9	80.8	
σ	6.1	4.9	6.7	
Median	81.4	84.5	82.0	

f-statistic = 1.31
degrees of freedom among samples = 2
degrees of freedom between replicates = 26

(b) Final ice meltiing temperatures°C.

north wall	0.0	1.0	2.0	3.0m
Mean	-18.3	-18.2	-17.5	
σ	0.7	0.66	0.31	
Median	-18.3	-18.2	-17.3	

f-statistic = 6.4

3.7.2: TYPE 4 INCLUSIONS

3.7.2.1: TRANSVERSE VARIATION IN HOMOGENIZATION TEMPERATURE

Three samples from slit "D" (table 3.3) in Deep Rake provided enough homogenization temperature data to allow statistical testing of transverse homogenization temperature measurements. Analysis of variance indicates that the homogenization temperatures are similar in type 4 fluid inclusions taken from the vein traverse. The sample from the

FIGURE 3.14: CROSS SECTION OF SALLET HOLE MINE.

Homogenization temperature means (μ), medians (m) and standard deviations (σ) are shown for type 4 inclusions at slits A, B, C, and D.

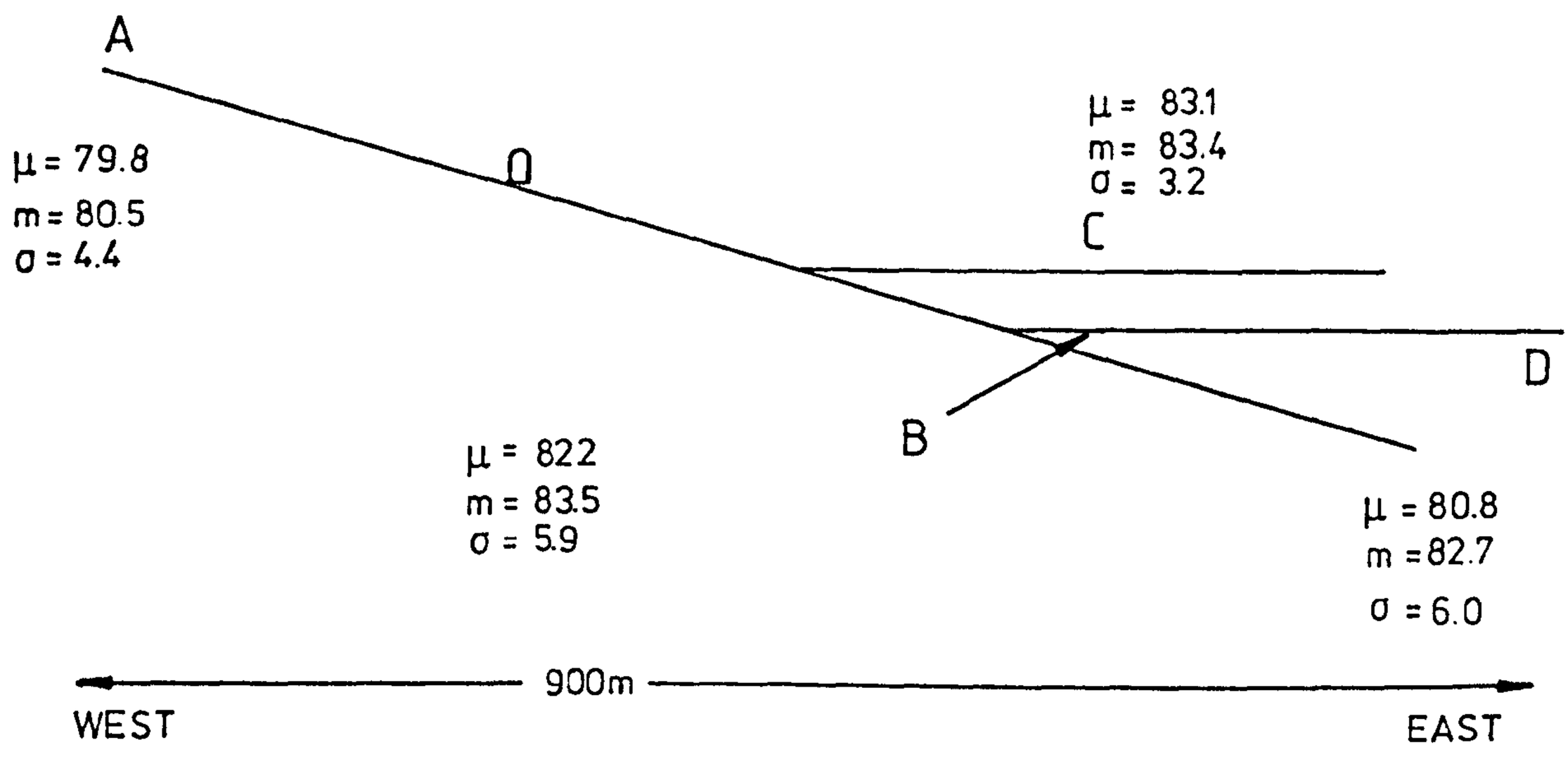

south wall of the vein does, however, show a lower mean final ice melting temperature than the other samples. Consequently the f-test fails at significance of less than 1%. Coefficients of skewness indicate that most of the samples are negatively skewed

3.7.2.2: LONGITUDINAL VARIATION IN HOMOGENIZATION TEMPERATURE

The populations of homogenization temperature measurements from four slits, labelled A, B, C and D on figure 3.14 were examined to determine longitudinal

temperature variation. One would expect that the greatest temperature change should occur between slit "A" and the slits in Deep Rake. An inspection of the means suggests this to be the case. However, testing of the populations using the Mann-Whitney U-test shows that the populations of homogenization temperatures from all the traverses were not dissimilar at a 5% level of significance apart from "A" against "C". The latter test was significant at 2%. An f-ratio of 1.31 for all the samples indicated that the homogenization temperature sample means are indistinguishable for the various slits at a 5% level of significance. Even taking the maximum longitudinal temperature difference possible, the lateral thermal gradient is still no more than $4\,^{o}C\ km^{-1}$.

3.7.2.3: SALINITY VARIATION

Means, medians and standard deviations of final ice melting temperatures for slits A, B, C and D are shown in figure 3.15. An f-ratio of 3.2 for all the final ice melting temperatures of the four slits indicates they have indistinguishable means at a 2.5% level of significance. Mann-Whitney U-tests on pairs of slits gave similar results.

3.7.3: COMPARISON OF TYPE 3 AND TYPE 4 FLUID INCLUSION DATA FROM SALLET HOLE MINE

Homogenization temperatures from the High Rake traverse

FIGURE 3.15

CROSS SECTION OF SALLET HOLE MINE.

Final ice melting temperatures for type 4 fluid inclusions. Means (μ), medians (m) and standard deviations (σ) are shown.

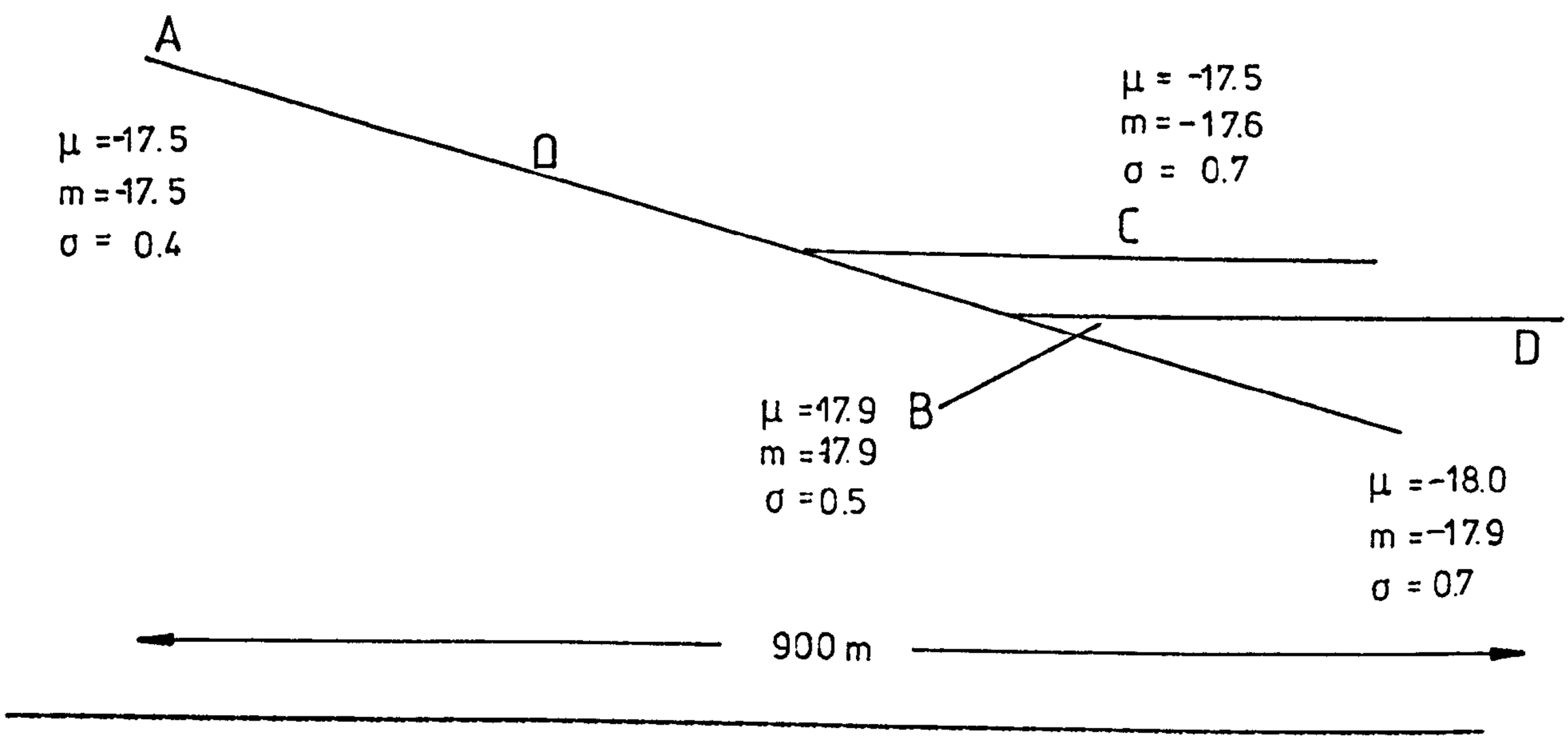

showed similar populations at a 5% level of significance (Mann-Whitney U-test) whereas slit "B" in Deep Rake gave a 59% level of significance for the same test. The conclusion to be drawn is that there is little evidence for change in depositional temperature from the type 3 mineralizing event to the type 4 event. A more tenuous conclusion may be that the two events were not separated by a considerable period of time.

3.8: COMPARISON OF THE HOMOGENIZATION TEMPERATURE POPULATIONS OF THE TYPES 3 AND 4 FLUID INCLUSIONS

Figure 3.16 shows the homogenization temperatures of these two inclusion types to fall into a very similar range. As reported earlier, the determined means of the two populations are 84.1°C ±13.4°C for type 3 and 84.4°C ±11.2°C for type 4. The calculated t-test statistic for the two populations was Ø.61, and therefore, the null hypothesis that the two samples are derived from the same population can be accepted at a 54% level of significance. A calculated f-statistic of Ø.36 for the two groups shows that the variance of the two populations are indistinguishable at a 5% level of significance. Therefore, it can be deduced that the two groups are derived from the same population and consequently no significant difference between the depositional temperatures of the groups is apparent. This conclusion is, however, based on the assumption that the filling temperature and the homogenization temperature of the two fluid inclusion types were similarly related.

Five samples which allowed measurement of suitable numbers of both types of inclusion gave similar results on testing. Four of the five samples tested, using the t-test, had similar populations at a 5% level of significance. The Mann-Whitney U-test gave similar results.

3.9: REGIONAL TEMPERATURE DISTRIBUTION

In order to quantify east-west variation in homogenization temperatures, sample means have been plotted on to a

Figure 3.16

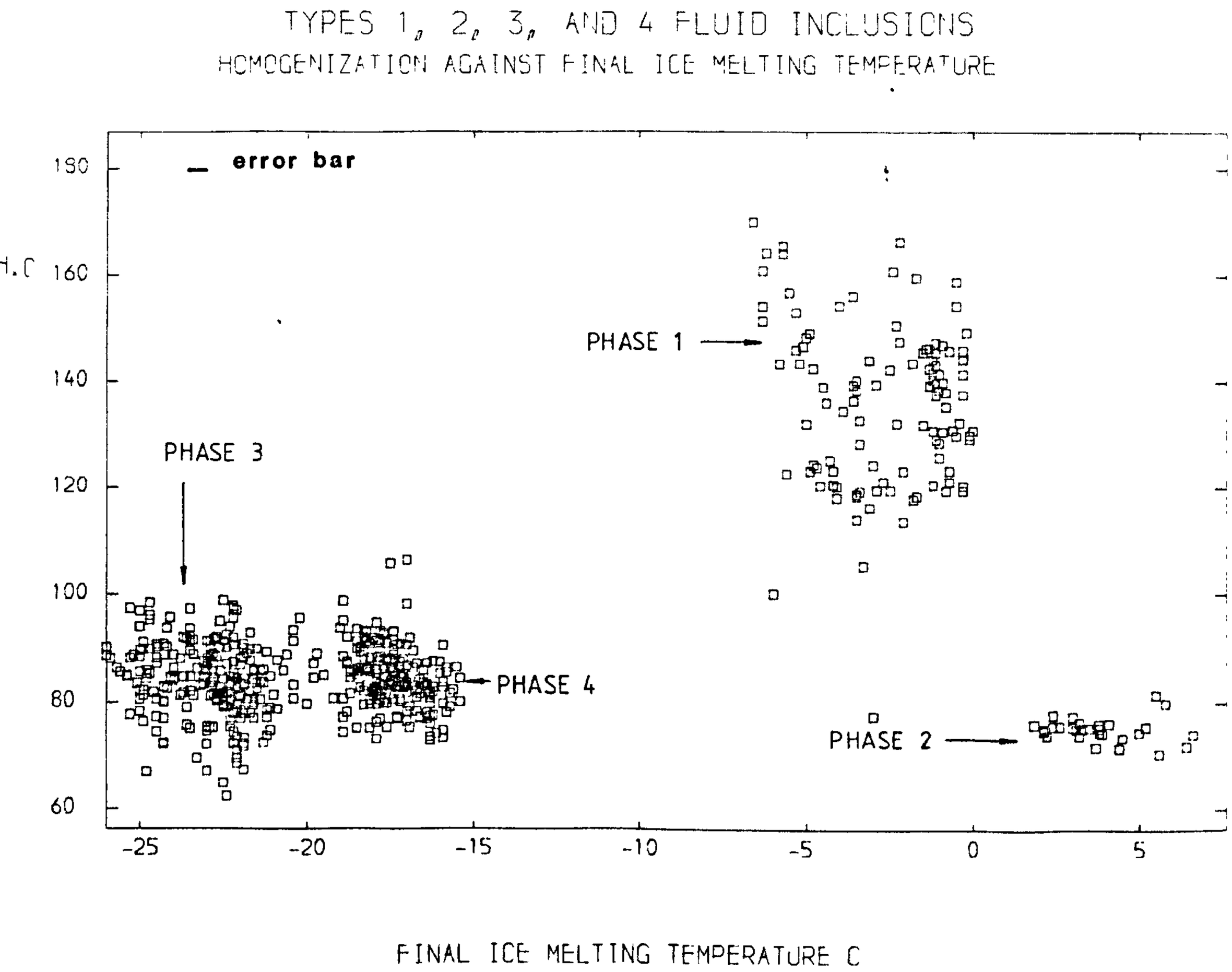

The diagram illustrates the discrete salinity-temperature ranges of the four ore fluids. Final melting of antarcticite has been plotted for the type 2 fluid inclusions.

grid and an arbitrary line drawn (A-B) to divide the Orefield into a eastern and western sector (figures 3.16 and 3.17). The data used for the comparisons are given in table 3.4. Means, medians and variance were compared for type 3 and type 4 fluid inclusion sample means drawn from the two sectors. Means and medians for the type 4 inclusions are slightly greater for the eastern sector when compared with the western. However, a t-test is unable to distinguish between the two populations at a 5% level of significance. The t-tests are unable to distinguish between the temperatures determined for the eastern and western sectors at a 74% and 67% level of significance for the phase 3 and 4 events respectively. An f-test indicates that east and western

TABLE 3.4

TYPE 3 AND 4 HOMOGENIZATION TEMPERATURES FROM WESTERN AND EASTERN DIVISIONS OF THE OREFIELD

Type 3 inclusions		Type 4 inclusions.	
West	East	West	East
84.3°C	86.Ø	86.7	86.4
76.8	83.3	83.8	75.6
77.5	81.9	85.5	83.4
85.8	81.4	77.7	8Ø.8
77.5	76.Ø	77.7	8Ø.8
88.Ø	82.2	82.7	81.8
83.6	82.Ø	82.9	91.3
8Ø.5	82.7	82.1	86.8
91.3	78.4	83.4	86.3
8Ø.9		84.9	85.3
8Ø.8		84.1	
85.1		8Ø.4	
f-statistic = Ø.1		f-statistic = Ø.2	
t-statistic = Ø.33		t-statistic = -Ø.43	

Figure 3.17

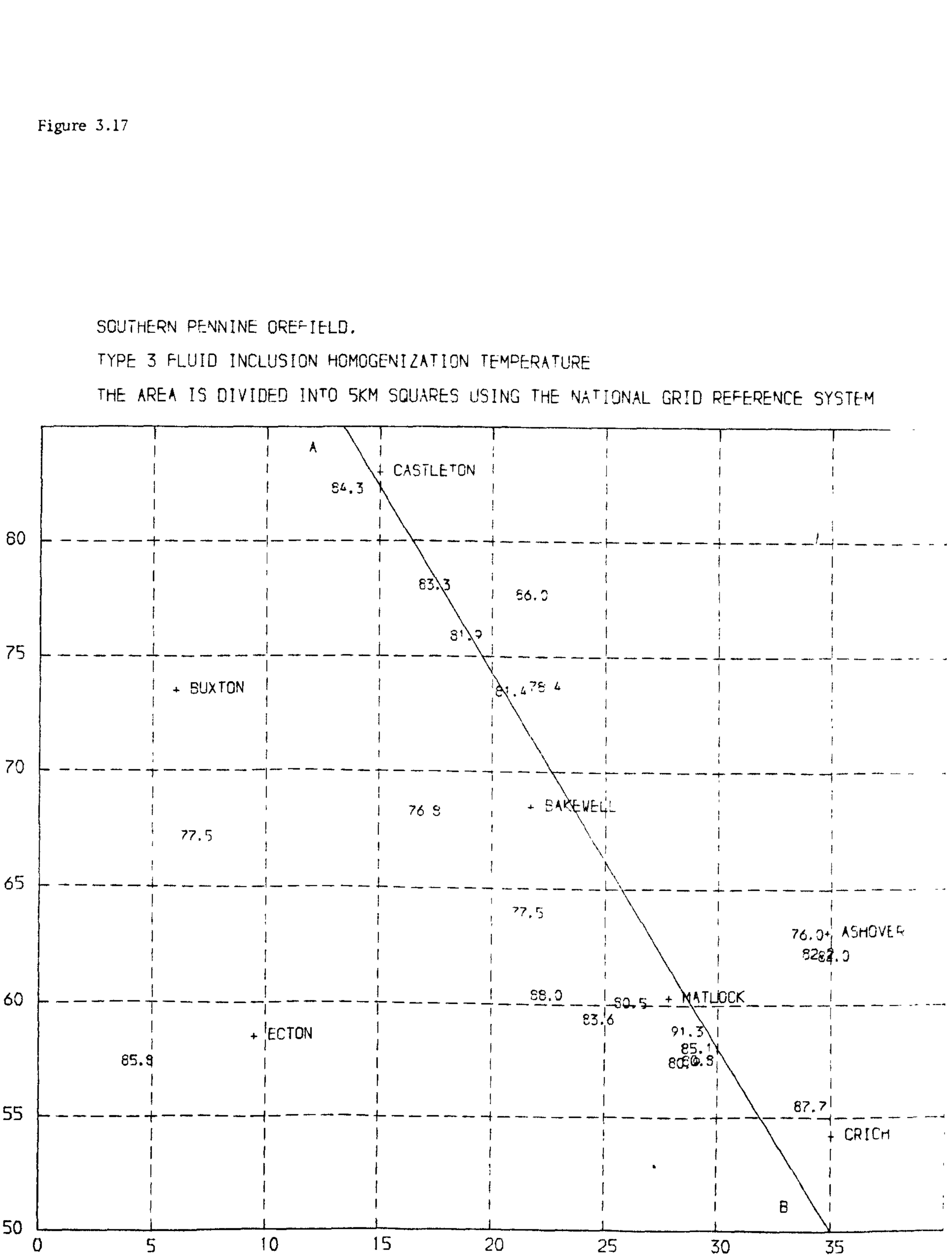

The line A-B is an arbitrarily drawn line, which is approximately parallel to the fluorite zone and divides an eastern and western half of the orefield in order to statistically compare the homogenization temperature populations.

Figure 3.18

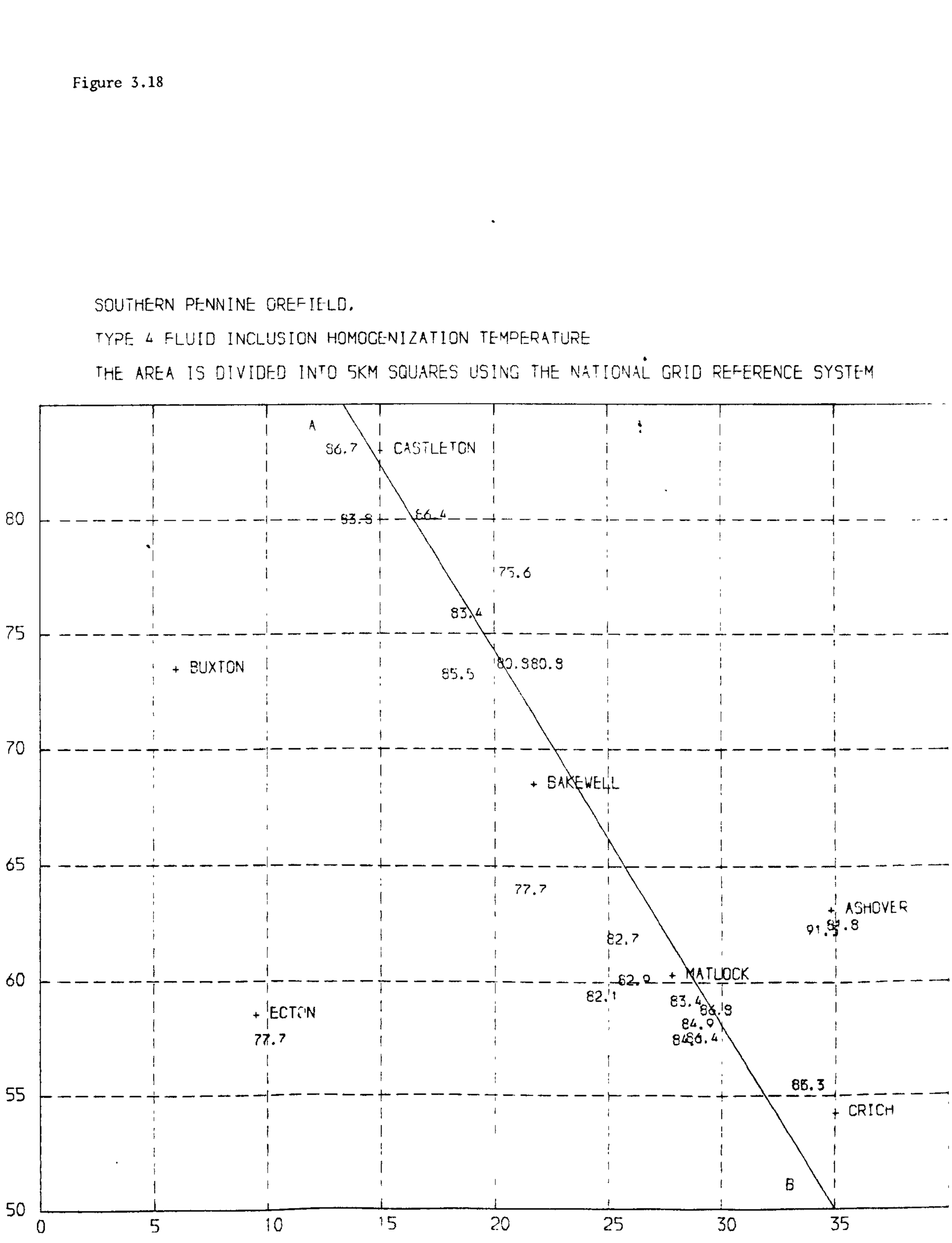

The line A - B is an arbitrarily drawn line, which is approximately parallel to to the fluorite zone and divides an eastern and western half of the orefield in order to statistically compare the homogenization temperature populations of the two division

populations of both types 3 and 4 have similar variance at a 5% level of significance. The significance of the test is slightly greater for the type 3 sample temperatures. Therefore, it seems reasonable to conclude that there were no significant lateral thermal gradients acting when the bulk of fluorite mineralization took place.

A further indication of the lack of regional temperature variation is given by the homogenization temperature means for fluorite samples from the Eakring 146 borehole. Fluorite samples taken from a depth of 801-802m gave type 3 and 4 sample means of $91.3\pm11^{o}C$ and $96.1\pm14^{o}C$. If a temperature correction of $12^{o}C$ is applied to account for 80bars excess pressure, and $24^{o}C$ is subtracted for the increased temperature with depth (geothermal gradient = $30^{o}Ckm^{-1}$), sample means closely approaching the population means for the block itself are calculated. Even if the corrections are ignored the maximum lateral gradient was $1.4^{o}Ckm^{-1}$.

3.10: CORRECTIONS FOR HOMOGENIZATION TEMPERATURES

Homogenization temperatures are only representative of the formation temperatures when entrapment of the fluid inclusion occurred at the equilibrium vapour pressure of the solution. There is no evidence of boiling, as would be indicated by a wide range in the degree of filling. Hence a minimum pressure required to restrain boiling of the type 1

fluids can be estimated. A confining pressure of 8.8 bars is required to stop pure water boiling at 175°C, the highest homogenization temperature recorded from the field (Weast, 198Ø).

Temperature corrections can only be applied to filling temperatures if an independent estimate of depth of formation or pressure can be made. Secondly, temperature corrections are only valid if homogenization occurs on the vapour-liquid curve of water. The only method of establishing the pressure acting on the system is to estimate the depth from the surface at which mineralization took place. To obtain this estimate, the age of mineralization must be determined.

3.1Ø.1: AGE OF SOUTHERN PENNINE MINERALIZATION

At the present time, field relationships probably provide the best evidence for the age of mineralization. The youngest sedimentary rocks cut by the veins of the Orefield are Permian in age (Ineson et al., 1972). Many of the igneous rocks of the field have been radiometrically dated and all appear to pre-date the mineralization. For example the Waterswallows Sill near Buxton has been dated by Stevenson et al. (197Ø) at 311Ma ±6Ma, which places the intrusion at the Namurian-Westphalian boundary. No mineralization has been observed in the Jurassic of the Midlands. Therefore, field evidence suggests a time span ranging from the Westphalian to the Upper Triassic.

Some attempts have been made to date the mineralization radiometrically (Moorbath, 1962; Ineson and Mitchell, 1973).

Moorbath used lead isotope ratios in galena to determine a modal age of 180Ma ±30Ma for mineral deposition. The Holmes-Houtermans model used to calculate the ages has been shown to be based on dubious assumptions and the values measured are not now considered as being geologically meaningful (Coomer and Ford, 1976).

Ineson and Mitchell (1973) used the potassium-argon (K-Ar) dating method to determine the age of clay mineral assemblages in hydrothermally altered igneous rocks. A wide range of ages were obtained, with a generalized bimodal distribution, suggesting significant activity at 270Ma and 235Ma. They do, however, suggest that mineralization may have been continuous from Upper Carboniferous to lower Jurassic times. The geological significance of K-Ar ages determined from clay mineral assemblages has been questioned (Shepherd et al.,1976; Rundle, 1981). The former paper examines evidence for the age of tungsten mineralization at the Carrock Fell Mine, Cumbria. K-Ar dating of biotite, muscovite and chlorite was carried out. A K-Ar date for muscovite formed during the greisenization was calculated as 383Ma ±4Ma, while co-existing chlorite gave an age range of 393 to 337 Ma. Ineson and Mitchell (1974) presented K-Ar dates for clay mineral assemblages from the same deposits. They suggested three distinct events which occurred at 282Ma, 231Ma, and 191Ma. Langley (1980) dated shales using the K-Ar method and found that the measured age ranges varied with the grain size of the clay minerals used. A Westphalian shale gave ages of 371Ma ±6Ma for a 31-53μm sieve fraction and 355Ma±5Ma for the 0.49-0.98μm fraction. Therefore, it seems judicious not to place too much emphasis on similarly

obtained K-Ar dates for mineralization in the Southern Pennines.

3.10.2: CALCULATING A TEMPERATURE CORRECTION

If mineralization occurred before the Hercynian Orogeny, then an estimate of the total thickness of the Namurian and Westphalian successions is required to calculate the temperature correction for fluid inclusion homogenization temperatures.

The thickness of the Namurian sediments in the southern end of the block has been measured as 373m in the Tansley borehole and 284m in the Ironville 3 borehole (Frost and Smart, 1979). Stages below H2 are considerably thinned. These thicknesses may, however, be unrepresentative since both boreholes are sited on anticlines where upwarping, contemporary with sedimentation, has resulted in condensed sequences. Sediments in the Stanton syncline for example are considerably thicker. Stevenson and Gaunt (1971), reported similar thinning of the E1 to H2 stages on moving from the gulf to the massif. The thickness of the E1-H2 sequence at Alport is 300m while at Hucklow Edge it is 42m. An isopachyte map for the Namurian of the East Midlands gives a thickness of 760m at the north of the massif and 300m at the southern end (Kent, 1966).

The thickness of Westphalian sediments that may have covered the Derbyshire block are more difficult to estimate. Frost and Smart reported that similar controls on sedimentation were active in the early part of Westphalian

times as had been acting in the the Namurian. The Westphalian A sediments thicken in the Edale and Widmerpool Gulfs. Variation in thickness of Westphalian B rocks indicate less control from block and basin sedimentation. The Westphalian A and B successions thicken from the south to the north. An example of this taken from Spink and Ford (1968) is the gradual thickening from the Leicestershire Coalfield (457m), in the south to the south Derbyshire Coalfield (640m) and the north Derbyshire Coalfield (770m) moving northwards. Isopachytes for the Westphalian indicate north-south thickness variation is more important than east-west variation. Thicknesses, formation densities, hydrostatic and lithostatic pressures are shown in figure 3.5

Hanor (1979) reported that in the Gulf Basin (USA), significant deviation away from hydrostatic pressure occurs in the depth range, 1.4km to 4.5km. Therefore, it seems reasonable to take a hydrostatic rather than a lithostatic estimate of pressure. However, both hydrostatic and lithostatic estimates are given in table 3.5. It is likely that brine density would increase at depth with increasing salinity but this would be compensated for by expansion of the brine on heating. Therefore, hydrostatic pressures calculated at a constant fluid density of $1000 kgm^{-3}$ are probably reasonable. Using the data of Potter (1977), a temperature correction for brines of 1 and 20 equivalent weight percent sodium chloride are shown in table 3.5. Although the fluids in inclusions from the Southern Pennines contain large quantities of calcium chloride, an equivalent weight percentage sodium chloride content probably yields a reasonable value.

TABLE 3.5

ESTIMATED DEPTHS OF MINERALIZATION FOR THE NORTHERN AND SOUTHERN HALVES OF THE DERBYSHIRE BLOCK AT THE END OF THE WESTPHALIAN AND ESTIMATED TEMPERATURE CORRECTIONS

(Pressures are calculated, disregarding temperature effects.)

PARAMETER	NORTH	SOUTH
Thickness (Namurian)	700m	300m
Thickness (Westphalian)	1200m	1200m
Hydrostatic pressure	190bars	150bars
Lithostatic pressure	474bars	372bars

(Density of Namurian, 2550kgm^{-3}, and Westphalian, 2470kgm^{-3}.)

CORRECTION (HYDROSTATIC)	(T = 100°C)	
1 equiv. wt% NaCl	25°C	20°C
20 equiv. wt% NaCl	31°C	28°C
CORRECTION (LITHOSTATIC)	(T = 100°C)	
1 equiv. wt% Nacl	48°C	40°C
20 equiv. wt% NaCl	45°C	36°C

These corrections have been provided to give some indication as to the maximum temperature at which mineralization could have taken place. If the bulk of the mineralization post-dates the Permian period, by which time the greater part of the Westphalian and Namurian sediments would have been removed from the block, only a small correction for pressure would be required. A thin Namurian cover and a 100-200m Triassic capping may have been all that overlaid the district in the Upper Triassic. Therefore, any post-Permian fluid inclusions probably require little or no temperature correction. The presence of methane within inclusions also negates the use of pressure corrections

(Hanor,1981). Type 1 inclusions, the most likely to have formed in pre-Permian times exhibit the highest gas pressures. Therefore, the temperature corrections have not been applied to the homogenization temperatures when plotting graphs or making any calculations.

3.11: FLUID INCLUSION TYPES REPRESENTING PHASES OF MINERALIZATION

The study of the distribution of fluid inclusions in thin section and paragenetic relationships to elucidate a sequence of hydrothermal events has been used by Chivas and Wilkins (1977) in studying the Koloula porphyry copper deposit at Guadalcanal and by Bloom (1981), studying stockwork molybdenum bodies. Isolation is thought not to be sufficient evidence for primary origin (Wilkins and Bird, 1980) but random distribution accompanied by isolation appears to be still one of the best criteria. Secondary inclusions are most usually formed by fracturing and re-healing of a mineral. If a mineral is exposed to repeated fracturing and healing, the earliest formed mineral should record all the phases of hydrothermal activity, assuming that the formation of coeval fluid inclusions occurs at each event. As multifaceted or negative crystal primary inclusions are initially rare, repeated fracturing may well significantly reduce their number or even remove them completely. As fracturing continues, secondary fluid inclusion planes will be intersected by later fractures, and

some of the earlier formed secondary inclusions will be destroyed also. The end result will be the breaking up of earliest formed inclusion planes until they are relatively randomly distributed. The most recently formed inclusions will be present in strong, undisrupted planes or curved arrays. Although this theory was applied by Chivas and Wilkins to complex porphyry copper deposits, the ideas seem to apply fairly well to fluid inclusion studies on the low temperature, polyphase fluorite mineralization of the Southern Pennine Orefield.

Thick double polished sections of fluorite were examined to decipher the sequence of hydrothermal events. The first assumption is that each fluid inclusion type represents a discrete hydrothermal phase. This assumption may well be incorrect, especially in the case of the type 3 and type 4 fluid inclusions. A second assumption is that each of inclusion types 1, 2, 3 and 4 contain fluids from which fluorite and possibly ore minerals were deposited. Fluid inclusion studies and REE geochemistry of the fluorite supports this assumption (Chapter 5).

Type 1 fluid inclusions can be unambiguously correlated with the earliest recorded stage of fluorite mineralization in the district. The largest deposits of this fluorite type occur in cavities in the boulder bed at Treak Cliff Cavern (Ford, 1969). The fluorite is usually purple, dark blue or clear. Smaller deposits have been identified in Dirtlow Rake (Castleton), Moss Rake, the Winnats Pass area, Ricklow Quarry, Watergrove Mine and Gateham Grange, Wetton. Ford (1969) noted that the Odin Rake cut through the cavity fillings of the boulder bed and filled easily accessible

vughs with a later generation of fluorite, and associated baryte, calcite, galena and sphalerite. Type 1 fluorite has been observed to contain types 1, 2, 3, and 4 fluid inclusions. An example of fluorite from the Old Tor Mine shows planes of type 1 inclusions terminating against an overgrowth of possibly type 2 fluorite. The transitional boundary is enhanced by a change in colouration and the presence of pyrite cubes at the interface. A similar relationship was observed in a sample from Watergrove Mine, where dark purplish-blue fluorite was covered by a later generation of pale mauve fluorite. Type 3 and 4 inclusions were abundant in both generations but type 1 inclusions were absent from the later phase. A similar but more ambiguous relationship was seen in fluorite from Murphy's Hole at Treak Cliff Cavern. Dark blue fluorite lining a cavity and separated from a later episode of fluorite mineralization by a thin layer of red clay, shows abundant type 1 inclusions. The later generation of coarsely crystalline yellow and blue fluorite contains type 2 inclusions only. Type 1 fluorite has not been observed to contain any sulphide inclusions and does not appear to have been precipitated along with any other contemporary mineral phases.

Type 2 fluid inclusions have been observed in fluorite from various localities and are nearly always accompanied by type 3 and type 4 inclusions. Type 2 inclusions have been noted in metasomatic fluorite from the Moor Farm quarry, Bonsall Moor, and from Butts quarry at the north end of the Ashover inlier. At the former locality, yellow cubes of fluorite infilling cavities contain type 3 and type 4 inclusion only. Assuming the cavity fillings post-date the

metasomatism, the inference is that the type 2 hydrothermal event pre-dates the type 3 and 4 events. Type 2 inclusions were also seen to be contained within fluorite from the north crosscut at Ladywash Mine. Rounded or elongate flattened type 2 inclusions occur in a band close to the fluorite-wall rock junction. Later fluorite contains what appear to be primary type 3 inclusions, and type 2 inclusions are absent. These relationships are interpreted as an early generation of type 2 fluorite being deposited on to the wall rock with later deposition of type 3 fluorite. No junction, however, can be identified separating the two generations. Another important locality for type 2 inclusions is fluorite from the Smalldale Pipe. The criteria for recognition of hydrothermal phases, as outlined above can be applied. Examination of thick sections shows that some samples contain types 2, 3 and 4 inclusions. Plate 3.2a shows the type 2 inclusions to be randomly distributed, with occasional discontinuous secondary planes. Type 4 inclusions dominate the section (plate 3.6a and 3.6b) and occur in densely packed and relatively continuous planes or curving arrays. A few secondary, type 3 inclusions are scattered over the section. Applying the ideas of Chivas and Wilkins (1977), it is concluded that the type 4 inclusions represent the youngest hydrothermal event.

Deciphering the age relationships of type 3 and type 4 inclusions is open to some ambiguity. The similarity in the population of homogenization temperatures drawn from the field as a whole and from individual sample populations suggests that the geothermal environment was little different during the two events. The phases may not be separated by a considerable period of time and they may even have over-

lapped. The plot of homogenization temperature against final ice melting temperature seems to rule out the mixing of the two brines at the site of deposition (Figure 3.16). A line parallel to the ordinate at -2Ø°C almost completely divides the two populations. Examination of numerous sections tentatively indicates that the type 3 inclusions pre-date type 4. A fluorite sample from Overton Hall Mine shows an early cubic generation of fluorite covered by a finer mass of late, bevel-edged material. Primary, plain cubic type 4 inclusions are present in the later fluorite with secondary type 3 and type 4 inclusions in the earlier deposit. Another sample from Masson Hill contains scattered primary negative crystal type 3 inclusions with abundant curving and planar arrays of type 4 fluid inclusions. Negative crystal type 4 inclusions have also been found in material from Fall Hill Quarry. On a regional level the abundance of type 4

TABLE 3.6

COMPARISON OF HOMOGENIZATION TEMPERATURES OF APPARENTLY COGENETIC OIL-WATER INCLUSIONS

Locality	Homogenization temp.°C.			
	aqueous	oil	Δ	TYPE
Gateham Grange	131.8	134.7	-2.9	1
Treak Cliff	133.4	132.2	Ø.6	1
Old Tor Mine	134.4	121.3	13.1	1
Eakring 146	1Ø4.2	89.9	14.3	4
Eakring 146	94.7	86.4	8.3	4
Eakring 146	98.9	83.6	15.3	3
Eakring 146	97.1	87.1	1Ø.Ø	3
Eakring 146	95.6	92.Ø	3.6	3
Gregory Mine	81.6	75.4	6.2	3
Gregory Mine	92.5	79.9	12.6	4

inclusions relative to type 3 seems to decrease moving west. Samples taken close to the Dinantian-Namurian boundary on the eastern margin of the field may contain type 4 inclusions exclusively. Despite the examples given above, type 3 and type 4 inclusion relationships are often ambiguous and localized overlap of the two phases is quite possible. If overlap did occur, two independent feeding channels are required if not independent sources.

Type 5 inclusions have been observed in association with types 1, 2, 3, and 4 fluid inclusions. Melting point measurements indicate that their fluid chemistry is similar to the type 2 fluid inclusions. This and their close association with the latter inclusion type suggests that the type 5 hydrothermal phase pre-dates the type 3 event. Type 6 inclusions probably post-date type 2 inclusions but their actual position in the fluid sequence could not be determined.

3.12: OIL INCLUSIONS

Oil inclusions are most commonly associated with type 1 fluid inclusions but they have also been found in association with types 3 and 4 in fluorite from the Gregory Mine and the Eakring 146 borehole. Type 1 fluorite localities include Treak Cliff, Odin Mine, Pindale Quarry, Windy Knoll and Gateham Grange, Wetton. They are readily recognized by their colour, refractive index, and ultra-violet fluorescence. The colour ranges from dark reddish brown through orange to

colourless. The refractive index is normally above that of fluorite (1.433). It is known that refractive index of the alkanes increases with increasing chain length (Buruss, 1981). Therefore, assuming the dominant compounds to be alkanes, the mean chain length is probably in excess of 1Ø. On exposure to U.V. light, the oils fluoresce a pale yellowish-green. Cooling to -15Ø^{o}C fails to freeze the liquid but the darker, more viscous oils appear to partly solidify to a brown waxy solid. Similar solids present at room temperature dissolve on heating to temperatures in excess of the homogenization temperature. Homogenization temperatures of cogenetic liquid-oil and aqueous inclusion pairs usually show the oil to have a significantly lower homogenization temperature. Differences in homogenization temperature (aqueous-oil) are shown in table 3.6 and range from -2.9^{o} to +15.3^{o}. Lower oil inclusion temperatures were ascribed by Roedder (1963) to the greater compressibilty of oils in comparison to brines. It is difficult to estimate a temperature correction for aqueous inclusions from the differences given in table 3.6 (Buruss, 1981). The chemistry of the organic compounds present has been discussed by Pering (1973) and their importance is discussed in later section, As a general conclusion, oil inclusions are not very abundant within the bulk of the fluorite of the district, as Rogers (1977) noted.

3.13: DISCUSSION AND CONCLUSIONS

A study of fluid inclusions in fluorite has revealed

four phases of fluorite deposition in the Southern Pennine Orefield. A total of seven inclusion types have been recognized, four of which represent stages of mineralization. Criteria for recognizing the inclusion types has been outlined. Highest temperatures of mineralization were attained in the first phase of mineralization. The inclusion fluids, however, contain only small quantities of dissolved salts. Generally, no correlation was found to exist between salinity and homogenization temperature. Nor is there any correlation between homogenization temperature ranges (2σ) and temperature means. These two conclusions apply even more strongly to the other three phases.

The second phase of mineralization is represented by type 2 fluid inclusions. These showed the lowest homogenization temperatures ($62^{o}C$-$82^{o}C$) and the highest salinities. Statistical tests showed that four widely spaced localities had the same sample means at a test significance of 5%. Evidently, hydrothermal convection was severely limited during this period of fluorite deposition.

Type 3 and 4 inclusion homogenization temperatures are very similar. Means and medians for the selected sample populations are 84.1^{o}, 84.2^{o} and 84.3^{o}, 84.4^{o} respectively. It may be that the two events were closely associated and even the possibility of some overlap cannot be ruled out. The discrete nature of the two melting point populations does, however, indicate that very little mixing of the two brines occurred at the site of deposition. The final ice melting temperature frequency distribution of the type 4 inclusions is slightly skewed suggesting that some dilution may have taken place.

It is clear from melting temperature measurements of the solid phases formed on freezing that the chemistry of the inclusion fluids cannot be completely dominated by sodium chloride. Final ice melting before -20.8^{o}C (Crawford, 1981) indicates either the presence of calcium or magnesium chlorides. Therefore, final ice melting temperatures cannot be expressed in terms of equivalent weight per cent sodium chloride. Final ice melting at -40^{o}C or final melting of antarcticite above 0^{o}C indicates very high calcium chloride concentrations in the brines.

A detailed study of fluid inclusions in material from High Rake and Deep Rake showed that longitudinal, vertical and transverse thermal gradients were very low during phases 3 and 4. A small temperature difference in sample means between High Rake and Deep Rake was observed. However, the lateral gradient was less than 4^{o}Ckm^{-1}. An interesting observation is that the proportion of type 4 to type 3 fluid inclusions in fluorite deposits is seen to increase towards the eastern margin of the field. This may indicate an easterly source for the type 4 ore fluid. Statistical testing shows that there is no reason to suggest that the regional distribution of fluorite deposits was controlled by east-west longitudinal thermal gradients, although the salinity of the type 4 ore fluid appears to have decreased very slightly as it moved west. Some other mechanism, other than cooling, is required to account for the clustering of the major fluorite deposits on the eastern margin of the Orefield.

The study has shown that the homogenization temperatures reported by Rogers (1977) were erroneously high. Where Rogers (1977) has given a final ice melting

temperature, typical of a type 3 or 4 fluid inclusion, corresponding mean homogenization temperatures for individual samples ranged from 75.6°C to 153.8°C. The mean homogenization temperature range determined for all type 3 and 4 inclusion samples in this study ranged from 75.6°C to 98.9°C, which closely agrees with the range determined by Moore (1980). The high values determined by Rogers (1977) were probably caused by poor contact between the mineral fragment and the stage and the very small surface area of the Leitz 1350 heating stage.

CHAPTER 4

CHEMISTRY OF THE ORE-FORMING FLUIDS

4.1: INTRODUCTION

The aim of this chapter is to reconstruct the physical and chemical conditions in which mineralization occurred. Thermometric fluid inclusion data and semi-quantitative chemical analysis of inclusion fluids may be used as a base for chemical modelling. The use of thermodynamics in constraining physicochemical parameters requires the initial assumption that the system was in equilibrium. Therefore, the subject of equilibrium in low temperature hydrothermal environments needs some discussion. The recognition of mineral assemblages which were stable as mineral deposition proceeded is useful for placing limits on the acidity, oxygen and carbon dioxide fugacity of the ore-forming environment. A study of the chemistry of present-day formation waters may also be used to estimate the concentration ranges of minor components within the fluids, such as barium and oxidized sulphur. Much of the chemical modelling assumes that equilibrium was established between the ore fluid and its surroundings, and therefore is only valid for non-mixing models of mineralization. The calculations associated with much of the modelling are presented in appendix 6.

4.2: MAJOR ELEMENT CHEMISTRY OF THE ORE FLUIDS

Any estimation of mineral solubility in an aqueous electrolyte requires a knowledge of the concentrations of the major dissolved salts, as well as estimates of partial gas pressures, pH, and temperatures. The molal concentration ranges of sodium, potassium, magnesium and calcium can be evaluated by combining cation ratios measured in fluid inclusion leachates with freezing point depression measurements in the ternary system $CaCl_2$-NaCl-H_2O. Ranges for various physical parameters are shown in table 4.1. The data has been summarized from information presented in chapter 3.

TABLE 4.1

ESTIMATED PHYSICAL PARAMETERS FOR THE ENVIRONMENT OF MINERALIZATION

Parameter	Phase 1	Phase 2	Phase 3	Phase 4
Fluid density* (kgm^{-3})	1000-1069	ca 1390	ca 1238	ca 1177
Hydrostatic Pressure	--------	20-190 bars	----------	----------
Lithostatic pressure	--------	20-474 bars	----------	----------
Minimum depositional temperature ^{o}C	100-171	62-82	65-99	73-106
Maximum depositional temperature ^{o}C	148-219	107-127	110-144	118-151

* at 25^{o}C

4.2.1: CATION RATIOS

Concentrations of sodium, potassium, calcium and magnesium in leachates from crushed fluorite containing one dominant fluid inclusion type were measured using atomic absorption spectrometry and emission spectrometry (See appendix 2). Analysis of calcium presents the most difficult problems since $CaCl_2$ does not move into solution as quickly as the alkali metal chlorides and fluorite itself contributes calcium to the leachate. The leaching method employed is outlined in appendix 2. Measurement of the calcium concentration is very important since it affects strongly the solubilities of fluorite and calcite as well as indirectly influencing the solubilities of all the gangue and ore minerals with the exception of quartz.

Na/K, Na/Ca and Na/Mg ratios were obtained for a number of samples containing types 2, 3 and 4 fluid inclusions and are reported in appendix 2. No attempt was made to determine similar ratios for the type 1 inclusions since samples were always contaminated with secondary, more saline inclusions. Anion concentrations are difficult to analyse quantitatively. Since the only commonly occurring high solubility salt of calcium is the chloride, chloride must be the dominant ion. The presence of chloride can be qualitatively determined by the addition of silver nitrate to an acidified solution. A white precipitate, soluble in ammonium hydroxide indicated the presence of chloride in all the leachates (Vogel, 1947). No precipitates were produced on addition of barium chloride solution, indicating the absence of sulphate. This test is,

however, of limited value as a consequence of its low sensitivity.

4.2.2: INTERPRETATION OF THE MELTING POINT DATA

Since the Na/Ca ratio for all the inclusion fluids is more than an order of magnitude less than the Na/Mg and the Na/K ratios, it is reasonable to interpret the freezing data in terms of the ternary system $NaCl-CaCl_2-H_2O$. Data for the system is available from Linke (1965) and Weast (1977). In figures 4.1 and 4.2, the molal Na/Ca ratios from the leachate analyses have been drawn On to a plot of molal sodium chloride against molal calcium chloride. On to this diagram isothermal contours for the system have been plotted directly from the data of Linke and Weast using a contouring subroutine from the GHOST library. The leachate ratios for the type 3 fluid show a wide range, and this may be narrowed by placing limits from the temperature at which the melting path departs from the $NaCl.2H_2O$-ice cotectic. This range is marked on figure 4.1 using an asterisk for the maximum and minimum ratios to distinguish them from .the leachate ratios. The difference is probably the result of contamination of the samples by other inclusion types. The type 4 fluid shows a relatively narrow compositional field and its position is in agreement with the melting sequence described in chapter 3. The composition of the type 2 inclusion fluid is easily constrained in terms of $CaCl_2$ and NaCl since the antarcticite + liquid field is very restricted at $+3^{o}C$. The chemical composition of the ore fluids are shown in figure 4.2. It is

Figure 4.1

Compositional range of the type 3 ore fluid plotted on to the ternary system $CaCl_2$-NaCl-H_2O.

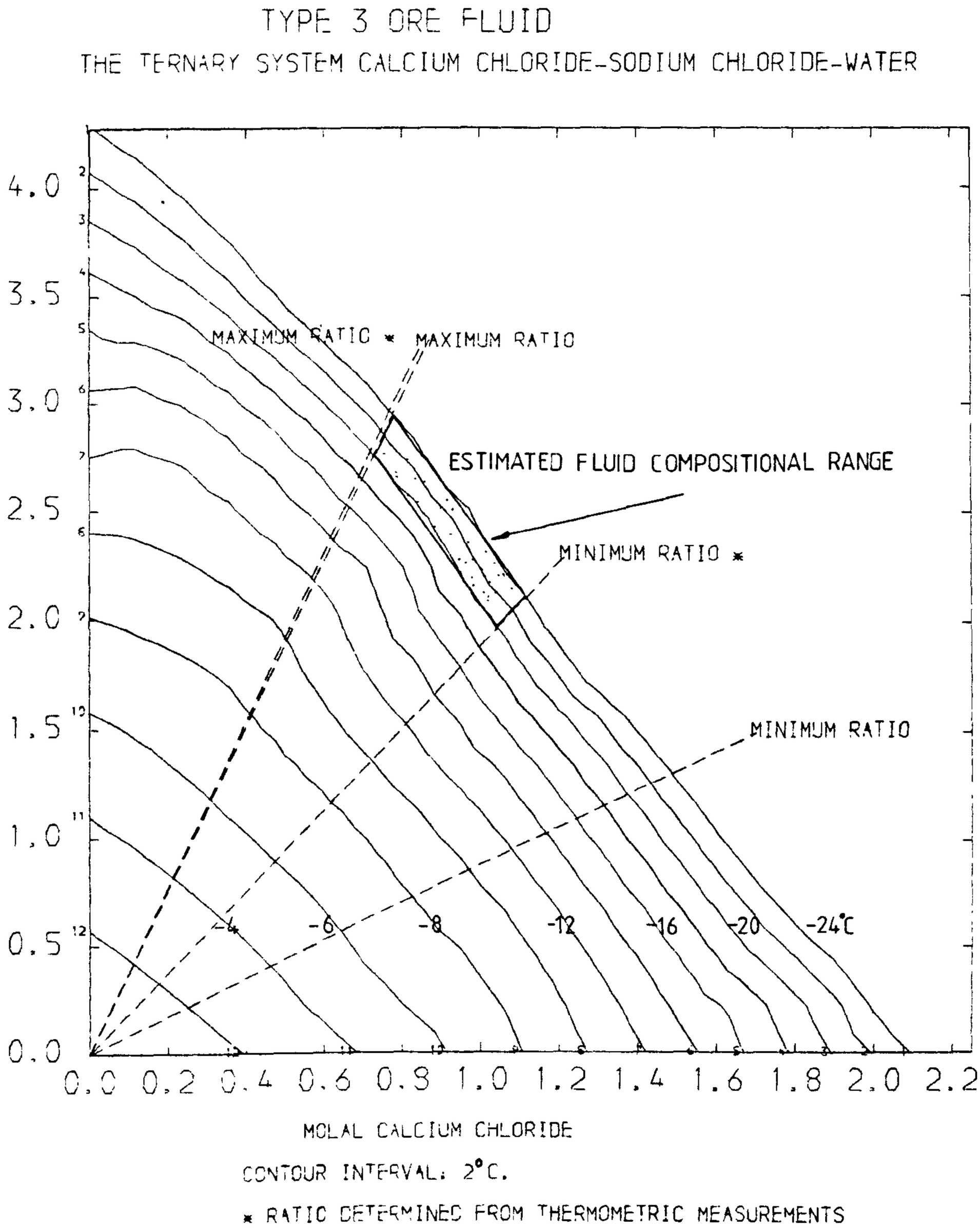

difficult to place any limits on the precision of the analyses, since it is impossible to assess the quality of the initially determined cation ratios and the accuracy of the ternary phase diagram. A precison of ±10% for the concentrations of all components in the ore fluids is probably reasonable.

TABLE 4.2

MAJOR ELEMENT CHEMISTRY OF THE ORE FLUIDS.

Molal concentration of cations for phases 2, 3 and 4.

Cation	Phase 2	Phase 3	Phase 4
Na^{+}	0.171-0.340	2.10-2.75	0.350-0.800
K^{+}	0.008-0.015	0.031-0.041	0.005-0.019
Mg^{++}	0.002-0.004	0.040-0.055	0.005-0.012
Ca^{++}	3.33-3.42	0.78-1.10	1.21-1.65
Cl^{-}	6.84-7.20	3.77-5.10	2.78-4.13
Stoichiometric ionic strengths.			
I(s)	10.4-10.5	6.5-6.8	4.7-5.3
Molal Ca^{++} , correcting* for the complex $CaCl^{+}$.			
Ca^{++}		0.39-0.48	0.51-0.55
Corrected m_{Cl^-} and ionic strength.			
Cl^{-}		3.4-4.5	2.1-3.0
I		3.7-4.7	2.6-3.6

* See appendix 6.1

re 4.2

Compositional range of the type 4 ore fluid plotted on to the ternary system $CaCl_2$-NaCl-H_2O

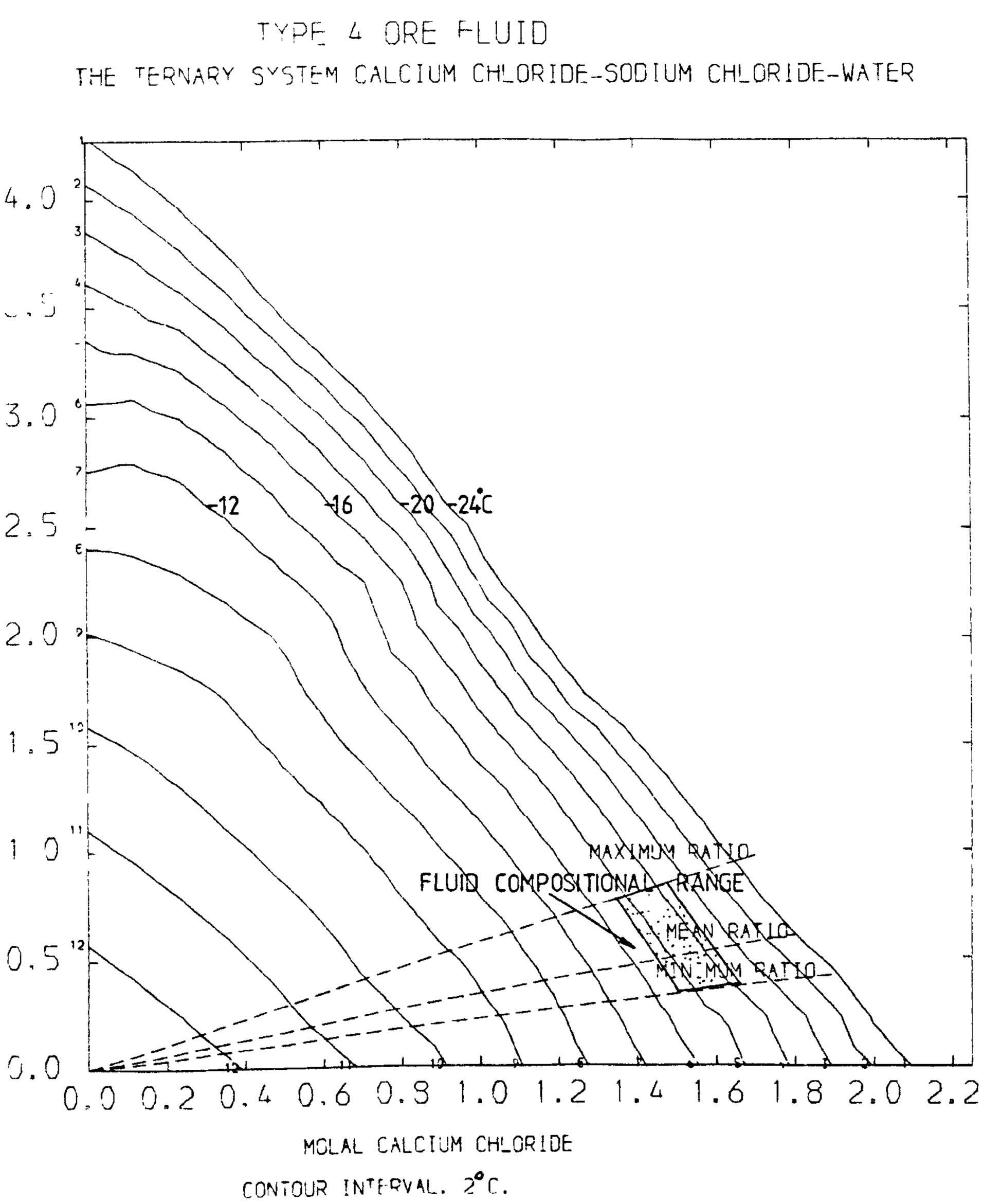

4.3: ACTIVITY COEFFICIENTS

Activity coefficients are used to relate molal concentrations to "effective concentrations" or activities (Krauskopf, 1979). The activity of an ion is the part of its concentration which affects its behaviour towards other ions and is simply related to a molal concentration by the equation:

$$a_i = \gamma_i \cdot m_i$$

where a_i is the activity, γ_i the activity coefficient and m_i the molality of the ith ion

Individual ion activity coefficients may be calculated for solutions of relatively low total dissolved salt content using an extended Debeye-Huckel equation (Davies (1962); Helgeson (1969); Truesdell and Jones (1974)). Values calculated become more inaccurate with increasing ionic strength. Ionic strength is defined in the equation:

$$I = \tfrac{1}{2} \quad \Sigma \quad z_i^2 . \quad m_i \qquad .$$

where I is the true ionic strength, z_i is the charge on the ith ion and m_i the molality of the ith ion. For a correct value to be obtained the molality of all complexes must be calculated. However, for the purposes of this study the only complex considered in the term was $CaCl^+$, giving

$$I = m_{Na^+} + m_{K^+} + m_{CaCl^+} + 3. (m_{Ca^{++}} + m_{Mg^{++}})$$

Individual ion activity coefficients were calculated for solutions with an ionic strength less than 3 using the equation,

$$\log\gamma_i^{\pm z} = \frac{A.\ z^2\ I^{\frac{1}{2}} + B'.\ I}{(1 + \mathring{a}_i\ B\ I^{\frac{1}{2}})}$$

where A and B are temperature dependant Debeye-Huckel coefficients (Helgeson, 1969). The $\mathring{a}_i$ term is the distance of closest approach of the ith ion and B' a deviation function which assumes an electrolyte dominated by sodium chloride (Appendix 5.2). Activity coefficients for the phase 3 fluid were taken from Sverjensky (1981) and for the phase 4 fluid, values were calculated from the equation of Helgeson (1969). The variation in individual mean salt activity coefficients with increasing ionic strength are shown in figure 4.3 taken from Helgeson et al. (1981). A mean salt activity coefficient is the square root of the products of the individual ion activity coefficients of the ions present in the salt (Garrels and Christ, 1965). It can be seen that values decrease rapidly to a minimum and then begin to increase on increasing the ionic strength. Activity coefficients are an important factor when considering mineral solubility. This can be easily demonstrated by considering the solubility of fluorite. In a saturated solution, the molality of calcium and fluoride ions are related by the equation

$$K_s = m_{Ca^{++}} \cdot m^2_{F^-} \cdot \gamma_{Ca^{++}}\gamma^2_{F^-} = a_{Ca^{++}} \cdot a^2_{F^-}$$

Figure 4.3

Variation in the mean salt activity coefficients of NaCl, KCl and $MgCl_2$ with increasing ionic strength.

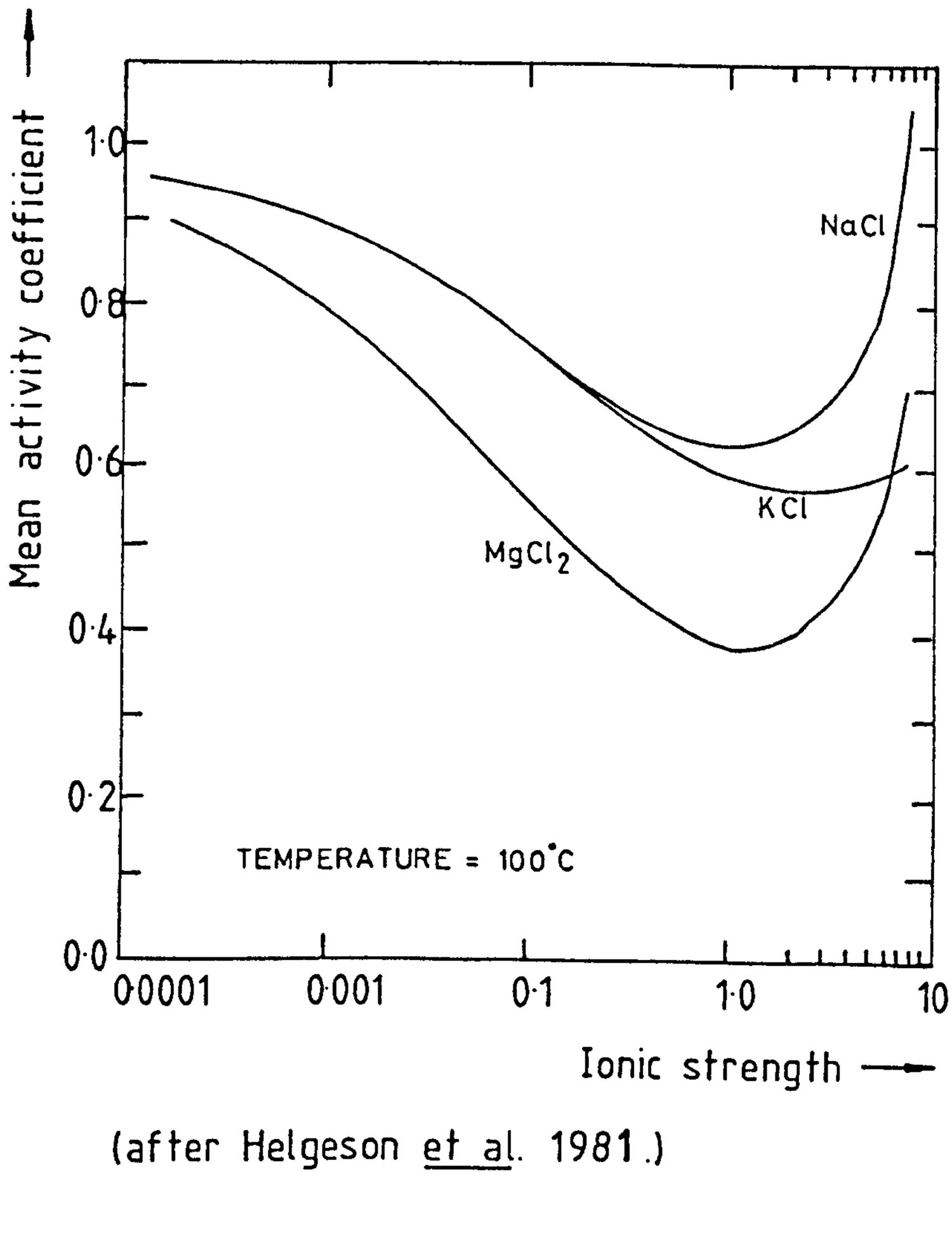

(after Helgeson et al. 1981.)

where K_s is the ion activity solubility product of fluorite. Since the molal concentration of calcium is unlikely to change significantly in the phase 2, 3 and 4 ore fluids, any change in the activity coefficients must be offset by a change in fluoride concentration and, therefore, a change in fluorite solubility. Diagrams used to show mineral stabilities generally use activities to express concentrations. It must be remembered that the molality of an ion is usually greater than or equal to its activity and the analytical concentration of the ion is much higher still, since complexing or ion-pairing must be considered. Little use of the phase 2 fluid composition has been made in calculating mineral stabilities, since activity coefficients cannot be estimated for such a highly saline fluid.

4.4.1: EQUILIBRIUM AND ORE DEPOSITION

Most thermodynamic calculations can only be satisfactorily applied to a system which is in a state of or has closely approached equilibrium. Equilibrium in ore deposits has been discussed in some detail by Barton *et al*. (1963) and Barton *et al*. (1977). In the latter paper the authors have concisely listed the aspects of equilibrium which require examination. These are :(1) the degree of attainment of equilibrium in aqueous species: (2) the degree of attainment of equilibrium between the ore fluid and the minerals being deposited from it: (3) the degree of attainment of equilibrium between the fluid and the wall rocks and the previously deposited mineral phases exposed to

the solution and (4) the degree to which the original state has been preserved, or to which it has been modified by post-depositional changes.

4.4.2: EQUILIBRIUM AMONG AQUEOUS SPECIES

Attainment of equilibrium among aqueous species is normally a rapid process (Barton et al., 1963). The one important exception is the inorganic reduction of aqueous sulphate (Ohmoto and Lasaga, 1982). This reaction is considered in some detail in section 4.7.

4.4.3: EQUILIBRIUM AMONG PRECIPITATING MINERAL PHASES AND THE ORE FLUID

Equilibration between solid mineral phases and aqueous solution is rapid compared to the time which ore-forming processes take to occur. Growth and dissolution of crystals can be discussed quantitatively in terms of ion activity solubility products (K_s) for specific mineral phases and the ion activity product (IAP) of the fluid in question. Percentage saturation can be expressed using the term:

$$\% \text{ saturation} = IAP/K_s \times 100\%$$

An attempt has been made by Barton et al. (1977) to relate the degree of saturation of a mineral in the ore fluid to the texture it displays. Figure 4.4 gives a suggested

Figure 4.4

The relationship between mineral textures and the degree of mineral saturation in an ore fluid. (Taken from Barton et al., 1977)

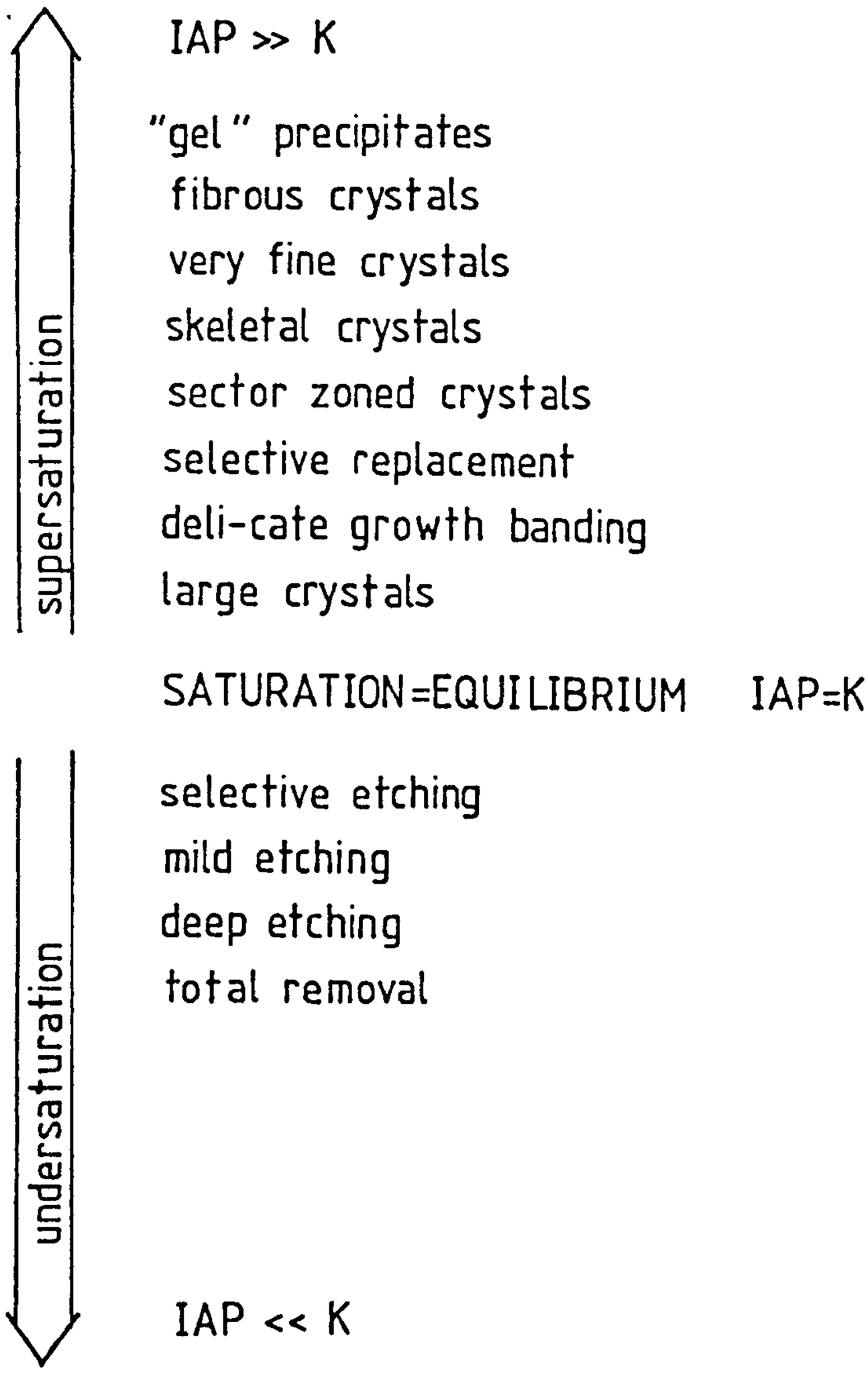

IAP = ion activity product of fluid
K = ion activity solubility product

relationship between mineral textures and the degree of saturation. This relationship proves useful, particularly when attempting to estimate important trace anion concentrations. Examples are the degree of saturation of calcium fluoride and calcium carbonate in the brines associated with phases 3 and 4. Much of the non-metasomatic fluorite in the Orefield shows delicate growth banding, and the occurrence of large cubic crystals, particularly in material deposited in the phase 3 and 4 events suggests that calcium fluoride was only very slightly saturated. In contrast, much of the baryte in the field displays colloform or fibrous textures suggestive of deposition in conditions of gross supersaturation. Dissolution is a difficult process to look at since, if there has been a complex fluid sequence, it is not always clear which fluid has been responsible for leaching a specific mineral. If the injection of fluid into the deposit was accompanied by tectonism, (Sibson et al., 1975) then evidence of a fluid may be preserved within fluid inclusions.

4.4.4: EQUILIBRIUM BETWEEN THE FLUID AND WALL ROCKS

In the Southern Pennine Orefield, the wall rocks are either limestone or dolomite. Evidence for equilibration between the wall rocks and the brine is useful in establishing pH limits for the fluid. Again corrosion textures are difficult to ascribe to a specific event. The slow moving solutions of phases 2, 3 and 4 would be expected to equilibrate with carbonates, especially considering the

low thermal gradients associated with these events. Type 3 inclusions are commonly associated with replacement deposits and presumably the fluid they contain was less equilibrated with carbonates than the phase 4 brines.

4.5: LIMITING SULPHATE CONCENTRATION

Constraints on the sulphate activities of the ore fluids are important since at 100°C, equilibrium between aqueous sulphur species is unlikely to be maintained if loss of total sulphur occurs by the removal of reduced sulphur species at a constant temperature and oxygen fugacity. The only sulphate mineral deposited by hydrothermal activity in the Southern Pennine Orefield is baryte, and therefore it may be reasonable to assume that the solubility product of barium sulphate controlled sulphate activity. Kramer (1969) applied factor analysis to subsurface brine analyses and noted a reciprocal relationship between the concentration of the two ions, again suggesting that control on the sulphate concentration of the fluid by baryte solubility. Brines rich in calcium and sodium are usually depleted in sulphates (Hanor, 1979) and this is attributed to processes of brine evolution (See chapter 6). Total molal sulphate (Graf et al., 1966; Downing and Howitt, 1969; Carpenter et al., 1974) concentrations of a number of very saline formation waters has been plotted against the molal sum of calcium and magnesium concentration (figure 4.5). An inverse relationship is apparent, which is shown as an upper concentration limit on the log molal sulphate versus molal magnesium + calcium

Figure 4.5

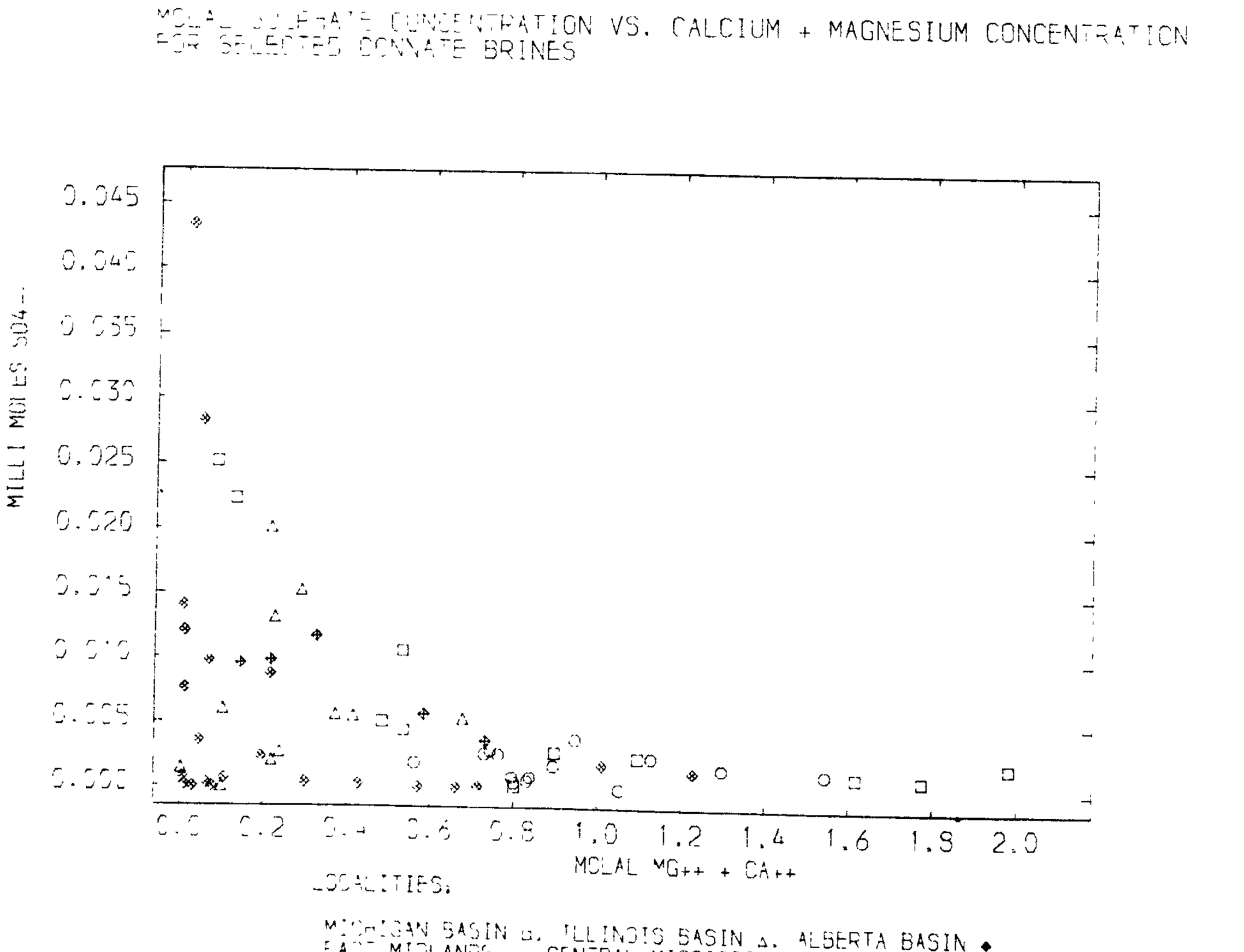

Figure 4.6

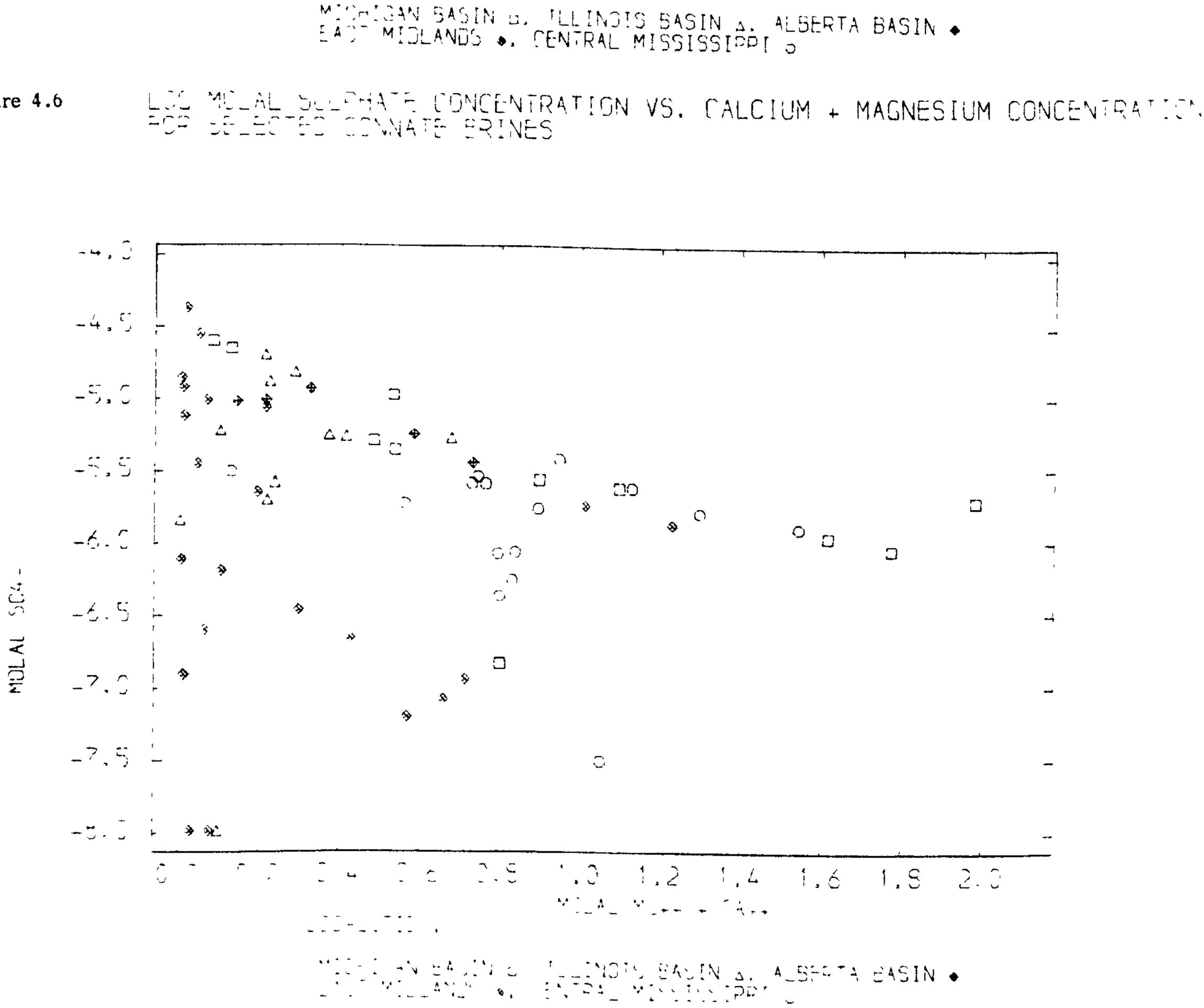

plot (figure 4.6). It appears that brines containing in excess of 1m calcium + magnesium do not usually contain more than $3x10^{-6}$ m total molal sulphate. This value may be taken as the expected maximum sulphate concentration that could have occurred in the phase 3 and phase 4 brines. If free ion activities are calculated (appendix 6.2), from this maximum total sulphate concentration, the free ion sulphate activities are found to be small (4×10^{-8} [phase 3]; 6×10^{-8} [phase 4]). These activities are small when compared with a postulated total sulphur activity of 10^{-5} (See section 4.8). They do not, however, represent equilibrium concentrations at 100°C, and if the residence time was prolonged, the activities would probably have fallen by two orders of magnitude. A maximum sulphate activity may be calculated by assuming saturation of calcium sulphate in the system (table 4.4, 4.5). Ellis and Mahon (1977) have suggested that the solubility of anhydrite may place an upper limit on the concentration of sulphate in a fluid, especially where calcium concentration is high. Although free sulphate activity must have been very low in the ore fluids, the ability of sulphate to form strong complexes with calcium and magnesium offsets the decrease in solubility due to the common ion effect. An upper limit of 0.05M SO_4^{-2} may be estimated from anhydrite solubility measurements at high ionic strengths and 100°C (Blount and Dickson, 1969). Maintenance of equilibria between aqueous sulphur species and reduction of sulphate is discussed at some length in section (4.8).

4.6: LIMITING BARIUM CONCENTRATION

The absence of anhydrite in hydrothermal deposits is usually considered to be the result of its increased solubility at lower temperatures. Since mineralization occurred over a small temperature range, increasing solubility on cooling does not explain the absence of anhydrite. The $[Ba^{++}]/[Ca^{++}]$ ratio of the ore fluid is probably a more important control. If the $[Ba^{++}]/[Ca^{++}]$ ratio of the fluid decreased then eventually anhydrite would become the stable solid sulphate phase. Similarly if the $[Ba^{++}]/[Ca^{++}]$ ratio increased, witherite would become the stable carbonate phase in place of calcite. Since neither anhydrite nor witherite occur within the field, the fluid composition must fall between the two stability boundaries. Plotting these stability boundaries on a graph of log $[Ca^{++}]/[H^{+}]$ against log $[Ba^{++}]/[H^{+}]$ (Helgeson, 1967), free ion concentration limits for barium may be estimated for the phase 3 and 4 hydrothermal events (Appendix 6.2). $[Ca^{++}]/[H^{+}]$ ratios have been calculated for the two events and are shown on figure 4.7. The diagram shows that the phase 4 fluid was able to stabilize higher concentrations of barium than the phase 3 fluid. The lower free ion concentration limit is 0.4-1.0ppm and is considerably higher than the sea water range 0.01-0.05ppm (Hanor, 1979). The difference is probably greater since the limits for the barium concentration of the hydrothermal fluids are represented as a free ion concentration limit. Total barium concentration will be increased as a result of sulphate, chloride and carbonate complexing. The maximum free barium molal concentrations at

Figure 4.7

Plot of log a_{Ca}^{2+}/ a_{H}^{+} against log a_{Ba}^{2+}/ a_{H}^{+} for the phase 3 and phase 4 ore fluids.

Boundary (a) divides the stability fields of baryte and anhydrite and boundary (b) defines the stability fields of calcite and witherite. Since anhydrite and witherite are not present within the mineral assemblage of the Orefield, it is assumed that mineral deposition took place in the calcite+baryte stability field. Since the pH of the fluids can be estimated and the calcium activity is known, the barium activity range for the two ore fluids may be estimated.

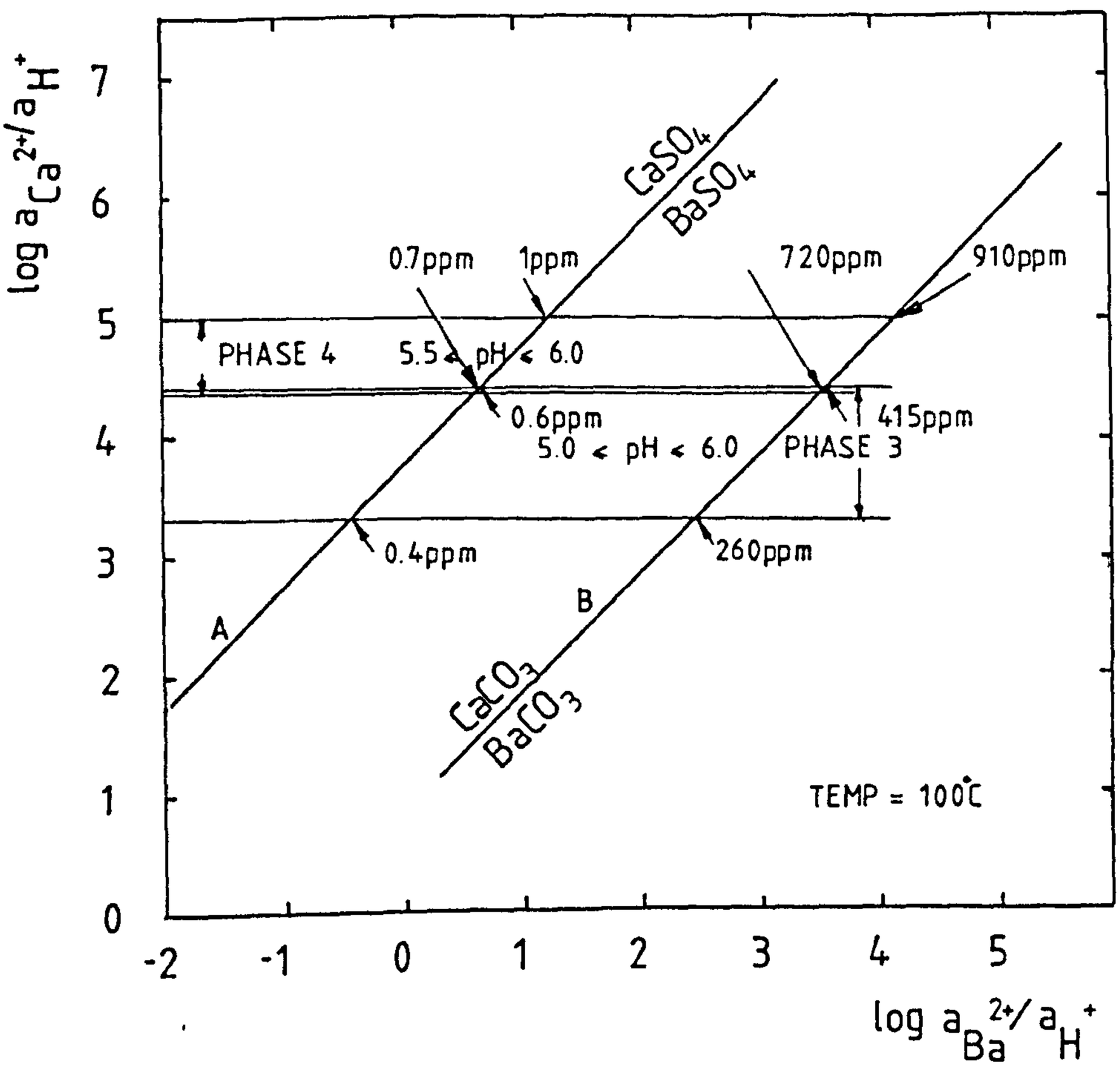

which calcite formation will take place are relatively low for the phase 3 event.

4.7: LIMITING ACIDITY

The formation of authigenic K-feldspar and muscovite in the vicinity of ore bodies and fractures which are considered to have carried ore fluids is often used to limit the pH of the ore-forming brine (Heyl et al., 1964; Giordanao and Barnes, 1981). Where the Southern Pennine ore fluids have interacted with siliceous rocks, stable silicates included chlorite, kaolinite, smectite and illite (Ineson and Mitchell, 1973). There is little evidence of K-feldspar and muscovite having been stable in the ore fluids. If the relative stabilities of these minerals are plotted on to a diagram of log $[Na^+]/[H^+]$ against log$[K^+]/[H^+]$, and the Na/K ratios of the ore fluids superimposed, it can be seen that both muscovite and probably K-feldspar were unstable in the phase 3 and 4 fluids. The minimum pH of the ore fluids can be estimated if an alteration assemblage of quartz+kaolinite+ smectite is used. Minimum pH values for the phase 3 and 4 ore fluids did not probably fall significantly below 5.2 and 5.9 respectively. These values were estimated from the point of intersection of the Na/K ratio line on to the smectite-kaolinite stability boundary (figure 4.8). Equilibration between fluids and silicates is known to take place slowly at low temperatures (Krauskopf, 1979), but if formation waters were resident in an aquifer for a sufficient period of time, equilibration may have occurred.

Figure 4.8

Stability relations of K-feldspar, muscovite, kaolinite, smectite and albite at 85°C and 1 atmosphere pressure as a function of $\log(K^+)/(H^+)$ and $\log (Na^+)/(H^+)$. Quartz saturation has been assumed. The stability fields were taken from Montoya and Hemley (1975).

Average molal concentrations of Na^+ and K^+ were used for fluids 3 and 4.

Phase 3 : $m_{Na^+} = 2.4$; $m_{K^+} = 0.012$.

Phase 4 : $m_{Na^+} = 0.58$; $m_{K^+} = 0.008$.

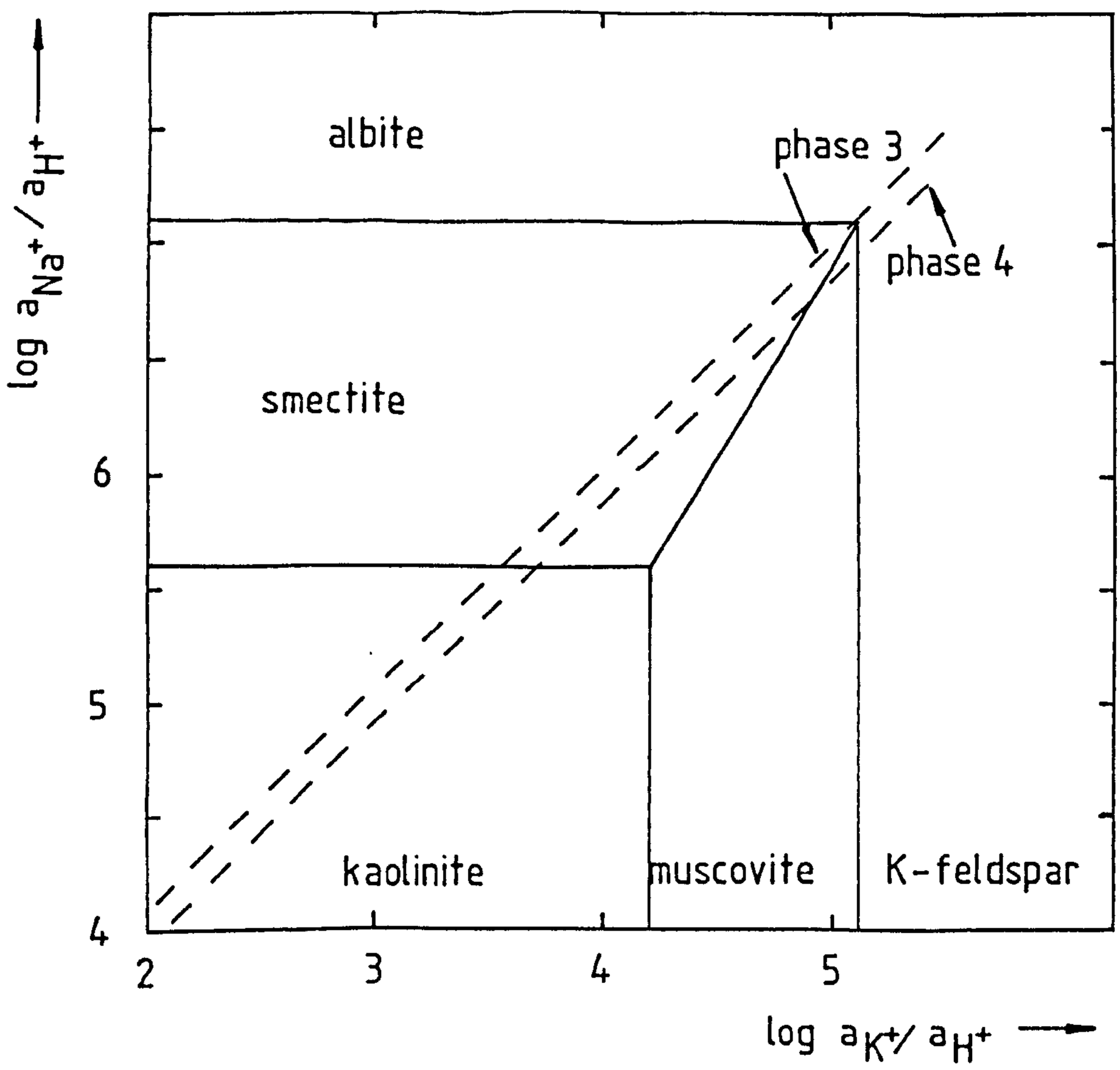

Evidence for brine-aluminium silicate equilibria in sedimentary aquifers comes from a study of moderately saline interstitial waters in recent sediments from the Kettleman Dome, California (Merino, 1975). Albite, K-feldspar, muscovite and sodium montmorillonite are present in the Tertiary sandstones. Plotting directly measured acidities, sodium and potassium concentrations of the interstitial brines on to an aluminium silicate stability diagram, points were found to group closely about the albite-K-feldspar-muscovite triple junction. Further evidence of brine-aluminium silicate equilibration was indicated by the alteration of kaolinite to muscovite at deeper levels of the formation, suggesting buffering of acid solutions. If the South Pennine mineralizing brines had been in prolonged contact with Namurian shales, then the mineral assemblage of quartz+kaolinite+mixed layer illite and smectite, reported by Spears and Amin (1981) for the sediments in the Tansley borehole may have adjusted th pH of the fluids.

The stability of calcite is strongly controlled by pH and if it can be proved that calcite was a stable mineral phase during fluorite deposition, then the acidity of the fluid can be well constrained. Plate 4.1 shows two sections where fluorite has been deposited on calcite. The scalenohedral crystal from Ladywash Mine appears practically uncorroded, indicating that the phase 3 fluid was neither significantly undersaturated with calcite nor oversaturated with fluorite. Ames (1961) showed that the replacement of calcite by fluorite is not inhibited by the formation of an inert layer of fluorite on the reaction boundary and this mechanism therefore cannot be used to explain the uncorroded

Plate 4.1

Textural relationships between early-formed carbonates and later fluorite.

1) A scalenohedral calcite crystal unaffected by exposure to the type 3 ore fluid. Sample from Ladywash Mine.
(f = fluorite; ct = calcite)

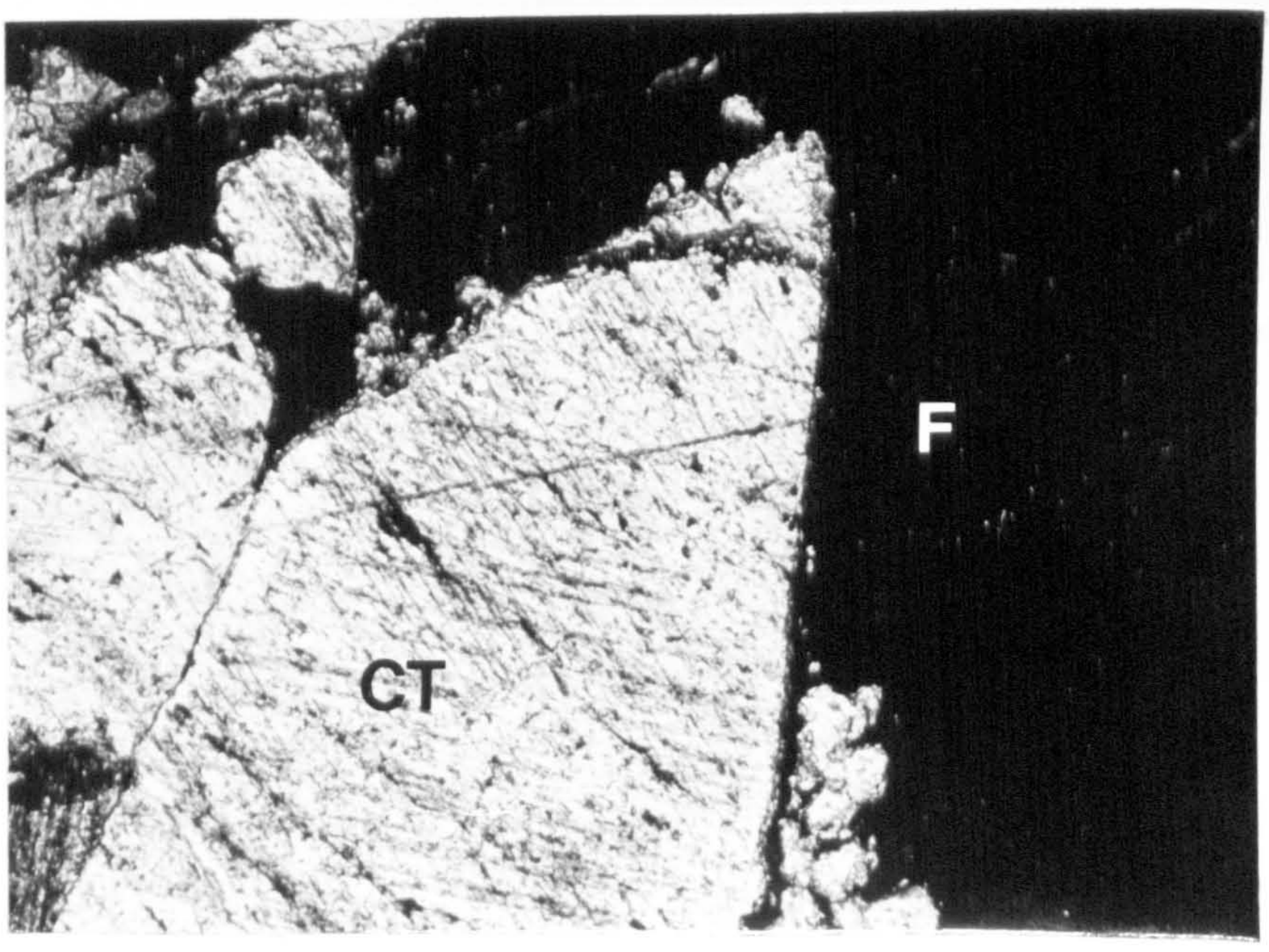

Width of field: 3.2mm

Uncorroded calcite crystal covered by later fluorite, probably deposited in the phase 3 hydrothermal event. Sample from Mill-town Quarry, Ashover.

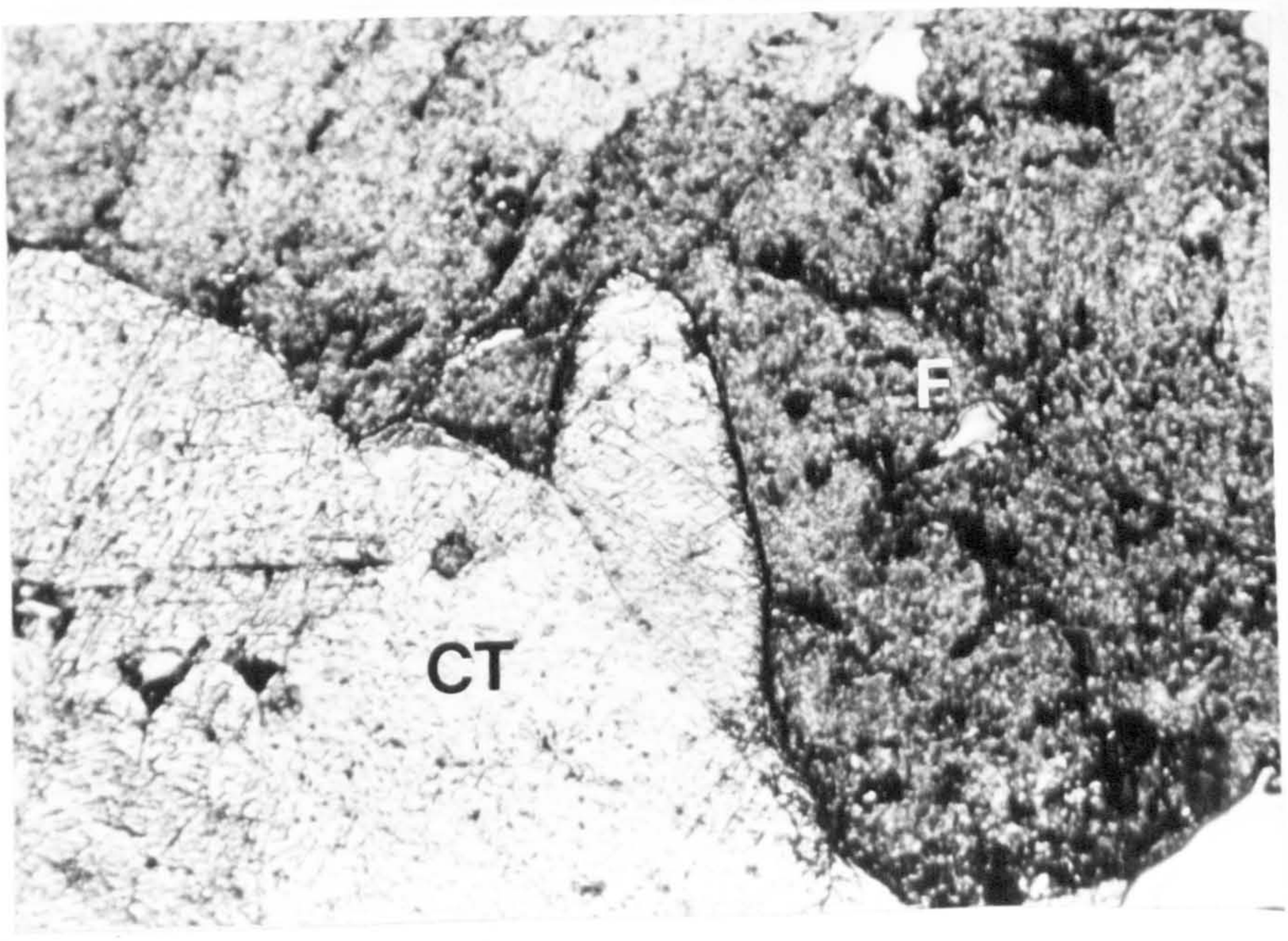

Width of field: 3.2mm

Plate 4.2

Textural relationships between early-formed calcite and later fluorite.

1) Fluorite (f) appears to have replaced dolomite and quartz. The sample was taken from Moor Farm (opencast site).

Dolomite = Do; Quartz = Q

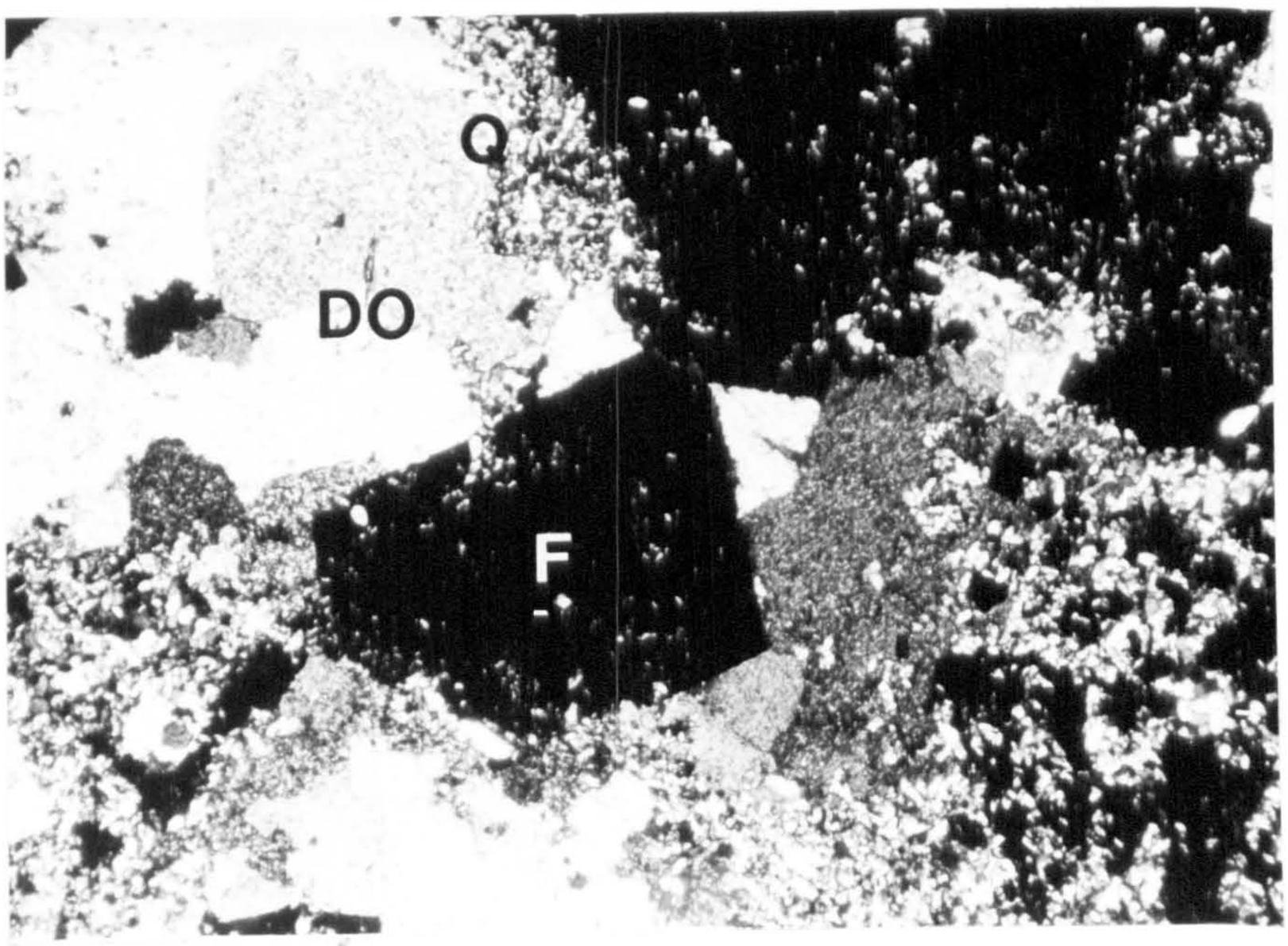

Width of field: 3.2mm

Corroded white calcite covered by later fluorite. Dissolution of the calcite may not, however, have occurred as a result of contact with the fluorite-forming ore fluid. The sample was taken from the Great Rake, Milltown Quarry.

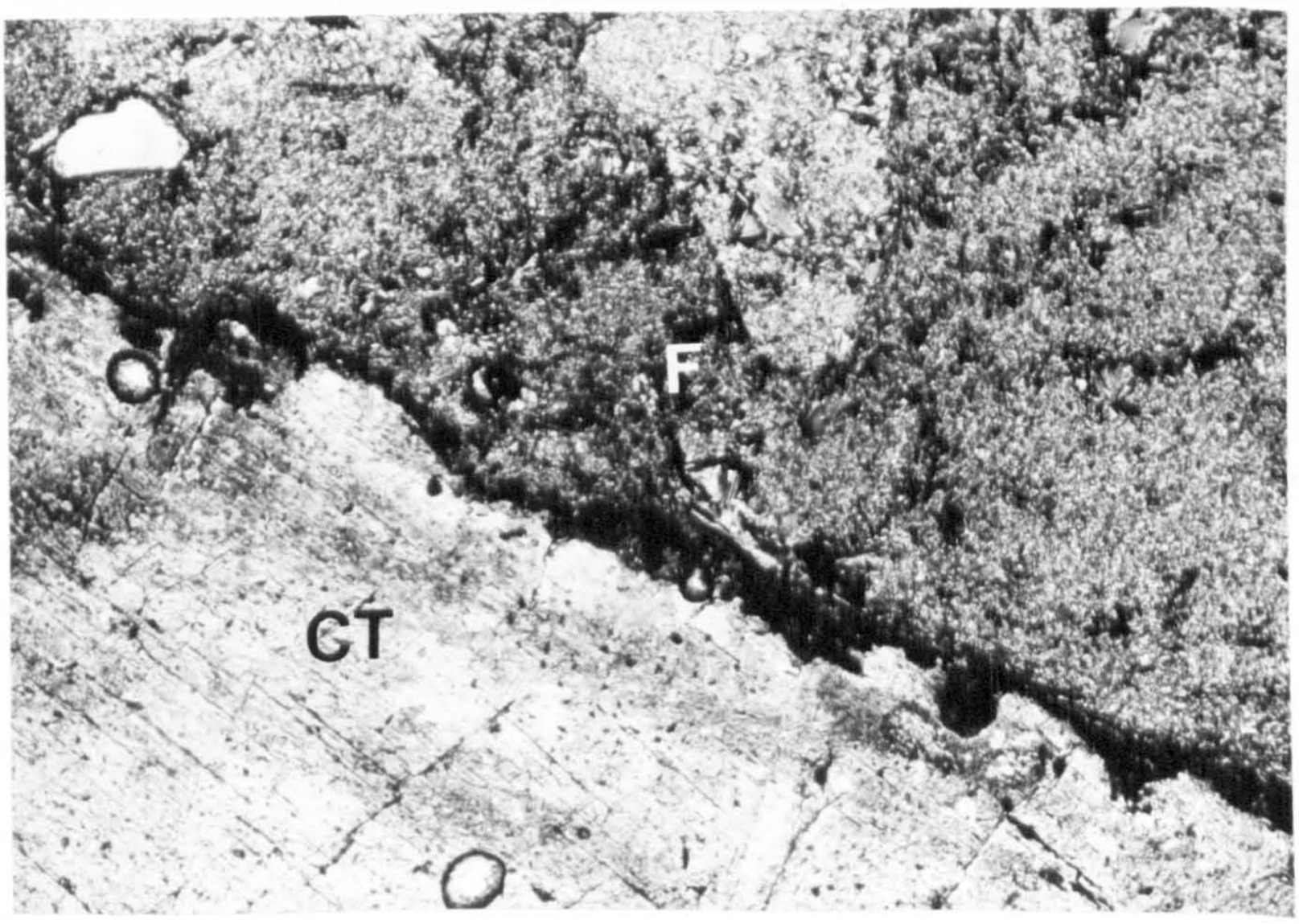

Width of field: 3.2mm

margin. Corrosion may occur simply as a result of the undersaturation of calcite, as would take place on cooling without pH change. The sample from the Great Rake (plate 4.2) shows a slightly corroded boundary of early white calcite, and could have been produced by the phase 3 ore fluid or an earlier hydrothermal event. Replacement (plate 4.2) of limestone by fluorite may take place as the result of changing the $[F^-]/[H^+]$ ratio (figure 4.11). Gas pressures estimated from crushing fluid inclusions suggests that carbon dioxide pressures did not exceed 16 atmospheres (appendix 6.15) in the third and fourth events. Therefore, if calcite was a stable mineral phase the pH cannot have been lower than approximately 5 in both fluids. The relationship between carbon dioxide fugacity, pH and calcite stability for phases 3 and 4 is shown in figure 4.12.

4.8:: LIMITING OXYGEN FUGACITY

The chemistry of the phase 3 and the phase 4 ore fluids can be described usefully in terms of oxygen fugacity and pH at 100°C, using a $\log fO_2$-pH diagram. Details of the theory and construction of such diagrams are given by Barnes and Kullerud (1961) and Holland (1965) and are summarized in appendix 6.5. The only aqueous sulphur species considered are SO_4^{--}, H_2S, and HS^-. The pH was never low enough to form HSO_4^- and solid sulphur (S_2). The boundaries between the sulphur species are shown as dashed lines. Sulphate is the only oxidized species while H_2S and HS^- represent the reduced species. Ohmoto and Lasaga (1982) have thrown some doubt on

the value of such diagrams at low temperatures. Using experimental data, they have determined the rate at which sulphate is inorganically reduced to sulphide at various acidities and temperatures. Some reaction rates are shown in table 4.3.

TABLE 4.3

REACTION RATES FOR INORGANIC SULPHATE REDUCTION (TOTAL SULPHUR = Ø.ØlM)

Temperature	Time (years)	
pH range	4 - 7	9
150°C	4×10^{3}	10^{9}
100°C	4×10^{5}	10^{12}
50°C	2×10^{8}	10^{16}

(Ohmoto and Lasaga, 1982)

If the total sulphur concentration is reduced by a factor of ten, the times are also reduced by the same factor. As can be seen, in alkaline conditions the reaction rates are exceedingly slow. Their conclusion is that if fluid flow was typical of a fracture system with cooling rates between Ø.ØØl and Ø.1°C hr^{-1}, equilibrium would not have been attained below 350°C. The very small thermal gradients estimated from the fluid inclusion homogenization temperatures for phases 3 and 4 indicate that flow rates were probably more similar to values associated with porosity-controlled flow, with a cooling rate of 10^{-4}°Chr^{-1}. Equilibration could then have occurred above 200°C. It is probable that the fluids were resident within an aquifer before moving into the limestone. If the fluids were resident for 40,000 years, aqueous

sulphate and reduced sulphur would have had time to equilibrate. If the sulphate concentration was similar to that measured in the Michigan Basin (Graf et al., 1966) and the Mississippi Valley Basin (Carpenter et al., 1974) initial sulphate activity would have been low ($1-4 \times 10^{-8}$). The fluid may have moved from the aquifer either isothermally or the movement may also have involved some heating. In the first case it can be presumed that sulphate activity had been reduced to the appropriate levels through normal processes of equilibration and that sulphur species were in equilibrium on initially entering the limestone or dolomite host rocks. In the second case the sulphate activity would have probably been two orders of magnitude too high, especially if heating occurred in the range 50°C-100°C. This disequilibrium would probably have had little effect on the calculated mineral stability boundaries since the ratio of reduced to oxidized sulphur would have remained high. If the oxygen fugacity of the system increased by some means, then equilibration may have occurred by the oxidation of reduced sulphur. It is more probable that deposition occurred in the oxygen fugacity range 10^{-57} - 10^{-55}. There is little evidence for the "equilibrium" coprecipit-ation of baryte and fluorite or baryte and galena (Robinson and Ineson, 1979). Bacterial reduction of sulphate in the temperature range 70-110°C is unlikely, although some laboratory strains are able to withstand sodium chloride concentrations up to saturation and temperatures up to 70°C (Postgate, 1979). Inorganic methods of sulphate reduction (Barton, 1967) have also been shown to be thermodynamically impractical (Sverjensky, 1981). Therefore, as ore deposition progressed, the sulphate

concentration of the ore fluid would have remained relatively constant while the reduced sulphur concentration would have fallen and hence the aqueous sulphate and sulphide concentrations would have moved away from equilibrium. The magnitude of this decrease would have, however, been very limited.

Sverjensky (1981) has estimated the solubility of galena in a fluid, very similar to the type 3 ore fluid. The maximum amount of lead sulphide such a solution could have carried was 10^{-6}m. If the total sulphur content of the fluid was 0.0001-0.00001m, removal of 10^{-6}m of reduced sulphur would not greatly have effected the sulphate/sulphide ratio or the total sulphur concentration. Hence, the aqueous sulphur species boundaries would remain within one log unit on the oxygen fugacity scale.

Assuming total sulphur concentrations for the ore fluid, both the oxygen fugacity and the pH may be further limited using sulphide mineral assemblage stabilities (Giordano and Barnes, 1981). LogfO_2-pH plots have been drawn for total sulphur concentrations of 0.01 and 0.00001m (figures 4.9 and 4.10). Probably the lowest total sulphur concentration to maintain sulphide stabilities is 10^{-7}. A useful upper limit on oxygen fugacity is the galena-anglesite stability boundary. There is little evidence of anglesite forming as a primary mineral within the orefield. A second upper limit is the haematite-pyrite stability boundary which depends on the reduced sulphur concentration in the sulphate stability field. Lowering of the reduced sulphur activity would lower the overall position of the boundary as would lowering the total sulphur activity of the system. The lowest

Figure 4.9

Plot of the logarithm of oxygen fugacity against the pH of the ore-forming environment.

A temperature of 100°C and a total sulphur activity of 10^{-5} has been assumed. Reduction of the total sulphur activity of the system has reduced the extent of the bornite+pyrite stability field. The shaded area shows the possible $\log fO_2$-pH range in which ore formation may have occurred.

PY = pyrite. CP = chalcopyrite. B = bornite. Po = pyrrhotite.

The fields within which mineral deposition took place have been shaded.

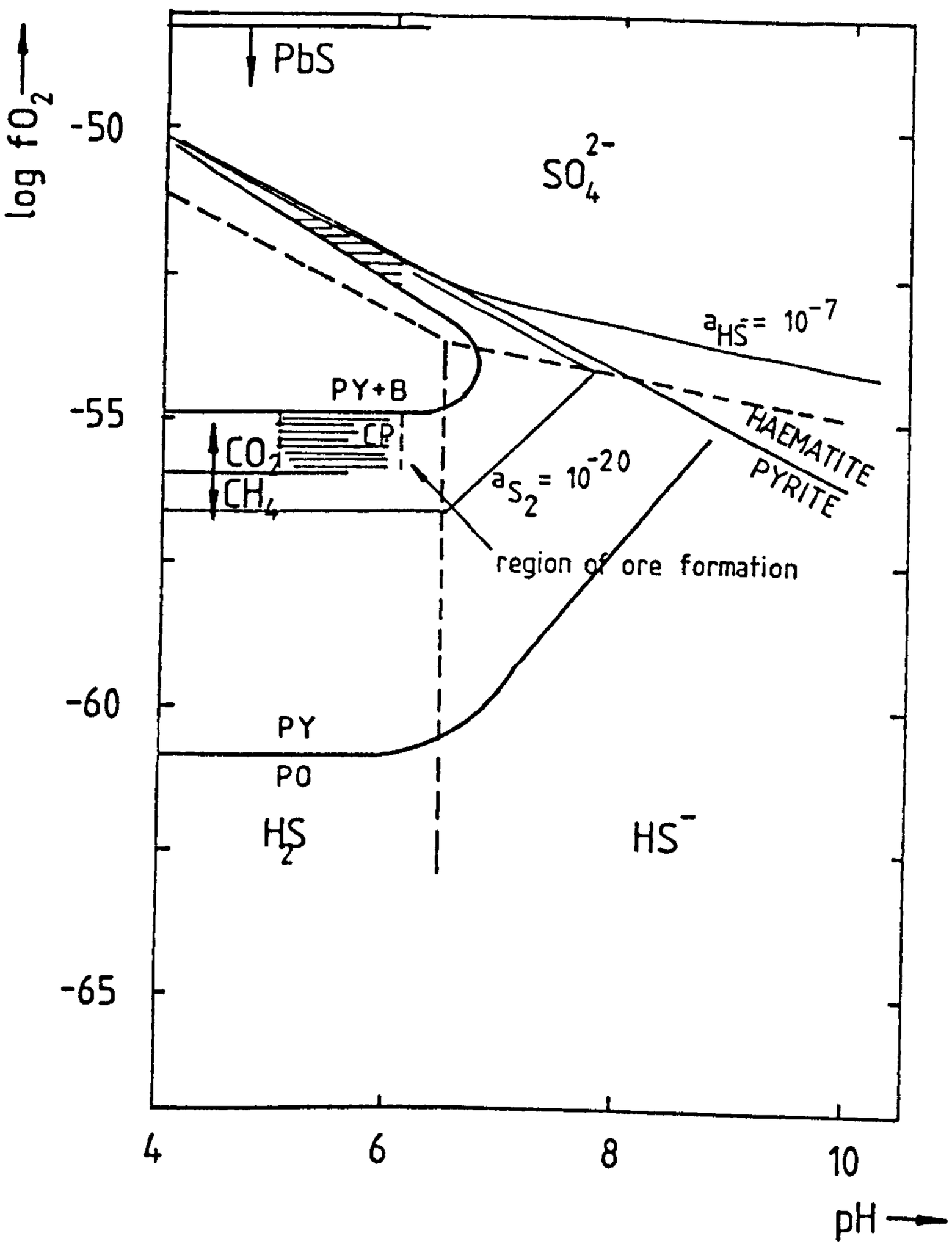

Figure 4.10

Plot of the logarithm of oxygen fugacity against the pH of the ore-forming environment.

A temperature of 100°C and a total sulphur activity of 10^{-3} has been assumed. Assuming a system in equilibrium, ore formation must have taken place below the haematite-pyrite stability boundary and above the pyrite-pyrrhotite boundary. Ore formation must also have occurred outside the pyrite+bornite stability field. The sulphur fugacity, calculated from the iron content of sphalerite, is shown as a contour on the diagram. The dashed lines divide the regions of reduced and oxidized sulphur speciation.

PY = pyrite. CP = chalcopyrite. B = bornite. Po = pyrrhotite.

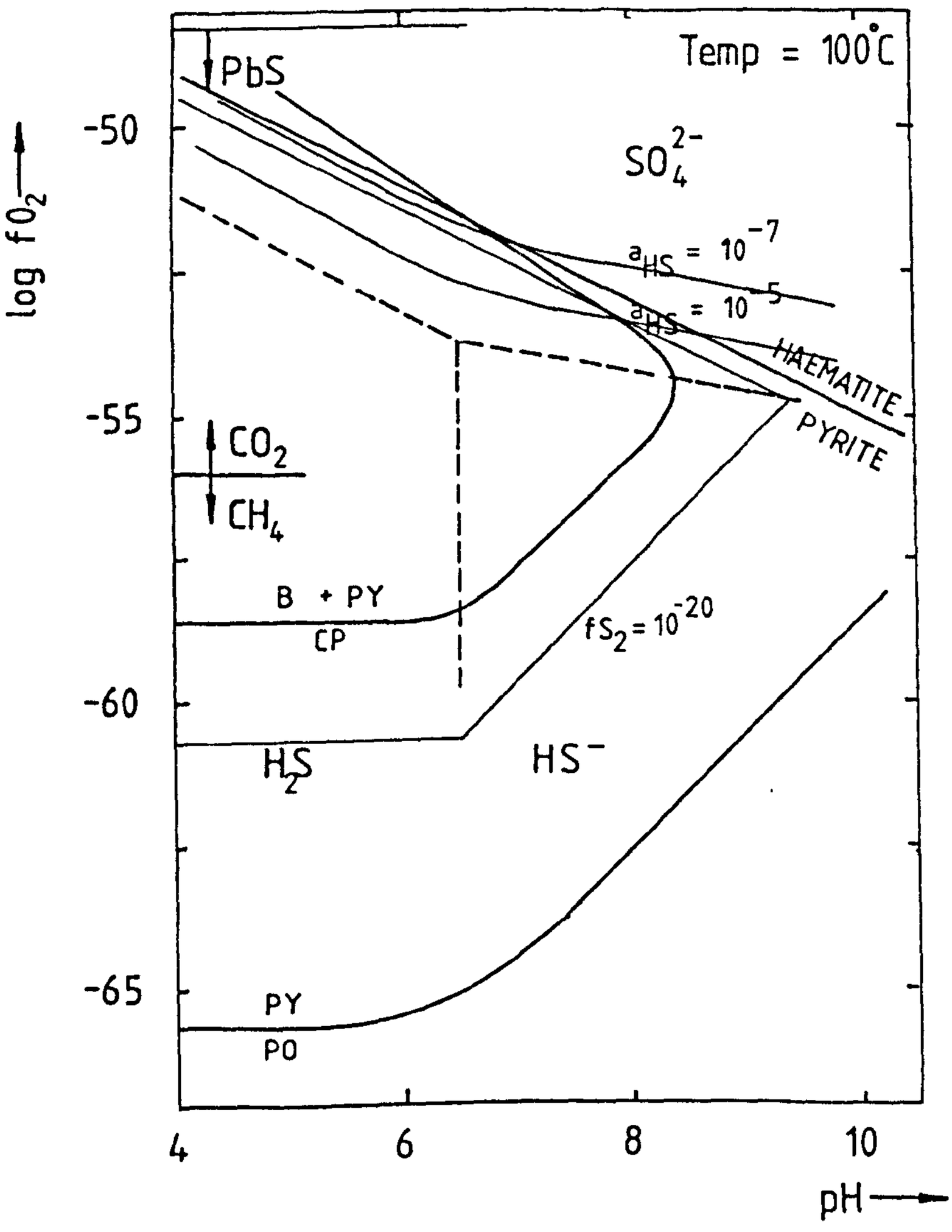

oxygen fugacity value permissible is formed by the pyrrhotite-pyrite stability boundary ($\log fO_2 = -62$). However, a more realistic limit may be formed by the CO_2/CH_4 stability boundary ($\log fO_2 = -56$). Below this boundary, CO_2 fugacity drops very rapidly and consequently carbonate stability decreases. The pyrite + bornite-chalcopyrite stability boundary is useful for further limiting both the oxygen fugacity within the extreme limits already described and the pH of the ore-forming environment. Bornite, like pyrrhotite is not found in association with galena and sphalerite within the district. As can be seen from figure 4.10, where the total sulphur concentration is 0.001m, the bornite + pyrite stability field is large. If the lower oxygen fugacity limit was 10^{-57}, the pH at which deposition occurred could not have been less than 8. At a lower total sulphur concentration ($\Sigma S = 10^{-5}$), the bornite + pyrite stability field is greatly reduced and ore deposition could have occurred between the $\log fO_2$-pH limits already suggested (10^{-57} -10^{-55}).

4.9: LIMITING SULPHUR FUGACITY

Sphalerite occasionally occurs as inclusions within fluorite associated with galena, pyrite and bravoite. Providing that the solution was saturated with iron disulphide during sphalerite deposition, the FeS content of the sphalerite may be used to estimate the sulphur fugacity of the ore-forming environment. Two equations have been used to make the estimate, both of which are based on the equation:

$$(FeS)_{sp} + 1/2S = (FeS_2)$$

The temperature of deposition T (^{o}K), may be estimated from fluid inclusion studies. The first equation used was:

$$\log X_{py} = 7.16 - 7730/T - 0.5 \times \log fS_2$$

$\log X_{py}$ is the mole fraction of FeS in sphalerite in the pyrite stability field (Toulmin and Barton, 1964). Temperature T was taken as $373^{o}K$ and the FeS mole fraction range as 0.0017-0.0003 (Appendix 3). The calculated sulphur fugacity range is $10^{-22} - 10^{-20}$. An alternative equation was given by Scott and Barnes (1971).

$$\log X_{py} = 6.65 - 7340/T - 0.5 \times \log fS_2$$

The different coefficients are derived from variations in the thermodynamic data used. Scott and Barnes equation gives a sulphur fugacity range of $10^{-20.5} - 10^{-19}$. These values are calculated from data which was gathered at temperatures in excess of $350^{o}C$, and extrapolation down to $100^{o}C$ obviously introduces errors (Barton and Skinner, 1979). The values do appear to be reasonable when a 10^{-20} sulphur fugacity contour is plotted on to the $\log fO_2$-pH diagrams (figures 4.9 and 4.10). The contours fall approximately on to the postulated $\log fO_2$-pH range.

4.10: LIMITING CARBON DIOXIDE FUGACITY

Carbon dioxide fugacity may be estimated in a number of ways. A total gas pressure can be estimated from the expansion of the vapour bubble on crushing a fluid inclusion. Using density data from Potter and Brown (1977) to estimate the degree of filling, a corrected maximum gas pressure at 100°C probably does not exceed 16 atmospheres. Nitrogen, methane and argon are probably present in minor amounts as well as carbon dioxide. Since the calcium activity of the fluid is known, the dissolved CO_2 and therefore the carbon dioxide fugacity can be calculated if calcite saturation is assumed. An estimate of the pH must also be made to satisfy the equation.

$$CO_2(g) + H_2O = 2H^+ + CO_3^{--}$$

Table 4.5 shows CO_2 fugacities calculated for phases 3 and 4. The higher calcium activity of the phase 4 fluid gives lower CO_2 fugacities than the phase 3 fluid (figure 4.12).

A further restriction on CO_2 fugacity may be applied if the ore fluid has produced replacement of limestone or calcite by fluorite. There is much evidence for fluorite metasomatism in the orefield, and such fluorite normally contains type 3 rather than type 4 fluid inclusions. The reason for this can be seen when the chemistry of the replacement process is examined.

Figure 4.11

Plot of the log of the $a_{CO_3^{2-}}/a_{H^+}$ ratio against the log of the $a_{F^-}^2/a_{H^+}$ ratio in the ore fluid.

The diagram is calculated for a system in equilibrium at 100°C. Fluorite saturation has been assumed in order to calculate the $a_{F^-}^2/a_{H^+}$ ranges for the type 3 and type 4 fluids. The diagram shows that if the two fluids adopted a pH of 6, fluoritization of limestone would progress at higher levels of carbonate activity in the phase 3 fluid than in the phase 4 fluid. Therefore, given similar conditions of ore formation, the type 3 fluid is more likely to produce limestone metasomatism than the phase 4 fluid.

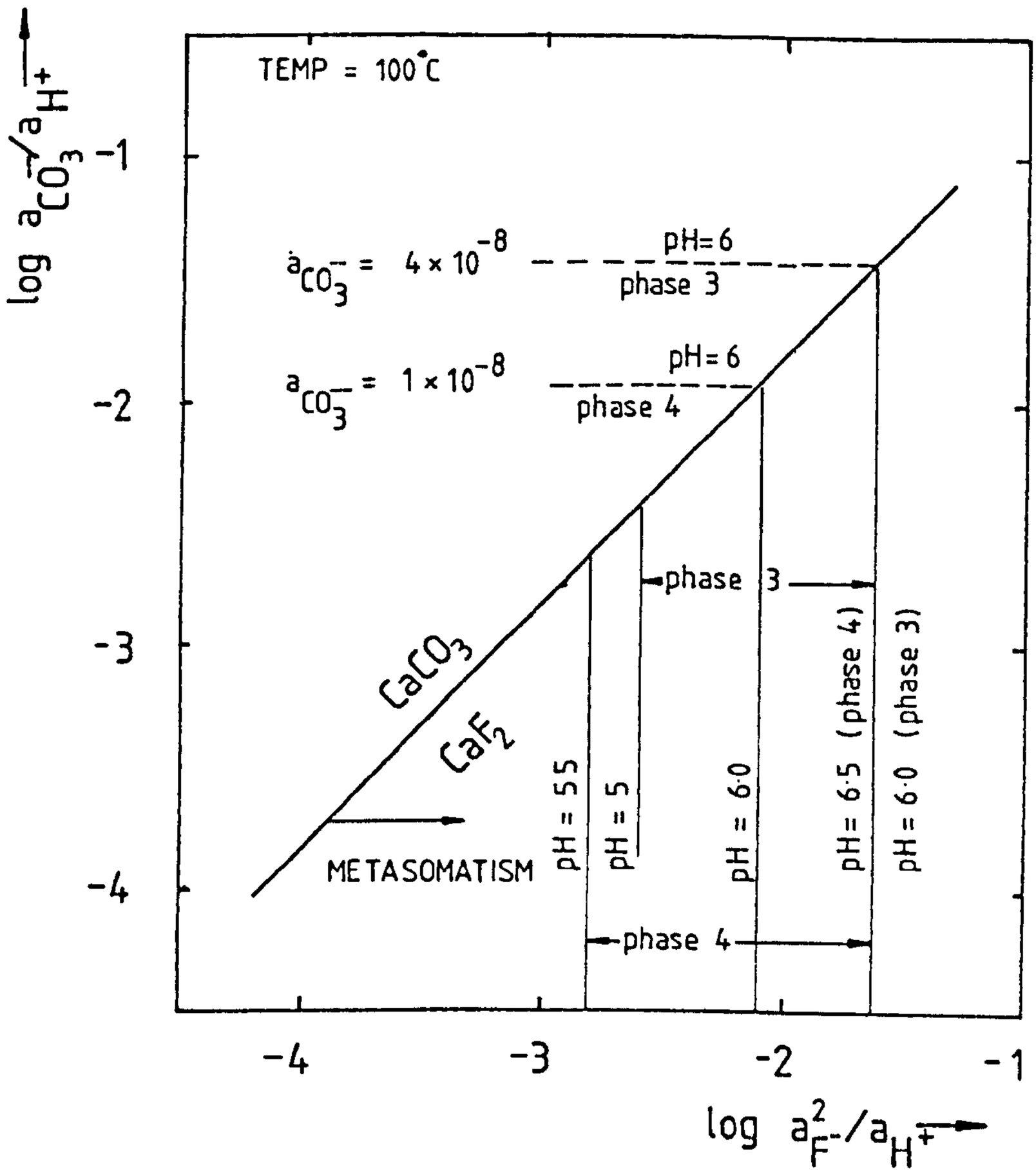

Figure 4.12

Plot of the logarithm of carbon dioxide fugacity against the pH of the ore fluid.

The stability of calcite may be shown for the phase 3 and phase 4 ore fluid in terms of CO_2 fugacity and pH. The stability boundaries have been calculated for the measured calcium activities of the two fluids at a temperature of $100^{o}C$.

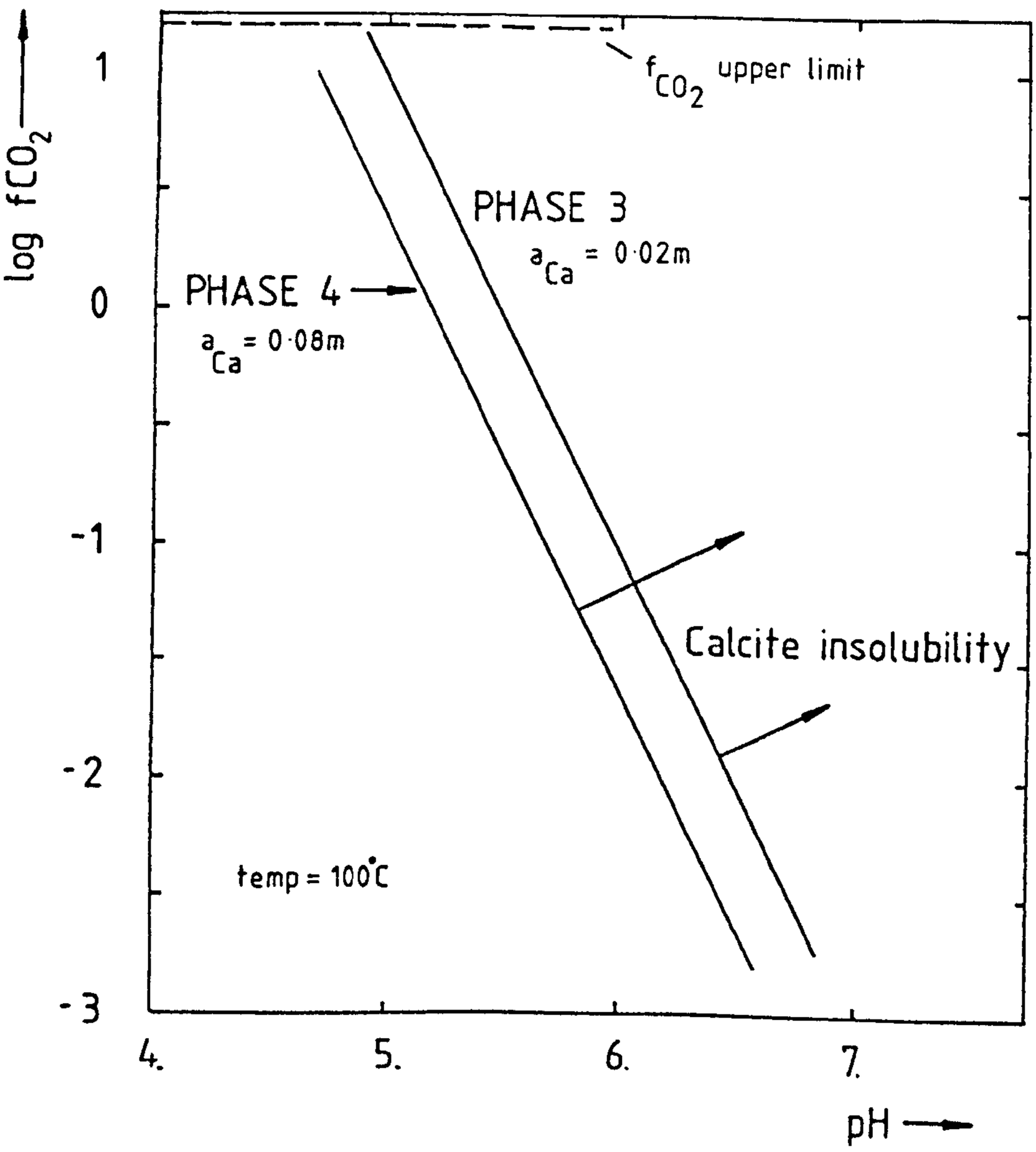

Replacement may occur by the reaction.

$$CaCO_3 + 2F^- = CaF_2 + CO_3^{--}$$

For fluorite deposition to take place, the fluid must have been saturated with calcium fluoride. Therefore, the fluoride activity may be calculated from the calcium activity of the ore fluid (table 4.5). Using the fluorite-calcite stability diagram (figure 4.11), it can be seen that to produce fluorite stability the $[F^-]/[H^+]$ ratio must have been relatively high. The dissolved CO_2 range at which replacement would have occurred is shown on the diagram. Figure 4.11 shows that if the phase 3 and 4 ore fluids had a similar pH (6), replacement would have occurred at carbonate activities four times greater in the phase 3 fluid when compared to the phase 4 brine.

4.11: DISCUSSION

Type 2, 3 and 4 fluid inclusions have been analysed for their major dissolved salt contents, and calcium and sodium were found to be the dominant cations. Expressing the composition of such fluids in terms of weight percent sodium chloride is clearly erroneous, although such an expression may produce a reasonably valid density estimate. Both potassium and magnesium concentrations were found to be low, although an inverse relationship between calcium and magnesium concentrations was observed (table 4.4 and 4.5), suggesting a possible control on magnesium activity by

dolomitization. Despite high calcium concentrations, the ionic strengths of the solution are calculated to be much lower than the stoichiometric ionic strengths when the formation of the complex $CaCl^+$ is taken into consideration. Unfortunately no satisfactory analysis of the phase 1 fluid could be made and the calculated ionic strength of the phase 2 fluid precluded the use of readily available thermodynamic data.

The absolute value of the association constant of $CaCl^+$ is probably questionable and the value used in the calculations (appendix 6.1) was taken from Giordano and Barnes (1981). Richardson and Holland (1979a) reported that in their experiments on fluorite solubility, the fit between experimental and calculated data was not improved significantly by taking the formation of $CaCl^+$ into account. Therefore the association constant may have a value closer to unity than that used. Macroscopic and microscopic textures displayed by much of the non-metasomatic fluorite formed in all four events suggests that deposition occurred from fluids which were only slightly saturated with calcium fluoride. In contrast much of the baryte in the field exhibits colloform or fibrous textures, characteristically produced in conditions of gross supersaturation. Therefore, it is reasonable to assume deposition of fluorite occurred within a system which was in, or had closely approached equilibrium, taking the simple evidence provided by mineral textures (Barton et al., 1977). Similar conclusions can be made for pyrite and bravoite, which both display delicate growth structures and are frequently included within phase 3 and 4 fluorites. Equilibrium textures would not be expected where a

solution with high metal concentrations mixed with a solution rich in reduced sulphur.

Calcium-rich fluids, present in sedimentary subsurface environments are uniformly depleted in sulphate ions. This may be attributed to the process of ultrafiltration, the common ion effect and removal by sulphate reducing bacteria (Graf, 1982). Therefore, it is postulated that these brines contained very low sulphate concentrations. An upper limit set by assuming the saturation of anhydrite produces a relatively low sulphate activity. It is more probable that the sulphate content of the fluid was controlled by the ion activity solubilty product of baryte (Kramer, 1969), as this mineral was the only sulphate compound to achieve saturation throughout the hydrothermal history of the deposits (table 4.5). Limits to barium activity have been placed by using the baryte-anhydrite and calcite-witherite stability boundaries to provide upper and lower values. The retrogressive temperature-solubility relationship of anhydrite is often given as the reason why anhydrite is not seen in hydrothermal ore deposits (Holland and Malinin, 1979), but this is probably not important when considering the Southern Pennine Orefield. Barium concentrations are often high in fluids dominated by calcium chloride, and this is presumably the result of the similarity in the chemical behaviour of the two elements

The acidity (pH) of the ore-forming fluids may have been limited by the clay mineral assemblage of potential reservoir rocks, the wall rock reactions at the site of ore deposition and sulphide mineral assemblages deposited from the brines. As a starting point, it seems unlikely that

solutions moving slowly through carbonate rocks could maintain a low pH level, given the estimated carbon dioxide fugacities and the calcium activities of the ore forming environment and it is suggested that buffering would occur quickly. The siliceous wall rock alteration assemblages suggest an approximate minimum pH of the ore fluids of 5.2 (phase 3) and 5.9 (phase 4). If the ore fluids had equilibrated with Namurian shales, the pH would probably not have fallen below this value at 100°C. Where fluorite has been deposited directly on to early-formed crystals of calcite, both corroded and uncorroded boundaries are observed. The former may be produced simply by undersaturation of the fluid with respect to calcite, a condition further indicated by the lack of any textural evidence suggesting coprecipitation of both calcite and fluorite. An upper limit to the pH is difficult to quantify, but sulphide solubilities may be useful since their solubility decreases with increasing pH (Anderson, 1973; Sverjensky, 1981). At a pH of 6, and a temperature of 100°C, galena solubility in a phase 3 fluid is approximately 0.2ppm. This concentration decreases by a factor of ten for each unit pH increase. Therefore, an upper pH limit has been taken as the neutral value (6.1) at 100°C. A total sulphur activity of 10^{-5} is favoured since the bornite+pyrite field is much reduced in terms of its oxygen fugacity-pH limits. Therefore, deposition may have occurred within the estimated pH range while maintaining calcite stability and retaining a chalcopyrite+pyrite sulphide assemblage.

Sulphur fugacities calculated from the iron contents of sphalerite broadly agree with the estimated oxygen fugacity-

pH limits. The use of sulphides to limit these parameters depends on the equilibration between aqueous suphur species. It has been argued that, although disequilibrium between oxidized and reduced sulphur was almost certain to have occurred, the high reduced to oxidized sulphur activity ratio ($\log fO_2$ = -57 - -55) present in the fluid together with the removal of only small quantities of reduced sulphur would not tend to significantly move sulphide stability boundaries.

Given the high calcium concentrations within the phase 2, 3 and 4 fluids and the maximum carbon dioxide pressures calculated from fracturing fluid inclusions, carbon dioxide fugacity probably never exceeded 16 atmospheres. Low carbon dioxide fugacities are further suggested by the abundant replacement deposits which may only have formed at high fluoride/carbonate activity ratios within the fluid. In such conditions, calcite undersaturation is probable but does not represent a necessary control on the metasomatic process (Ames, 1961).

4.12: CONCLUSIONS

1) Calcium and sodium chlorides were the dominant salt components in the ore fluids. Calcium chloride was the dominant salt in the type 2, 4 and 5 brines.

2) Delicate growth banding in large, well formed crystals of fluorite with intricately formed sulphide inclusions suggests mineral deposition in conditions of mineral saturation [equilibrium].

TABLE 4.4.

PHYSICAL AND CHEMICAL CHARACTERISTICS OF TYPE 1, 2 AND 5 FLUID INCLUSIONS

	Type 1	Type 2	Type 5
Fluid density at 25°C	1000-1069	ca 1390	ca 1282 kgm^{-3}
Temperature, °C	100-171	62-82	66.3, 68.3
Total Na	0.0-1.7	0.17-0.34	0.0-0.3m
Total Ca	-	3.33-3.42	2.5-2.6m
Total Mg	-	0.002-0.004	-
Total K	-	0.008-0.015	-
Stoiciometric ionic strength.			
I	ca 2.	10.4-10.5	ca 8.

3) By analogy with high salinity $CaCl_2$-NaCl formation waters, sulphate concentration was probably low in the main ore-forming fluids. Saturation of anhydrite provides an upper limit for free molal sulphate concentration.

4) An aluminium silicate alteration assemblage of smectite+ kaolinite+quartz indicates the type 3 and 4 ore fluids had a pH of approximately 5.2 and 5.9. A upper pH limit of 6 is required for sulphide transport in a single solution.

5) The concentration of iron in sphalerite indicates a sulphur fugacity for the type 3 and 4 ore fluids in the range 10^{-19} to 10^{-22}.

TABLE 4.5

SOME ESTIMATED PHYSICOCHEMICAL PARAMETERS FOR PHASES 3 AND 4

Parameter	Phase 3	Phase 4
Density (25°C)	ca 1238 kgm^{-3}	ca 1137 kgm^{-3}
Temperature range	65-99°C	73-106°C
Total Na	2.10-2.75	0.35-0.80
Total K	0.031-0.041	0.005-0.019
Total Mg	0.04-0.055	0.005-0.012
Total Ca	0.78-1.10	1.21-1.65
Total Cl	3.77-5.10	2.78-4.13
Stoichiometric ionic strength	ca 6.5-6.8	ca 4.7-5.3
Parameters estimated at 100°C.		
Total sulphate From oil-field brine	← 3 x 10^{-6}m →	
Free molal sulphate from anhydrite saturation (upper limit): molal SO_4^{--}	$1.4x10^{-3}$ - $1.7x10^{-3}$	$2.7x10^{-4}$ - $2.9x10^{-4}$
Total molal sulphate from anhydrite solubility:	← 0.05m →	
Free molal barium	$2.9x10^{-6}$ - $3x10^{-3}$ m	$5x10^{-6}$ - $7x10^{-3}$ m
Fluorite solubility from data of Richardson & Holland (1979).		
Free molal fluoride	$4.6x10^{-4}$	$3.4x10^{-4}$
Total fluoride	$2.4x10^{-3}$m	$2.3x10^{-3}$ (table 7.7)
Free molal fluoride (Data from Helgeson , 1969)		
Molal F-	$1.7x10^{-4}$ - $1.9x10^{-4}$	$1.3x10^{-4}$ - $1.4x10^{-4}$
Free molal CO_3^{2-} from calcite saturation (Helgeson, 1969).		
Molal CO_3^{2-}	$2.4x10^{-7}$ - $3.0x10^{-7}$	$3.8x10^{-8}$ - $4.2x10^{-8}$
Oxygen fugacity	$-57<\log fO_2>-55$ or	$-52<\log fO_2>-51.5$
pH	5 - 6.1	5.5 - 6.1
sulphur fugacity	← 10^{-22} —	10^{-19} →
carbon dioxide fugacity	5. - 0.04	1.3 - 0.14

(fugacities expressed in atmospheres)

6) The high reduced to oxidized sulphur ratio in the fluids and the small degree of disequilibrium occurring as a result of sulphide deposition allows the use of sulphide stability diagrams. A maximum total sulphur activity for the system of 10^{-5} is necessary to maintain chalcopyrite+pyrite stability in the pH range 5-6 at 100°C.

Ranges for various physicochemical parameters are shown in table 4.4 and 4.5.

CHAPTER 5

RARE EARTH ELEMENT GEOCHEMISTRY

5.1: INTRODUCTION

No detailed work on REE geochemistry on the fluorite and calcite has been done on the deposits of the Southern Pennine Orefield. Dunham (1952) did, however, comment on the colouration of fluorite and its relationship to REE element abundances. Howie et al. (1982) published three analyses of the REE content of fluorite from the district and Smith (1974) published a detailed study of yttrium, lanthanum and cerium variation in the fluorite veins of the Ashover and Crich inliers. The behaviour of lanthanides in hydrothermal solutions has not been particularly well established and the subject requires an in-depth review. Knowledge of fluid inclusion homogenization temperatures and ore fluid chemistry enables a comparison between REE abundance and the physicochemical environment to be drawn. Since conditions of mineralization are well established, it can be thermodynamically assessed whether valency changes in the REE can occur. This is particularly important when trying to establish the cause of europium anomalies. The measured REE abundances may also yield information concerning the source of the lanthanides and possibly fluorine in the ore fluid and the mechanisms of REE transport and mineral precipitation.

5.2: DETERMINATION OF REE ABUNDANCES

REE abundances were measured using an inductively coupled plasma (ICP) source spectrometer. The method of REE separation and REE determination was the same as that outlined by Walsh et al. (1981). The machine used was a Philips PV 8210 15-m ICP spectrometer (Kings College, London University). Dissolution of fluorite requires a slightly different method from that applied to silicates. The powdered fluorite sample was decomposed in 20ml of perchloric acid in a PTFE beaker and evaporated to dryness. If the fluorite had not completely dissolved the process was repeated. Using this process no fusion was required. Calcite was dissolved in 20ml of hydrochloric acid (10%) as was limestone. Calcite dissolved completely but dissolution of limestone left an insoluble residue. This residue was filtered and ignited in a silver crucible at 800°C with 0.5g of sodium hydroxide for 20 minutes. After cooling the fused material was dissolved in 20ml of hydrochloric acid (25%). Six columns were used for REE separation with either a standard or a blank sample present in one of the columns on all batches. The REE analyses are given in table 5.2.

5.2.1: PRECISION AND ACCURACY

Since the concentrations of the REE in the minerals analysed are very low, the determinations of some of the

lanthanides were made close to the detection limits of the I.C.P. spectrometer. The detection limits for the REE on the I.C.P have been given by Walsh et al. (1981) and are shown in table 5.1. To estimate the precision of the REE abundances determined in the fluorite, the concentrations of lanthanides in a single sample were measured three times. The results of the test and the confidence limits (2σ) are shown in table 5.1.

TABLE 5.1

CONFIDENCE LIMITS FOR REE ANALYSES AND DETECTION LIMITS

REE	Replicates			±2σ	Detection limit
	1	2	3		
La	Ø.58	Ø.9Ø	Ø.65	Ø.32	Ø.75
Ce	1.83	2.1Ø	1.58	Ø.52	Ø.86
Sm	Ø.48	Ø.4Ø	Ø.47	Ø.Ø8	Ø.11
Eu	Ø.18	Ø.17	Ø.17	Ø.Ø1	Ø.Ø2
Dy	Ø.79	Ø.81	Ø.77	Ø.Ø4	Ø.Ø5
Ho	Ø.15	Ø.15	Ø.15	-	-
Yb	Ø.34	Ø.3Ø	Ø.29	Ø.Ø5	Ø.Ø4
Lu	Ø.Ø5	Ø.Ø3	Ø.Ø4	Ø.Ø2	Ø.Ø1

Accuracy is difficult to assess since no fluorite standards were available. The standard used to estimate percentage recovery was supplied by Dr. J. N. Walsh. The mean percentage recovery was found to lie between 93% and 95% for all the REE analysed. Certain lanthanides were affected by interference from calcium. Examples were lanthanum, neodymium and gadolinium.

Table 5.2
RARE EARTH ELEMENT ANALYSES OF FLUORITE, CALCITE AND LIMESTONE

MINERAL	La	Ce	Sm	Eu	Dy	Ho	Yb	Lu	Locality	Inclusion type
Fluorite	0.58	1.83	0.48	0.18	0.79	0.15	0.34	0.05	Fall Hill Quarry	4
"	2.7	0.90	0.36	0.08	0.22	0.05	0.06	0.02	Pindale Quarry	3?
"	1.22	0.81	0.20	0.06	0.26	0.05	0.06	0.01	Treak Cliff Cavern	2
"	2.60	2.04	0.74	0.14	0.83	0.18	0.33	0.04	Treak Cliff Cavern	1
"	1.06	0.77	0.39	0.11	0.54	0.11	0.19	0.01	Ladywash Mine	3
"	1.23	1.23	0.72	0.15	1.29	0.29	0.45	0.05	Treak Cliff Cavern	1
"	1.13	1.05	0.32	0.07	0.22	0.05	0.07	0.01	Smalldale Quarry	2
"	1.02	1.22	0.37	0.09	0.46	0.11	0.13	0.02	Masson Hill (opencast)	3
"	1.21	2.01	0.40	0.12	0.49	0.12	0.18	0.02	Ladywash Mine	3
"	0.87	0.96	0.39	0.12	0.59	0.13	0.21	0.03	Overton Hall Mine	4
"	0.54	0.72	0.36	0.10	0.49	0.12	0.16	0.02	Royal Mine	4
"	2.33	2.02	0.81	0.18	0.67	0.15	0.25	0.08	Winnats Pass	1
Calcite (Late)	1.36	1.00	0.27	0.07	0.25	0.06	0.11	0.01	Blende Vein, Magpie Mine	
" (Early)	1.03	0.84	0.28	0.06	0.20	0.05	0.13	0.01	Moor farm (opencast site)	
Calcite (Late)	6.90	9.00	1.70	0.40	1.57	0.32	0.67	0.10	Smalldale Quarry	
" (early)	2.30	3.10	0.80	0.16	0.58	0.11	0.27	0.04	Tearsall Quarry	
Limestone	2.23	2.05	0.36	0.08	0.27	0.06	0.17	0.02	Tunstead Quarry	
Limestone	1.87	1.21	0.33	0.08	0.23	0.06	0.15	0.01	Smalldale Quarry	

5.3: INTRODUCTION TO REE GEOCHEMISTRY OF FLUORITE AND CALCITE

There are numerous factors which influence the partitioning of an element between a precipitate and a parent solution. In the case of the lanthanides these factors are partly nullified since they represent a series of homologous cations of similar size and charge. There are two major controls on the REE content of a hydrothermal mineral. These are; (1) crystallographic and; (2) environmental. Crystallographic control is the availabiltiy of suitable sites within the lattice and environmental control is influenced by the prevailing physico-chemical conditions of mineralization.

5.4: CRYSTALLOGRAPHIC CONTROLS

The ionic radius and the electronegativity of an ion have a control on an element's ability to enter the lattice of a mineral. In the case of this discussion the ion being replaced is calcium, which has an ionic radius of 12nm in eight-fold coordination (Whittaker and Muntus, 197Ø). Substitution is not extensive between elements whose ionic radii differ by more than 15%. Substitution is, however, greater at higher temperatures because a higher energy state serves to increase the vibratory motion of the ions, and so the crystal structure expands and becomes more susceptible to accepting appropriate ions (Krauskopf 1979). Figure 5.1 shows the type of REE pattern produced if fractionation occurs as a

Figure 5.1

Ionic Radii of calcium and the REE in eight-fold coordination.

Ca = 12nm: La =12.6nm: Ce = 12.2nm: Nd = 12nm: Sm = 11.7nm: Eu^{2+} = 13.3nm: Eu^{3+} = 11.5nm: Dy = 11.1nm: Ho = 11nm: Yb = 10.6nm: Lu = 10.5:

Data from Whittaker and Muntus, 1970.

Percentage difference in ionic radii of Ca^{2+} and the REE plotted against atomic number. The pattern produced indicates the nature of REE distribution if ionic radii is the only control on lanthanide fractionation.

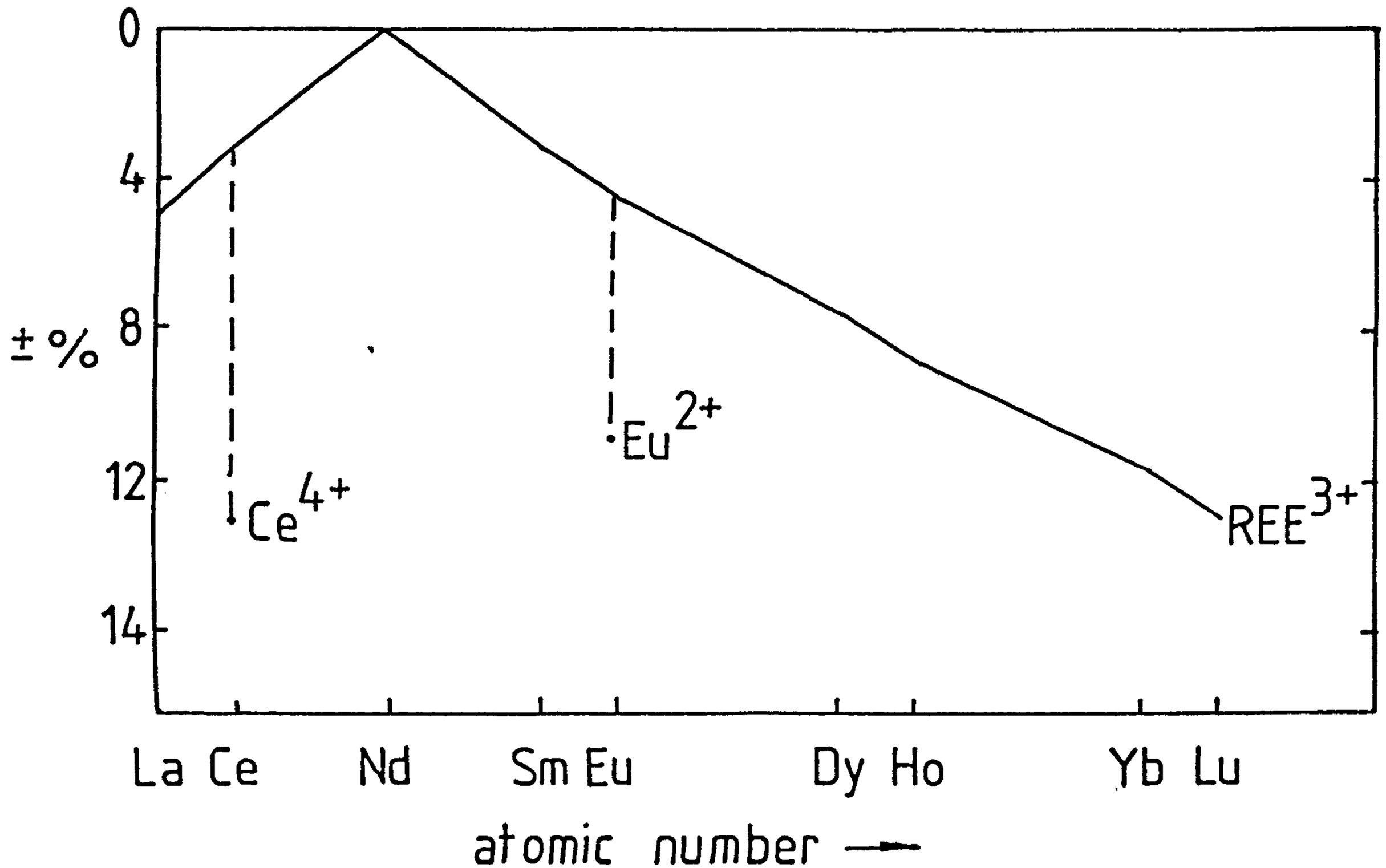

consequence of the deviation of the ionic radii of the lanthanides from that of calcium. The light rare earth elements (LREE) substitute with greater ease than the heavier members (HREE). The Eu^{++} ion has a larger ionic radius than the Eu^{3+} ion, suggesting that in reducing conditions a negative anomaly may occur. Since the charge imbalance between the calcium ion and the substituting REE ion has been nullified, however, substitution of Eu^{++} for calcium may produce a positive anomaly. The relative effects of charge and size of an ion cannot be readily quantified. Oxidization of Ce^{3+} to Ce^{4+} will produce a strong negative anomaly.

The ability of fluorite and calcite to hold large quantities of the lanthanides cannot be doubted. Calcite from the Harz Mountains has been found to be enriched in lanthanum by 500 times chondrite and in lutetium by 100 times chondrite (Moller et al., 1979) and a sample of green fluorite from Cornwall shows an enrichment of x540 and x50 respectively (Howie et al.,1982). Hence it can be assumed that fluorite and calcite can store large quantities of the REE if they are available and that both minerals have high effective distribution coefficients.

5.5: PHYSICOCHEMICAL ENVIRONMENT

The distribution of lanthanide ions between mineral species and aqueous solution is also influenced by the physicochemical environment. A particularly important aspect is the availability of anions for REE complexing.

The partition coefficient (K_p) is defined thermodynamically

as an ion activity product A for the lanthanide ion Ln^{3+}.

$$K_p = A \cdot (Ln^{3+}_{solid}) / A \cdot (Ln^{3+}_{soln})$$

Hence, anything affecting the activity product of the lanthanide ion in solution could be as important as crystallographic constraints on influencing the effective distribution coefficient.

It is known that when precipitation of a mineral occurs that a double electrically charged layer is set up on the growth surface of a mineral. Ions diffuse through this layer, and the rate of diffusion is obviously controlled by the charge on the ion as well as the charge on the growth surface. Therefore, trace element distribution is heavily dependant on the complexing of the ions. In turn, the nature of the complexes is controlled by the major element chemistry of the ore fluid as well as gas fugacities, pH, temperature and pressure. Complexing in the lanthanides can be expressed in the equation:-

$$Ln^{3+} + nA^{x-} \overset{\beta_n}{=} Ln\ A_n^{3-nx}$$

where A can be Cl^-, F^-, SO_4^{--}, and CO_3^{--} and β_n is the complex stability constant. Bilial et al.(1979a) have shown that the dominant REE complex in the fluorite bearing system is the mono-fluoride complex, LnF^{2+}. At fluoride activities of 10^{-4}m, as estimated for the Pennine ore fluids, it is unlikely that LnF_2^+ or LnF_3^o will form in any quantity. Low carbonate activities present even assuming that fluorite

deposition occurs while the system is saturated with respect to calcium carbonate, nullifies any affect of strong carbonate complexes. Hydroxyl complexes are unimportant in the pH range in which deposition of fluorite took place (pH < 6). Chloride ions do not play any role in complexing while sulphate ions form weak mono-sulphate complexes which cannot stabilize useful quantities of REE, even assuming anhydrite saturation.

Figure 5.2 shows the stability of several lanthanide mono-fluoride and mono-sulphate complexes at 25°C. The gross stability or association constant β_n is defined as:-

$$\beta_n = \frac{a_{Ln^{3+}} \cdot \ {}_A{}^{3-nx}}{a_{Ln^{3+}} \cdot \ a_A^{n}x-}$$

The pattern produced shows maximum stability at terbium mono-fluoride with decreasing values moving to the HREE and even greater decrease toward the LREE. This is partly explained by the decrease in the ionic radii from the LREE to the HREE with the consequent strengthening of the bond between ligand and cation. Bilial and Becker (1979b) investigated the variation in the stability constants of the REE mono-fluoride complexes with increasing ionic strength. They found from an experimental study that maximum complex stability occurs in a Ø.5 molal NaCl solution, suggesting that REE fractionation will be greatest in this type of solution. Guichard et al., (1979) suggested that complexing may not only stabilize the REE in solution but may actively compete with the crystallizing mineral phases for the lanthanides. If this

Figure 5.2

Stability of selected REE mono-fluoride and mono-sulphate complexes.

The association constant β_n is defined in the equation;

$$\beta_n = \frac{a_{Ln}\, A^{3-nx}}{a_{Ln}^{3+} \cdot a_{(A^{x-})^n}}$$

where Ln is the selected REE and A is the ligand (SO_4^{2-} or F^-)

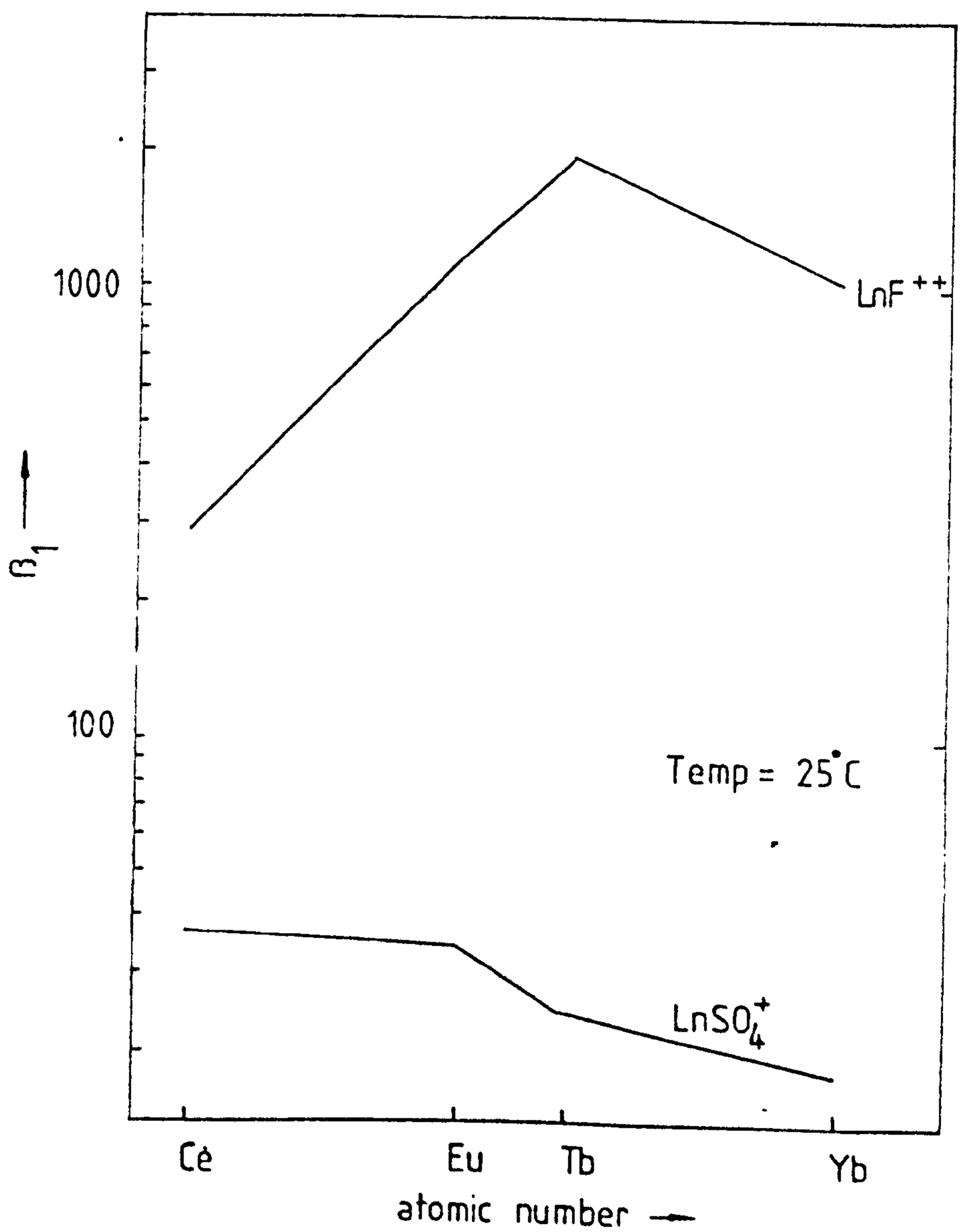

were the case, interpretation of REE contents would be made considerably more difficult.

The ability of REE to undergo cation exchange on contact with various clay minerals may also be important. Clay minerals probably represent efficient scavengers of the REE and a solution which has been in prolonged contact with shales would be expected to be considerably depleted in the lanthanides. Since calcium chloride brines are considered most likely to have been generated by membrane filtration in shales, scavenging of the REE should be extensive. In reducing conditions, ion exchange could possibly remove trivalent REE ions more effectively than the divalent europium ion, thus producing a positive anomaly in the ore fluid. Ce^{4+} would probably be removed more efficiently than Ce^{3+}, thus producing a negative anomaly. As a starting point for examining lanthanide distributions in fluorite, some average REE patterns for common rock types are shown in figure 5.3. Lanthanide concentrations are generally normalized to chondritic abundances (Nakamura, 1974), although solutions which have possibly evolved in, or at least have been in prolonged contact with, shallow crustal rocks could be more reasonably normalized to an average shale. All the rock types plotted, apart from limestone, show a marked negative europium anomaly, while limestone alone shows a small negative cerium anomaly, as does sea water. Granites and shales have the highest mean values with a decrease to sandstones and limestones. All the patterns show LREE enrichment.

Figure 5.3

Chondrite normalized REE abundances for average granite, shale, sandstone and limestone. The patterns have been plotted from data given by Wedepohl (1974).

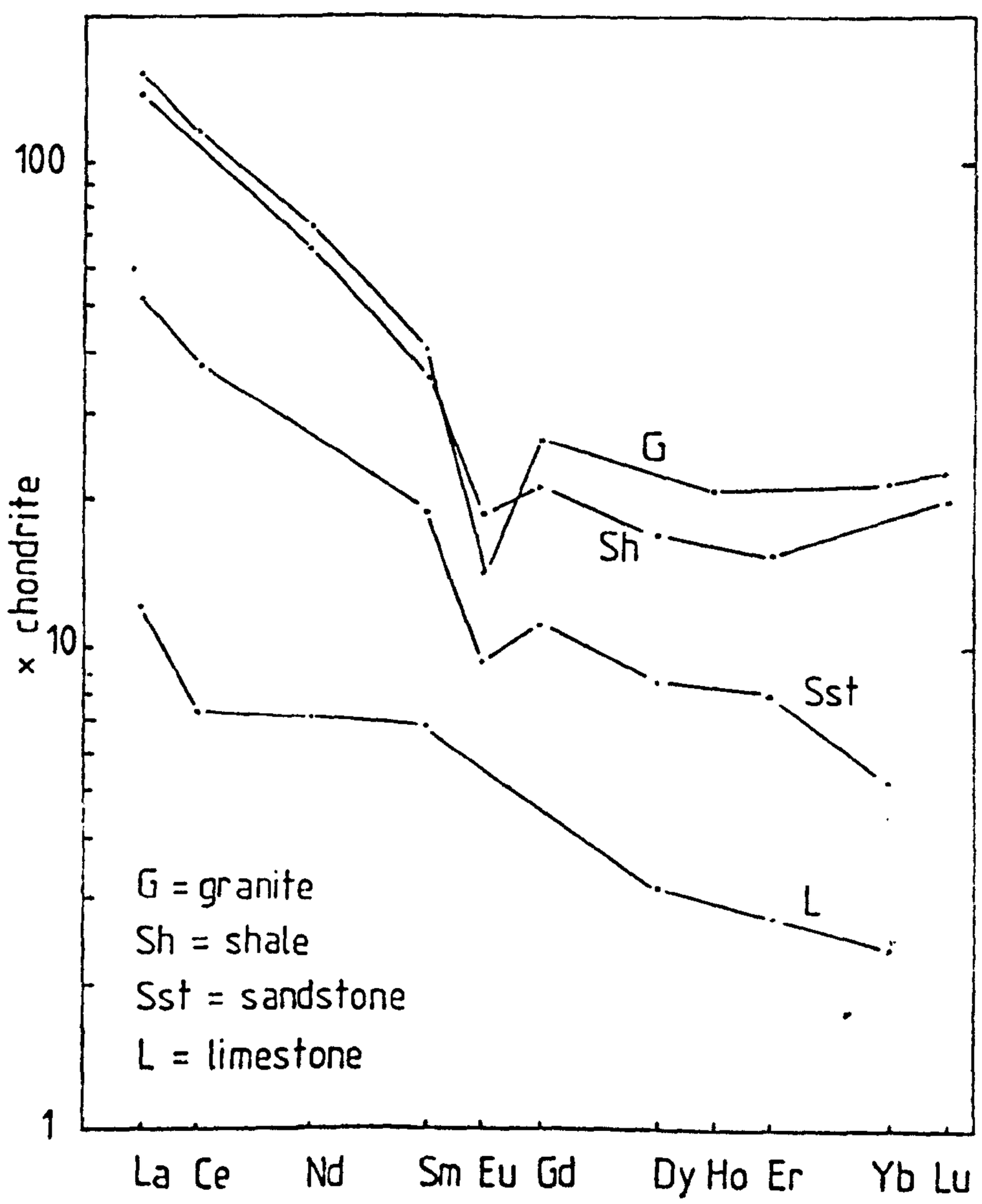

5.6: LANTHANIDE ABUNDANCE IN FLUORITE AND CARBONATES

Brattner et al.(1972) noticed a correlation between the REE distribution in fluorite and the position of fluorite in the paragenetic sequence. These are; (1) preferential concentration of the LREE in early stages of mineralization ;(2) normal chondritic distribution in intermediate stages and; (3) preferential concentration of the HREE in later stages.

5.6.1: THE TERBIUM/CALCIUM-TERBIUM/LANTHANUM DIAGRAM

Moller et al., (1976) presented a diagram which would graphically show the observations of Brattner et al. (1972) as well as representing the processes of limestone metasomatism (assimilation) and reworking of earlier-formed fluorite (remobilization). The theory behind the Tb/Ca-Tb/La diagram requires some discussion. Terbium is used to represent the HREE since it forms the strongest mono-fluoride complex of the trivalent lanthanides. Deposition of fluorite in a closed system is considered initially. The early crystallized fluorite would be rich in the LREE since they form the least stable complexes. As crystallization proceeds, Moller et al suggested that the fluoride activity of the fluid will decrease rapidly and the ratio of HREE to LREE in the precipitating fluorite will increase, thus producing a fractionation trend. The ratio of HREE to calcium in the mineral should also increase. Hence, if the REE abundances were measured in such a deposit and a Tb/Ca-Tb/La diagram

constructed, a diagonal trend should be obtained with the earliest-formed material plotting at the bottom left hand corner of the diagram. For volumetric considerations alone, a closed system is seems improbable, therefore, Moller and Morteani (unpub. paper) presented a second model. Their model for the open system is based on the assumption that source regions will be hotter than the surrounding environment and that flow rates in fractures close to the source will be consequently higher. HREE-rich fluorite should precipitate from relatively unfractionated solutions close to the source while on moving away from the source the HREE/LREE ratio of the mineral will increase. A third model proposed by the author is the possibility of a fluoride-rich solution mixing with a calcium-rich solution. It would be reasonable to assume that the major contribution of lanthanides to the fluorite would come from the solution with the high fluoride activity and that little REE fractionation would occur. Therefore, a vertical trend, similar to that obtained from limestone metasomatism may be produced. The processes of fractionation, metasomatism and remobilization are shown in figure 5.4.

5.6.2: REMOBILIZATION AND ASSIMILATION

It is very likely that both these processes have produced deposits in the Southern Pennine Orefield. Moller and Morteani (unpub. paper) suggested mechanisms of REE fractionation for both processes. When remobilization occurs, they suggest that the F^-/Ca^{++} and the CO_3^{2-}/Ca^{2+} activity ratios

Figure 5.4

Types of trends which may be observed on a Dy/Ca-Dy/La diagram

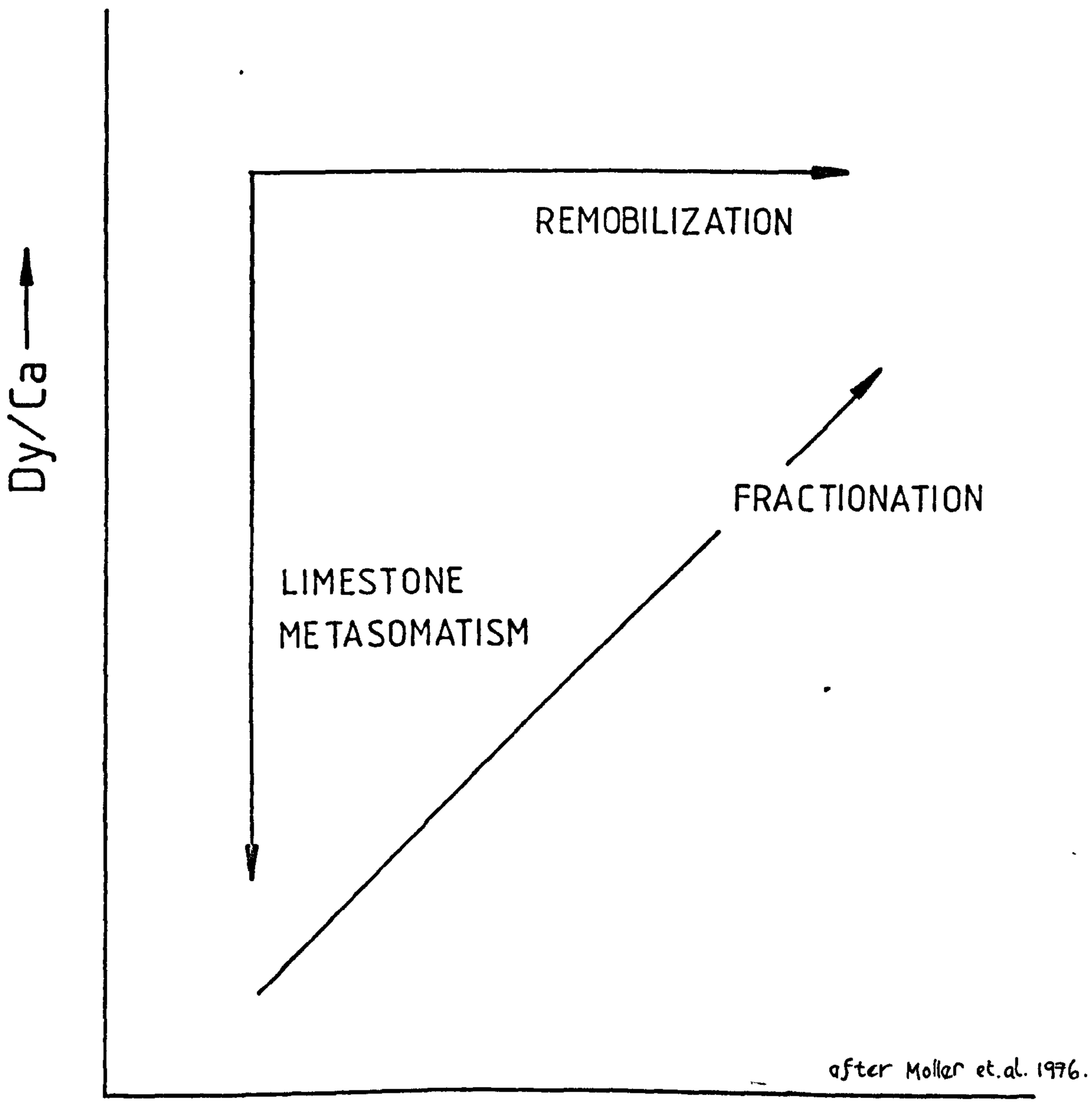

will be high in the solution where movement of fluorite and calcite is taking place respectively. The ligand activities may well be higher in this type of solution than in the primary ore fluid. The HREE will probably be completely taken up into solution with possibly some loss of the LREE. The terbium/calcium ratio, they suggest will probably remain fairly constant, thus producing a horizontal scatter on the diagram. Metasomatism, as mentioned earlier in the case of fluid mixing will most likely show as a vertical scatter on the Tb/Ca-Tb/La diagram. A modified plot of Yb/Ca-Yb/La was used to plot values for calcite (Parekh and Moller, 1977). Parekh and Moller consider that carbonate complexing, prevalent in a solution staturated in calcite, may shift the maximum HREE stability from terbium to ytterbium.

5.6.3: ORIGIN OF EUROPIUM ANOMALIES

The mechanism by which a europium anomaly is formed may be complex, since such an anomaly may be produced by either a depletion of europium in the ore fluid or the presence of divalent europium ions, formed at low oxygen fugacities. It is also possible that some ligands could stabilize the Eu^{2+} ion as a complex. Thermodynamic data may be used to clarify the conditions required for reduction of trivalent europium to take place. Unfortunately, most of the thermodynamic data available for europium complexes requires theoretical extrapolation to the temperatures found in mineralizing environments. Sillen and Martell (1971) provide the equilibrium constant for the reaction at $25^{o}C$:-

$$Eu^{3+} + e^{-} = Eu^{2+}$$

The equilibrium constant may be calculated at elevated temperatures using the equation:-

$$\log K_{T_1} = \log K_{298} + \frac{\Delta H}{2.303.\ R} \cdot \frac{(T_1 - 298)}{T_1.\ 298}$$

In the equation, logK is the log of the equilibrium constant at temperature T (373°K), ΔH is the enthalpy of association, T is the temperature at which the properties of the reaction were measured (298°K) and R is the gas constant (Ø.ØØ2). Using the reaction;

$$\tfrac{1}{4}O_2 + H^{+} + e^{-} = \tfrac{1}{2}H_2O$$

given by Hogfeldt (1982), the stability of divalent and trivalent europium species may be plotted onto an oxygen fugacity-pH diagram, using the combined reaction.

$$Eu^{2+} + \tfrac{1}{4}O_2 + H^{+} = \tfrac{1}{2}H_2O + Eu^{3+}$$

The association constant at 25°C for the trivalent europium mono-fluoride complex is given by Bilial and Koss (1980), although no values for entropy or enthalpy are given. Hogfeldt (1982) does, however, give the enthalpy of association for the yttrium mono-fluoride complex (ΔH=1.2 $kcalmol^{-1}$) which may be used to produce a rough extrapolation to 373°K. This reaction:

$$EuF^{+} + \tfrac{1}{4}O_2 + H^{+} = \tfrac{1}{2}H_2O + EuF^{++}$$

gives stability line (1) shown in figure 5.5. Looking at the upper and lower limits of oxygen fugacity at which ore deposition is likely to occur, it is obvious that a very high pH would be required for EuF^{+} stability (pH>7). The divalent ion behaves in a similar way to barium and strontium, and therefore, it is probable that $EuSO_4^o$ is one of the strongest complexes formed by Eu^{++}. No association constant is available for the complex but Garrels and Christ (1965) suggest that association constants for all the alkaline earth mono-sulphate complexes are similar. Therefore, the association constant was taken to be the same as that for $CaSO_4^o$ and the value was taken from Giordano and Barnes (1981) as (K_a=316). The position of the boundary formed by the equation;

$$EuSO_4^o + F^{-} + \tfrac{1}{4}O_2 + H^{+} = \tfrac{1}{2}H_2O + EuF^{++} + SO_4^{2-}$$

indicates that even at sulphate activities equivalent to anhydrite saturation, the type 3 and 4 ore fluids would not stabilize the Eu^{++} ion (figure 5.5). In conclusion, therefore,

Figure 5.5

Stability of trivalent and divalent europium fluoride and sulphate complexes as a function of oxygen fugacity and pH of the environment.

Boundary (1) divides the regions of EuF^{++} and EuF^{+} stability.
Constant fluoride activity (1×10^{-4}m) and temperature is assumed(temperature = $100^{o}C$).
Line (2) indicates the boundary between EuF^{++} and $EuSO_4^o$ complex stabilities.
This line is calculated for $CaSO_4$ saturation of the phase 3 ore fluid.
Line (3) again shows the stability fields of EuF^{++} and $EuSO_4^o$ but for a sulphate activity similar to that found in oil-field brines of similar bulk chemical composition as tne ore fluids.
Lines (4) and (5) represent approximate upper and lower limits of oxygen fugacity in the environment of mineral deposition.

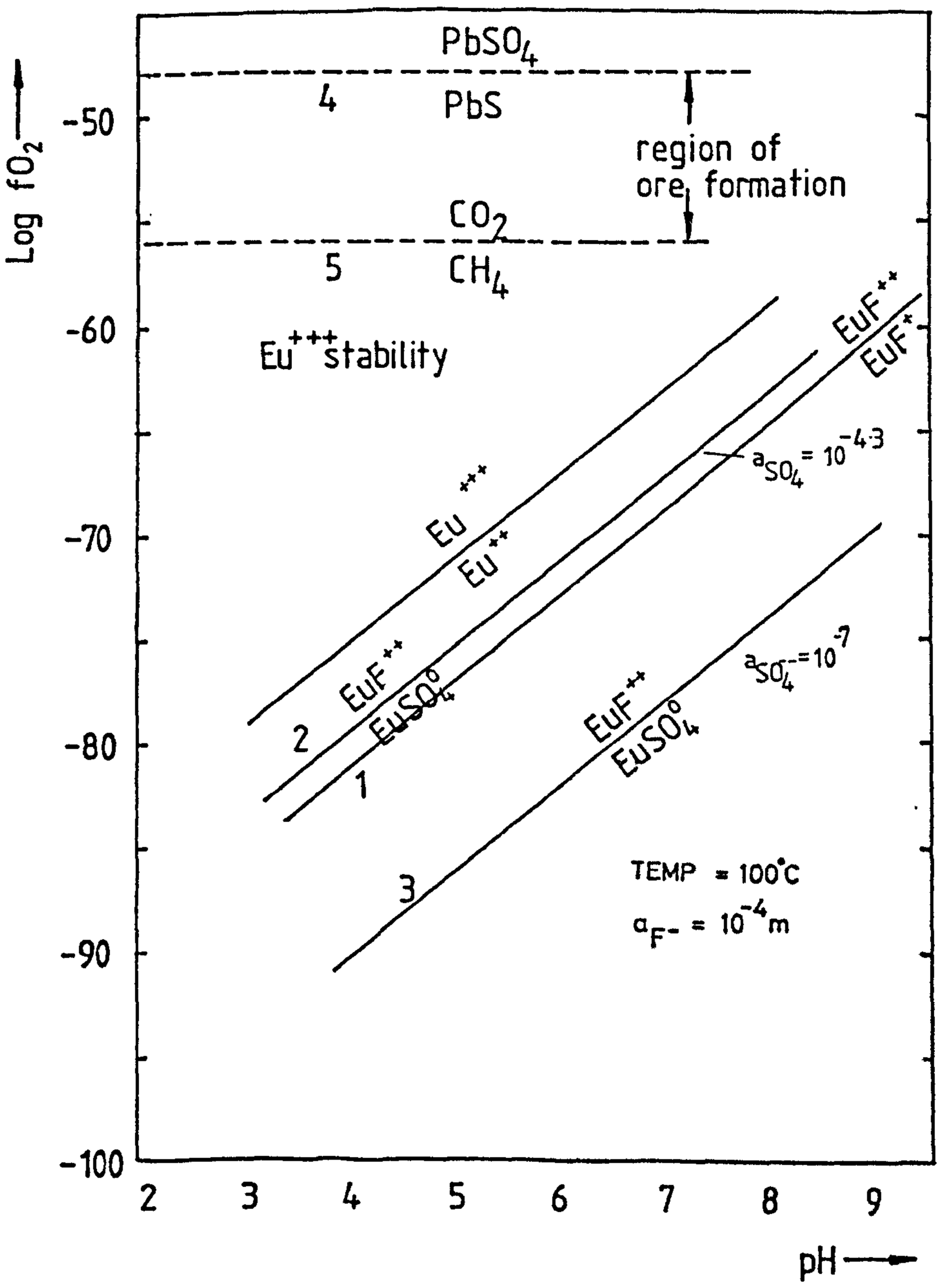

fluoride is the only important complexing ligand when the ore fluid is saturated with fluorite in both the divalent and trivalent states of the europium ion. The divalent ion will only occur in the region of carbonate instability and pyrrhotite stability or at high pH's. Therefore, it is probably reasonable to conclude that any europium anomaly is produced from an anomaly within the REE concentration of the ore fluid itself rather than as a function of the redox conditions. The thermodynamic data are presented in appendix 6.12.

5.7: LANTHANIDE CONTENT OF FLUORITE FROM DERBYSHIRE

On initial inspection of the chondrite normalized REE patterns (figure 5.6), all the samples plotted are seen to be LREE enriched and to have very low total abundances. Most of the patterns plot below the standard limestone values given by Wedepohl (1971). Each of the fluorite types, defined on the basis of the primary fluid inclusions they contain, will be discussed individually.

5.7.1: TYPE 1 FLUORITE

Samples of this fluorite were taken from Treak Cliff Cavern and its vicinity and are possibly not representative of a regional type of fluorite. All the samples show negative cerium and europium anomalies. Cerium anomalies may be inherited by one of three ways; (1) ore fluids produced by

Figure 5.6.

Chondrite normalized REE abundances for fluorite samples from the Southern Pennine Orefield

The number on each pattern refers to the associated primary fluid inclusion type. Two diagrams have been plotted purely to prevent the diagrams becoming cluttered. Total REE abundance can be seen to be low and all patterns show LREE enrichment.

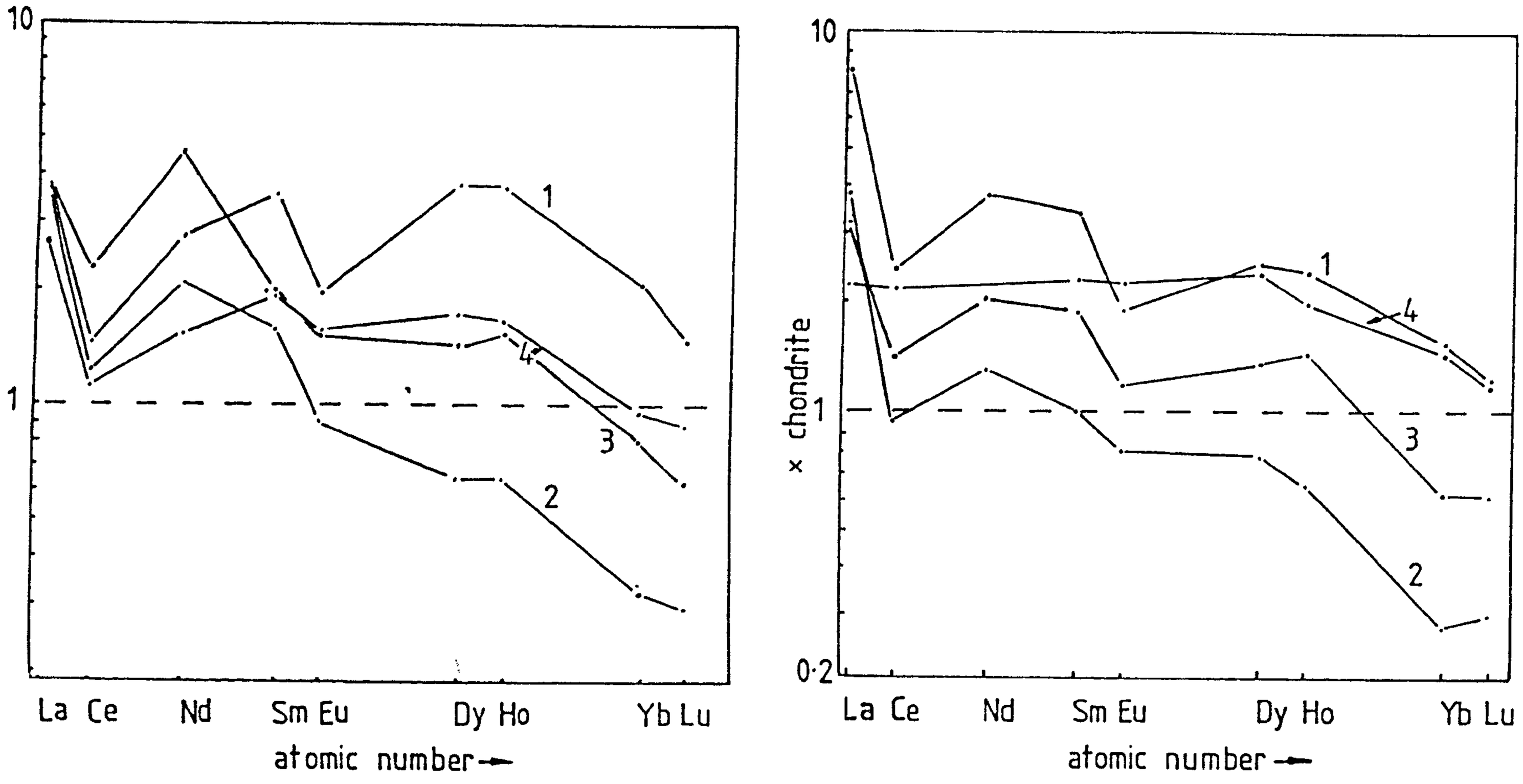

concentration of sea water or marine pore waters would automatically inherit the negative cerium anomaly present in sea water; (2) pure marine carbonates inherit negative cerium anomalies from sea water and this could be passed on to a brine migrating through limestones or carbonate-cemented sedimentary rocks or it could be acquired on intensive metasomatism of marine carbonates; (3) the leaching of oxidized sediments such as desert sandstones may convert Ce^{3+} to Ce^{4+}. Ce^{4+} is very easily adsorbed on manganese and iron oxyhydrates and will probably undergo ion exchange on contact with clay minerals more readily than the accompanying trivalent lanthanides. There can be little doubt that the ore fluids have evolved from sea water and that processes such as metasomatism and dolomitization of carbonates have occurred. The very low abundances of the REE suggest prolonged contact with an ion exchange media.

The higher total lanthanide content of the type 1 fluorite in relation to the other fluorites may be attributed to the physicochemistry of the environment. Thermometric fluid inclusion measurements indicate a relatively low ionic strength, which as stated earlier, favours mono-fluoride complexing (Bilial et al., 1979b). They also indicate higher temperatures of deposition than the other fluorite types (ca 140°C). Calcium activity is probably low and therefore, could not suppress fluoride content. In such favourable conditions for REE transport, it is surprising that more REE were not incorporated into the lattice. The conclusion must be that the ore solution has had extensive interaction with REE scavengers such as the clay minerals or iron or manganese oxide.

Moving to the Dy/Ca-Dy/La diagram figure 5.7, which should show the same features as a Tb/Ca-Tb/La plot, the three points show a higher HREE/Ca ratio than the other fluorites, which can be interpreted as an environment richer in the REE. The Dy/La ratio, however, differs little from the ratios in fluorite precipitated from the ore solutions containing high calcium concentrations.

5.7.2: TYPE 2 FLUORITE

This type of fluorite has the lowest total lanthanide content. The samples plotted were taken from Treak Cliff Cavern and Smalldale Quarry. Again the total lanthanide content can be best explained in terms of the depositional environment. The major element concentration ranges of this ore fluid were calculated to be NaCl (Ø.17m-Ø.34m), $CaCl_2$ (3.3-3.4m) and $MgCl_2$ (Ø.ØØ2-Ø.ØØ4m). The high calcium concentration would obviously suppress fluoride activity in the ore fluid as a result of the common ion effect. The limited amount of fluoride available for complexing is suggested by the low Dy/Ca ratio seen on the plot of Dy/Ca against Dy/La (figure 5.7). The phase contains inclusions with the lowest homogenization temperatures (62°-82°C) of the four groups. The two points are seen to plot in close proximity, which would also be expected from the fluid inclusion evidence. Another reason for the low REE contents may be related to evolution of the mineralizing brines. To produce a brine which is so highly concentrated in calcium chloride by filtration of meteoric and pore waters, suggests

Figure 5.7

Plot of Dy/Ca against Dy/La for a number of fluorite samples from the Southern Pennine Orefield.

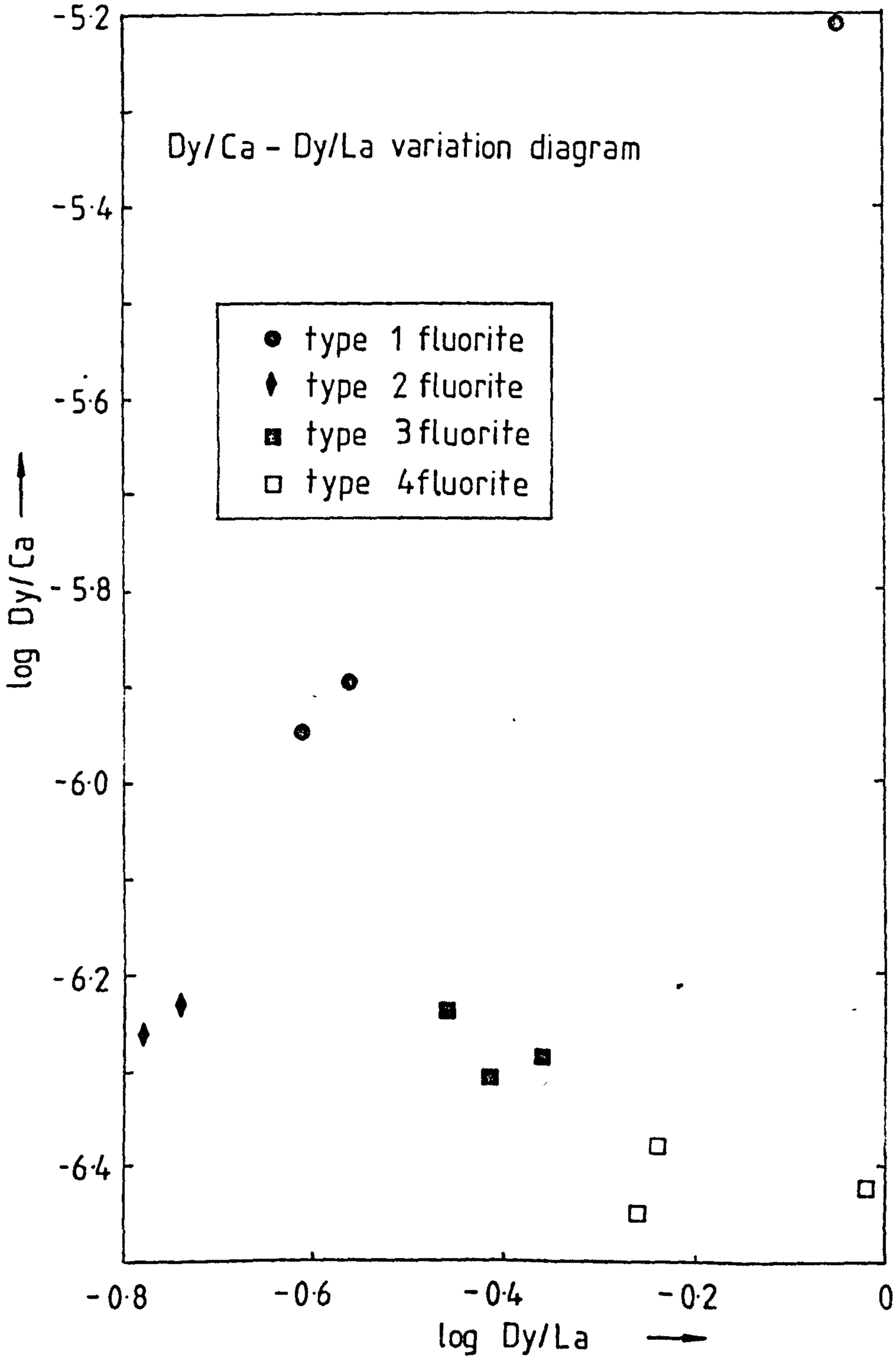

that the solution took a considerable period of time to evolve and therefore, prolonged contact with REE scavenging clay minerals would occur. The very high total dissolved salt concentration may also be indicative of a phase of evaporative concentration at the surface (See chapter 6). Europium does not show a very strong negative anomaly and its concentration is slightly below chondritic abundance. The cerium anomaly can be explained by the same processes listed in the last paragraph.

5.7.3: TYPE 3 FLUORITE

In both the chondrite normalized plots (figure 5.7), the type 3 fluorite has the second lowest REE abundances. The samples were taken from Ladywash Mine at Eyam and the Masson Hill opencast site. The homogenization temperatures of primary inclusions range from 86°C to 89°C. The low values cannot be ascribed to low fluoride activity in the ore-forming fluid alone, since a major chemical analysis of the fluid gives NaCl (2.1-2.75m), $CaCl_2$ (Ø.78-1.1m) and $MgCl_2$ (Ø.Ø4-Ø.Ø55m). This corresponds to a free fluoride ion concentration in the ore fluid of 3.4ppm (1.8×10^{-4}m). Possibly the difference in depositional temperatures has a strong effect on the REE content. There is some correlation between the total abundances and the homogenization temperatures of the four phases although how this correlation would change with a larger sample size is unknown. Fluorite types 3 and 4 form nearly all of the economic fluorite deposits of the district, so both solutions must have been

saturated with fluoride. The relative degree of supersaturation is difficult to estimate; however, the presence of delicate growth banding and the sometimes large crystals of fluorite found in deposits suggests that the ion activity solubility product of fluorite did not significantly exceed saturation (Barton et al., 1977). Both samples show negative cerium and small negative europium anomalies.

The Dy/Ca-Dy/La variation diagram shows the three samples to plot closely together. The environmental Dy/Ca ratio is similar to that of the type 2 fluorite while the Dy/La ratio shows relative enrichment in the HREE.

5.7.4: TYPE 4 FLUORITE

The samples analysed came from Fall Hill Quarry and Gregory Mine at Ashover and the Royal Mine. Of the two patterns plotted on figure 5.6, they are relatively flat, with one showing a negative cerium anomaly. Fluid inclusion analysis showed the dominant cation in the ore fluid to be calcium. A calculated analysis is NaCl (Ø.35-Ø.8m) and $CaCl_2$ (1.21-1.65m). This corresponds to a free fluoride concentration of 2.5ppm at 1ØØ°C. The Dy/Ca - Dy/La shows close clustering of the points (figure 5.7). The fluorite also shows the highest HREE/LREE fractionation. Using the standard interpretation of the diagram one might deduce that fluorite types 2, 3, and 4 represented a remobilization series. However, as mentioned earlier the type 2 fluorite has a very limited distribution and there is little evidence that it formed extensive deposits. Type 4 fluorite may well,

however, represent remobilized type 3 fluorite, since nearly all type 3 material contains secondary type 4 inclusions.

5.8: SIGNIFICANCE OF EUROPIUM ANOMALIES IN DERBYSHIRE FLUORITE.

As mentioned earlier, REE are potentially mobile on hydrothermal alteration of feldspar-bearing rocks (Alderton et al.,1980). Alteration of particularly calcic feldspar will produce a positive europium anomaly within a brine. Shepherd et al. (1982) has plotted normalized REE abundances for a Caledonian granite with both whole rock, apatite and K-feldspar fractions. K-feldspar has a large positive anomaly whereas apatite shows a pronounced negative anomaly. The normalized REE plot for the whole rock shows a slight negative europium anomaly. Theoretically, an anomalously high europium concentration in the fluid could produce a negative anomaly in the fluorite if very low oxygen fugacities were apparent at the site of mineral formation. However, it has already been shown thermodynamically that reduction of Eu^{3+} at 100°C is unlikely. The presence of pyrite inclusions in fluorite rather than pyrrhotite rules out reduction of Eu^{3+} in the pH range 5 to 7. Therefore, it seems reasonable to conclude that the small negative europium anomalies were inherited from the solution itself. Leaching of a granite therefore, seems unlikely if K-feldspar is the only phase to decompose. Decomposition of apatite or possibly micas could, however, hide any positive europium anomaly created by the break-down of feldspar. Carboniferous shale also has a small negative europium anomaly (Shepherd et al., 1982).

Figure 5.8

Chondrite normalized REE abundances for calcite and limestone samples taken from the Southern Pennine Orefield. All the patterns show LREE enrichment and both negative cerium and europium anomalies are apparent.

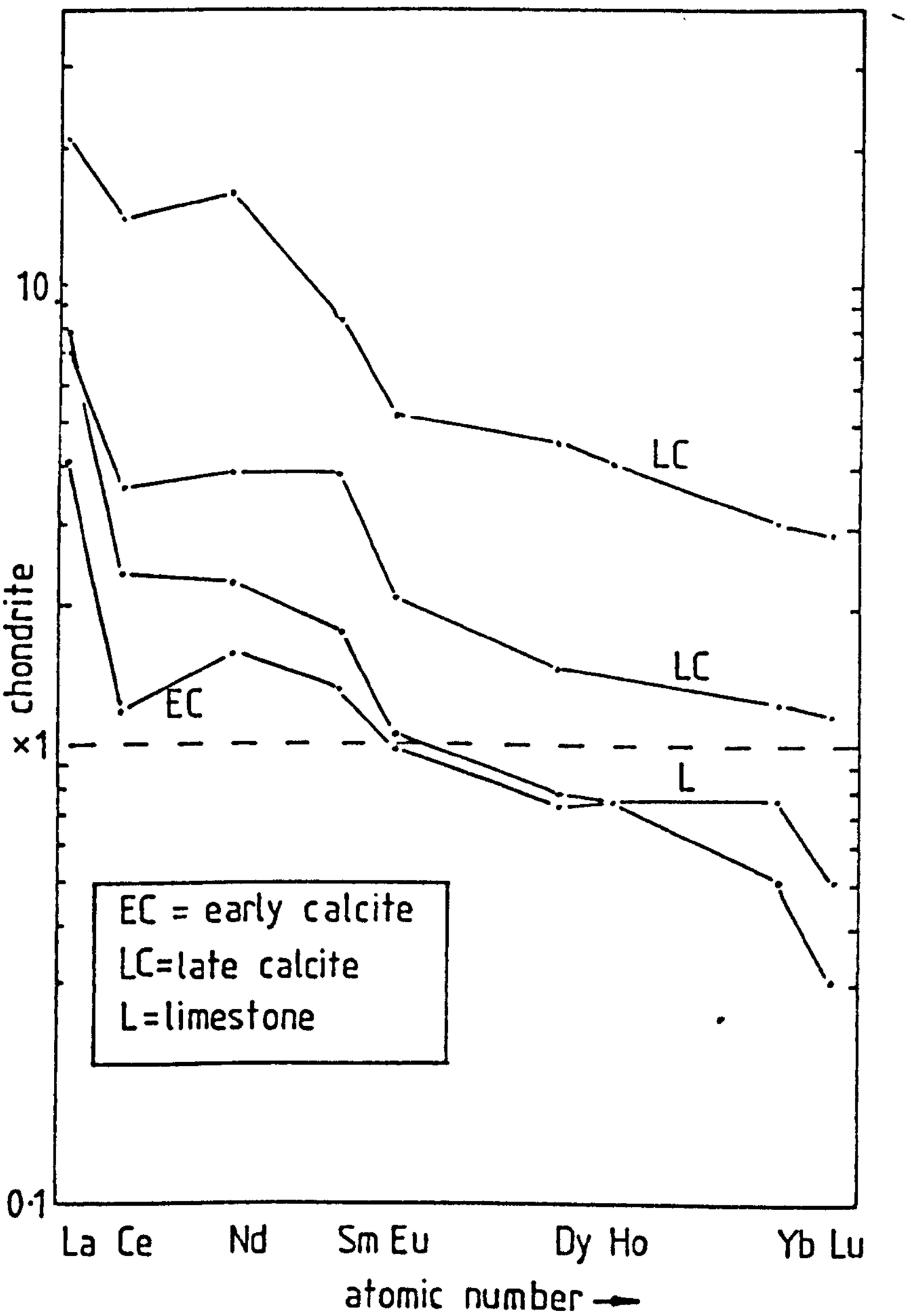

Figure 5.9

Plot of Yb/Ca against Yb/La for a number of early and late calcite samples as well as limestone. The vertical distribution of points for the calcite may indicate precipitation by mixing of two solutions with differing Yb/Ca ratios.

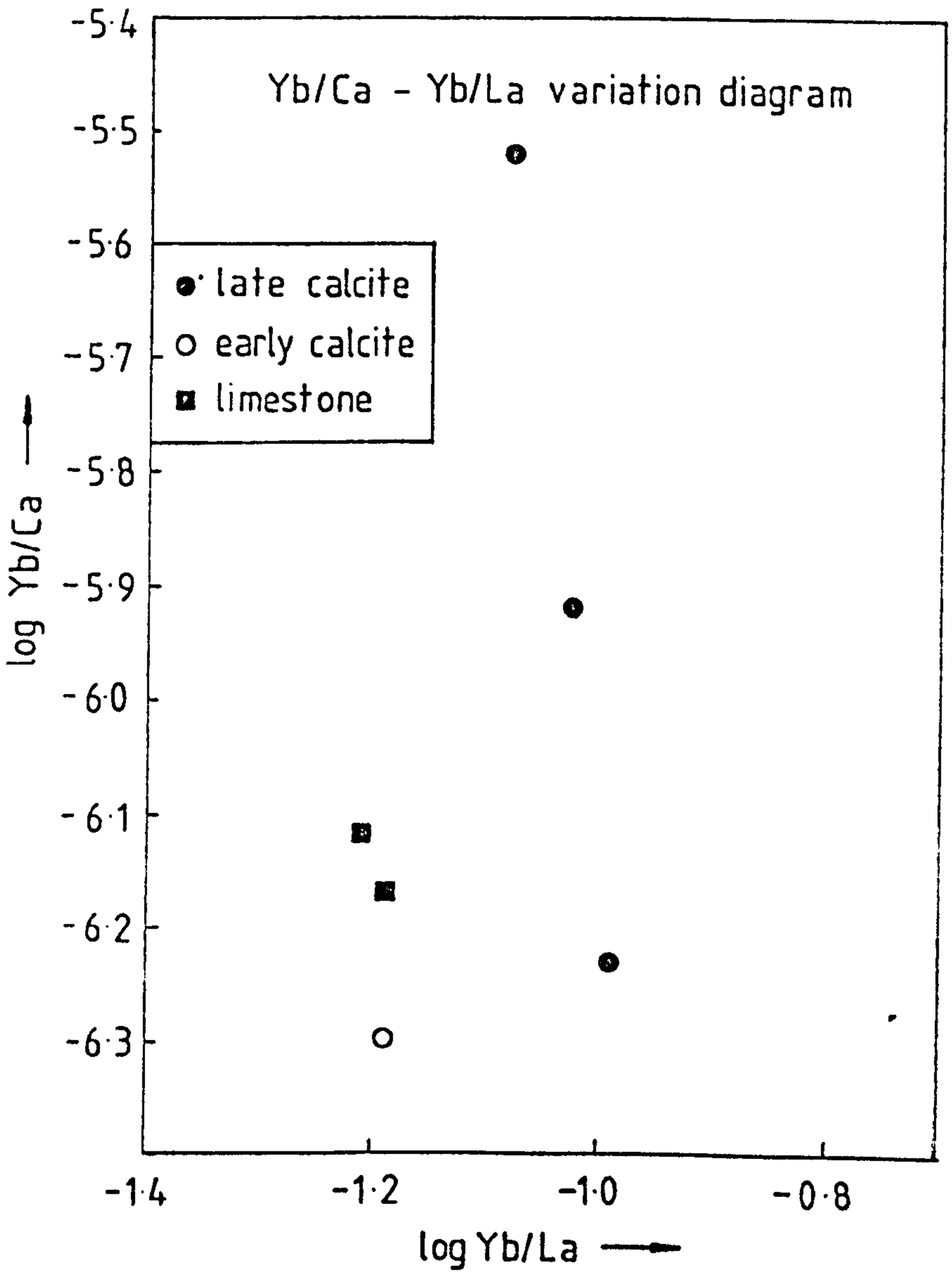

5.9: CARBONATES FROM DERBYSHIRE

The chondrite normalized pattern for the limestone plots below the mean value shown in figure 5.8. The pattern shows LREE enrichment as well as a slight negative cerium anomaly. The sample was taken from the Tunstead Limestone Quarry (Bee Low Limestone), well away from the intensely mineralized eastern margin of the district. Another sample taken from a limestone quarry near Bradwell showed similar abundances. Early white columnar calcite taken from the wall of a vein (Dirtlow Rake, Sheldon) shows very low abundances of the REE. Two other samples of early calcite were analysed and had lanthanide concentrations below the detection limits of the I.C.P. spectrometer. This suggests that the initial mineralizing solutions were extremely depleted in the REE.

A Yb/Ca-Yb/La plot is used to represent lanthanide fractionation in carbonate systems (Parekh and Moller, 1977). The variation diagram shows the solutions to have had a lower HREE/Ca ratio than the original diagenetic pore waters (figure 5.9). Three samples of late calcite collected from Smalldale, Moor Farm and Tearsall opencast sites plot in a vertical arrangement on the diagram. Assuming a single phase of mineralization, one could interpret this as a metasomatic trend (Moller et al., 1979). Paragenetic relations show that the calcite occurs as the last phase of mineralization, filling open cavities within the fluorite deposits. Hence a better interpretation is the mixing of a carbonate-rich solution carrying REE complexes with a calcium-rich solution.

Small europium anomalies are also present on the chondrite normalized plots.(figure 5.8).

5.10: DISCUSSION

The factors which control REE emplacement in hydrothermally formed fluorite and calcite have been reviewed. From a theoretical point of view, complexing of the REE seems to be the most important factor in controlling fractionation between fluids and crystallizing solid phases. It can be proved that the mono-fluorides are the only important REE complexes in a system saturated with fluorite. Marchand et al. (1976) suggested that the the REE were transported as chlorides, and consequently little fractionation between solution and mineral would occur, since the association constants of these complexes are similar for the LREE and the HREE. The work of Bilial and Becker (1979a) readily disproves this hypothesis for a system saturated with calcium fluoride. Therefore, the REE distribution pattern of a mineral cannot be considered to be representative of the REE pattern of the ore-forming fluid or the rock from which the lanthanides were leached. Total REE abundances may be explained to some extent by looking at the chemistry of then ore-forming fluids. The chemistry of the type 1 fluid makes it potentially the best carrier of REE. This type of fluorite does show the highest total lanthanide content of the four fluorite groups. The chondrite normalized REE distribution patterns also show a peak in the region of Dy, which one would expect if mono-fluoride complexing was the main factor influencing

fractionation. The high calcium content of the type 2 fluid would be expected to suppress fluoride activity and produce low REE abundances. This conclusion is supported by the analytical data.

The clustering of the fluorite types into groupings on the Dy/Ca - Dy/La variation diagram indicates that precipitation of fluorite occurred in a stable environment where little fractionation of the lanthanides was taking place. The uniformity also suggests that the brines were thoroughly mixed before deposition of fluorite occurred. Mixing processes may, however, have produced the late calcite.

The cerium anomaly in both the fluorite and the carbonates suggests either a sea water origin for the ore fluids or the dissolution of carbonates formed in a marine environment. There is a possibility that the brines passed through oxidized sediments such as desert sandstones, and Ce^{4+} was removed by adsorption. Removal of the REE through contact with iron or manganese oxides could also deplete the total lanthanide abundance.

The LREE enrichment may be produced by several factors. Many sedimentary and igneous rocks show LREE enrichment (Wedepohl, 1971). Crystallographic control also probably favours the emplacement of the LREE into the fluorite lattice. A third process which may produce a general LREE enrichment is ion exchange by clay minerals. As a general rule for ion exchange, the replacing power of an ion increases with increasing atomic number for ions of the same valency (Grim, 1968). Therefore, if a fluid leaches or passes through a shale, there will probably be an increase in the

LREE/HREE ratio of the solution, provided that exchange sites remain active.

The unusual chondrite normalized REE patterns for fluorite from South West England, Cumbria (Howie et al., 1982) and the Northern Pennine Orefield (Shepherd et al., 1982) must principally result from REE abundances in the hydrothermal solutions themselves and therefore, be strongly related to the lanthanide source. Mineral phases with high REE contents such as apatite and biotite (Wedepohl, 1971) are likely to be unstable in the ore fluids and represent good sources of the lanthanides. It has been shown that the negative europium anomaly could not have been introduced as a result of the redox conditions and therefore, must have been present in the brines. Leaching of orthoclase or plagioclase feldspar would produce a positive anomaly in the fluid but this could be masked by the large negative europium anomalies which would result from the destructive leaching of apatite and biotite. Therefore, leaching of an underlying crystalline basement or immature Namurian sandstones could account for the observed REE distribution patterns in the fluorite. Leaching of marine carbonates could provide similar REE distribution patterns if some enrichment of the HREE occurred.

5.11: CONCLUSIONS

Important conclusions arising from the preceding discussion are:

1) The availability of ligands for complexing and the strength of the various REE complexes was probably the most important control on the fractionation of the lanthanides between solids and solution and in determining the total REE content of the precipitating mineral phases.

2) The uniformity of the REE chondrite normalized patterns suggests that fluorite was deposited from a well-mixed ore fluid.

3) The negative europium anomalies, present in some of the chondrite normalized REE patterns was inherited from the ore fluid. Leaching of biotite and apatite may have produced these anomalies. The negative cerium anomaly was most probably inherited from the sea water component of the mineralizing brines.

4) The LREE enrichment could have been generated as a result of fluid interaction with source or wall rocks, as a result of fractionation from crystallographic control or through REE cation exchange between the fluids and clay minerals.

CHAPTER 6

ORIGIN OF THE MINERALIZING BRINES

6.1: INTRODUCTION

Ranges for the activities of major elements, trace elements and gases as well as pH limits have been established for the ore fluids in chapter 4. In the present chapter the major element chemistry, determined from inclusion leachate analyses and 87Sr/86Sr isotope ratios are used to place constraints on the origin of the hydrothermal fluids. The major dissolved salt species generally behave as buffers and cannot be readily removed from a fluid as ore deposition proceeds (Helgeson, 1970). Therefore, the cation ratios may be compared with ratios measured in present-day brines from various geological environments so as to give some clue as to their origin. In order to produce a complete model of ore genesis it may be useful to look at the initial evolution of the ore-forming fluids, which were very homogeneous and presumably derived from a well mixed reservoir source.

6.2: CHEMICAL COMPOSITION OF THE MINERALIZING BRINES

6.2.1: TYPE 1 ORE FLUID

The relatively high first observed melting temperature of the type 1 fluid inclusions indicates that calcium and magnesium were not important components (Crawford, 1981) in the solution. Very low salinities determined from inclusions in fluorite from Treak Cliff (Ø.2 equivalent wt % NaCl), Faucet Rake (Ø.5 equivalent wt % NaCl) and Watergrove Mine (No melting point depression) indicate salinities less than that of sea water. The highest salinities were determined in inclusions in purple fluorite from Pindale Quarry (9.3 equivalent wt % NaCl) and Moss Rake (1Ø equivalent wt% NaCl). Fluids with salinities less than that of sea water could be meteoric waters, dehydration waters (Graf and Anderson, 198Ø) or possibly the filtrate produced by membrane filtration (reverse chemical osmosis). Oil inclusions were associated with the type 1 fluids, suggesting that a component of the solution may have been derived from an oil-field brine. The large variation in both temperature and salinity is also suggestive of fluid mixing having taken place. This idea is also supported by the work of Pering (1973). Pering observed a bimodal distribution in chain lengths of the aliphatic hydrocarbons contained within purple fluorite from Treak Cliff Cavern. Maxima occur at C17 and C27 suggesting the mixing of hydrocarbons from the Edale shales and from the Dinantian limestones. Another interesting

Figure 6.1

Triangular diagram illustrating the magnesium-calcium-sodium concentrations of various high salinity brines and sea water and fluid inclusion analyses. Points are plotted as percentage gram-equivalent concentrations.

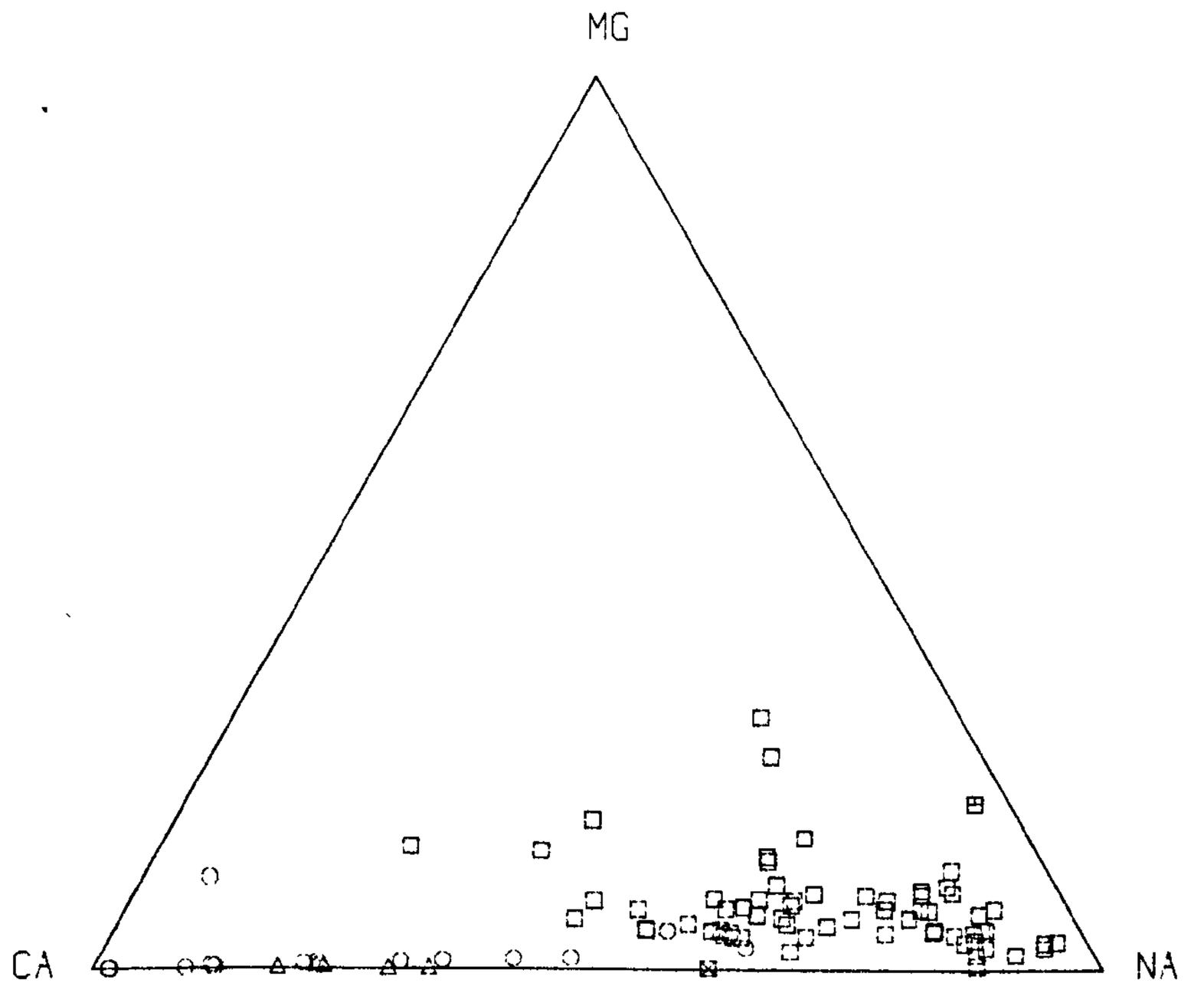

KEY

OILFIELD BRINES □. SUDBURY BASIN △. OCEAN WATER ⊞
SALTON SEA BRINE ⊠. FLUID INCLUSION ANALYSES ○

feature is the presence of the carbonyl group (=C=O), which Pering considered to be the result of bacterial alteration, post-dating mineralization. Such alteration, however, could not readily occur in inclusions which had been sealed at temperatures in excess of 140°C. Therefore, a second explanation may be the high oxygen fugacity prevailing at the time of deposition. Mixing of descending meteoric water at 100°C with brine (10 equivalent wt % NaCl) at 150°C presents density problems. Density differences (Potter and Brown, 1977) of the two fluids suggest that a 50°C temperature increment would not be sufficient to make the hotter fluid less dense than the meteoric water.

6.2.2: TYPES 2, 3, 4, AND 5 ORE FLUIDS

The presence of oil within type 1, type 3 and type 4 fluid inclusions suggests a genetic link with oil-field brines. Compositions plotted on to a Mg-Ca-Na triangular diagram (figure 6.1) show that the fluids were more depleted in magnesium than typical oil-field brines. This depletion is emphasized when molal magnesium concentration is plotted against molal calcium (figure 6.2). Removal of magnesium as a result of chloritization of aluminium silicates and adsorption by clay minerals has been shown to occur when an oil-field brine at 200°C interacts with a greywacke (Bischoff et al., 1981). Dolomitization probably played a major part in removal of magnesium although calculations suggest that both dolomite would not have been a stable phase in either the type 2 or type 4 brines. Chloritization was probably the

Figure 6.2

Plot of molal magnesium concentration against molal calcium concentration for some high salinity formation waters and the ore fluids (phases 3 and 4) The phase 2 and 5 fluids would plot in boxes to the right of and below the phase 4 fluid composition.

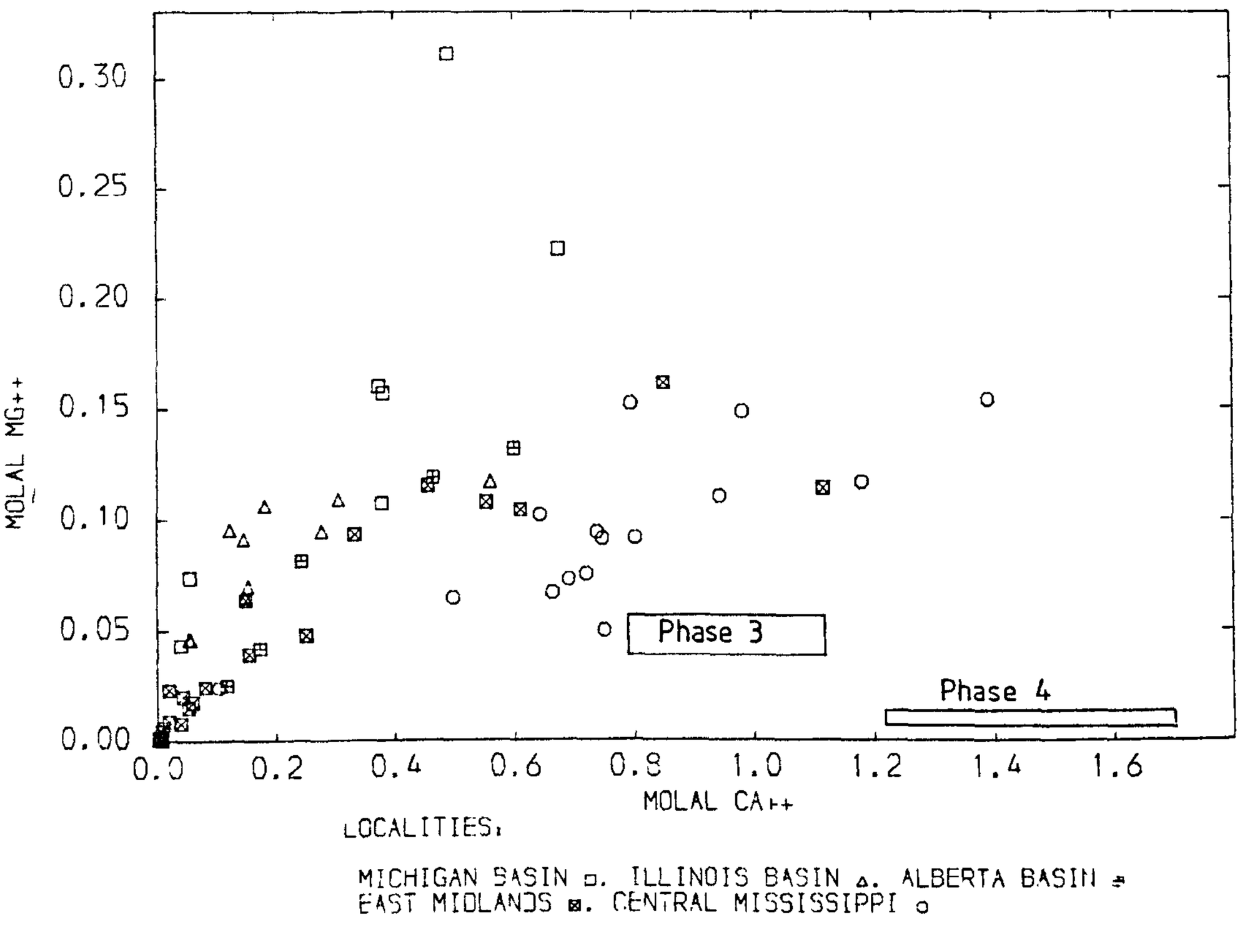

final magnesium removing process, if fluid-wall rock equilibria occurred at 100°C. Sea water has a considerably higher Mg/Na ratio than either typical oil-field brines or the ore fluids. Therefore, if concentration of sea water, which contains 35g of salts per 1 , produced the brines, considerable removal of magnesium must have taken place. The most distinctive feature of the type 2, 3 and 4 brines are their very low Na/Ca ratios. The type 3 brine has a Na/Ca ratio which is similar to brines found in the deeper parts of sedimentary oil-field basins, such as the Mississippi Valley and Michigan Basins. Calcium usually increases in concentration with increasing salinity and depth and examples have been cited by Graf et al., (1966) and Collins (1975). This relationship is shown in figure 6.3, plotted from the data of Graf et al., Carpenter et al., (1974) and Collins. The Central Mississippi Valley Basin brines show this trend particularly well. The Ca/Na ratio has also been plotted for the type 3 ore fluid. Although a deep origin for the type 3 brine may be implied, there are exceptions, such as the brines from the Michigan Basin which occur at relatively shallow levels. The type 2 and type 4 brines are more difficult to classify. High salinity brines with a high Ca/Na ratio have been found in Lower Cambrian evaporites lying on the Siberian Platform (Krotova, 1957), in the low grade metasediments of the Sudbury Basin (Frape and Fritz, 1982) and in the Salton Sea brines. Frape and Fritz (1982) reported brines with a total dissolved salt content of up to 240g l^{-1}. The Ca/Mg ratio was very high at <3290. The type 2 ore fluid for comparison has a Ca/Mg molal ratio of 5630 and a total dissolved salt content of approximately

Figure 6.3

PLOT OF DEPTH BELOW THE SURFACE AGAINST TOTAL DISSOLVED SALT CONTENT FOR SELECTED OILFIELD BRINES

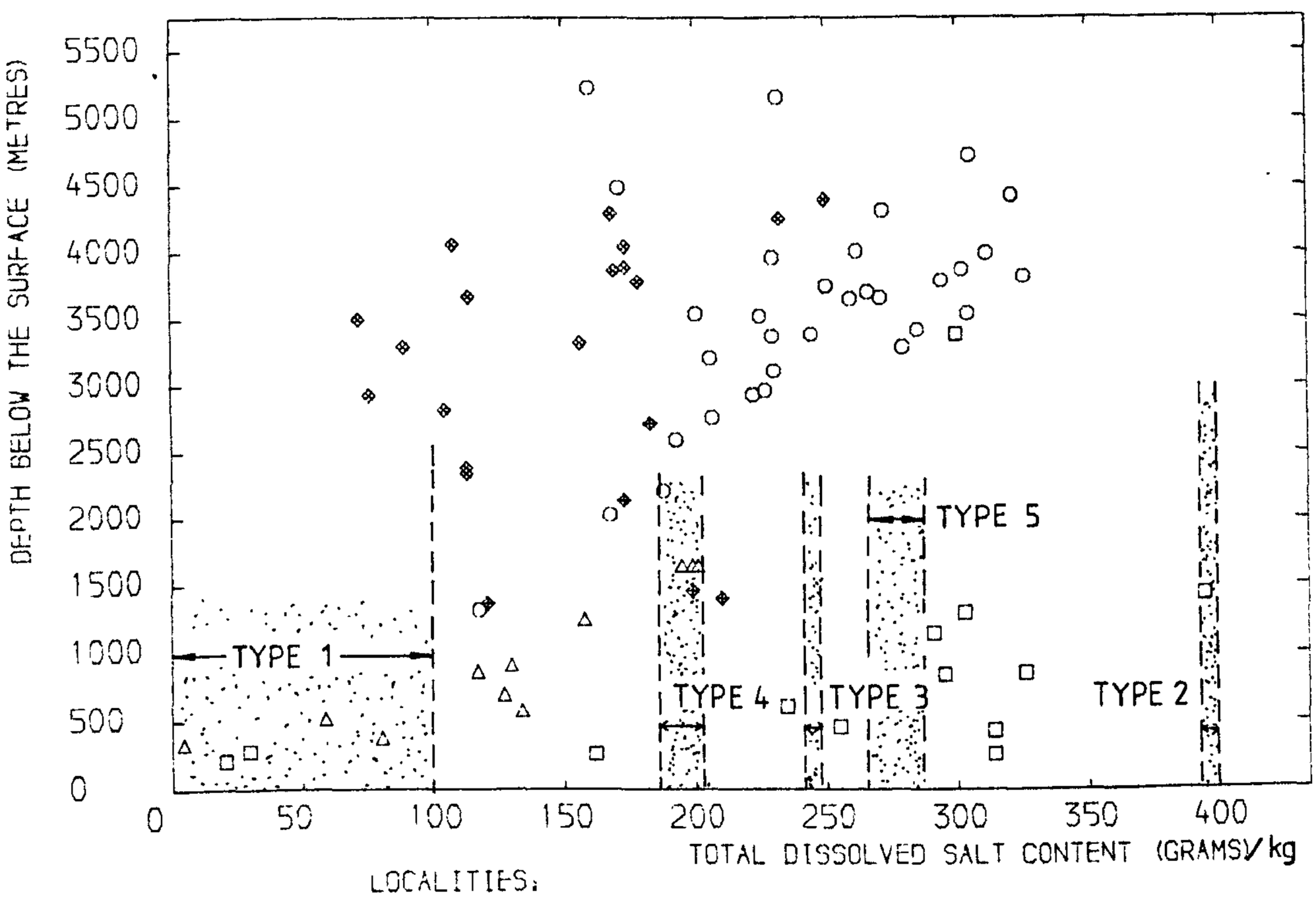

LOCALITIES:

MICHIGAN BASIN □. ILLINOIS BASIN △. ALBERTA BASIN ◆
LOUISIANA BASIN, ⊕. CENTRAL MISSISSIPPI ○

400g l^{-1}. Despite a stable isotope study of the brines Frape and Fritz (1982) were unable to suggest a specific origin for the saline waters. The brines in the Siberian Platform, although having very high total dissolved salt content (500-687g l^{-1}, have high Mg/Ca ratios. Krapenchenko (1964) attributes this to genetic processes such as dololomitization and dissolution of carnallite. Bentor (1969) reported analyses of brines from various formations in Israel and observed a decrease in Na/Ca ratios on the increasing age of the host rock. Bentor suggested that high calcium concentrations may be produced by membrane filtration of pore waters followed by a stage or stages of evaporative concentration. This overcomes the problem of decreasing efficiency of the filtration process as the concentration of the residual fluid increases (See section 6.5.2). The Salton Sea brine (White et al., 1963), although containing very little magnesium, has a considerably higher K/Na ratio in comparison to the type 2 and 4 brines (figure 6.4).

In conclusion the type 3 fluid can reasonably be classified as an oil-field brine while the Na/Ca ratios of the type 4 and particularly the type 2 and 3 brines are significantly lower than those reported for even the most concentrated oil-field waters. Calcium may have been gained as the fluids migrated. Bischoff et al. (1981) reported, in their experiments on alteration of greywacke by brine with an initially high calcium concentration, that calcium is released by albitization of labradorite and dissolution of calcite and dolomite. Frape and Fritz (1982) suggested that a decrease in the Na/Ca ratio of groundwater may be a fundamental process in the maturation of all such waters.

Figure 6.4

Triangular diagram illustrating the potassium-sodium-magnesium concentrations of various high salinity formation waters and sea water as well as fluid inclusion compositions. Points are plotted as percentage gram-equivalent concentrations.

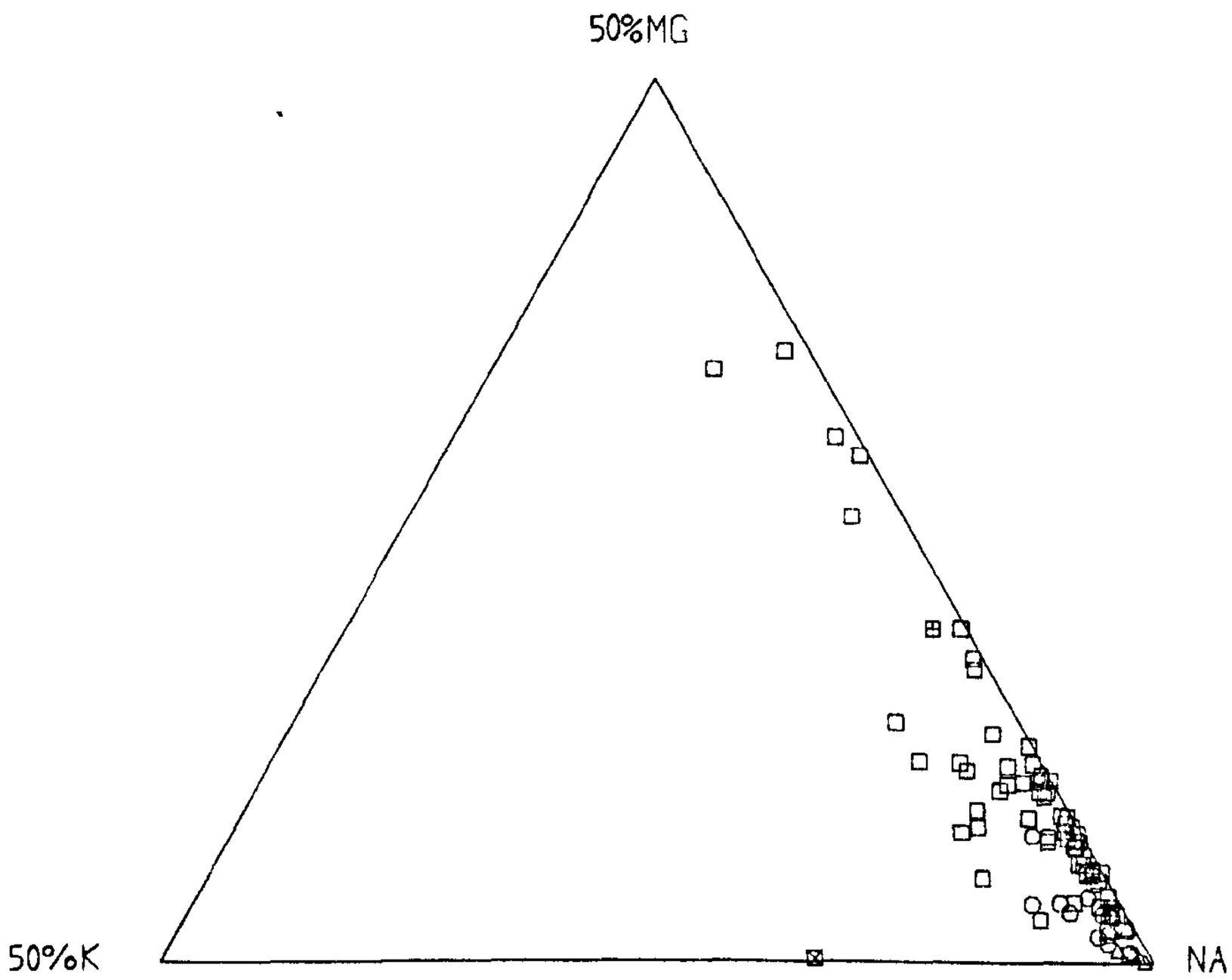

KEY

OILFIELD BRINES □. SUDBURY BASIN △. OCEAN WATER ⊞
SALTON SEA BRINE ⊠. FLUID INCLUSION ANALYSES ○

Some type of concentration process other than simple membrane filtration is probably necessary to account for the chemistry of the type 2 and type 5 brines. The recognition of calcium as being an important component of ore fluids associated with hydrothermal fluorite deposits is becoming more apparent. Recent fluid inclusion studies by Kesler (1977), Moore (198Ø) and Deloule (1982) have revealed high calcium concentrations in the ore fluids. Kesler (1977) reported a fluid inclusion study of the Manto fluorite deposits of Coahuila, Mexico observed some high salinity inclusions in the Cerro El Pilote district. In freezing studies Kesler noted the final melting phase was hydrohalite, which melted at Ø°C. Analysis of the inclusion leachate, however, gives a molal Na/Ca ratio of Ø.Ø45. Since only a pure NaCl solution can produce melting of hydrohalite at Ø.1°C, the phase was probably antarcticite and, therefore, the solutions had a similar composition to the type 2 and 5 brines. Kesler also reported the presence of halite daughter crystals in similar inclusions. These high salinity fluids are considered to have been produced by the concentration on boiling of the more dilute ore-forming fluids found in inclusions in fluorite in other associated deposits after the intrusion of a rhyolite. Concentration by boiling is unlikely in the Southern Pennine Orefield, but generation of a calcium-rich brine by membrane filtration with subsequent concentration by evaporation on a Triassic land surface could not be ruled out. The mechanism by which the fluid moves to the surface and then sinks back into the ground is, however, difficult to visualize.

6.3: D/H RATIOS IN THE ORE-FORMING BRINES

Moore (1980) gave a δD range (-100‰ -8‰) for the fluid inclusions in fluorite from Derbyshire. This range is considerably greater than the reported ranges for the Northern Pennine Orefield (Moore, 1980) and the Mississippi Valley (Hall and Friedman, 1963). The range for the Mississippi Valley is shown in figure 6.5, taken from Taylor (1979). The large range could be produced by trapping water from different levels of a deep sedimentary basin. Hitchon and Friedman (1969) reported that the δD range for the Alberta Basin formation waters was -134‰ to +30‰. In connate waters, δD usually increases with increasing salinity. Other effects causing variation may be mixing of connate waters with meteoric waters, hydroxide exchange with clay minerals, membrane filtration, and reaction with hydrocarbons (Taylor, 1979). Given that at least four distinct fluids were responsible for fluorite mineralization and that all the aforementioned processes are likely to have taken place the value of δD values is limited without accompanying $\delta^{18}O$ values.

Figure 6.5

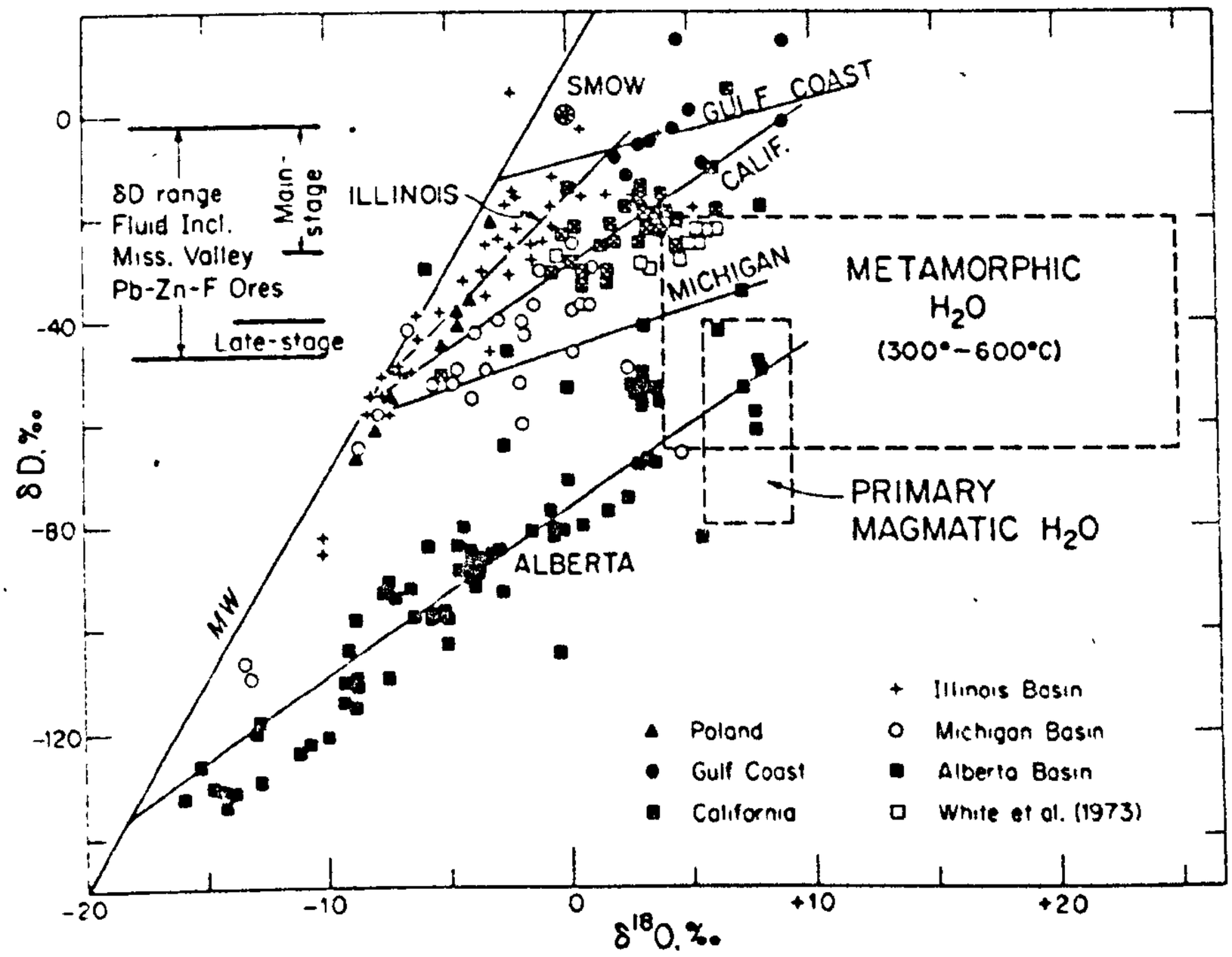

Plot of δD vs. δO^{18} for oil-field brines from North America (Clayton et al.,1966; Hitchon and Friedman, 1969; Kharaka et al., 1973) and Poland (Dowgiallo and Tongiorgi, 1972). Also shown are S.M.O.W. and the calculated fields of both primary magmatic and metamorphic waters. The δD range of Mississippi Valley-Type ore deposits is also shown (Hall and Friedman, 1963).
(Taken from Taylor, 1979)

6.4: STRONTIUM ISOTOPE GEOCHEMISTRY

6.4.1: 87SR/86SR RATIOS IN FLUORITE AND CALCITE

Minerals such as calcite, fluorite and baryte contain negligible concentrations of rubidium so that the measured 87Sr/86Sr ratios represent the corresponding ratio in the ore fluid. Interpretation is also simplified by there being no fractionation in the strontium isotope system. 86Sr/87Sr ratios have been used to place constraints on models of ore-genesis by various workers (Barbieri et al., 1977; Kesler and Jones, 1981; Barbieri et al., 1982; Kessen et al., 1981). The strontium isotope ratios of marine carbonates varied during the Palaeozoic and Mesozoic periods but were globally uniform. Strontium isotope ratios for marine carbonates have been presented by Peterman et al. (197Ø) and Veizer and Compston (1974). Visean marine carbonates have a restricted strontium isotopic ratio of Ø.7Ø77 (Peterman et al, 197Ø), while Palaeozoic marine carbonates have a range of Ø.7Ø7-Ø.7Ø9. Rocks derived from possible mantle sources show low 87Sr/86Sr ratios. Oceanic basalts, for example, have a mean initial 87Sr/86Sr ratio of Ø.7Ø37, when intruded (Faure and Powell, 1972). Determination of the 87Sr/86Sr ratios in six gangue minerals from the Southern Pennine Orefield are given in table 6.1

TABLE 6.1:

87SR/86 SR RATIOS FOR FLUORITE AND CALCITE.

Mineral	Locality	87Sr/86Sr ratio
Fluorite	Masson Hill	Ø.71Ø12 ± 4
Fluorite	Overton Hall Mine	Ø.71Ø11 ± 22
		Ø.71Ø1Ø ± 3
Fluorite	Smalldale Quarry	Ø.7Ø848 ± 5
		Ø.7Ø861 ± 3
Fluorite	Treak Cliff Cavern	Ø.7Ø818 ± 4
		Ø.7Ø836 ± 7
Calcite (early calcite)	Blende Vein, Magpie Mine	Ø.7Ø827 ± 4
		Ø.7Ø829 ± 8
Calcite (late calcite)	Moor Farm (Opencast)	Ø.7Ø993 ± 7
		Ø.71ØØ3 ± 2

The fluorite samples from Smalldale Quarry, Treak Cliff Cavern and the calcite sample from Magpie Mine show possible 87Sr/86Sr heterogeneity. There is good evidence to suggest that these specimens represent replaced limestone wall rock, and the ratios which fall between the Visean marine carbonate value (Ø.7Ø77) and the highest ratios measured in the fluorite samples could be produced by limestone metasomatism. Primary, type 3 inclusions were identified in the sample from Masson Hill and primary type 4 inclusions in the sample from Overton Hall Mine. Both these samples were of fluorite which had grown in an open vugh. Similarly the late calcite sample was taken from a scalenohedral crystal which had grown in an open cavity. All the ratios exceeded the the Visean marine carbonate value.

6.4.2: INTERPRETATION OF THE 87SR/86SR ISOTOPIC RATIOS

The high values indicate that the brines must have been in contact with a more radiogenic host rock than the Carboniferous Limestone, and that strontium must have been added to the system by wall rock exchange with minerals other than strontium-bearing carbonates. The fluorite samples from Masson Hill and Overton Hall Mine which formed in an open cavity have very similar ratios despite having been deposited in different mineralizing events. This similarity could be the result of the evolutionary processes which have produced the increase in the 87Sr/86Sr ratios, if one assumes that the ore fluids were derived from sea water. It is interesting to note also that the late calcite has a similar 87Sr/86Sr ratio to the fluorite from Masson Hill and Ashover, despite the fact that the calcite mineralization differs from the fluorite mineralization in that it does not appear to be associated with any Pb-Zn-CaF_2-Ba formation. The high values give no support to the suggestion of a deep-seated mantle source for the fluids (Evans and Maroof, 1976), although leaching of rubidium-rich basement rock could not be ruled out. A solution vertically rising from the Charnian basement at a depth of 2km could be expected, however, to rapidly exchange radiogenic strontium with marine carbonate strontium, thus reducing the 87Sr/86Sr ratio of the fluid (Sunwall and Pushkar, 1979). Therefore, it may be tentatively concluded that the fluids have migrated laterally through or descended vertically into the limestone host-rock. Strontium isotope ratios have been measured in oil-field brines from

Ohio (Sunwall and Pushkar, 1979) and Kansas and Colorado (Chaudhuri, 1978). 87Sr/86Sr ratios range from Ø.7Ø92-Ø.7341. The high values again suggest that marine carbonates cannot represent the source of the strontium. Sedimentary rock-forming minerals such as illite, smectite, potassium feldspar and mica are rich in rubidium, and therefore, shales and greywackes can generate high 87Sr/86Sr ratios in short periods of time. Shepherd et al. (1982) have plotted a 87Sr/86Sr evolution diagram for the Carboniferous limestone, Namurian shale and Devonian granite in the proximity of the North Pennine Orefield. Two hundred million years ago, the shales would have only have had a slightly higher 87Sr/86Sr ratio than the fluorite. Leaching of biotite and plagioclase, derived from Caledonian granites and present in the Namurian sandstones, could also have increased the 87Sr/86Sr ratio of the ore fluids. In the leaching of shales alone, the leachate probably has a lower 87Sr/86Sr ratio than the shale itself (Bofinger et al., 1968), since strontium is supplied by the most soluble strontium-bearing phase [marine carbonates]. Regardless of the origin of the ore fluid, the results indicate epigenetic mineralization, with the introduction of strontium from a source lying outside the host rock.

6.5: EVOLUTION OF THE ORE FLUIDS

6.5.1: DISSOLUTION OF EVAPORITES

Clearly, large volumes of brine were involved in the mineralizing process in order to produce the chemical

homogeneity of the fluids seen in the fluid inclusions in fluorite. The geological environment in which such fluids can be produced is obviously a constraint on when and where mineralization can occur. The mechanism by which highly saline brines are evolved is the subject of some debate. Russel (1933) proposed membrane filtration (reverse osmosis) to produce calcium-sodium brines while Carpenter et al. (1974) and Carpenter (1978) suggested that dissolution of evaporite sequences can be used to explain the formation of all saline brines.

6.5.2: MEMBRANE FILTRATION (REVERSE CHEMICAL OSMOSIS)

This mechanism is based on the fact that clay minerals are surrounded by a zone of negative charge known as the Guoy layer. When clay mineral particles are forced together and the layers overlap, the zones of negative charge remain permeable but resist ions passing through in solution to varying degrees. Obviously, very high hydraulic pressure gradients have to be applied across the almost impermeable membrane to produce any filtering effect. According to Berner (1971), a shale buried to a depth of 300m should attain membrane properties. Increasing the calcium to sodium ratio of a brine is considered to be one of its most important functions. Kharaka and Berry (1973) noted in an experimental study that bicarbonate anions passed through the membrane more easily than sulphate which in turn passed through more easily than chloride. Hanshaw and Coplen (1973) also presented the results of some experimental work on

ultrafilters. The theory by which they were able to model the behaviour semi-permeable membranes indicates that the efficiency of the process will drop with the increasing concentration of the residual fluid. Hence, eventually the dissolved salt concentration of the effluent will be almost equal to that of the residual fluid. Kharaka and Smalley (1976) carried out filtration experiments at increased temperatures and varied pressures, using bentonite and kaolinite as the filters. As Kharaka and Berry had suggested, calcium is retarded with respect to sodium at very slow rates of filtration. At increased temperatures (80°C) the relative retardation of calcium with respect to sodium was increased but the filtration ratios were more closely grouped. The maximum concentration achieved in the reservoir solution was $6g\ litre^{-1}$, still considerably less than the $400g\ litre^{-1}$ observed in some analyses from the Michigan Basin.

6.5.3: DISSOLUTION OF EVAPORITES

Manheim and Horne (1968) and Manheim (1970) suggested that membrane filtration defied the principles of hydrology. They observed that the high pressure gradients required to produce filtration were not available in modern sedimentary sequences and the passage of very large volumes of both pore and meteoric water was difficult to account for in what are almost impermeable rocks. Graf (1982) has suggested that recent research has answered many of the problems. It is thought that rapid sedimentation of fine grained material; lateral tectonic compression; aquathermal pressuring; and

dehydration of gypsum will be able to produce the required degree of over-pressuring. Carpenter (1978), however, suggested that all concentrated brines could be produced from evaporites in one of three ways; (1) dissolution of evaporites; (2) interstitial fluids expelled from an evaporite sequence; (3) incongruent alteration of evaporite minerals. He suggested that sulphate may be lost through precipitation of calcium sulphate and reduction; carbonate through precipitation of calcite and potassium by formation of authigenic potassium micas. High calcium concentrations are obtained by dolomitization of calcium carbonate. There are several problems with this idea. Analyses of oil-field brines usually show a positive correlation between calcium and magnesium (figure 6.2) concentration. A second problem is that considerable quantities of calcium are used up in removing sulphate and carbonate ions and therefore vast quantities of calcite would require dolomitizing. The model also fails to show why an inverse relationship between the concentrations of sodium and calcium should occur (figure 6.3) on increasing the dissolved salt content of a fluid. Although evaporite sequences are present in the Triassic strata adjoining the Southern Pennine Orefield, the high calcium concentration of the type 3 and 4 brines by dolomitization would have produced vast quantities of dolomitized carbonates as well as epigenetic anhydrite deposits. The apparent lack of such deposits seems to favour reverse chemical osmosis as a mechanism of brine generation.

6.5.4: VOLUME OF ORE FLUID REQUIRED FOR FLUORITE MINERALIZATION

In many models of ore genesis it is often assumed that the ore fluid only passes through a vein system once, and after which it is either lost to the surface and or diluted by ground-water. In a single solution model, a favourable quantity of fluorite deposited from 1 kg of fluid would be 10mg. Taking a brine density of 1150kgm^{-3} at 100^{o}C, this corresponds to 11.5mg of fluorite from 1 litre of fluid. An estimate of the quantity of fluorite present in the district is difficult to make. However, Ford and Ineson (1971) reported that the Glebe Mine alone had produced between 980 000 and 1 980 000 tonnes of fluorite up to that time. Laportes produce approximately 250 000 tonnes of fluorite per annum and they have been operating for over 40 years in the South Pennines (Ford, personal communication). A total of 20 M tonnes of fluorite for the district as a whole is probably not unreasonable. In a single solution model, each tonne of fluorite required $1.0x10^{8}$ kg of ore fluid. Therefore, a total of $2x10^{15}$ kg of fluid were required to produce the fluorite deposits. Using the density stated above, this corresponds to 1738km^{3} of brine. If the mass of fluorite deposited was equally split between the phase 3 and phase 4 events the volume of the pore water may be estimated.

Membrane filtration (reverse chemical osmosis) appears to be the best way of generating calcium-rich brines, and if it is assumed that all the pore water is supplied by compacting sediments [principally shales], the volume of the

sedimentary basin required may be estimated. Prior to diagenesis, shales may contain 3500 litres of pore water per cubic metre. Of this, 75% is lost on burial to 100m and is expelled to the surface while 5% is retained even at considerable depths of burial (Hanor, 1979). Therefore, one cubic metre of shale may yield 700 litres of pore water. If the 700 litres undergoes filtration, the model of Graf et al., (1966) may be used to calculate the volume of ore fluid produced. Graf et al.'s model makes some very optimistic assumptions. These are:-

1) Shale ultrafilters have perfect efficiency, except for the specific brine losses provided for by the model.
2) All sulphate is reduced bacterially and replaced by an equivalent amount of bicarbonate. This also allows for the possibility of sulphate passing through the membrane with the equivalent quantity of sodium.
3) All bicarbonate passes through the shale barrier with the equivalent amount of sodium.
4) All magnesium is lost in dolomitization and is replaced by an equivalent quantity of calcium.

The equations used are:-

$$X = 1.79 \cdot \left(\frac{m_{Ca} + m_{Mg}}{2} \right) + 1.86\, m_{Na}$$

$$Y = 258 \cdot \left(\frac{m_{Ca} + m_{Mg}}{2} \right) + 80.4\, m_{Na}$$

Where X is the volume of pore water and Y the volume of meteoric water required to produce one volume of ore fluid.

TABLE 6.2:

VOLUME OF PORE WATER REQUIRED TO PRODUCE THE TYPE 3 AN 4 BRINES

	Type 3	Type 4
Volume of pore water used	6.5l	3.5l
Volume of meteoric water used	69.9l	323l
Volume of ore fluid per cubic metre of shale (litres)	1Ø7	2ØØ
No. of litres required for mineralization	$8.7x1Ø^{14}$	$8.7x1Ø^{14}$
Volume of shale (km^3)	813Ø	435Ø

Table 6.2 shows gives an indication as to the volume of fluid and the size of the shale basin required to generate the ore fluid in a non-circulatory system. The volume of the ore fluids alone would fill a sea 1ØØØm deep, 8Ømm long and 22km wide. Clearly the storage of this quantity of fluid in a position where it could be moved into the Orefield presents problems. The calculated total shale volume of $12480km^3$ corresponds to a shale basin 8Ømm long, 26km wide and 6km deep. Given that a considerable volume of meteoric water must be added to increase calcium concentrations, evolution of these fluids must have taken a considerable period of time. The model can be altered by increasing the amount of fluorite deposited from a litre of ore fluid. However, this can only be increased by a certain amount since fluorite in Derbyshire does not show textures typical of supersaturation. Basins such as the Widmerpool, Gainsborough and Edale Gulfs were

probably incapable of producing the volumes of brines required.

Ziegler (1981) has reconstructed the palaeogegraphy of north west Europe from Silurian times to the present day. Sedimentary sequences capable of generating large quantities of ore fluids can be identified. Worley and Ford (1977) suggested that the fluids could have been derived from the Dinantian shales of the North Sea Basin. The extent of these shales is not well known. Dinantian shales also occur in the Irish Sea basin. Thick Namurian sediments occur in the Rhenish Basin (2000m) and the Bowland-Craven Basin (1000m). On moving north, into the North Sea, Namurian sediments give way to red beds. Westphalian sediments reach their thickest in the North German Lowlands (3500m), but also maintain their thickness moving from England on to the European mainland. Thick Triassic sequences occur in the Worcester Graben, the Cheshire Graben and the Carlisle basin in the west. In the North Sea, thick successions occur in the North Danish Basin (6000m) and the Viking Trough (3000m).

Triassic sedimentation was controlled by tensional tectonism, with the rapid filling of subsiding grabens. All these basins could have generated high salinity brines through over-pressuring as a result of sediment compaction or aquathermal pressuring. Aquathermal pressuring is likely to have occurred in the North Sea Grabens, where increased thermal gradients occurred as a result of crustal thinning. Tensional tectonism would also have favoured fluid movement. Dense fluids may move towards the surface if a reservoir at lithostatic pressure is fractured (Jones and Wallace, 1974) or if shear stress is rapidly released from a reservoir with

stress-induced porosity (Sibson et al., 1975).

6.6: DISCUSSION

The association of oil with the type 1, 3 and 4 fluids indicates that oil-field brine was probably an important fluid component. The organic geochemistry of the hydrocarbons (Pering, 1973) and the wide range in final ice and homogenization temperatures is suggestive of fluid mixing at the site of deposition. Interaction between a moderately saline formation water and highy oxygenated descending meteoric water is a possibility. The composition of the type 3 brine is similar to that of a deep formation water, although depletion in magnesium has occurred probably as a result of dolomitization and chloritization of sedimentary minerals. The type 2, 4 and 5 brines have unusual compositions, although the type 4 fluid is closest to an oil-field brine. The type 4 brine is similar in composition to fluids present in the low grade metasediments of the Sudbury Basin, although the origin of the latter is unknown (Frape and Fritz, 1982). The type 2 and 5 fluids could have been initially produced by membrane filtration with final stages of concentration by surface evaporation (Bentor, 1969). 87Sr/86Sr ratios for fluorite and calcite suggests interaction of the ore fluids with radiogenic (rubidium enriched) wall rocks, other than marine Palaeozoic or Mesozoic carbonates. Leaching of a Charnian-type basement cannot be ruled out but is unlikely while there is no evidence for the contribution of juvenile strontium.

Contribution of radiogenic strontium from the overlying Namurian shales is probably the best possibility as suggested by Moore (1980) and Shepherd et al. (1982) for the Northern Pennine Orefield.

A simple model of brine evolution and ore genesis suggests that a shale basin of considerable size is required to produce the quantities of ore fluid needed. The Namurian sediments of the Bowland-Craven basin or the Triassic sediments of the Cheshire-Severn or Viking Grabens were probably the best source. The homogeneity of the brines suggests that brine generation did not occur concurrently with mineralization but points to storage and mixing within an intermediate reservoir. A circulatory model of ore genesis could have considerably reduced the volumes of brine required. A mechanism of reducing the pH and the potassium content of the fluid is necessary if the brines were to have effectively leached the source rocks on each cycle. The uniformity of the REE concentrations in the fluorite and the fluid compositions also places restrictions on a circulatory model of mineralization.

A single solution "one pass" model of mineralization is possible. If the ore fluids contained 10ppm or 1ppm CaF_2, and a fluid flow of 1µms occurred through the top 100m of limestone, 1738km^3 or 17380km^3 of fluid could have moved through the orefield in 1837Ø years or 183700 years, depending on the concentration used. Two hundred thousand years is not a geologically long period of time, considering the postulated age range for the ore deposits. Such a mechanism would provide an "open system" for geochemical modelling and would avoid the inherent difficulties of

isothermal fluid circulation.

6.7: CONCLUSION

Important conclusions arising from the prece ding discussion are:

1) The presence of abundant oil in type 1 fluid inclusions and the more rare occurrence of oil in type 3 and 4 inclusions suggests that oil-field brines formed a component of the ore fluids.

2) The high $CaCl_2$/NaCl ratios in the type 2, 4 and 5 ore fluids indicates, however, that these brines at least were not typical of present-day subsurface sedimentary formation waters.

3) 87Sr/86Sr ratios for fluorite range from Ø.7Ø82 to Ø.71Ø1, indicating that the ore fluids had interacted with wall rocks or source rocks enriched in radiogenic strontium with respect to Visean marine carbonates.

4) The ore fluids were probably produced by membrane filtration but attainment of total dissolved salt concentrations of up to $4ØØgl^{-1}$ may have required other mechanisms of brine evolution.

5) Twenty million tonnes of fluorite would have required at least $1740km^3$ of ore fluid (1Ømg per kg fluorite), and if

derived from shales, a shale volume of 12 480km^3. Formations capable of generating such large quantities of brines are limited. Possible sources are the Namurian sediments of the Bowland-Craven basin and the Triassic sediments of the North Sea Graben and the Severn-Cheshire basin.

CHAPTER 7

ASPECTS OF ORE FORMATION

7.1: INTRODUCTION

In any model of ore formation it is important to establish the source of the ore-forming components themselves, their mode of transport and the mechanisms of mineral deposition. The physicochemical environment of mineralization has already been established in chapters 3 and 4 and provides a framework within which the various processes may be modelled and their importance evaluated.

The potential of various source rocks may be estimated by looking at the measured abundances of the appropriate elements and calculating the stability of the host mineral phases on exposure to the predicted fluid conditions. The behaviour of fluorite in hydrothermal environments has been investigated by a number of researchers and their data may be usefully applied in order to evaluate which processes will most efficiently precipitate fluorite. Fluid inclusion data are particularly valuable when trying to estimate to what extent fluid mixing and cooling have controlled mineral solubility. Since fluorite from the Orefield contains inclusions of galena and sphalerite, a model of ore genesis must be able to account for the measured sulphur isotope ratios for sulphides and be compatible with the chemistry of sulphide solubility.

7.2: SOURCES OF FLUORINE AND THE BASE METALS

It has been suggested in chapter 6 that the evolution of an ore-forming fluid such as those associated with mineralization in the Southern Pennine Orefield involved prolonged contact with shales at some time. Leaching of shales by formation waters has been proposed as a mechanism of generating metal-rich solutions involved in mineralization at Pine Point (Billings et al. 1969) and in the formation of copper deposits (Boyle 1968). Carpenter et al. (1974) reported that galena and baryte, precipitating as scale on oil-well piping in the Central Mississippi Valley oil-field were probably derived from leaching of shales. Lead isotope data for the fluids themselves and for possible source rocks were used to justify this hypothesis. Very high lead and zinc concentrations in waters from certain stratigraphic units were measured. Concentrations of up to 65ppm Pb and 285ppm Zn were determined. Carpenter et al. (1974) suggested that mobilization of the base metals occurred as the result of injection of potassium-rich fluids and the consequent expulsion of metals as a result of the recrystallization of mixed-layer potassium clay minerals. This argument was not supported by the experimental work of Long and Angino (1982) who found that calcium chloride solution is much more effective in mobilizing metals than potassium chloride solution of the same ionic strength. Destabilization of potassium silicates as a result of interaction with potassium-depleted hydrothermal fluids may be more important

in leaching base metals. Long and Angino (1982) also noted that leaching of shales at temperatures in excess of 90°C may not increase the efficiency of the leaching process. Therefore, the type 2, 3 and 4 fluids were probably particularly effective in leaching base metals from shales, especially when the high calcium concentrations of the fluids are taken into consideration.

Leaching of fluorine is more problematical, with little experimental or theoretical work having been done on the subject. High fluorine concentrations in fluid and gas phases are known to be associated with late stages of acid magmatism and, therefore, a genetic link with acid magmatism has often been proposed to explain the formation of fluorite deposits. Since there appears to be no obvious genetic association with acid magmas in the Southern Pennine Orefield, other sources of fluorine must be looked for. Possible sources of barium and the base metals will also be examined.

7.3: SELECTION OF SOURCE ROCKS

Initially, some constraints may be placed upon the sources of both base metals and fluorine in the light of the conclusions drawn in chapter 6 and in the introductory notes on the Orefield itself. These constraints are.

(1) Fluorite deposits filling veins but also metasomatically replacing limestone are sited at the top of a 1.8km succession of carbonates directly beneath a sequence of shales and sandstones. No correlation is known to exist between basement highs and centres of intense mineralization.

Fluorite deposits are thought to die out at depth. These facts are suggestive of fluids moving laterally or descending into the limestone from an overlying formation.

(2) Strontium isotope ratios in fluorite and calcite indicate contact with rocks enriched in rubidium relative to Visean marine carbonates. It is known that strontium isotopes fairly readily equilibrate when a fluid enters a carbonate environment and therefore it seems unlikely that the ore-forming fluids passed through a column of 1.8km of marine carbonates. Similarly metasomatism of limestone after considerable contact with carbonates is unlikely. However, as a cautionary note, it must be remarked that feeder channels could possibly have become insulated as a result of the high fluid/wall rock ratios producing rapid metasomatism or as a result of the silicification of the walls of the feeder channels. No feeder channels have, however, been identified in the Orefield. On the other hand, the high permeability of limestone would provide slow moving solutions with plenty of opportunities to interact with the wall rocks and therefore the hyposthesis of mobilization of fluorine and base metals from post-Dinantian rocks is favoured in preference to a basement source. The source rock potential of the Dinantian limestones themselves must also be examined.

7.3.1: DINANTIAN LIMESTONES

It is possible that fluorine was derived from the host rocks themselves. In the Buxton district, the fluorine content of the limestones is low (100ppm $\pm$100ppm), with the

highest values having been recorded from the Brigantian Monsal Dale limestones (300ppm ±300ppm) (Harrison, 1981). The Buxton district probably provides the most reliable concentrations for South Pennines since fluorite deposits in the area are very limited. The Bakewell district shows limestones with low values in Asbian material but considerably increased concentrations of fluorine (6700ppm ±16000ppm) in the Brigantian (Bridge and Gozzard, 1981). These high values may, however, represent contamination of limestone through movement of fluorine in the ground water away from the nearby fluorite deposits. Bridge and Gozzard (1981) suggested from the results of cluster analysis of the trace element concentrations that the fluorine is present as fluorapatite. Fluorine concentrations in limestones given by Wedepohl (1971) range from 20 to 510ppm.

TABLE 7.1

ZINC, COPPER AND LEAD CONCENTRATIONS (PPM) IN THE BEE LOW LIMESTONES AND THE MONSAL DALE LIMESTONES OF THE BUXTON DISTRICT.

	Zn	Pb	Cu
Bee Low limestone	11 ± 14	6 ± 20	5 ± 8
Monsal Dale Limestone	14 ± 12	8 ± 14	3 ± 4

The main problem in postulating the limestone as source of fluorine is the difficulty of producing a mechanism which can scavenge and transport the element and cause precipitation at centres of high concentration given the

physicochemical constraints already outlined. Secondly it is probable that the higher concentrations may not represent primary depositional values. The limestones have very low base metal concentrations. Harrison (1981) reported the concentrations of Zn, Pb and Cu in the Bee Low and Monsal Dale limestones and values are given in table 7.1. Therefore, even if fluorine could have been derived from the limestone the base metals would probably have had to be mobilized from elsewhere. Worley and Ford (1977) suggested that Dinantian shales in the North Sea basin could be the source of fluorine and the base metals.

7.3.2: NAMURIAN AND WESTPHALIAN SANDSTONES

Immature, feldspathic sandstones, such as those in the Rough Rock (G1), Chatsworth (R2) , Kinderscout (R1)and Heyden Rock (R2) Formations, contain some muscovite, biotite and feldspar. Apatite is also present in smaller quantities. The minerals are derived from either a Caledonian granitic or gnissose granitic province (Stevenson and Gaunt, 1973) and are, therefore, likely to contain relatively high fluorine concentrations. Concentrations of fluorine in these minerals were drawn from Wedepohl (1971).

Microcline and orthoclase	300ppm
Biotite	800-35000ppm
Muscovite	200-7700ppm
fluorapatite	13500-33600ppm

Concentrations of fluorine in microcline and orthoclase could be due to the presence of fluid inclusions. It is improbable that much fluorine was lost during the weathering and transportation processes which produced the sandstones (Carpenter, 1969).

7.3.3: RELEASE OF FLUORINE INTO THE FLUIDS

The ionic radius of the fluoride ion is very similar to that of the hydroxide ion and substitution may take place fairly readily. Obviously an acidic solution in equilibrating with a mica or clay mineral will be buffered to some degree by the release of hydroxide ions into the solution. Therefore acidic solutions are unlikely to be good fluoride scavengers. The effect of temperature changes on the scavenging ability of hydrothermal fluids may be estimated from the data of Munoz and Luddington (1974), (1977) in the case of the micas, although their data requires considerable extrapolation which obviously leads to large errors. Roberson (1966) collected similar data for hydroxide-fluoride exchange in apatite.

Munoz and Luddington (1974) experimentally derived thermodynamic data for the equation:-

$$\text{Ø.5 Biotite (OH)} + \text{HF} = \text{Ø.5 Biotite (F)} + H_2O$$

A regression for the equilibrium constant is:-

$$\log K = 2552/T\ (^{o}K) - \text{Ø.31}$$

Using association constants for HF and H_2O (Appendix 6.13), the equilibrium constants for the reaction at low temperatures may be calculated. The fluoride activity of a brine in equilibrium with biotite (annite) is shown in figure 7.1 at various pH values and temperatures. The plot suggests that on cooling of a fluid at a constant pH value, fluorine will be adsorbed into the mica rather than released. Muscovite behaves in a very similar way to biotite (Munoz and Luddington, 1977). Biotite is not usually seen as an authigenic mineral in Mississippi Valley-type ore deposits. Clearly the complete decomposition of a mica is the most favourable occurrence for significant fluorine release. However decomposition to a clay mineral is more likely and clay minerals can themselves store considerable quantities of fluorine. In this respect silica saturation is of great importance. The lack of quartz as a cogenetic mineral phase in association with fluorite may not necessarily indicate undersaturation of silica in the ore fluids. It may indicate that only a small degree of cooling has taken place during ore deposition. It is probable that a fluid which had evolved in a siliceous aquifer would be saturated in silica whereas considerable periods of residence within a carbonate host would produce undersaturation. Since alteration assemblages occurring where ore fluids have interacted with lavas or tuffs suggest the presence of some silica in solution, saturation will be assumed. Albitization of labradorite has occurred in the Matlock Lower Lava (Smith et al., 1967) and this reaction uses silica:-

Figure 7.1

The diagram shows a plot of temperature against $\log(F^-)$ in which fluoride activity in equilibrium with annite at set pH levels is shown. The equilibrium constant for the reaction was taken from Munoz and Luddington (1974).

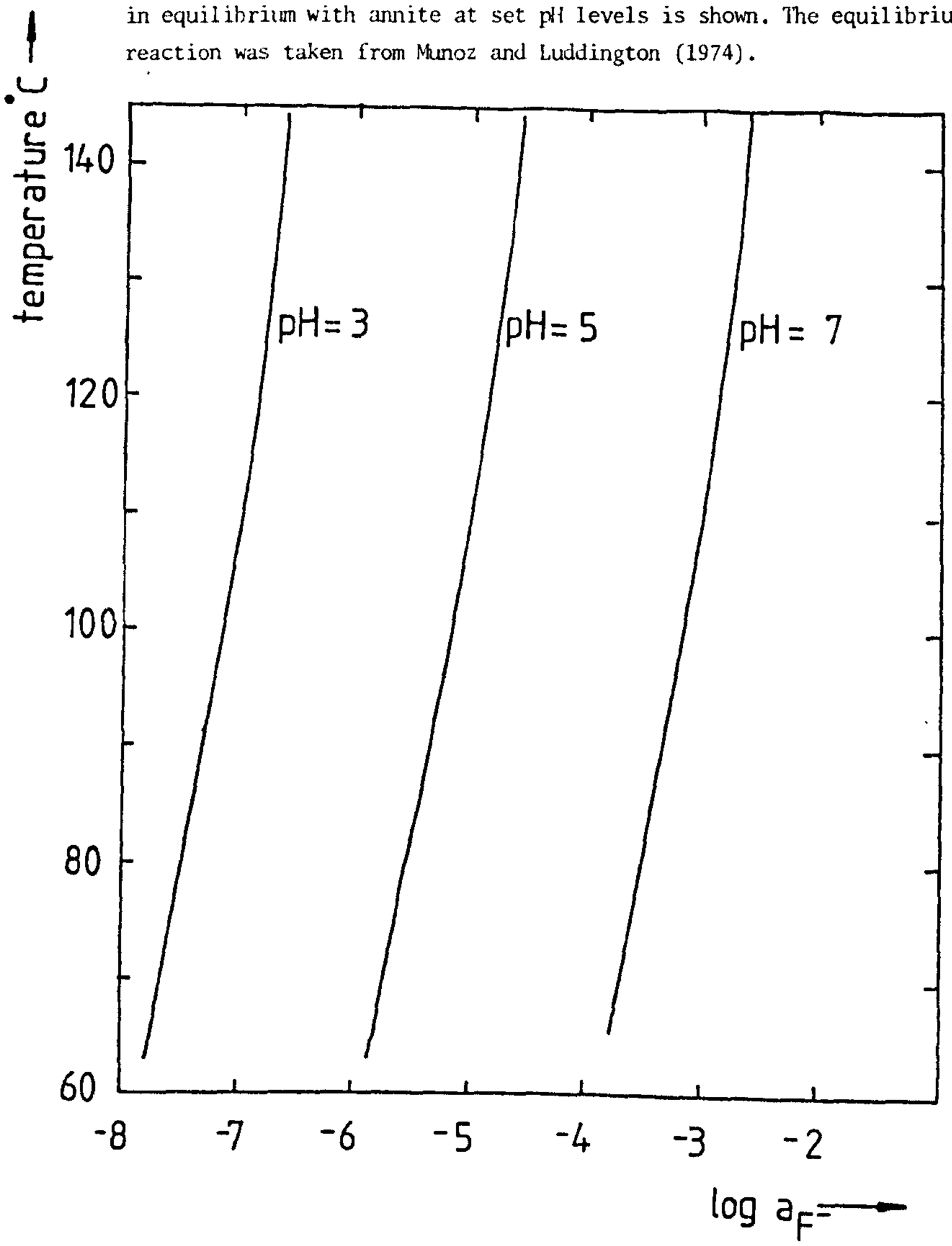

$$2Na^{+} + CaAl_2Si_2O_8 + 4SiO_2 = 2NaAlSi_3O_8 + Ca^{++}$$

Other minerals formed in alteration processes are kaolinite, chlorite, illite and smectite (Ineson and Mitchell, 1973). The main problem with using alteration assemblages as a guide to fluid chemistry is the uncertainty as to which fluids were responsible for which mineral suite. In figure 7.2, the stability of muscovite, K-feldspar and kaolinite has been plotted to show the effects of changing the temperature and therefore the potassium activity of the ore fluids while keeping the pH within a constant range(See appendix 6.14.1). At quartz saturation K-feldspar is an unstable phase below 150^{o}C in both the phase 3 and phase 4 fluids. In the neutral to slightly acidic pH ranges used muscovite is also unstable in both fluids below 100^{o}C. The phase 3 ore fluid would be able to stabilize both K-feldspar and muscovite more successfully than the phase 4 fluid given the same pH.

Fluorapatite may contain considerable quantities of fluorine, although not as much as is indicated by the stoichiometric formula. Chloride and hydroxide ions may substitute for fluoride. Stevenson and Gaunt (1971) reported the presence of apatite in the Rough Rock, Roaches Grit and Kinderscout Grit Formations. Fluorine may be removed from apatite as a result of hydroxide-fluoride exchange and mineral dissolution. Roberson (1966) and more recently Stauffer (1982) reviewed the thermodynamic data for fluor- and hydroxy-apatite. The equation for the exchange reaction is:

$$Ca_{10}(PO_4)_6(OH)_2 + 2F^{-} = Ca_{10}(PO_4)_6F_2 + 2OH^{-}$$

Figure 7.2

The diagram shows the stability relations of K-feldspar, muscovite and kaolinite at 25°C, 60°C, 100°C and 150°C at 1 atmosphere pressure and as a function of log $(K^+)/(H^+)$ and log(H_4SiO_4). The estimated $(K^+)/(H^+)$ ranges for the phase 3 and 4 ore fluids have been plotted on to the diagram. The free molal potassium concentrations for the phase 3 and 4 fluids are 0.035 and 0.01m respectively.

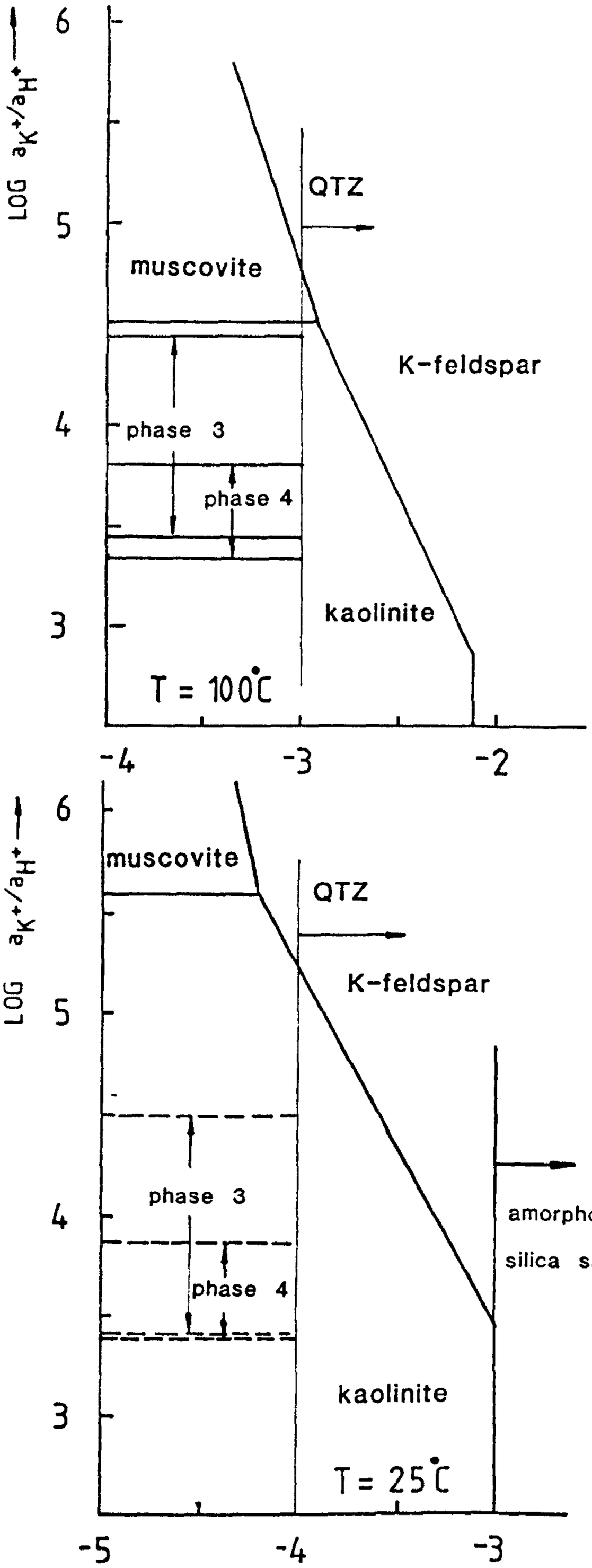

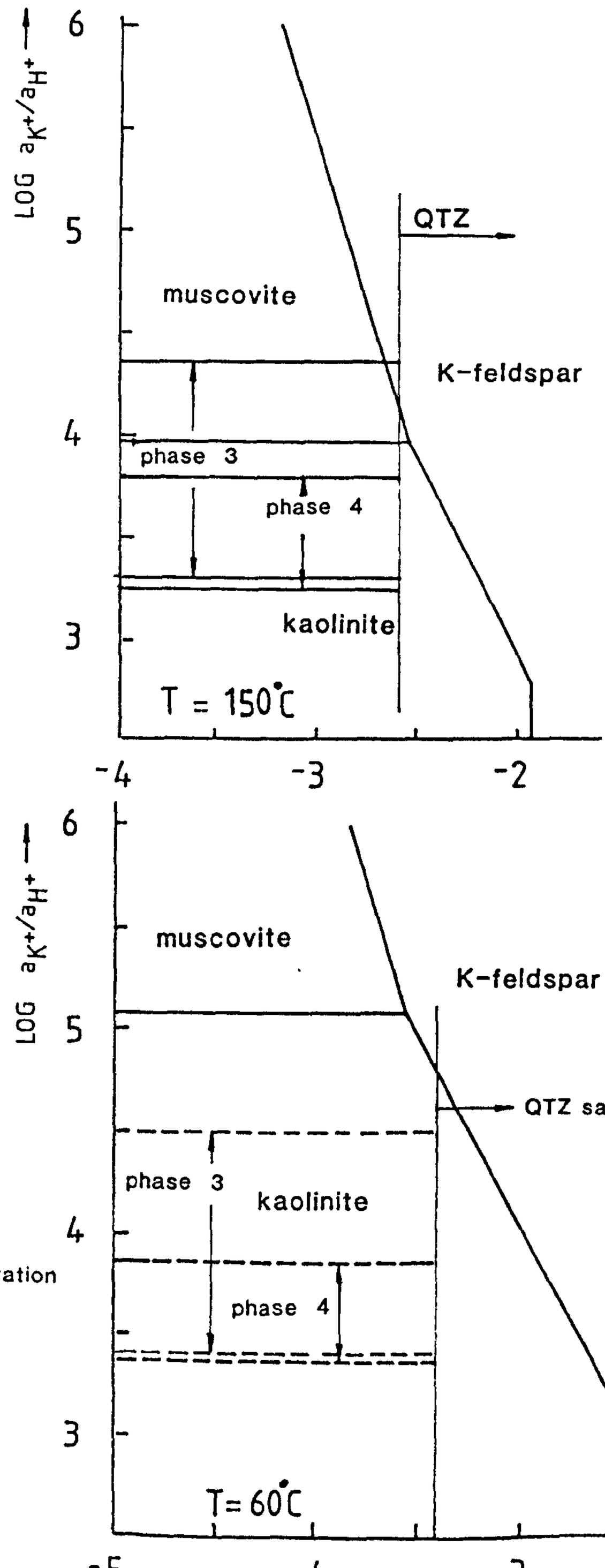

Using thermodynamic data from Krauskopf (1979), the equilibrium constant can be extrapolated to higher temperatures using the equation given in section 5.6.3. The free energy and enthalpy of the reaction at 25°C are -9.Ø kcal mol^{-1} and 9.58 kcal mol^{-1}. The equilibrium constant at 1ØØ°C is 8.Ø. Using these values and the association constant for water at 1ØØ°C (appendix 6.13), the activity of fluoride in equilibrium with fluorapatite at a pH of 6 is calculated to be approximately five orders of magnitude less than the fluoride activity at fluorite saturation.

The dominant aqueous phosphate species in the pH range (5-7) is $H_2PO_4^-$, rather than HPO_4^{--}, the dominant species in sea water. The equation for the solubility of apatite may be:-

$$Ca_5(PO_4)_3F + 6H_2O = 5Ca^{++} + 3H_2PO_4^- + 2F^- + 6OH^-$$

The stability boundary formed by the equation is plotted on a diagram (figure 7.3) showing activity of fluoride against pH (appendix 6.14.2). The plot shows that unless the dihydrogen phosphate activity falls below two orders of magnitude of that of sea water, apatite will remain a stable mineral phase. Complexing of phosphate will be considerably greater than corresponding complexing in sea water, but whether it will be sufficient to destabilize apatite is doubtful.

In conclusion hydroxide-fluoride exchange involving fluorapatite will probably make no contribution to the fluorine content of the ore fluid in the pH range 5 to 7. Dissolution of apatite could occur at very low total

Figure 7.3

Dissolution of fluorapatite as a function of fluoride activity and pH at set dihydrophosphate activities and 100°C.

The boundary at (a) represents fluorite saturation of the phase 3 ore fluid at 100°C, based on the calcium activity of the fluid. The line below represents a similar boundary for the phase 4 ore fluid.

The line (c) shows a boundary, to the right of which, fluorapatite will remain a stable solid phase in the fluid, which has a total phosphorous content of 0.07ppm. It is assumed that 50% of the dihydrophosphate ion is complexed.

The line (b) shows the dihydrogen phosphate activity at which dissolution of fluorapatite will take place at fluoride activities in excess of fluorite saturation. The boundary is approximate.

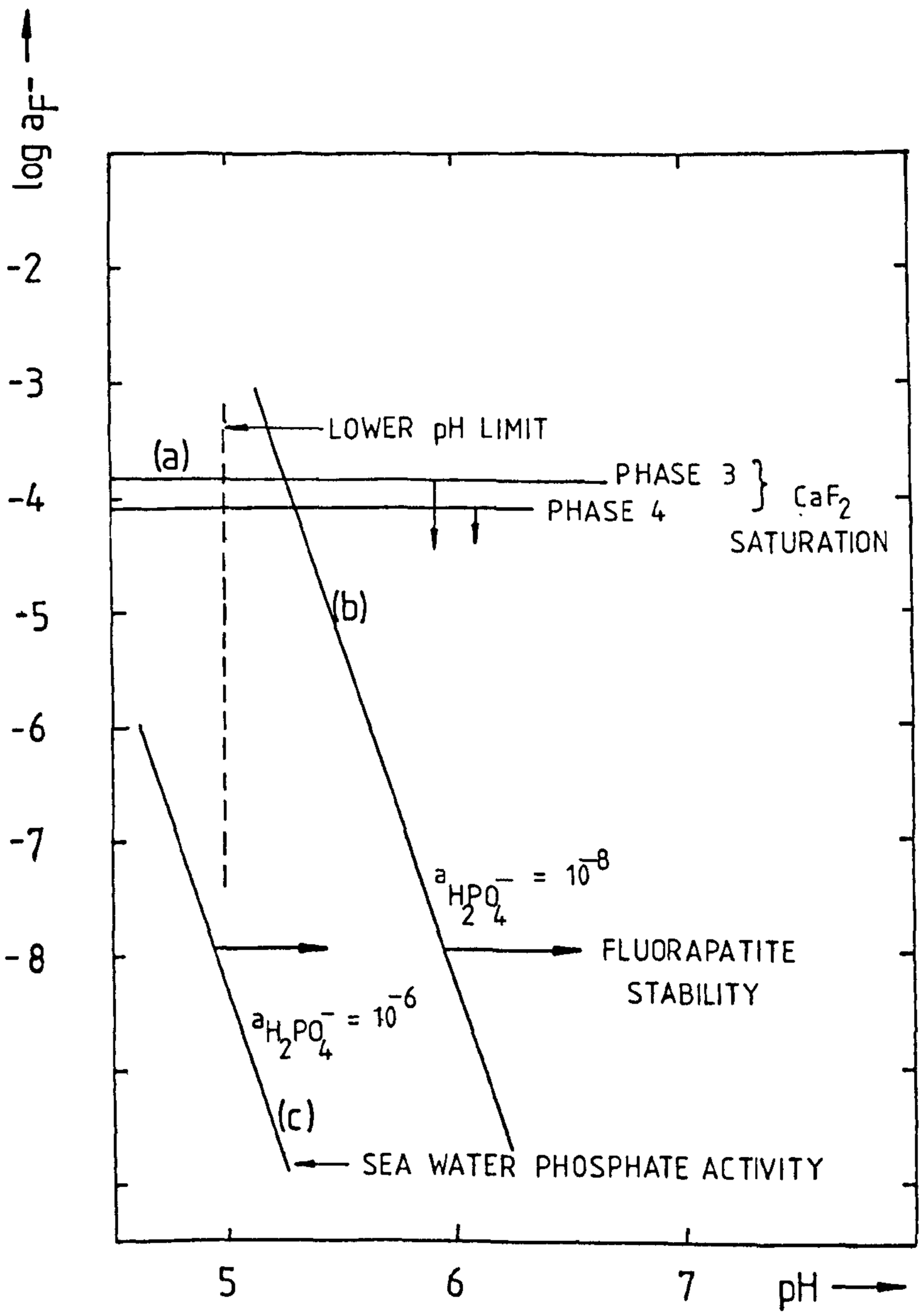

phosphate concentrations. Sea water contains Ø.Ø7ppm phosphorus and Collins (1975) noted that most formation waters contain less than 1ppm of the element. Therefore, it is doubtful whether phosphate concentrations could be reduced enough for the fluids to be able to decompose fluorapatite.

7.3.4: QUANTITATIVE REMOVAL OF FLUORINE

Three of the Namurian sandstones which are likely to contain high concentrations of fluorine are the Lower and Upper Kinderscout Grits, and the Rough Rock Grits. Modal analyses of the mineral content are taken from Stevenson and Gaunt (1971). The fluorine source potential of these formations has been estimated, assuming that muscovite, biotite and K-feldspar are completely decomposed by the hydrothermal fluids (table 7.2).

TABLE 7.2

ESTIMATED FLUORINE CONTENT OF IMMATURE NAMURIAN SANDSTONES

Modal mineralogical analysis

Member	Feldspar	K-Mica	Biotite
Rough Rock	1Ø%	3%	14%
U. Kinderscout Grit	11%	2%	8%
L. Kinderscout Grit	16%	1%	2%
Fluorine yield mg/kg	3ØØ	16ØØ	415Ø
Fluorine yield (kg) per cubic metre (24ØØkg)			
Rough Rock Flags	7.2×10^{-2}	Ø.12	1.39
U. Kinderscout Grit	$8.Ø\times10^{-2}$	7.7×10^{-2}	Ø.79
L. Kinderscout Grit	Ø.12	3.9×10^{-2}	Ø.2Ø

The calculation is based on the premiss that all the silicates have an equal density and that the modal ratios are directly related to weight ratios. The calculation does suggest that the sandstones form good potential sources of fluorine. They also have the advantage over shales of a having a high porosity. If all the feldspar and mica were completely destroyed, a sandstone (100m thick x 5km wide x 30km long) such as the Rough Rock Grit could yield enough fluorine to form the fluorite deposits of Derbyshire. It is more likely, however, that biotite would be converted to chlorite, smectite or kaolinite and potassium feldspar to kaolinite or smectite. The instability of both muscovite and potassium-rich illite would remove two of the major fluorite-bearing sedimentary mineral phases, and release fluorine into the system. The fluorine adsorbing potential of both kaolinite and chlorite are probably considerably poorer than the minerals they are replacing. In conclusion, the immature Namurian sandstones are good fluorine sources and the $[K^+]/[H^+]$ activity ratio of all the mineralizing brines indicates that the fluorine-bearing mineral phases would be unstable when in contact with the ore-fluids. In an ideal situation complete removal of K-feldspar, muscovite and biotite could occur but replacement by more stable alteration products is more probable.

TABLE 7.3

LEAD,ZINC,COPPER AND BARIUM CONCENTRATIONS IN MARINE AND NON-MARINE SHALES FROM THE TANSLEY BOREHOLE. THE AVERAGE VALUES FOR ALL SHALES WERE TAKEN FROM KRAUSKOPF (1979)

Element	marine	non-marine	average (ppm)
Pb	37±16	155±44	20
Zn	80±17	103±15	90
Cu	47±17	140±41	50
Ba	415±83	415±115	600

7.3.5: SOURCES OF BARIUM AND THE BASE METALS

Spears and Amin (1981) measured the base metal concentrations in Namurian shales from the Tansley Borehole. Concentrations of Pb, Zn, Cu and Ba are given in table 7.3

The measured abundances show that the Namurian shales are slightly enriched in the base metals relative to the average shale composition but not abnormally so. The shales probably represent a good source for the base metals. K-feldspar may contain high lead concentrations while biotite may contain high zinc concentrations (Wedepohl, 1971). Therefore, dissolution of biotite and K-feldspar may add base metals as well as fluorine to the ore fluid. Martin-Kaye (1982) suggested that Westphalian sediments may also have been capable of supplying sufficient quantities of lead and zinc to form the Pennine deposits. It is known that base metals are transported in organic complexes in fresh water and flocculation and precipitation occur when mixing with salt water takes place in an estuarine environment

(Sholkovitz 1978). Therefore, the Coal Measures and Namurian estuarine sediments form good potential sources for the base metals.

Other potential sources include the possibility of high base metal concentrations in formation waters contributing to the ore fluids themselves (Carpenter et al., 1974; Billings et al., 1968), or remobilization of metals syngenetically or syndiagenetically deposited with carbonates (Roberts, 1973; Boast et al. 1981)

7.4: CONSTRAINING MODELS OF MINERAL DEPOSITION

7.4.1: AN EQUATION FOR FLUORITE SOLUBILITY

An equation for fluorite solubility is useful for indicating the fluorine carrying capacity of a fluid and its ability to deposit the mineral when component concentrations of the system change. Richardson and Holland (1979a) showed that the important complexes controlling fluorite solubility are NaF^{o}, MgF^{+} and CaF^{+}. At low pH values and high Fe^{++} activities, the complexes HF^{o} and FeF^{+} may also be included in the expression. Anderson (1977) outlined a simple method of calculating galena solubility in hydrothermal solutions and such a method may be used to calculate fluorite solubility. A mass balance for the total fluoride concentration in the system may be written:

$$\Sigma m_{F^-} = m_{F^-} + m_{NaF^o} + m_{MgF^+} + m_{CaF^+} + m_{FeF^+} + m_{HF^o}$$

Concentrations of the complexes can be estimated from the corresponding association constants, activity coefficients and cation and ligand concentrations. The following complexes have been used to calculate total fluoride in the system:

$$m_{NaF^o} = K_{NaF^o}\, m_{Na^+}\, m_{F^-}\, (\gamma_{Na^+}\, \gamma_{F^-}) = K'_{NaF^o}\, m_{Na^+}\, m_{F^-}$$

$$m_{CaF^+} = K_{CaF^+}\, m_{Ca^{++}}\, m_{F^-}\, \frac{(\gamma_{Ca^{++}}\gamma_{F^-})}{\gamma_{CaF^+}} = K'_{CaF^+}\, m_{Ca^{++}}\, m_{F^-}$$

$$m_{MgF^+} = K_{MgF^+} \; m_{Mg^{++}} \; m_{F^-} \; \frac{(\gamma_{Mg^{++}}\gamma_{F^-})}{\gamma_{MgF^+}} = K'_{MgF^+} \; m_{Mg^{++}} \; m_{F^-}$$

$$m_{FeF^+} = K_{FeF^+} \; m_{Fe^{++}} \; m_{F^-} \; \frac{(\gamma_{Fe^{++}}\gamma_{F^-})}{\gamma_{FeF^+}} = K'_{FeF^+} \; m_{Fe^{++}} \; m_{F^-}$$

$$m_{HF^\circ} = K_{HF^\circ} \; a_{H^+} \; m_{F^-} \; \frac{(\gamma_{F^-})}{\gamma_{HF^\circ}} = K'_{HF^\circ} \; a_{H^+} \; m_{F^-}$$

K is the association constant for the appropriate complex and K' is the same constant with a correction factor for activity coefficients (molal equilibrium constant). Association constants are given in table 7.4. Using the mass balance equation total fluoride solubility is given by the equation:

TABLE 7.4

ASSOCIATION CONSTANTS FOR IMPORTANT FLUORINE-CONTAINING COMPLEXES

COMPLEX	LOG EQUILIBRIUM CONSTANT TEMPERATURE	
	50°C	100°C
Ω NaF°	-0.117	0.012
Ψ MgF^+	2.00	2.24
Ψ CaF^+	1.36	1.76
Ω FeF^+	1.45	1.74
Φ HF°	3.52	3.75

Data from Richardson and Holland[Ψ] (1979b), Krauskopf[Φ] (1979), Deloule[Ω] (1982).

$$\Sigma m_{F^-} = m_{F^-} . (1 + m_{Na^+} K'_{NaF^o} + m_{Mg^{++}} K'_{MgF^+} + m_{Ca^{++}} K'_{CaF^+} + m_{Fe^{++}} K'_{FeF^+} + a_{H^+} K'_{HF^o})$$

If ø is the complexing factor, then the equation is:

$$\Sigma m_{F^-} = m_{F^-} . \phi$$

The free fluoride molality can be estimated from the calcium concentration of the ore fluid if it is assumed that the solution was saturated with fluorite. This is given in the equation:

$$m_{F^-} = \frac{K_s}{\gamma Ca^{++} . m_{Ca^{++}}} . \gamma_{F^-}^{-1}$$

where $2m_{Ca^{++}} \geqslant m_{F^-}$

The expression is very reliant on the quality of the activity coefficients and gives poor absolute values. However, the equation may be useful for estimating how much fluoride a solution may dissolve, relative to the free molal concentration of fluoride in the system. Similar equations have been used to estimate the effects of dolomitization and cooling on the type 3 and 4 fluids.

7.4.2: ISOTHERMAL MINERAL DEPOSITION

Changes in the activity of the calcium or fluoride ions will effect the solubility of fluorite. Changes in the activities of minor components within the brine may have effected the stability of fluoride complexes and produce fluorite supersaturation. Fluid mixing will be considered in a later section.

7.4.2.1: CHANGING THE CALCIUM ACTIVITY

Since the ion activity solubility product of fluorite is dependant on the calcium activity in the solution, increasing the calcium activity in a fluid already saturated with fluorite would produce fluorite deposition. Calcium may have been added to the system through the dissolution of limestone. For example, limestone dissolution resulting from a pH change from 4 to 6 at 100°C, with an initial calcium concentration of 1.1m, would produce a 0.005% increase in the total molal calcium concentration of the solution. Therefore, unless calcium is added to the solution by destabilizing a strong calcium complex, high calcium concentrations would act as a buffer and would probably not have influenced fluorite deposition.

7.4.2.2: CHANGING FLUORIDE ACTIVITY

Since the fluoride activity of the type 2, 3 and 4 fluids was compelled to be low, activity of fluoride could be changed by orders of magnitude as a result of small changes in the strength of fluoride complexes. Complexes may have been weakened as a result of precipitation of the appropriate cations. Complexes may also have been effected by changes in pH and oxygen fugacity. Sodium, calcium, magnesium, aluminium, iron, boron, silicon and hydrogen ions all form fluoride complexes.

7.4.2.3: SODIUM FLUORIDE COMPLEXES.

Sodium, like calcium was present in the brines at high concentrations. It was, however, probably completely dissociated (Helgeson, 1969) and was also difficult to remove in the low temperature hydrothermal environment. The NaF^{o} and Na_2F^{+} complexes are weak and were probably best destabilized by cooling.

7.4.2.4: MAGNESIUM FLUORIDE COMPLEXES

The complex MgF^{+} is stronger than NaF^{o} and CaF^{+} (Richardson and Holland, 1979a). A good mechanism by which magnesium could have been removed from the solution was the process of dolomitization.

$$Mg^{++} + 2CaCO_3 = MgCa(CO_3) + Ca^{++}$$

Not only would magnesium have been removed from solution, thus destabilizing the MgF^+ complex but calcium would also have been released. Figure 6.2 shows a plot of molal magnesium concentration against molal calcium concentration for a number of deep formation waters from the East Midlands (Downing and Howitt, 1968), Central Mississippi Valley (Carpenter et al., 1974) and the Illinois, Michigan and Alberta basins (Graf et al., 1966). A generalized positive correlation is present between calcium and magnesium concentrations. If the ore fluids were derived from deep formation waters, then at some stage in the evolution of the brines magnesium has been preferentially removed with respect to calcium. Removal of Ø.1-Ø.2m Mg^{++} could have significantly reduced the stability of the MgF^+ complex concentration and produced fluorite saturation. An estimate of the change in stability can be made by calculating the change in complexing factors (ϕ) (Anderson, 1977) for a Ø.15m change in the total magnesium concentration of the phase 4 ore fluid. The association constants for the complexes MgF^+ and CaF^+ at 1ØØ°C given in table 7.4. Taking the only contributing fluoride complexes to be MgF^+ and CaF^+, the total fluoride concentration of the system can be expressed in the equation:

$$\Sigma m_F = m_{F^-} \cdot \quad \phi$$

where $\phi = 1 + m_{Mg^{++}} K'_{MgF^+} + m_{Ca^{++}} K'_{CaF^+}$

On the loss of Ø.15m Mg^{++} the complexing factor changes from 11.8 to 6.3 (Initial fluorite saturation was assumed and activity coefficients were taken from appendix 5.1). The

calculation indicates that more than 50% of the total molal fluoride concentration could have been removed from solution. Dolomitization of limestone or formation of authigenic chlorite could remove magnesium from a formation water. Two problems are apparent when considering the role of dolomitization in fluorite deposition. Firstly, very large volumes of carbonates must be dolomitized (Richardson and Holland, 1979b) and secondly, there is no indication of a dolomite-fluorite association in the Orefield. It is also necessary for dolomite to have been a stable mineral phase in the ore fluids. The degree of dolomite saturation may be estimated from the molal magnesium and calcium concentrations in the ore fluids assuming calcite saturation at 100°C. The ion activity solubility product (K_s) of dolomite is not easily measured at low temperatures and therefore, large errors are attached to any values. The value used here was taken from Helgeson (1969).

$$K_s \doteq a_{Ca^{++}} \cdot a_{Mg^{++}} \cdot a^2_{CO_3^{2-}} = 10^{-19.67}$$

Using the activities given in chapter 4, the percentage saturation ranges for the phase 3 and 4 ore fluids are 57-600% and 9-13% respectively. The phase 2 fluid was probably also undersaturated with dolomite. The values, calculated on the basis of calcite saturation, indicate that the phase 3 fluid was just saturated with dolomite and the phase 4 fluid was undersaturated. The low magnesium activities in the phase 2 and 4 fluids my have resulted from the growth of authigenic chlorite or adsorption by smectites during fluid migration.

7.4.2.5: ALUMINIUM FLUORIDE COMPLEXES

Nordstrom and Jenne (1977) and Deloule (1982) have suggested that aluminium fluoride complexes may have been capable of transporting fluoride. Aluminium forms fluoride complexes in the reaction:

$$Al^{3+} + nF^{-} = AlF_n^{3-n} \qquad n = 1,2,3,4,5 \text{ \& } 6.$$

Calculation of the association constants of the first three complexes indicates that they are particularly strong (Deloule, 1982). Unfortunately the complexes are easily hydrolyzed in comparatively acid solutions. Aluminium concentration in oil-field brines is comparatively low (Collins, 1975) and is the result of the very low solubility of gibbsite ($Al(OH)_3$). At the estimated pH range for the environment of mineralization, and given the published solubility data for gibbsite, it can be easily shown that aluminium could not complex fluoride ions at the concentrations required.

7.4.2.6: CHANGES IN pH

Richardson and Holland (1979b) showed that acid solutions (pH<3) are required for the HF^{o} complex to significantly effect fluorite solubility (Figure 7.4). Given the buffering capacity of limestones and shales (Long and

Figure 7.4

The quantity of fluorite precipitated by cooling NaCl solutions at varying pH values from 260°C to 25°C.

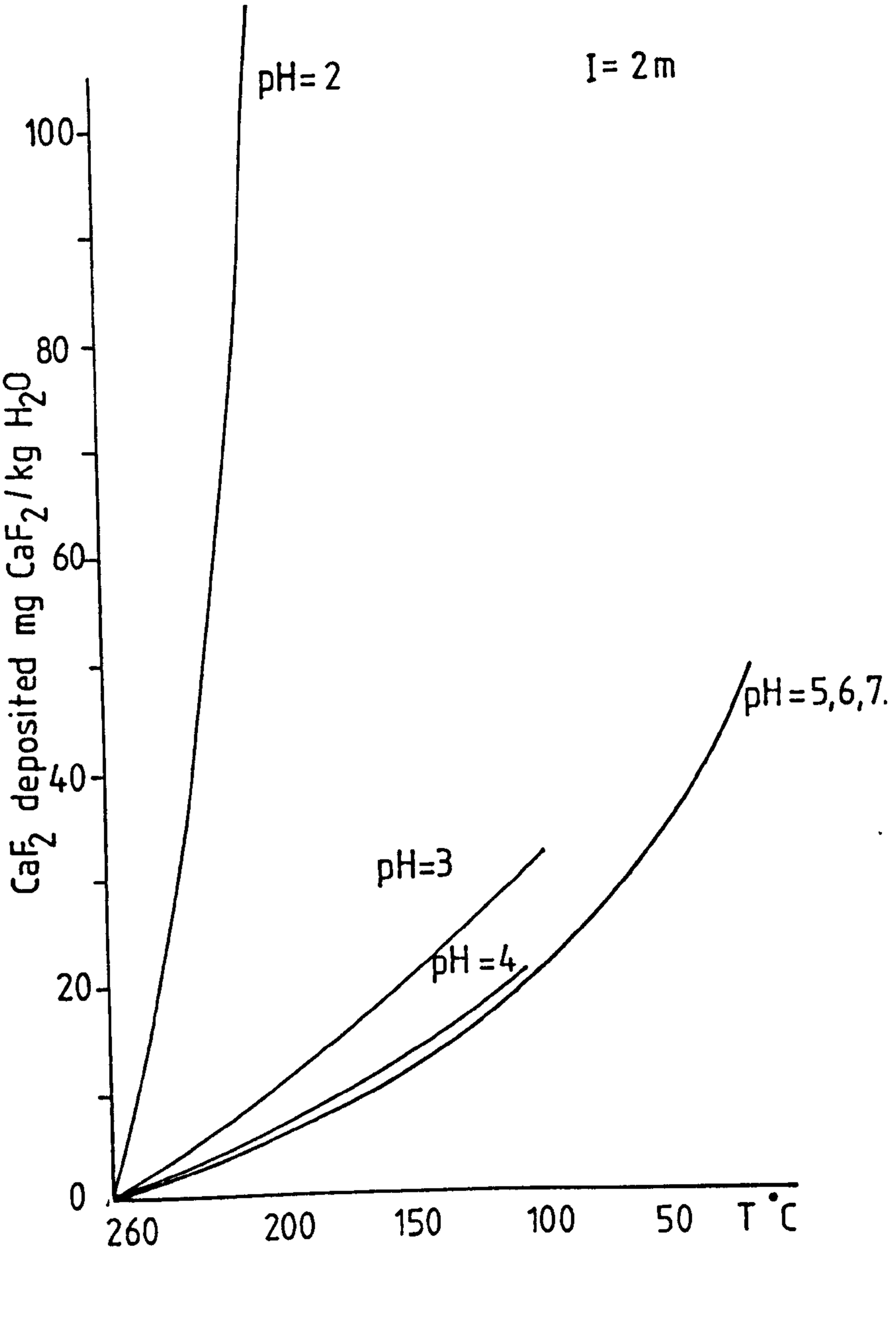

Angino, 1982) on acid solutions, it is unlikely that the HF complex played an important role in fluorite mineralization in the Orefield.

7.4.2.7: IRON FLUORIDE COMPLEXES

The association constants for both Fe^{2+} and Fe^{3+} fluoride complexes have been calculated by Deloule (1982). The trivalent iron fluoride complexes are very strong, but their instability in the redox conditions present in a mineralizing environment precludes their formation. Divalent iron fluoride complexes are considerably weaker than their trivalent counterparts. Moore (1980) measured the concentration of iron in fluid inclusions from the Southern Pennine Orefield and estimated a molal concentration range of 0.005-0.2m. Since pyrite, chalcopyrite and bravoite solubility influenced molal free iron concentration, it is likely that this concentration range is too high. Carpenter et al. (1974) reported a maximum iron concentration of 0.008m in formation waters from the Central Mississippi Valley and Collins (1975) reported maximum total iron concentration of 0.02m for all oil-field brines.

7.4.2.8: RELATIVE STABILITY OF FLUORIDE AND HYDROXIDE COMPLEXES

Using association constants for calcium, magnesium and iron hydroxides and fluorides (Hogfeldt (1982); Deloule

(1982)), the pH range at which the following type of reaction occurs may be estimated.

$$M^{n+} F_m^{n-m} + mOH^- = M^{n+} OH_m^{n-m} + m_F-$$

The reaction has the advantage that the cation supplying the fluoride may be removed by another ligand without any solid mineral phase either being precipitated, removed or altered. Unfortunately, calculations show that $MgOH^+$ and $CaOH^+$ are only important in solutions with a pH in excess of 7. Aluminium fluorides become unstable in the pH range 5-6, but the low solubility of $Al(OH)_3$ prevents the transition being a useful depositional mechanism.

7.4.3: LIMESTONE METASOMATISM

Many fluorite deposits appear to have formed as a result of the replacement of limestone. Fluorite would have replaced limestone if the fluoride/carbonate ratio reached an appropriate level in the ore fluid (section 4.11) and if the fluid was saturated with calcium fluoride. The important point to note is that pH levels are not a controlling factor in limestone replacement (Ames, 1961). The results of calculations presented in section 4.11 show that the type 3 fluid would have more efficiently replaced carbonates than the type 4 fluid. Ames (1961) showed that the surface area of the carbonate was an important control on the rate at which the replacement process took place. The field work of Firman and Bagshaw (1974) and Worley (1976) supports this

hypothesis.

7.4.4: ISOTHERMAL MINERAL DEPOSITION THROUGH FLUID MIXING

TABLE 7.5

FINAL ICE MELTING TEMPERATURE RANGES, STANDARD DEVIATION RANGES AND ESTIMATED SALINITY VARIATION IN TERMS OF GRAMS OF SODIUM CHLORIDE

Phase	1	3	4
Final ice melting temperatures	-6.6-Ø.Ø	-26 to -2Ø	-19.8 to -15.5
range (2σ)	Ø.2-1.6	Ø.3-1.7	Ø.3-Ø.9
±2σ expressed as NaCl variation ($gl t^{-1}$)	±7 - ±54	±1Ø - ±58	±1Ø - ±31

Mixing is an attractive depositional mechanism for both fluorite and associated sulphides since it overcomes the problems of single solution mineral solubility. Mixing of two fluids of differing chemical composition as a mode of depositing fluorite has been proposed by Hall and Friedman (1963), Dunham (1966), Kesler (1977) and Zimmerman and Kesler (1981). Richardson and Holland (1979b) showed that isothermal dilution of a fluoride-bearing solution would generally cause a reduction in the level of the ion activity product of fluorite within the fluid. However, a more effective depositional mechanism is the mixing of a fluoride-rich solution with a calcium-rich formation water. This type of model has been suggested by Dunham (1966) and Sawkins (1966). The amounts of calcium fluoride which may be precipitated in

ideal conditions is very large and therefore overcomes problems associated with the volume of ore fluids required to pass through a vein system.

Variation in final ice melting temperature measurements may be used to investigate the possible degree of fluid mixing. The standard deviation and the range ($\pm 2\sigma$) in final ice melting temperatures are presented for hydrothermal

TABLE 7.6

MEAN MELTING TEMPERATURES FOR AN EASTERN AND WESTERN DIVISION OF THE OREFIELD

Phase 4		Phase 3	
West	East	West	East
-17.1	-18.1	-21.6	-25.1
-17.9	-16.5	-22.6	-22.9
-17.6	-18.Ø	-22.Ø	-23.Ø
-16.3	-18.Ø	-24.3	-23.8
-17.2	-17.2	-22.3	-21.9
-16.8	-19.7	-23.3	-23.8
-17.1	-18.3	-23.4	-24.8
-16.7	-17.5	-22.6	
-16.3	-17.9	-22.1	
-17.7	-18.9	-22.Ø	
-17.6			
-17.1			

f-statistic = 8.53
Mann-Whitney U-test significant at Ø.ØØ7

f-statistic = 4.49
t-test significant at Ø.Ø7

phases 1, 3 and 4 in table 7.5.

The variation in NaCl content shows that the composition of the fluid fluctuated in all three phases to a relatively high degree. However, since there is no stratigraphic control on mineralization, the salinity variation may have altered through time, rather than having been present during any

specific instance during mineral deposition. Temporal salinity variation is indicated when salinity variation over the whole Orefield is examined. In figures 7.5 and 7.6, the Orefield has been divided into a western and eastern region, with the dividing line roughly parallel to the fluorite zone. The final ice melting temperature means for the eastern and western divisions for the phase 3 and 4 events are shown in table 7.6.

As can be seen, lateral salinity variation within the phase 3 and 4 events was relatively small when one takes into account the size of the Orefield (25x35km). The salinity of the phase 4 fluid may have increased from west to east but the final ice melting temperatures indicate that the phase 3 fluid composition was indistinguishable in the two divisions at a 7% level of significance. If mixing was the depositional mechanism for precipitating fluorite, then the process must have been remarkably uniform. No correlation between final ice melting temperatures and homogenization temperatures is apparent in the populations determined for mineralization phases 2, 3 and 4. Some type 1 inclusion sample populations do, however, show a positive correlation, suggesting the mixing of a warmer, moderately saline brine with a cooler, relatively dilute fluid.

Mixing of two solutions which had similar salinity can be ruled out since the high calcium concentration of both the type 3 and type 4 solutions would severely limit the amount of fluorine such brines could transport. Fluorine could only be supplied by a brine which had a low calcium activity. A fluid with a similar final ice melting temperature as the type 4 fluid could be composed of only sodium chloride, but

Figure 7.5

SOUTHERN PENNINE OREFIELD.

TYPE 4 FLUID INCLUSION FINAL ICE MELTING TEMPERATURE

THE AREA IS DIVIDED INTO 5KM SQUARES USING THE NATIONAL GRID REFERENCE SYSTEM

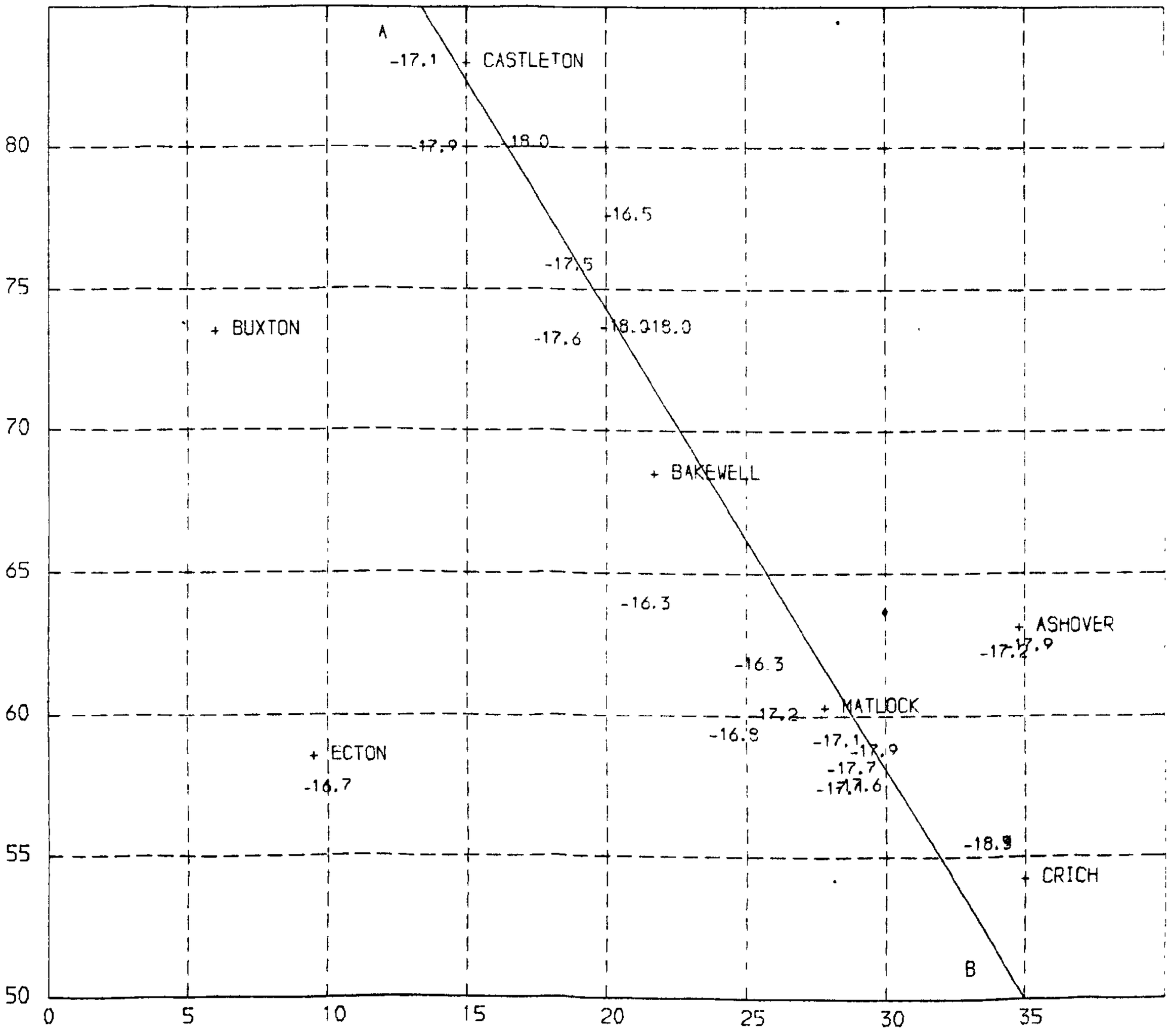

The line A-B is an arbitrarily set boundary, approximately parallel to the fluorite zone, providing and eastern and western division of the Orefield in order to statistically compare the respective final ice melting temperature populations.

Figure 7.6

SOUTHERN PENNINE OREFIELD.

TYPE 3 FLUID INCLUSION FINAL ICE MELTING TEMPERATURE

THE AREA IS DIVIDED INTO 5KM SQUARES USING THE NATIONAL GRID REFERENCE SYSTEM

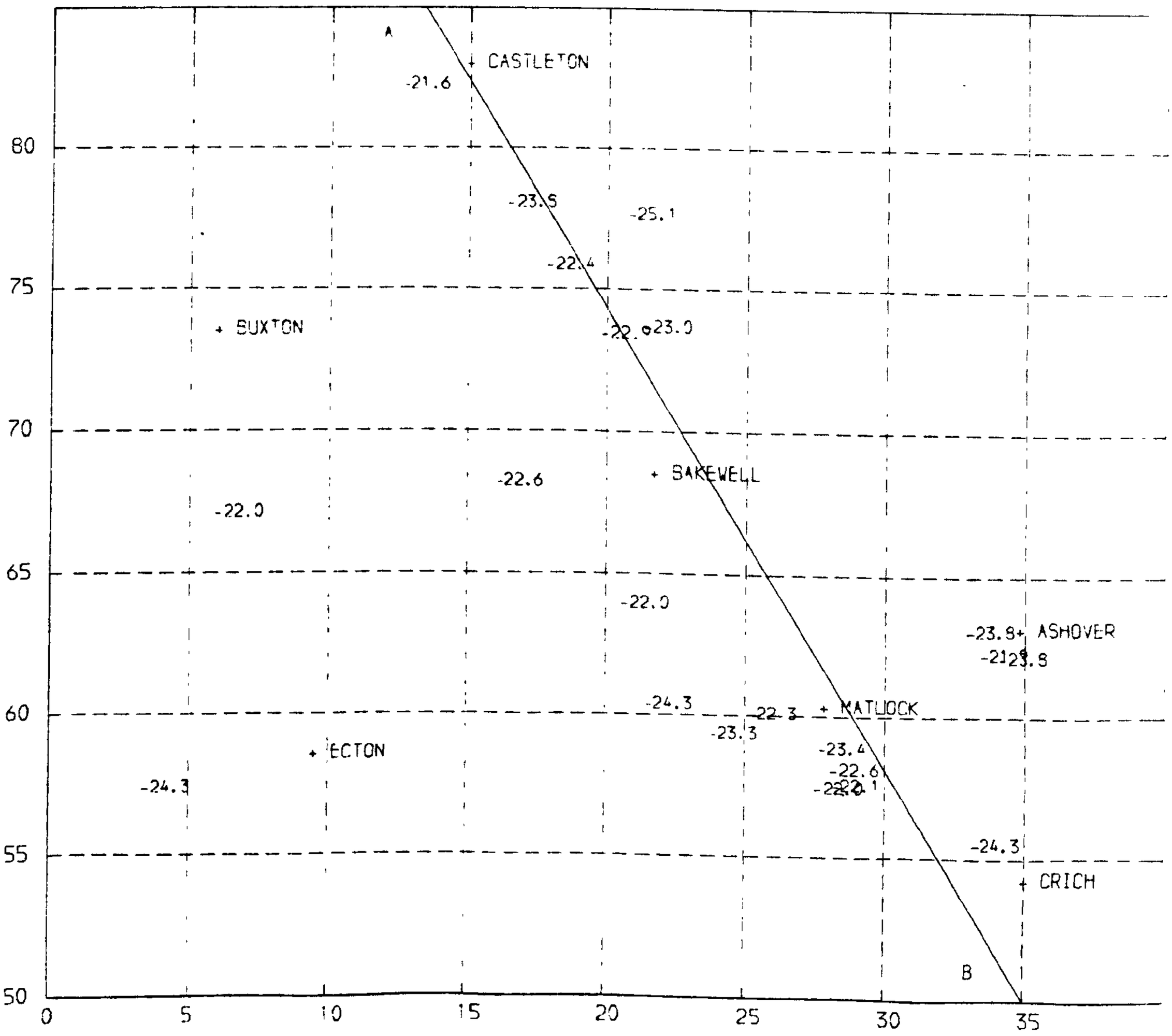

The line A-B is an arbitrarily set boundary, approximately parallel to the fluorite zone, providing an eastern and western division of the Orefield, in order to statistically compare the respective melting temperature populations.

such a solution could be easily recognized by observing the temperature at which hydrohalite melts. The presence of hydrohalite at between -40° and -22°C within type 3 and 4 fluid inclusions indicates the presence of quantities of calcium in both fluids as does a final ice melting temperature below -21°C. Hanor (1979) suggested that analyses of formation waters showed that high fluoride concentrations are present in relatively dilute fluids with high HCO_3^- and SO_4^{2-} abundances and not usually in concentrated NaCl dominated brines.

Very uniform mixing of a dilute fluoride-rich brine with the calcium-rich fluids cannot be ruled out but the process seems unlikely, given the extent of the Orefield. The low total REE abundances and the very uniform lanthanide distribution patterns offer little support to the hypothesis of mineral deposition by fluid mixing. To obtain the patterns it is probably necessary that the fluoride-rich fluid was very depleted in the REE. It would be expected, however, that the fluoride-rich solution would be the REE carrier, given the stability of REE fluoride complexes.

7.4.5: FLUORITE DEPOSITION AS A RESULT OF FLUID COOLING

For fluid cooling to occur, heat must either be lost through convection of the ore fluid or loss to the wall rocks. The remarkable homogeneity of the depositional temperatures, particularly in the phase 2, 3 and 4 mineralizing events does not seem to favour heat loss to the wall rocks or loss as a result of rapid fluid convection. As

in the case of measured salinity variation, the standard deviation in the mean homogenization temperature of any given sample population is relatively large, but the temperature variation over the Orefield as a whole is small (Table 7.7).

Therefore it may be inferred that the thermal variation represents a temporal variation of the geothermal gradient rather than high thermal gradients at the site of mineral deposition. The effect of cooling on the various solutions is investigated in the following section.

7.4.5.1: TYPE 1 FLUID

If the cooling range is taken as being two standard

TABLE 7.7

DEPOSITIONAL TEMPERATURE RANGES FOR INDIVIDUAL SAMPLES AND FOR THE TOTAL POPULATIONS FOR THE FOUR MINERALIZING EVENTS.

	Mineralizing events 1	2	3	4
Temperature range expressed as 2σ	9.0-30.2		4.4-20.0	3.4-12.2
Population mean	136.5	75.1	84.1	84.3
Range (2σ)	28.6	6.2	13.4	11.2

deviations of the homogenization temperature, then the cooling interval ranges from 9°C to 30°C. The data presented by Richardson and Holland (1979b) suggested that cooling of solutions containing 0.5 wt% NaCl up to 3 wt% NaCl over the temperature range 260°C to 100°C would result in fluorite

dissolution rather than precipitation. At the maximum salinity observed in any type 1 inclusion (10 wt% equiv. NaCl), cooling over a temperature range of 25°C would produce less than 5mg of fluorite per kg of ore fluid. Substitution of calcium for sodium in the fluid will probably not improve the quantity of fluorite deposited. Therefore, it is reasonable to conclude that the type 1 fluorite deposited at Treak Cliff and Watergrove Mine could not have been precipitated as a result of fluid cooling.

7.4.5.2: TYPE 2 FLUID

The very small temperature variation associated with this phase of mineralization seems to rule out cooling as a depositional mechanism.

7.4.5.3: TYPE 3 AND 4 FLUIDS

The cooling range expressed as two standard deviations of the homogenization temperature population indicates that the possible cooling intervals for the two phases were relatively similar (Table 7.7). The contribution which various complexes make to the overall solubility of fluorite may be investigated by calculating a theoretical complexing coefficient form the equations and data given section 7.7, section 7.4.1 and appendicies 5.1 and 5.2. The calculated contributions of the various complexes at 50°C and 100°C for the phase 3 and 4 ore fluids are given in table 7.8.

TABLE 7.8

COMPLEXING COEFFICIENTS FOR THE PHASE 3 AND 4 ORE FLUIDS AT 50°C AND 100°C

	Phase 3		Phase 4	
temperature	50°C	100°C	50°C	100°C
Complex				
NaF	1.49	1.65	0.18	0.22
MgF	1.63	0.68	0.27	0.42
CaF	2.29	1.75	2.29	4.88
FeF	0.18	0.09	0.15	0.27
F	1.0	1.0	1.0	1.0
Total	6.59	5.17	3.89	6.78
Free molal fluoride	1.72×10^{-4}	4.6×10^{-4}	2.19×10^{-4}	3.4×10^{-4}
Total fluoride	1.13×10^{-3}	2.38×10^{-3}	8.52×10^{-4}	2.3×10^{-4}

The results of the calculations shown in table 7.8, indicate that sodium and calcium were the most important ions available for fluoride complexing. Iron concentration was taken as 0.02m and appears to have had little influence on fluoride complexing. The calculation is in agreement with the experimental data of Richardson and Holland (1979a), with the complexing factor actually increasing on cooling the phase 3 fluid. The latter fluid having a slightly higher ionic strength than the phase 4 fluid, especially when calcium complexing is considered. The solubility product of fluorite increases on cooling from 100°C and therefore the decrease in solubility of fluorite in the type 3 fluid is purely due to the change in the activity coefficient of the calcium and fluoride ions. In the type 4 solution, changes in both the complexing factor and the activity of calcium decrease the solubility of fluorite. If the destabilization of the complex $CaCl^+$ on cooling were allowed for, the quantity of fluorite

precipitated may increase. In conclusion, the calculations suggest that fluorite may have been deposited on cooling both ore fluids in the temperature range 100°C-50°C. Although this range is considerably greater than the observed range, trends are probably similar. The calculation also suggests that more fluorite would have been deposited from the type 4 fluid than the type 3 fluid on cooling a given volume of fluid over the same temperature interval. It is also apparent that both fluids were capable of holding a significant part of their fluoride contents within complexes at 100°C.

7.5: SULPHIDE SOLUBILITY

Since much of the fluorite of the district contains solid inclusions of galena and sphalerite, any model of fluorite deposition must also explain the formation of cogenetic sulphides. Problems of sulphide precipitation and transport occur because of their very low solubility products. Three types of model have been proposed in recent years to explain the transport and deposition of lead and zinc in low temperature sulphide deposits. The first model involved the mixing of two fluids, one carrying the base metals and the other carrying reduced sulphur (Anderson, 1975; Beales and Onasick, 1970; Beales, 1975; Beales and Jackson, 1966). Skinner (1967) suggested that base-metal-rich solutions may encounter reduced sulphur already present at the site of mineral precipitation. A second model suggests the transport of the base metals with sulphate (Barton, 1967). The sulphate is reduced as a result of the oxidation

of organic material or methane. Sverjensky (1981) has shown that the latter reaction is thermodynamically impractical even in the most favourable circumstances. A third model allowed base metals to be transported together with reduced sulphur at low concentrations (Helgeson, 1970; Anderson, 1973; Sverjensky, 1981).

Analysis of fluid inclusion melting temperature data for the Orefield does not indicate fluorite deposition by fluid mixing. This conclusion is at variance with the model of ore genesis proposed by Robinson and Ineson (1979), based on sulphur isotope measurements. They suggested that the sulphur isotope ratios indicated the mixing of two reduced sulphur sources. Unfortunately, no measurements were made to establish whether there existed a "sulphur isotope stratigraphy" (Nielsen ,1979) as has been identified in other low temperature sulphide deposits. Reduced sulphur could have been derived by the leaching of sedimentary sulphides from shales, with varying degrees of inorganic reduction of sea water sulphate depending on the period of fluid residence and the physicochemical environment. Ohmoto and Rye (1979) suggested that the Hansonburg galena deposits of New Mexico acquired their reduced sulphur in this way. In such a situation, similar sulphur isotope ratios as those recorded may well be produced. The range in sulphur isotope ratios for galena included in fluorite is -14.8‰ to -4.0‰ (Robinson and Ineson, 1979), which is considerably smaller than the total range for all sulphides of -23.2‰ to +6.6‰. The sulphur isotope range for baryte has little significance when considering a fluorite-sulphide system, since there is little evidence to indicate that the two minerals were precipitated

as a coeval mineral assemblage. Therefore, in the opinion of the author, the measured sulphur isotope ratios do not necessarily imply fluid mixing at the site of mineral precipitation.

7.5.1: ZINC/LEAD RATIOS IN ROCKS AND FLUIDS AND PRECIPITATION OF GALENA AND SPHALERITE

There is a dominance of galena over sphalerite in both Northern and Southern Pennine Orefields. In a mixing situation, where fluids with high base metal concentrations meet fluids with high reduced sulphur activities, one would expect precipitation of all the lead and zinc in the ore fluid, when one takes into account the high insolubility of both galena and sphalerite. It might be argued that the absence of sphalerite or the presence of high galena/ sphalerite ratios in a deposit merely indicates that the fluid was depleted in zinc with respect to lead. However, certain facts seem to suggest that an ore fluid would have had a Zn/Pb ratio in excess of one. Lead solubility is more restricted than zinc solubility since both the sulphate and the sulphide of lead are less soluble than the corresponding zinc salts. It is also generally recognized that the base metals are transported as chloride complexes, since the complexes are both relatively strong (Barnes, 1979) and chloride is the most abundant ligand in a high salinity ore fluid. Comparison of association constants for the chloride complexes (Helgeson, 1969) of lead and zinc shows that zinc forms slightly stronger members. Possible sources for base

metals in the fluids such as shale, granite and pore water have Zn/Pb ratios of 2.5, 4.5 and 163 respectively (Krauskopf, 1979). Experimental studies (Long and Angino, 1982) in which shales were leached by chloride brines showed that Zn/Pb ratios were higher in the fluid than the corresponding rock. Leaching of the Ninnescah shale which had a whole rock Zn/Pb ratio of Ø.55 produced a fluid with a Zn/Pb ratio 2.Ø. Leaching of the other shales generally produced fluids with high Zn/Pb ratios, as would would be expected if metal ion complexing were the major control on mobilization. The calcium chloride dominated formation waters of the Central Mississippi Valley basin contain relatively high base metal concentrations with Zn/Pb ratios ranging from 1 to 32 (Carpenter et al., 1974). Therefore, not only is zinc more abundant than lead in most common rock types and formation waters, but zinc is also more soluble in chloride, sulphate or sulphide dominated aqueous electrolytes. Leaching of K-feldspar alone could have produced high Pb/Zn ratios in the ore fluids. However, the absence of positive europium anomalies in the chondrite normalized REE plots for fluorite is not indicative of exclusive leaching of K-feldspar.

From the above argument it may be speculated that the Southern Pennine ore fluids may have contained Zn/Pb ratios in excess of one. If mineral deposition occurred as the result of a sulphide-rich fluid mixing with base metal-rich formation water, the process must have been very finely balanced in order that galena would precipitate and sphalerite remain soluble. Figure 7.7 shows the relative solubilities of galena and sphalerite in a brine similar to

Figure 7.7

The diagrams show the stoichiometric solubilities of galena and sphalerite in a fluid containing 2.8 molal NaCl and 0.64 molal $CaCl_2$ (dissociated) at pressures corresponding to the liquid-vapour pressure for water. (Taken from Sverjensky, 1981)

(a) Galena solubility

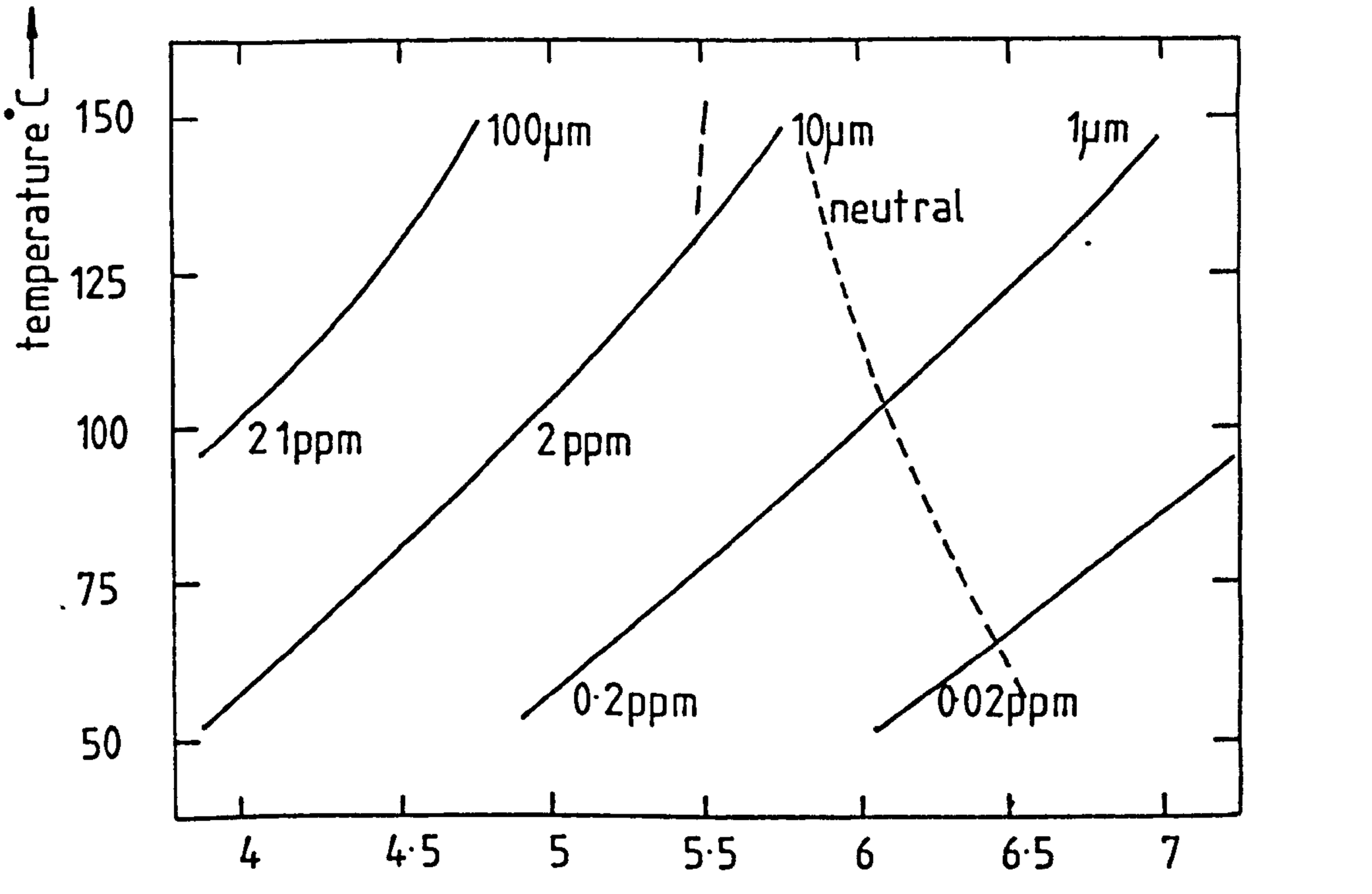

(b) Sphalerite solubility.

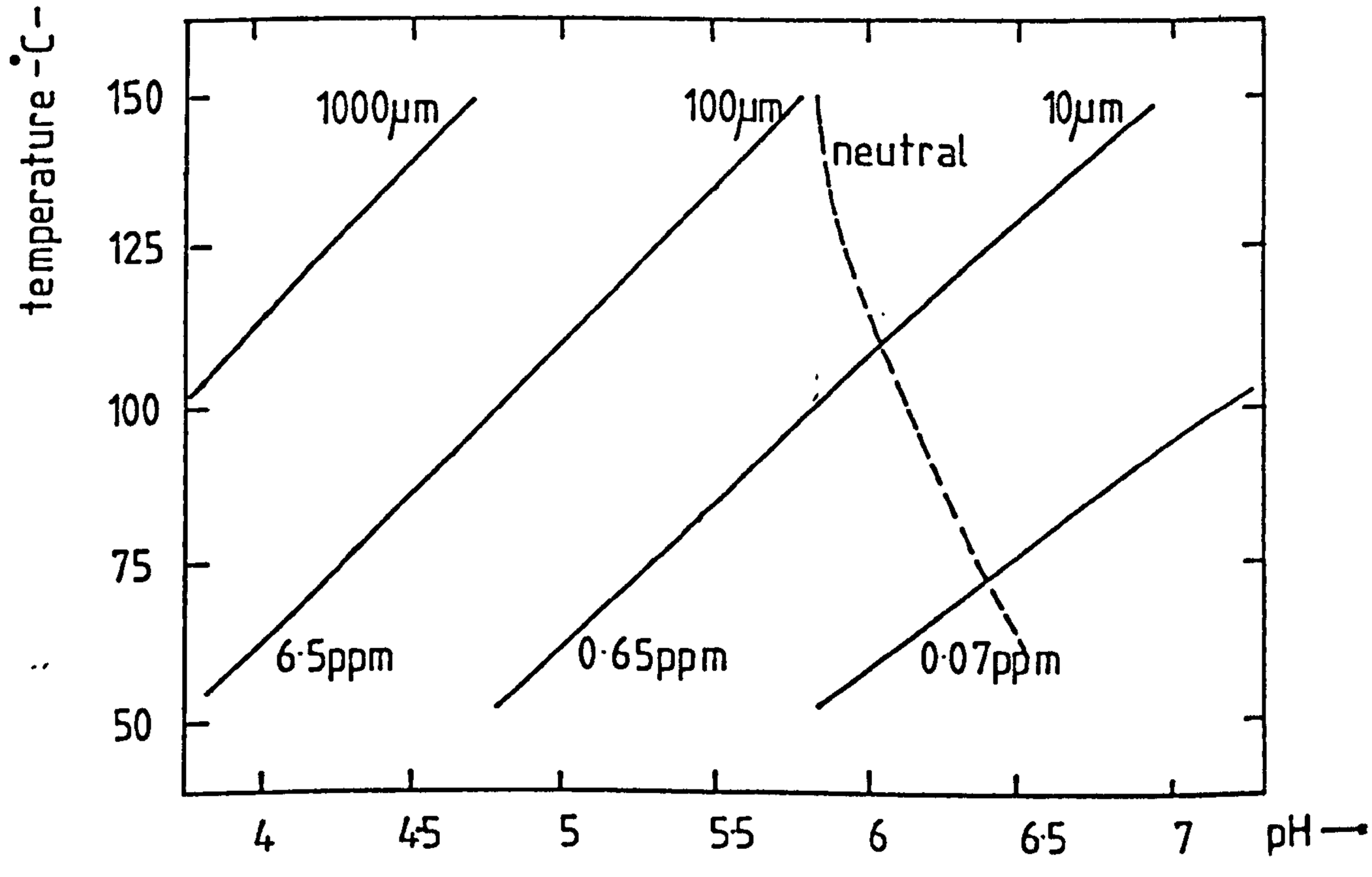

the type 3 ore fluid as a function of temperature and pH.

Sphalerite does occur in the Orefield but mainly concentrated in deposits lying on the eastern margin of the field. The delicate nature of such a process can be shown by calculating the levels of reduced sulphur required to deposit galena but not sphalerite in a hypothetical ore fluid containing 5ppm Zn and 2ppm Pb at 100°C. The solubility of galena and sphalerite as a function of reduced sulphur (HS^-)* activity and pH are given by the following equations:

$$ZnS + H^+ = Zn^{++} + HS^- \qquad \log K = -11.03$$

$$PbS + H^+ = Pb^{++} + HS^- \qquad \log K = -12.51$$

The solubility of galena and sphalerite in a hydrothermal fluid may be calculated using the method of Anderson (1977) and the data of Sverjensky (1981). The two equations for the solubility of the sulphides are constructed in a similar way to the equation for fluorite solubility.

$$\Sigma m_{Pb^{++}} = m_{Pb^{++}} + m_{PbCl^+} + m_{PbCl_2^o} + m_{PbCl_3^-} + m_{PbCl_4^{2-}}$$

$$\Sigma m_{Zn^{++}} = m_{Zn^{++}} + m_{ZnCl^+} + m_{ZnCl_2^o} + m_{ZnCl_3^-} + m_{ZnCl_4^{2-}}$$

Using the appropriate association constants for the lead and zinc chloride complexes (Helgeson, 1969) and a fluid containing $4.1 m_{Cl^-}$, the complexing factors were calculated in order to relate total lead and zinc concentrations with their corresponding free molal concentrations. The complexing factors are:

*Stable reduced sulphur species should be H_2S rather than HS^-.

$$\Sigma m_{Pb}^{++} = m_{Pb}^{++} \quad . \quad 13600$$

$$\Sigma m_{Zn}^{++} = m_{Zn}^{++} \quad . \quad 17000$$

Single ion activity coefficients for lead and zinc are Ø.Ø5 and Ø.Ø7 respectively. The activity of lead and zinc may now be calculated and refitted into the equation relating these activities with pH and reduced sulphur activity. If a pH of 5 is assumed and all the zinc must remain in solution, then the reduced sulphur activity cannot exceed $1Ø^{-6}$. This would allow the deposition of 1.4ppm of galena before sphalerite began to precipitate. The permanent retention of a remarkably low reduced sulphur activity in an ore fluid mixing environment seems unlikely and since only low sulphur activities are permissable, all the reduced sulphur could be carried with the base metals. Therefore the mixing hypothesis becomes redundant. The only argument against this idea is that it could be suggested that the ore fluids had a low Zn/Pb ratio, an argument which seems difficult to justify geochemically.

In a single solution model of hydrothermal mineralization, mineral zonation develops in response to the changing solubilities of mineral phases .(Susak and Crerar, 1982). The most soluble mineral phases precipitate closest to the source where changes in pH, oxygen fugacity and temperature, to mention just three controls, are greatest. The widespread occurrence of lead within the South Pennine Orefield and the restricted occurrence of zinc, probably reflects the poorly developed mineral zonation of the field, produced as a result of physicochemical changes in a single mineralizing solution. This hypothesis does not, however,

contradict the suggestion that baryte was formed as a result of fluid mixing.

7.6: DISCUSSION

Since there is no proven association between acid magmatism and mineralization in the Southern Pennines as has been suggested for number of similar deposits (Hall and Friedman 1963; Sawkins, 1966; Kesler, 1977), other potential fluorine sources have been investigated. Asbian limestones in the eastern part of the Orefield are known to contain high fluorine concentrations (Bridge and Gozzard, 1981). The fluorine is probably present within fluorapatite, a mineral phase which may be difficult to dissolve in the ore fluids. The high fluorine concentrations may also be due in part, to the diffusion of fluorine away from centres of mineralization through groundwater movement. The Namurian sandstone-shale succession could represent a good source of both fluorine and the base metals (Shepherd et al., 1982). Some of the Namurian sandstones have compositions which are broadly granitic, and were certainly derived from a granitic or gnissose-granitic province to the north (Stevenson and Gaunt, 1971). Biotite, muscovite, K-feldspar may contain fluorine. Biotite and K-feldspar may also contain high concentrations of zinc and lead respectively (Wedepohl, 1971). The origin of the lead is not as problematical as that of the fluorine, since high lead and zinc concentrations have been found in a number of formation waters (Carpenter et al., 1974; Billings et al., 1969). It has also been demonstrated that chloride brines can

effectively leach base metals from shales (Long and Angino, 1982). Spears and Amin (1981) have shown that the Namurian shales of the Tansley borehole contain base metal concentrations slightly higher than the average abundances in shale, given by Krauskopf (1979), and as such represent a potential source for the metal sulphides. The Westphalian sediments may also contain high metal concentrations since it is known that organic complexes stabilizing lead and copper in fresh water, flocculate on estuarine waters mixing with sea water (Sholkovitz, 1978).

Using the calculated fluid compositions for the phase 3 and 4 brines, it has been shown that K-feldspar and muscovite were both unstable at the temperatures at which mineralization was occurring. The reason for this is the low potassium activity of the fluids. Calculations also suggest that fluoride/hydroxide ion exchange between clay minerals, micas or apatite and the ore fluids would probably remove fluorine from the aqueous phase at the estimated pH levels (5-6) of the ore-forming environment.

An expression relating fluorite solubility to the chemistry of the ore fluid has been presented, based on the method used by Anderson (1977) for estimating galena solubility. The lack of good activity coefficients and the possibly incomplete nature of the expression precludes the calculation of absolute solubility data. However, the equation may be used to estimate the importance of complexing, and the effects on complexing of processes such as dolomitization and cooling.

The contribution which various complexes make towards fluorite solubility have been evaluated for the phase 3 and 4

fluids. At 100°C, NaF^{o} and CaF^{+} were important in the phase 3 fluid and CaF^{+} only in the phase 4 fluid. The various mechanisms of fluorite precipitation suggested by Richardson and Holland (1979b) have been investigated. Examination of $[Mg^{++}]/[Ca^{++}]$ ratios in the ore fluids and formation waters suggests that the fluids were depleted in magnesium. Removal of a postulated 0.15m $MgCl_2$ would have produced 50% loss of fluorite from an initially saturated solution. Calculation, however, shows that even at calcite saturation, dolomite would have been an unstable phase in the type 4 ore fluid. The phase 3 fluid could have been slightly saturated with dolomite and dolomitization could have produced some fluorite deposition. Field evidence suggests that dolomitization proceded mineralization in the Southern Pennine Orefield (Ford, 1969; Ixer, 1978), although whether Zechstein brines, probably saturated or just undersaturated with calcium sulphate could have produced the dolomitization is questionable (Baker and Kastner, 1981). Formation waters with very low sulphate concentrations would probably form much more effective dolomitizing agents.

Changes in pH of the ore fluid on entering the limestone can probably be discounted as a depositional mechanism as can hydrolysis of fluorine-bearing complexes. Limestone metasomatism was probably one of the most important depositional mechanisms. Fluorite may have replaced limestone, irrespective of the pH of the ore fluid. The main control on the process would have been the degree of saturation of fluorite. Since cation exchange is not thought to take place during metasomatism, the solubility of calcite in the ore fluid is not an important control. Richardson and

Holland (1979b) suggested that fluid mixing or cooling were the most important methods of precipitating fluorite in a hydrothermal environment. Mixing is the most attractive mechanism since it allows large quantities of minerals to be formed from relatively small quantities of fluid. The only limit is that fluorite from the Orefield generally shows equilibrium textures (Barton et al., 1977) which are unlikely to have been produced in conditions of gross supersaturation. Since the range in final ice melting temperatures for an individual sample is not very much less than that for the total population, temporal salinity variation of a single solution is implied rather than continuous mixing of fluids. A dilute fluid containing 100-1000ppm fluorine could have mixed with the formation waters in a very slow and uniform way over the entire Orefield but the practicability of such process seems doubtful.

Surprisingly, very few fluid inclusion studies have been made in which homogenization-melting temperature paired measurements have been recorded. An exception is a study of the strata-bound fluorite deposits of Sweetwater Tennessee (Zimmerman and Kesler, 1981). They showed that there was an inverse correlation between melting and homogenization temperatures which they interpreted as evidence for fluid mixing. No such trend was observed in the type 3 or 4 fluid inclusion data but a positive correlation was observed in a number of type 1 samples. This suggests that the type 1 fluorite may possibly have been deposited by a combination of fluid mixing and cooling.

The type 1 fluid shows the greatest cooling range but the calculations of Richardson and Holland (1979b) indicate

that cooling of moderately saline brines would generally produce fluorite dissolution or undersaturation. The type 3 and 4 fluids have similar cooling ranges. A maximum range which would incorporate 99% of determined homogenization temperature values would be 27°C and 22°C for the phase 3 and 4 events respectively. Calculations do suggest that fluorite could precipitate as the result of cooling in the range 100-50°C, but the amounts deposited would probably be significantly lower than 10mg fluorite per kilogram of ore fluid. The uniformity of the homogenization temperatures across the Orefield suggests that the whole block was maintained at a relatively uniform temperature. Therefore significant heat loss to the wall rocks is unlikely. Fluid convection would be limited by the shale capping to the limestone. Taking these considerations into account, the efficiency of the cooling process must have been limited.

In conclusion, it is difficult to specify which depositional processes listed by Richardson and Holland (1979b) were responsible for precipitating fluorite in the Orefield. The replacement of limestone by fluorite is undoubtedly important, but some fluorite has also been directly precipitated from the ore fluids. Fluid inclusion evidence neither supports large degrees of fluid mixing nor fluid cooling. A single solution model of ore deposition seems preferable on the grounds of fluid inclusion salinity studies and such a model is compatible with data on galena and sphalerite solubility. Cooling, though relatively inefficient, could have produced the deposits over an extended period of time. Replacement of limestone could have produced the bulk of the deposits and later stages of

hydrothermal activity could have remobilized some of the fluorite. A major advantage of the replacement process is that it does not require radical changes in pH, temperature or a dual anion and cation source.

7.7: CONCLUSIONS

Important conclusions arising from the previous discussion are:

1) Immature Namurian sandstones containing biotite, muscovite and feldspar could have acted as a fluorine source for the ore deposits. Decomposition of these fluorine-bearing mineral phases by fluids with low $[K^+]/[H^+]$ ratios at 100°C could have released fluorine, providing that the aluminium silicate alteration products were less capable of holding fluorine than the primary minerals.

2) Lead and zinc may have been derived from high salinity formation waters, as a result of the leaching of Namurian and Westphalian shales or from the leaching of carbonates containing syngenetically or syndiagenetically emplaced base metals.

3) Part of the fluorine present in the ore fluids was almost certainly complexed. The complexes NaF^o and CaF^+ were important in the type 3 fluid and CaF^+ only in the type 2, 4 and 5 fluids.

4) Dolomite was possibly just saturated in the type 3 ore fluid and probably undersaturated in the type 2 and 4 fluids. Therefore it seems unlikely that dolomitization of carbonates produced fluorite deposition.

5) Uniform homogenization temperatures for the main ore-forming events indicate that the importance of fluid cooling was very limited. Uniform final ice melting temperatures are not suggestive of fluorite deposition through fluid mixing. Limestone metasomatism with later remobilization of fluorite were probably the two most important genetic processes.

6) A geochemical argument against fluid mixing for precipitation of the sulphides has been proposed. It is based upon the theory that leaching of most source rocks would produce fluids with Zn/Pb ratios in excess of unity. Deposition of sulphides in conditions of high reduced sulphur activity as a result of mixing would produce orebodies with correspondingly high sphalerite/galena ratios. The dominance of galena over sphalerite in the Southern Pennine Orefield is suggested to be the result of the lower solubility of galena with respect to sphalerite in a single mineralizing fluid. Galena was probably deposited as a result of increasing pH of the ore fluids on entering the limestone host rock.

CHAPTER 8

CONSTRAINTS ON MODELS OF ORE GENESIS

8.1: INTRODUCTION

This chapter attempts to summarize some of the constraints on ore genesis which have become apparent from the fluid inclusion thermometric and geochemical research already reported in earlier sections. The volumes, compositions and origins of the ore fluids, the potential sources of the hydrothermal minerals and the physicochemistry of ore deposition are discussed. Where relevant, the applicability of theories of ore genesis proposed for the Southern Pennine Orefield and other related lead-zinc-fluorite deposits has been commented upon.

8.2: FLUID INCLUSION MICROTHERMOMETRY AND ORE GENESIS

The most important finding of the study is the recognition of not less than four phases of fluorite mineralization in the Southern Pennine Orefield. The nature of the final ice melting temperature and homogenization temperature ranges for each fluid inclusion type clearly indicates that each phase of hydrothermal activity occurred as a discrete temporal event. Each event was characterized by very uniform temperatures and uniform ore fluid compositions over a wide

area. The uniformity in temperature suggests that heat loss from the fluids to the wall rocks was very limited as was the rate of fluid flow. The lack of any determinable east-west thermal gradients indicates that the clustering of the fluorite deposits on the eastern margin of the orefield was not the result of elevated longitudinal temperature gradients as suggested by Mueller (1954). Concentration of fluorite and an increased ZnS/PbS ratio could have been the result of higher ore-forming cation activities in the ore fluids, if a non-mixing hypothesis of mineral deposition is adhered to. There is some evidence that slight dilution and cooling of the type 4 ore fluid probably occurred on moving westward. As Rogers (1977) concluded, oil inclusions are very rare in the bulk of the fluorite deposits. This discovery is in contradiction to the statement by Spooner (1981), that oil inclusions are ubiquitous in low temperature Pb-Zn-F deposits. The lack of hydrocarbons within fluid inclusions lends little support to the mechanism of sulphide deposition in which sulphate is reduced to produce sulphides, as a result of the oxidation of organic compounds.

8.3: ORIGIN OF THE ORE FLUIDS

The origin of the ore fluids has an important bearing on models of ore genesis. The phase 1 ore fluid was atypical of other fluids involved in Pennine mineralization. The fluid inclusions contain a relatively low salinity brine. However, homogenization temperatures in some cases exceed the highest uncorrected sample means for fluorite (Smith, 1974), drawn

from the fluorite zone of the North Pennine Orefield (Atkinson et al., 1982). In contrast to the other ore fluids, the type 1 brine was associated with quantities of oil. Pering (1973) noted a bimodal distribution in the length of the carbon atom chains in the aliphatic hydrocarbons. Pering attributed this to the mixing of hydrocarbons derived from the Edale shales and the Dinantian limestones. The presence of carbonyl compounds and the lack of cogenetic sulphides is possibly suggestive of high oxygen fugacities having existed at the site of deposition. Correlation between final ice melting points and homogenization temperature, for some samples, is also indicative of fluid mixing.

The type 2, 4, and 5 brines were characterized by very high calcium chloride concentrations, with lesser quantities of sodium chloride present. The fluids were notably depleted in magnesium, and an inverse correlation between magnesium and calcium concentration suggests that the fluids were involved in dolomitizing processes. The very low concentration of magnesium indicates that dolomite would not be a stable mineral phase in the type 2 and 4 ore fluids at 100°C and at calcite saturation. Therefore, processes such as cation exchange with clay minerals and chloritization of aluminium silicates may have been the final processes to remove magnesium. Brines with moderately high Ca/Na ratios are found at depth in thick sedimentary sequences, and are thought to be produced as a result of membrane filtration (Graf, 1982). The Ca/Na ratios present in the type 2, 4 and brines are atypical of oil-field brines. Another difference is the lack of correlation between high calcium and high magnesium concentrations in the ore fluids, a relationship

which is a characteristic of oil-field brines. It is known that the efficiency of the filtration process decreases on increasing the concentration of the residual fluid, and it is debatable whether such a process could produce brines with a salt concentration in excess of $400gl^{-1}$. Therefore, an evaporative stage of concentration for the type 2 and 5 ore fluids cannot be ruled out. Fluids with very high Ca/Na ratios have been found in metasediments from the Sudbury basin (Frape and Fritz, 1982). The type 3 brine was more typical of a modern-day oil-field brine and the presence of ver rare petroleum inclusions in the type 3 and 4 brines is suggestive of an oil-field derivation or component in the ore fluids.

8.4: CALCIUM CHLORIDE AND SOLUBILITY OF ORE MINERALS

A number of recent fluid inclusion studies have shown calcium chloride to be an important component of fluorite-forming ore fluids. Fluid inclusions with high calcium concentrations have been found by Kesler (1977) in deposits from Mexico, Moore (1980) in fluorite from the North Pennine Orefield, Sverjensky (1981) in material from the Viburnum Trend and Deloule (1982) in fluorite from Le Burc and Montroc in the Massif Central. Experimental studies of fluorite, galena and sphalerite solubility in "typical" Mississippi Valley-type ore fluids have usually used the fluid inclusion compositions determined by Hall and Friedman (1963). Examples are Richardson and Holland (1979b), Anderson, 1973, Cadek *et al.*, (1982). Thermochemical data for solubility calculations is

often based on the initial assumption that all hydrothermal fluids were dominated by NaCl (Helgeson 1969; Helgeson et al., 1981). The solubility of most minerals in equilibrium with a fluid, increases with an increase in the ionic strength of that solution. The ionic strength of two fluids, one dominated by NaCl and the other by dissociated $CaCl_2$ and both having relatively similar final ice melting temperatures ($-21^{o}C$) are calculated to be 3.9 and 5.9 respectively (Weast, 1980). Although, the two aqueous electrolytes would show similar behavior on a heating-freezing stage, unless careful observation were made, the solubilities of fluorite and the sulphides would be very different in the two liquids.

8.5: THE VOLUME OF ORE FLUIDS INVOLVED IN MINERALIZATION

A number of authors have suggested a relationship between the de-watering of a sedimentary basin and the formation of Mississippi Valley-type ore deposits (Dozy, 1970; Beales and Onasick, 1970) on the flanks of such basins and sited on structural "highs".

The volume of ore fluid required for mineralization in a "one pass" model of mineralization has been calculated assuming that 10mg of fluorite was precipitated from a kg of brine. In Derbyshire, before mining, there may have been 20Mt of fluorite, which would have required 1738km^3 of brine to produce the deposits. It could be argued that much greater quantities of fluorite could be precipitated in a mixing model of mineralization (Richardson and Holland, 1979). The practicality of the mechanism (section 8.7), the REE content

of the fluorite, the delicate growth textures displayed by both fluorite and included sulphides and the uniform composition of the ore fluids all favour a single solution mineralization model.

If one assumes that the mineralization occurred in the Triassic, then the ore fluids must have been generated in a fairly limited number of deep sedimentary basins. Thick Namurian sediments occur in the Rhenish Basin (2000m) and the Bowland-Craven Basin (1000m). Westphalian sediments reach their thickest in the North German Lowlands but retain a substantial from the north of England on to the north European mainland. Thick Triassic sequences occur in the Worcester Graben, the Cheshire Graben and the Carlisle basin in the west as well as in the North Sea. Triassic sedimentation was controlled by tensional tectonism, with the rapid filling of subsiding grabens. All these basins could have generated high salinity brines through overpressuring as a result of sediment compaction or aquathermal pressuring. Aquathermal pressuring is likely to have occurred in the North Sea Grabens, where increased thermal gradients occurred as a result of crustal thinning.

The homogeneity of the ore fluids seems to rule out contemporaneous brine generation and mineralization. Presumably, brines were concentrated in the basins themselves. Fluid migration towards the ore field could have occurred as the result of the release of lithostatic fluid pressure and a return to hydrostatic pressure on fracturing a thick sedimentary sequence (Jones and Wallace, 1974), sediment overpressuring with fluid expulsion at the basin margins and seismic pumping as a result of the release of

shear stress (Sibson et al., 1975). How far such a brine could migrate as a result of some of these processes is unknown. Migration as a result of simple convection seems doubtful given the extremely high densities of some of the mineralizing brines. Fluid circulation with leaching, ore transport and deposition occurring in a single cycle is possible, and would have considerably reduced the volumes of brine involved in mineralization. The leaching capacity of the brine would require rejuvenation by decreasing the pH and the potassium activity of the fluid. In the absence of high thermal gradients, mechanisms of fluid circulation also require an explanation. Fluid movement could have occurred as a result of seismic processes, especially when the very active nature of Triassic siesmicity is taken into account (Anderton et al., 1979). An intermediate reservoir was also probably necessary in order to modify and homogenize the brine compositions.

8.6: SOURCES OF THE ORES

Worley and Ford (1977) suggested that F, Pb, Zn, and Ba could be derived from leaching Dinantian sediments which lie to the east of the Orefield. 87Sr/86Sr ratios for strontium in fluorite are higher than those typical of Visean marine carbonates. Therefore pervasive leaching of Dinantian carbonates is unlikely although Dinantian shales could have been a potential source rock. Lead and zinc concentrations are relatively small in unmineralized carbonates to the west

of the Orefield (Harrison, 1981). Fluorine concentrations are greater, but could be the result of post-depositional ground water movement. If the fluorine is present as fluorapatite, the ore fluids could probably neither destabilize the mineral or remove fluorine through ion exchange. For these reasons Dinantian carbonates can be rejected as a source of the ores.

A Namurian sandstone and shale sequence probably provides the best source for F, Pb, Zn and Ba for the north Pennine (Moore, 1980; Shepherd et al., 1982) and south Pennine hydrothermal ore deposits. It has been shown that minerals present in the immature sandstones, such as biotite, muscovite and K-feldspar would have been unstable in the type 3 and 4 ore fluids at 100°C. Biotite may contain high concentrations of fluorine and zinc while K-feldspar may contain lead and fluorine. If the dissolution of these aluminium silicates occurred, considerable quantities of Pb, Zn and F could be released into the ore fluids. If alteration to clay minerals occurred, probably lesser quantities of fluorine would be released.The exclusive leaching of K-feldspar may be ruled out since all the fluorite shows chondrite normalized negative rather than positive europium anomalies. The less porous Namurian shales also contain moderate base metal concentrations (Spears and Amin, 1981) as well as reduced sulphur in sedimentary pyrite. Zinc and lead may have been concentrated during the evolution of the ore fluids. Present day formation waters in the central Mississippi Valley Basin (Carpenter et al., 1974) and the Michigan Basin (Billings et al., 1968) contain high base metal concentrations. The source of fluorine is probably more problematical than the source of the base metals. Calcula-

tions show that fluorine cannot be removed by hydroxide-fluoride anion exchange in the pH range 5-6. Therefore, in neutral ore fluids, fluorine must be gained by dissolution of fluorine-bearing phases or addition of fluorine-bearing fluids.

8.7: ORE TRANSPORT AND DEPOSITION

Fluid mixing as a depositional mechanism for both ore and gangue minerals in low temperature Mississippi Valley-type ore deposits has had popular support over recent years (Beales and Jackson, 1966; Beales and Onasick, 1970; Anderson, 1975). Similarly, mixing models have been proposed for Pennine ore genesis (Worley and Ford, 1977; Robinson and Ineson, 1979; Shepherd et al., 1982). There is, however, remarkably little evidence of any sort that the Pennine fluorite deposits formed as a result of fluid mixing. The hydrological practicality of such a mechanism is doubtful in itself (Ohle, 1980). The delicate growth textures displayed by fluorite and included sulphides indicate mineral growth in conditions, only slightly in excess of mineral saturation (Barton et al., 1977). Variation in final ice melting temperatures is very small in the two inclusion types which represent the main fluorite and ore-forming stages. Since there is no stratigraphic control on the inclusions measured, salinity variation could represent slight variation in the composition of the ore fluid as the mineralizing events proceeded. Lack of fluid inclusion salinity variation leaves two alternatives. The first is the possible mixing of two

brines of similar salinity. This can be dismissed since a $CaCl_2$-NaCl brine only has a very limited potential for transporting fluorine. The second may be the mixing of a fluid containing a very high fluoride concentration with the a $CaCl_2$-NaCl dominated ore fluid. Such a process would have to be very uniform over a considerable area. During the mixing process, the composition of the resultant brine would be required to maintain a constant Dy/Ca ratio. In order to do this, it is probably necessary that the fluoride-rich fluid contained very low total REE abundances. The conditions of such a mechanism are probably hard to meet.

Anderson (1975) suggested that the pH dependancy of sulphide solubility precludes single solution transport of the sulphides at 100°C while maintaining calcite stability. Anderson's argument is based on the the definition of an ore-forming fluid (1ppm minimum of all components) and on galena solubility estimates in fluids of considerably lower ionic strength than the type 2 or type 3 fluids. In the south west Wisconsin orefield, McLimans et al. (1980) have reported the presence of a sphalerite stratigraphy which extends for considerable distances. Such evidence clearly favours the possibility of low temperatures sulphide deposition from a single solution. Sverjensky (1981) has recalculated galena and sphalerite solubility in fluids of higher ionic strength than used by Anderson (1975) and has estimated considerably higher solubilities in such brines.

An argument which does not seem to have been looked at is the relevance of Zn/Pb ratios within an orefield. If a base metal rich brine encountered high concentrations of reduced sulphur, it would be expected that the ZnS/PbS ratios

of the deposit would reflect the Zn/Pb ratio of the ore fluid. Formation waters which have been found to contain base metals have Zn/Pb ratios in excess of 1 (Billings et al., 1968; Carpenter et al., 1974). Leaching experiments conducted using chloride-rich brines show that zinc is leached from shales more readily than lead (Long and Angino, 1982). This could be the result of the stronger chloride complexes formed by zinc, the easier release of zinc from cation exchange sites in clay minerals or the destabilization of zinc-bearing phases in the rock. Unless it was possible to generate a lead-rich brine, depleted in zinc, deposition of purely lead sulphide by fluid mixing of a base metal and reduced sulphur source is practically impossible.

It is more probable that the dominance of galena in the orefield is a function its lower solubility. Sphalerite occurs on the eastern margin of the field where zinc concentrations in the ore fluid may have been higher and pH changes greater. All the galena and sphalerite could have been precipitated as a result of pH change on the fluid moving from the Namurian to the Dinantian sediments, with possible cooling of the fluid taking place. Concentrations of lead in the ore fluid need not have exceeded 1ppm, without producing problems of ore fluid volume. If the ore fluids contained 1ppm CaF_2, and a fluid flow of 1µms occurred through the top 100m of limestone, 17380km^3 of fluid could have moved through the orefield in 183700 years. Two hundred thousand years is certainly not a prohibitively long period of time. Deposition of fluorite is more problematical than deposition of the sulphides since the solubility of fluorite is unaffected by pH changes in the range 4-8 (Richardson and

Holland, 1979b). The importance of fluid cooling was obviously limited, since the homogeneity of fluid inclusion homogenization temperatures indicates a lack of either heat loss to the wall rocks or loss through rapid fluid flow. Fluorite dissolution would have occurred on cooling the type 1 brine. Calculations indicate that fluorite would have been preciptated on cooling the type 3 and 4 fluids. However, the maximum cooling intervals are 20°C and 12°C respectively.

It is unlikely that dolomitization of carbonates produced any fluorite, although removal of magnesium from the type 3 and 4 ore fluids may have brought the fluoride in the brines closer to a saturation level. Replacement of calcite by fluorite was probably the most effective depositional mechanism. The process only requires fluorite saturation in the ore fluid and a favourable F^-/CO_3^{2-} ratio. The mechanism is independent of the pH of the system. The type 3 fluid was probably more effective in replacing limestone than the other brines. This is supported by the presence of type 3 fluid inclusions in many of the metasomatic replacement deposits.

8.8: SUGGESTIONS FOR FURTHER RESEARCH

Further studies of variation in depositional temperature of fluorite through the study of homogenization temperatures of fluid inclusions is probably of very limited value. A more extensive study of fluid inclusion final ice melting temperatures could possibly resolve the age relations and the extent of the five hydrothermal events more completely. The work would be, however, severely limited by

the lack of primary inclusions.

A study of the δD, $\delta^{18}O$ isotope ratios of the inclusion fluids and the 87Sr/86Sr ratio of the enclosing minerals would undoubtedly be of interest in providing more information about the sources of the fluids, interaction of fluids with the wall rocks, mixing of different fluid reservoir sources and mechanisms of mineral deposition. A new method of determining δD and $\delta^{18}O$ from the same inclusion fluid sample would need to be developed, since $\delta^{18}O$ is normally determined from the isotopic composition of the host oxide mineral. The wide δD range (-100‰ to -8‰) for fluid inclusions in fluorite from the Orefield suggests that study of stable isotopes could have good potential. Measurement of δD and the 87Sr/86Sr ratio in a fluid and the containing mineral allows the study of both the solvent and the solute in the ore-forming brine (Norman and Landis, 1983). A 87Sr/86Sr ratio range of 0.7082 to 0.7101 is probably large enough to resolve characteristic ranges for the five ore fluids. The evolutionary relationship of the fluids could be studied and an indication as to whether mineralization occurred in a truly open system or a closed or semi-closed circulatory system may be determined. Again, the main problem with such a study would be the ability to relate a specific host mineral to an inclusion fluid. Strontium isotope ratios could also be determined for baryte in order to establish whether baryte was deposited from a fluid with the same 87Sr/86Sr ratio as the fluorite-forming brines. Such a study could be extended to all the low temperature fluorite-baryte-calcite deposits in the British Isles. Strontium isotope ratios for potential source rocks are also

required in order to make the studies more profitable.

Although processes of fluorite deposition have received much attention, mobilization of fluorine during interaction of high-salinity fluids with wall rocks has attracted little attention. The potential of source rocks could be evaluated by measuring fluorine concentrations in unweathered and unaltered samples.

There is also little literature concerning the movement of the REE during mineral dissolution and alteration in low temperature hydrothermal environments. The unusual forms of some chondrite normalized REE patterns (Howie et al., 1982) clearly indicate that that the source rock and fluid-rock interaction has a strong influence on lanthanide abundance in a mineral such as fluorite. Experimental studies on the fractionation of lanthanides during fluid-wall rock interaction involving mineral dissolution, alteration and ion exchange would be valuable when using the REE to interpret fluid evolution. There is also a dearth of thermodynamic data for the REE complexes, particularly at elevated temperatures. A more complete knowledge of the nature of REE complexing in a variety of aqueous electrolytes at elevated temperatures would be of great use in understanding the movement of the lanthanides in a hydrothermal environment.

CHAPTER 9

CONCLUSIONS

A summary of the more important conclusions presented in the various chapters of this thesis are listed below.

1) Seven fluid inclusion types have been recognized, at least four of which contain samples of what were fluorite-forming hydrothermal fluids.

2) Homogenization temperature ranges for the four important inclusion types are: 100-171°C for type 1 inclusions: 62-82°C for type 2 inclusions: 65-99°C for type 3 inclusions: 73-106°C for type 4 inclusions.

3) Final ice melting temperature ranges for inclusion types are: -6.6°C to 0°C for type 1 inclusions: -26.0°C to -20.0°C for type 3 inclusions: -19.5°C to -15.4°C for type 4 inclusions. Antarcticite was the final melting phase in the type 2 inclusions and final melting occurred in the temperature range 1.8°C to 6.6°C.

4) Homogenization temperature ranges for the type 3 and type 4 fluid inclusions are very similar, suggesting that the two events may have occurred within a short span of time.

5) The four fluorite-forming events cannot be distinguished

in paragenetic sequences by changes in coloration or the nature of included material within the fluorite. Fluorite containing primary type 1 fluid inclusions does, however, clearly pre-date fluorite formed in other mineralizing phases and this relationship can be recognized in the field.

6) There is no evidence of east-west thermal gradients having been important in any of the hydrothermal events.

7) Oil inclusions are associated with type 1, 2 and 3 fluid inclusions but are very rare except in association with type 1 fluid inclusions. Homogenization temperatures of the oil inclusions are generally slightly lower than similar temperatures determined from cogenetic aqueous inclusions.

8) Final ice melting temperatures fall into very restricted ranges indicating mineral deposition from fluids of relatively constant composition.

9) Calcium and sodium chlorides were the dominant salt components in the ore fluids. Calcium chloride was the dominant salt in the type 2, 4 and 5 fluids.

1Ø) Delicate growth banding in large, well-formed fluorite crystals containing intricately structured sulphide inclusions indicates mineral deposition occurred in conditions closely approaching equilibrium.

11) By analogy with present-day high salinity formation waters, sulphate concentration in the ore fluids was probably

low.

12) An alteration assemblage of smectite+kaolinite+quartz indicates the type 3 and 4 ore fluids had a minimum pH of 5.2 and 5.9 respectively. An upper pH limit of 6 would have been necessary for sulphide transport and deposition from a single solution.

13) Oxygen fugacity ranged from 10^{-57} to 10^{-55} atm and sulphur fugacity fell in the range 10^{-19} to 10^{-22} atm.

14) The availability of ligands for complexing and the relative strengths of the REE fluoride complexes was probably the major control on the fractionation of the lanthanides between crystallizing phases and the hydrothermal solution.

15) The uniformity of the REE chondrite-normalized patterns suggests fluorite deposition occurred as a result of non-mixing processes taking place in an open system.

16) Negative europium anomalies in some of the chondrite-normalized distribution patterns for fluorite were inherited from the solution itself. Leaching of biotite and apatite may have produced these anomalies. Negative cerium anomalies may have been inherited from sea water.

17) LREE enrichment could have been produced as a result fluid interaction with wall or source rocks, or a result of crystallographic control on fractionation between fluids and the precipitating mineral phase.

18) The presence of abundant oil inclusions in association with type 1 fluid inclusions and the more rare occurrence of oil in association with type 3 and 4 inclusions suggests that oil-field brines formed a component of the ore fluids.

19) The high $CaCl_2$/NaCl ratios in the type 2, 4 and 5 inclusion fluids, indicates that these brines were not typical of present-day high salinity formation waters.

20) 87Sr/86Sr for the fluorite ranged from 0.7082 to 0.7101, suggesting that the ore fluids had interacted with rocks enriched in radiogenic strontium with respect to Visean marine carbonates.

21) The ore fluids were probably generated by membrane filtration but attainment of total dissolved salt concentrations in excess of $400gl^{-1}$ may have necessitated other mechanisms of fluid evolution.

22) Immature sandstones containing biotite, muscovite and K-feldspar could have acted as the fluorine source for the fluorite deposits. Decomposition of fluorine-bearing mineral phases by fluids with low $[K^+]/[H^+]$ ratios at 100°C could have released fluorine into the system, providing that aluminium silicate alteration products such as kaolinite and smectite were not capable of absorbing all the fluorine.

23) Lead and zinc may have been derived from formation waters or from the leaching of Namurian or Westphalian

shales.

24) Part of the fluorine present in the ore fluids was almost certainly complexed in the form CaF^{+} and NaF^{o}.

25) Dolomite may have just been a saturated mineral phase in the type 3 ore fluid and was almost certainly undersaturated in the type 2 and 4 ore fluids. Therefore dolomitization of carbonates is unlikely to have produced fluorite mineralization.

26) Uniform homogenization temperatures for the main ore-forming events indicate that the importance of cooling as a depositional mechanism for fluorite was severely limited. Uniform final ice melting temperatures determined from inclusions are not suggestive of fluorite deposition from fluid mixing. Metasomatic replacement of limestone by fluorite with later stages of fluorite remobilization were probably the most important genetic processes.

27) A geochemical argument against fluid mixing for precipitation of the sulphides has been proposed. It is based upon the argument that leaching of most source rocks would produce Zn/Pb ratios in excess of unity. Precipitation of galena and sphalerite from such fluids by exposure to high levels of reduced sulphur would produce ores in which the ZnS/PbS ratio reflected the Zn/Pb ratio of the base metal-carrying ore fluid. The dominance of galena as the major sulphide mineral in the Southern Pennine Orefield with sphalerite present on the eastern margin of the field is

considered to be the result of single solution mineral zonation in response to the differing solubility products of galena and sphalerite.

REFERENCES

Alderton, D.H.M., Pearce, J.A. and Potts, P.J., (198Ø) Rare earth element mobility during granite alteration: Evidence from Southwest England. Earth Planet. Sci. Letters, 49, pp149-165.

Ames, L.L. (1961) The metasomatic replacement of limestones by alkaline fluoride-bearing solutions. Econ. Geol., 56, pp73Ø-739.

Anderson, G.M. (1973) The hydrothermal transport and deposition of galena and sphalerite near 1ØØ°C. Econ. Geol., 68, pp48Ø-492.

Anderson, G.M. (1975) - Precipitation of Mississippi Valley-type ores. Econ. Geol., 7Ø, pp937-942.

Anderson, G.M. (1977) - Thermodynamics and sulphide solubilities. In Short course in application of thermodynamics to petrology and ore deposits. Greenwood, H.J. , ed., Mineralog. Assoc. of Canada, Vancouver, pp136-15Ø.

Anderton, R., Bridges, P.H., Leeder, M.R. & Sellwood, B.W. (1979) - A dynamic stratigraphy of the British Isles. George Allen & Unwin, London, 3Ølp.

Atkinson, P, McM. Moore, J. and Evans, A.M. (1982) - The Pennine Orefields of England with special reference to recent structural and fluid inclusion investigations. Bull. du B.R.G.M., 2, sect. 2, no. 4, pp149-156.

Baker, P.A. & Kastner, M. (1981) - Constraints on the formation of sedimentary dolomite. Science, 213, pp214-216

Bamford, D., Nunn, K., Prodehl, G. & Jacob, B. (1977) - LISPB-III Upper crustal structure of northern Britain. Jour. geol. Soc. London, 133, pp481-488.

Barbieri, M., Masi, U. & Tolomeo L. (1982) - Strontium geochemistry in the epithermal barite deposits from the Apuan Alps (Northern Tuscany, Italy). Chem. Geol., 35, pp351-356.

Barbieri, M., Masi, U. & Tolomeo, L. (1977) - Geochemical evidence on the origin of the fluorite epithermal deposit at Monte Delle Fate near Cerveteri (Latium central Italy). Miner. Deposita, 12, pp393-398.

Barnes, H.L. (1979) - Solubilities of ore minerals. In Geochemistry of hydrothermal ore deposits. Barnes, H.L., ed., 2nd ed. Wiley, New York, pp4Ø4-46Ø.

Barnes, H.L. & Czamanske (1967) - Solubilities and transport of ore minerals. In Geochemisty of hydrothermal ore deposits. Barnes, H.L., ed., Holt, Rinehart & Winston, New York, pp334-381.

Barnes H.L. & Kullerud, G. (1961) - Equilibria in sulphur containing aqueous solutions in the system Fe-S-O and their correlation during ore deposition. Econ. Geol., 56, pp648-688.

Barrett, T.J. and Anderson, G.M. (1982) - The solubility of sphalerite and galena in NaCl brines. Econ. Geol., 77, pp1923-1933.

Barton, P.B. (1967) - Possible role of organic matter in the precipitation of the Mississippi Valley ores. Econ. Geol. Mon. 3, pp 371-378.

Barton, P.B., Bethke, P.M., Toulmin, P. (1963) - Equilibrium in ore deposits: Min. Soc. Am., Spec. Paper No. 1, pp171-185.

Barton, P.B., Bethke, P.M., & Roedder, E. (1977) - Environment of ore deposition in the Creede Mining district, San Juan Mountains, Colarado. III: Progress toward interpretation of the chemistry of the ore-forming fluid for the OH vein. Econ Geol 72, ppl-25.

Barton, P.B, & Skinner B.J. (1979) - Sulphide mineral stabilities. In Geochemistry of hydrothermal ore deposits: Barnes, H.L., ed., 2nd ed., Wiley, New York, pp278-403.

Beales, F.W. (1975) - Precipitation mechanisms for Mississippi Valley-type ore deposits. Econ. Geol., 70, pp943-948.

Beales, F.W. & Jackson S.A. (1966) - Precipitation of carbonate reservoirs as illustrated by Pine Point ore field, Canada. Trans. Instn Min. Metall., (Sect. B, Appl. earth Sci.), 75, B278-B285.

Beales, F.W. & Onasick, E.P. (1970) - Stratigraphic habitat of Mississippi Valley-type orebodies. Trans. Instn Min. Metall. (Sect. B, Appl. earth sci.), 79, B145-B154.

Bentor, Y.K. (1969) - On the evolution of subsurface brines in Israel. Chem. Geol., 4, 83-110

Berner, R.A. (1971) - Principles of chemical sedimentology. McGraw-Hill, New YorK.

Bilial, B.A. & Becker, P. (1979)- Complex formation in geo-chemical systems: II Stability of rare earth fluoro-complexes in fluorite bearing model-system at various ionic strengths. Jour. Inorg. Nucl. Chem., 41, pp1607-1608.

Bilial, B.A., Hermann, F., Fleischer, W. (1979) - Complex formation of trace elements in geochemical systems: I Potentiometric study of fluorocomplexes of rare earth elements in fluorite-bearing model-systems. Jour. Inorg. Nucl. Chem., 41, p347.

Bilial, B.A., Koss, V. (1980) - Complex formation of trace elements in geochemical systems: III Studies on the distribution of fluorocomplexes of rare earth elements in fluorite-bearing model-systems. Jour. Inorg. Nucl. Chem., 42, pp629-630.

Billings, G.K., Kesler, S.E. & Jackson, S.A. (1969) - Relation of zinc-rich formation waters of Northern Alberta, to the Pine Point ore deposit. Econ. Geol., 64, pp385-391.

Bischoff, J.L., Radtke, A.S. & Rosenbauer, R.J. (1981) - Hydrothermal alteration of graywacke by brine and seawater: Roles of alteration and metal chloride complexing on metal solubilization at 200°C and 350°C. Econ. Geol., 76, pp559-676.

Bloom, M.S. (1981) - Chemistry of inclusion fluids: Stockwork molybdenum deposits from Questa, New Mexico and Hudson Bay Mountain and Endako, British Columbia. Econ. Geol., 76, pp1906-1920.

Blount, C.W. & Dickson, F.W. (1969) - Solubility of anhydrite ($CaSO_4$) in NaCl-H_2O from 100°C to 450°C and 1 to 1000 bars. Geochim. cosmochim. Acta, 33, pp227-245.

Boast, M.B., Coleman, M.L. & Halls, C. (1981) - Textural and stable isotopic evidence for the genesis of the Tynagh base metal deposit, Ireland. Econ. Geol., 76, pp27-55.

Bofinger, V.M., Compston, W. & Vernon, M.J. (1968) - The application of acid leaching to Rb-Sr dating of a mid Ordovician shale. Geochim. cosmochim. Acta, 32, pp823-833.

Boyle, R.W. (1968) - The source of metals and gangue elements in epigenetic deposits. Mineral. Deposita, 3, pp174-177.

Brattner, P., Jacob, K.H., Luck, J., Moller, P., Rusick, U., & Szacki, W. (1972) - Zur Fraktionierung der Seltenen Erden in Fluoriten. Erzmetall., 25, pp389-394.

Bridge, D. & Gozzard, J.R. (1981) - The limestone resources of the country around Bakewell, Derbyshire (1981) - Miner. Assess. Rep. Inst. Geol. Sci., No 79.

Burruss, R.C. (1981) - Hydrocarbon fluid inclusions in studies of sedimentary diagenesis. In Fluid inclusions: applications to petrology. Hollister, L.S. & Crawford, M.L., eds., Mineralog. Assoc. Canada, short course handbook, 6, pp138-156.

Butcher, N.J.D. (1976) - Fluorite mineralization in the South Pennine Orefield. PhD thesis, University of Leicester.

Cadek, J., Majer, V. & Malkovsky, M. (1982) - Transport of fluorine in low temperature hydrothermal brines. Bull. du B.R.G.M., 2, sect. 2, no. 4, pp379-382.

Carlon, C.J. (1978) Baryte mineralization in the British Isles. PhD thesis, University of Manchester.

Carpenter, A.B., (1978) - Origin and chemical evolution of brines in sedimentary basins. Oklahoma Geol. Surv. Circ., 79, pp60-77.

Carpenter, A.B., Trout, M.L. & Pickett, E.E. (1974) - Preliminary report on the origin and chemical evolution of lead- and zinc-rich oil field brines in central Mississippi. Econ. Geol., 69, pp1191-1206.

Carpenter, R. (1969) - Factors controlling the marine geochemistry of fluorine. Geochim. cosmochim. Acta, 33, pp1153-1167.

Chaudhuri, S. (1978) - Strontium isotopic composition of several oilfield brines from Kansas and Colarado. Geochim. cosmochim. Acta, 42, pp329-331.

Chen, C-T.A. & Marshall, W.L. (1982) - Amorphous silica solubilities IV. Behaviour in pure water and aqueous sodium chloride, sodium sulphate, magnesium chloride and magnesium sulphate solutions up to 350 deg C. Geochim. cosmochim. Acta, 46, pp279-287.

Chivas A.R. & Wilkins, R.W.T. (1977) - Fluid inclusion studies in relation to hydrothermal alteration and mineralization at the Koloula porphyry copper prospect, Guadalcanal. Econ. Geol., 72, pp153-169.

Clauer, N., O'Neil, J.R. & Bonnot-Courtois, C. (1982) - The effect of natural weathering on the chemical and isotopic compositions of biotites. Geochim. cosmochim. Acta, 46, pp1755-1762.

Clayton, R.N., Friedman, I., Graf, D.L., Mayeda, T.K., Meents, W.F. & Stump, N.F. (1966) - The origin of saline formation waters: I Isotopic composition. Jour. Geophys. Res., 71, pp3869-3882.

Coomer, P.G. & Ford, T.D. (1975) - Lead and sulphur isotope ratios of some galena specimens from the South Pennines and North Midlands. Mercian Geol., 5, pp291-304.

Collins, A.G. (1975) - Geochemistry of oilfield brines. Elsevier. 496p.

Cope, F.W. (1949) - The Woo Dale borehole, near Buxton. Q. Jl. geol. Soc. Lond., 105, p5.

Cope, F.W. (1973) - Woodale borehole, near Buxton, Derbyshire. Nature (Physical Sciences), 243, pp29-30.

Cope, F.W. (1979) - The age of the volcanic rocks in the Woo Dale Borehole, Derbyshire. Geol. Mag., 116, pp319-320.

Crawford, M.L. (1981) - Phase equilibria in aqueous fluid inclusions. In Fluid inclusions: applications to petrology. Hollister, L.S. & Crawford, M.L., eds, Mineralog. Assoc. Canada, short course handbook, 6, pp75-100.

Crawford, M.L., Kraus, D.W. & Hollister, L.S. (1979) - Petrologic and fluid inclusion study of calc-silicate rocks, Prince Rupert, British Columbia. Am. Jour. Sci., 279, 1135-1159.

Davis, J.C. (1973) - Statistics and data analysis in geology. Wiley, New York, 550p

Davies, C.W. (1962) - Ion association. Butterworths, London.

Deloule, E. (1982) - The genesis of fluorspar hydrothermal deposits at Montroc and the Tarn as deduced from fluid inclusion analysis. Econ. Geol., 77, pp1867-1874.

Downing, R.A. & Howitt, F. (1969) - Saline ground-waters in the Carboniferous rocks of the East Midlands in relation to the geology. Q. Jl. Eng. Geol. London., 1, pp241-269.

Dozy, J.J. (1970) - A geological model for the genesis of the lead zinc ores of the Mississippi Valley. Trans. Instn Min. Metall. (Sect. B., Appl. earth sci.), 79, B163-B170.

Dunham, K.C. (1952) - Fluorspar. Spec. Rep. Mineral Resour. G.B., H.M.S.O., London, 143p.

Dunham, K.C. (1948) - Geology of the northern Pennine Orefield. Vol, 1, Tyne to Stainmore. Mem. Geol. Surv., G.B., H.M.S.O., London, 357p.

Dunham, K.C. (1966) - Role of juvenile solutions, connate waters and evaporitic brines in the genesis of lead-zinc-fluorite-barite deposits. Trans. Instn Min. Metall. (Sect. B., Appl. earth sci.), 75, B226-229.

Dunham, K.C. (1973) - A recent deep borehole near Eyam, Derbyshire. Nature, 241, pp84-85.

Ellis, A.J. & Mahon, W.A.J. (1977) - Chemistry and geothermal systems. Academic Press, New York, 392p.

Evans, A.M. & Maroof, S.I. (1976) - Basement controls of mineralization in the British Isles. Mining. Mag., 134, pp401-411.

Faure, G & Powell, J.L. (1972) - Strontium isotope geology. Springer-Verlag, Berlin, 188p.

Firman, R.J. & Bagshaw, C. (1974) - A re-appraisal of the controls of non-metallic gangue mineral distribution in Derbyshire. Mercian Geol., 5, pp145-161.

Ford, T.D. (1969) - The stratiform ore deposits of Derbyshire. In Sedimentary ores: ancient and modern. Proc. 15th inter-university geological congress, Leicester, 1967.

Ford, T.D. (1969b) - The Blue John deposits of Treak Cliff in relation to the Boulder Bed. Proc. Yorks. Geol. Soc., 37, pp153-158.

Ford, T.D. (1976) - The ores of the South Pennines and Mendip Hills, England - a comparative study. In handbook of strata-bound and stratiform ore deposits, vol. 5, regional studies, ed. Wolf, K.M., Elsevier, Amsterdam, pp161-195.

Ford, T.D. (1971) - The fluorspar mining potential of the Derbyshire Orefield. Trans. Instn Min. Metall. (Sect. B., Appl. earth sci.), 80, B126-210.

Frape, S.K. & Fritz, P. (1982) - The chemistry and isotopic composition of saline groundwaters from the Sudbury Basin, Ontario. Canadian Jour. Earth Sci., 19, pp645-661.

Frost, D.V. & Smart, J.G.O. (1979) - Geology of the country north of Derby. Mem. Geol. Surv. G.B.

Garrels, R. M. & Christ, C.L. (1965) - Solutions, minerals and equilibria. Harper and Row, New York, 450p.

Giordano, T.H. & Barnes, H.L. (1981) - Lead transport in Mississippi Valley-type ore solutions. Econ. Geol., 76, pp2200-2211.

Graf, D.L. (1982) - Chemical osmosis, reverse chemical osmosis and the origin of subsurface brines. Geochim. cosmochim. Acta, 46, pp1431-1448.

Graf, D.L. and Anderson, D.E. (1981) - Geochemical inputs for hydrologic models of deep lying sedimentary units: loss of mineral hydration water. Jour. Hydrol., 54, pp297-314.

Guichard,F., Church, Th. M., Treuil, M., & Jaffrezic, H. (1979) - Rare earths in barites: Distribution and effects on aqueous partitioning. Geochim. cosmochim. Acta, 43, pp983-997.

Graf, D.L., Friedman, I, Meents, W.F. & Shimp, N.F. (1966) - The origin of saline formation waters: III Calcium chloride waters. Illinois Geol. Surv. Circ., 397, 60p.

Green, A.H. & Strahan, A. (1887) - Carboniferous limestone, Yoredale Rocks and Millstone Grit of North Derbyshire. Mem. Geol. Surv. G.B., 2nd ed.

Grim, R.E. (1968) - Clay Mineralogy. 2nd ed., McGraw-Hill, New York.

Hall, W.E. & Friedman, I. (1963) - Composition of fluid inclusions, Cave-in-Rock, fluorite district, Illinois and Upper Mississippi Valley zinc-lead district. Econ. Geol., 58, pp886-911.

Hanor, J.S. (1979) - The sedimentary genesis of hydrothermal fluids. In Geochemistry of hydrothermal ore deposits. Barnes, H.L. ed., Wiley, New York, pp137-172.

Hanor, J.S. (1981) - Dissolved methane in sedimentary brines: Potential effect on the P.V.T. properties of fluid inclusions. Econ. Geol., 75, pp603-609.

Hanshaw, B.B. & Coplen, T.B. (1973) - Ultrafiltration by a compacted membrane. II Sodium in exclusion at various ionic strengths. Geochim. cosmochim. Acta, 37, pp2311-2328.

Helgeson, H.C. (1967) - Solution chemistry and metamorphism. In Researches in geochemistry, 2, P.H. Abelson, ed., Wiley, New York, pp362-404.

Helgeson, H.C. (1969) - Thermodynamics of hydrothermal systems at elevated temperatures and pressures. Am. Jour. Sci., 267, pp729-804.

Helgeson, H.C. (1970) - A chemical and thermodynamic model of ore deposition in hydrothermal systems. In Fiftieth anniversary symposia, B.A. Morgan, ed., Min. Soc. Am. Spec. Paper 3, pp155-186.

Helgeson, H.C., Kirkham, D.H. & Flowers, G.C. (1981) - Theoretical prediction of aqueous electrolytes at high pressures and temperatures. IV. Calculation of activity coefficients and apparent molal and standard relative partial molal properties to 600°C and 5kb. Am. Jour. Sci., 281, pp1249-1516.

Heyl, A.V. (1969) - Some aspects of genesis of zinc-lead-baryte-fluorite deposits in the Mississippi Valley, U.S.A. Trans. Instn Min. Metall. (Sect. B., Appl. earth sci.), 78, B148-160.

Heyl, A.V., Hosterman, J.W. & Brook, M.R. (1964) - Clay mineral alteration in the upper Mississippi Valley zinc-lead district: Clays and clay minerals. Conf., 12th, Atlanta, 1963, Proc., pp445-453.

Hitchon, B. & Friedman, I. (1969) - Geochemistry and origin of formation waters in the Western Canada sedimentary basin. I Stable isotopes of hydrogen and oxygen. Geochim. cosmochim. Acta, 33, pp1321-1349.

Hogfeldt, E. (1982) - Stability constants of metal-ion complexes. Part A: Inorganic Ligands. IUPAC Chemical data series, no. 21, Pergamon Press, 310p.

Holland, H.D. (1965) - Some applications of thermochemical data to problems of ore deposits. II Mineral assemblages and the composition of ore-forming fluids. Econ. Geol., 60, pp1101-1166.

Holland H.D. and Malinin, S.D. (1979) - The solubility and occurrence of non-ore minerals. In Geochemistry of hydrothermal ore deposits, Barnes, H.L. ed., Wiley, New York, pp461-508.

Hollister, L.S., Crawford, M.L., Roedder, E., Burrus, R.C. & Spooner, E.T.C. (1981) - Practical aspects of microthermometry. In Fluid inclusions: applications to petrology. Hollister, L.S. & Crawford, M.L., eds, Mineralog. Assoc. Canada, short course handbook, 6, pp278-304.

Houghton, G., McLean, A.M., Ritchie, P.D. (1957) - Compressability, fugacity and water-solubility of carbon dioxide in the region of 0-36atm. and 0-100 deg.C. Chem. Eng. Sci., 6, pp132-137.

Howie, R.A., Pegram, E. & Walsh, J.N. (1982) - The content of rare earth elements in English fluorites: a preliminary study. Jour. Russel Soc., 1, pp22-25.

Ineson, P.R. & Al-Kufaishi, F.A.M. (1970) - The mineralogy and paragenetic sequence of Long Rake Vein at Raper Mine, Derbyshire. Mercian Geol., 3, pp337-351.

Ineson, P.R. and Ford, T.D. (1982) - The South Pennine Orefield: its genetic theories and eastward extension. Mercian Geol., 8, pp285-303.

Ineson, P.R. & Mitchell, J.G. (1973) - Isotopic age determinations on clay minerals from lavas and tuffs of the Derbyshire Orefield. Geol. Mag., 109, pp501-512.

Ineson, P.R. & Mitchell, J.G. (1974) - K-Ar isotopic age determinations from some Lake District mineral localities. Geol. Mag., 111, pp521-537.

Ineson, P.R., Richardson, R.T. and Wood, G.H. (1972) - A baryte-galena vein in the Magnesian Limestone at Whitwell, Derbyshire. Proc. Yorks. Geol. Soc., 39, pp139-149.

Ixer, R.A. (1978) - The emplacement of a fluorspar flat at Masson Hill, Matlock, Derbyshire. Mercian Geol., 6, pp245-255.

Ixer, R.A. and Townley, R. (1979) - The sulphide mineralogy and paragenesis of the South Pennine Orefield, England. Mercian Geol., 7, pp51-63.

Johnson, D.A. (1974) - Relative stabilities of dipositive and tripositive lanthanoid ions in aqueous solution. Jour. Chem. Soc., Dalton Trans., pp1671-1675.

Jones, C.M. (1980) - Deltaic sedimentation in the Roaches Grit and associated sediments (Namurian R2b) in the South West Pennines. Proc. Yorks. Geol. Soc., 43, pp39-67.

Jones, P.H. & Wallace, R.H. (1974) - Hydrologic aspects of structural deformation in the northern Gulf of Mexico basin. Jour. Res. U. S. Geol. Surv., 2, pp511-517.

Kent, P.E. (1966) - The structure of the concealed Carboniferous rocks of north-eastern England. Proc. Yorks. Geol. Soc., 35, pp323-352.

Kent, P.E. (1967) - A contour map of the sub-carboniferous floor of the North Midlands. Proc. Yorks. Geol. Soc., 36, pp174-194.

Kesler, S.E. (1977) - Geochemistry of the manto fluorite deposits of Northern Coahuila, Mexico. Econ. Geol., 72, pp204-218.

Kesler, S.E. & Jones L.M. (1981) - Sulphur and strontium isotope geochemistry of celestite, barite and gypsum from the Mesozoic basins of north eastern Mexico. Chem. Geol., 31, pp211-224.

Kessen, K.M., Woodruff, M.S. & Grant, N.K (1981) - Gangue mineral 87Sr/86Sr ratios and the origin of Mississippi Valley-type mineralization. Econ. Geol., 76, pp913-920.

Kharaka, Y.K. & Berry, F.A.F. (1973) - Simultaneous flow of water and solutes through geological membranes. I. Experimental investigation. Geochim. cosmochim. Acta, 37, pp2577-2604.

Kharaka, Y.K., Berry, F.A.F. & Friedman, I (1973) - Isotope composition of oil-field brines from Kettlemen Dome, California and their geologic implications. Geochim. cosmochim. Acta, 37, pp1899-1903.

Kharaka, Y.K. & Smalley, W.C. (1976) - Flow of water and solutes through compacted beds. Am. Assoc. Petrol. Geol. Bull., 60, pp973-980.

Konnerup-Madsen, J. (1979) - Fluid inclusions in quartz from deep-seated granitic intrusions, South Norway. Lithos, 12, 13-23.

Kramer, J.R. (1969) - Subsurface brines and mineral equilibria. Chem. Geol., 4, pp37-50.

Krapchenko, L.N. (1964) - On the genesis of deep-seated brines of the Siberian platform. Geochemistry International, 6, pp1107-1114.

Krotova, V.A. (1957) - Conditions of formation of calcium chloride waters in Siberia. Petroleum Geology, 2, pp545-552.

Krauskopf, K.B. (1979) - Introduction to geochemistry. 2nd ed., McGraw-Hill, Tokyo.

Langley, K.M. (1980) - Dating sediments by a K-Ar method. Nature, 276, pp56-57.

Lawler, J.P. and Crawford, M.L. (1983) - Stretching of fluid inclusions resulting from a low temperature microthermometric technique. Econ. Geol., 78, pp527-pp529.

Linke, W.F. (1965) - Solubilities of inorganic and metal-organic compounds. 4th ed., vol. 2, Am. Chem. Soc., 1914p.

Long, D.T. & Angino, E.K. (1982) - The mobilization of selected trace metals from shales by aqueous solutions: effects of temperature and ionic strength. Econ. Geol., 77, pp646-652.

Manheim, F.T. (1970) - Critique of membrane filtration concepts as applied to the origin of subsurface brines. Amer. Assoc. Petrol. Geol. Bull., 54, pp858.

Manheim, F.T. & Horn, M.K. (1968) - Composition of deeper subsurface waters along the Atlantic continental margin. Southeastern Geol., 9, pp215-236.

Marchand, L., Joseph, D., Touray, J.C. & Treuil, M. (1976) - Criteres d'analyse geochemique des gisements de fluorines bases sur l'etude de la distribution des lanthanides; application au gite du Maine (71 Cordesse, France). Miner. Deposita, 11, pp357-379.

Maroof, S.I. (1976) - The structure of the concealed pre-Carboniferous basement of the Derbyshire Dome from gravity data. Proc. Yorks. Geol Soc., 41, pp59-69.

Martin-Kaye, P. (1982) - Contribution to the study of the Pennines (U.K.). Bull. B.R.G.M., 2, sect. 2, no. 3, pp317-318.

Macdonald, A.J. & Spooner, E.T.C. (1981) - Calibration of the Linkam TH600 programmable heating cooling stage for microthermometric exmination of fluid inclusions. Econ. Geol., 76, pp1248-1258.

McLimans, R.K., Barnes, H.L. and Ohmoto, H. (1980) Sphalerite stratigraphy of the Upper Mississippi Valley zinc-lead district, Southwest Wisconsin. Econ. Geol., 75, pp351-361.

Merino, E. (1975) - Diagenesis of tertiary sandstones from the Kettleman North Dome, California. II. Interstitial solutions: distribution of aqueous species at 100°C and chemical relation to diagenetic mineralogy. Geochim. cosmochim. Acta, 39, pp1629-1645.

Moller, P & Morteani, G. (1982) - On the geochemical fractionation of rare earth elements during the formation of calcium minerals and its application to the problems of the genesis of ore deposits. In press.

Moller, P., Morteani, G., Hoefs, J. & Parekh, P.P. (1979) - The origin of the ore-bearing solution in the Pb-Zn veins of the western Harz, Germany as deduced from rare earth element and isotope distribution in calcites. Chem. Geol., 26, pp197-215.

Moller, P., Parekh, P.P. & Schneider, H.J. (1976) - Application of Tb/Ca-Tb/La abundance ratios to the problems of fluorspar genesis. Miner. Deposita, 11, pp111-116.

Montoya, J.W. & Hemley, J.J. (1975) - Activity relations and stabilities in alkali feldspar and mica alteration reactions. Econ. Geol., 70, pp577-594.

Moorbath, S. (1962) - Lead isotope abundance studies on mineral occurrences in the British Isles and their geologic significance. Proc. Roy. Soc. London, A254, pp295-360.

Moore, G.R. (1980) - A chemical and isotopic study of fluid inclusions from the Northern Pennine Orefield. Ph.D. thesis, University of Durham.

Morgan, J.W. & Wandless (1980) - Rare earth element distribution in some hydrothermal minerals: evidence of crystallographic control. Geochim. cosmochim. Acta, 44, pp973-980.

Mueller, G. (1951) - A genetical and geochemical survey of the Derbyshire mineral deposits. Ph.D thesis, University of London.

Mueller, G. (1954) - The distribution of coloured varieties of fluorite within the thermal zones of Derbyshire mineral deposits. Internat. Geol. Cong. 19th Algiers, 1952. Comptes rendus, sec 13, pt15, pp523-529.

Munoz, J.L & Luddington, S.D. (1974) - Fluoride-hydroxyl exchange in biotite. Am. Jour. Sci., 274, pp396-413.

Munoz, J.L. & Luddington, S.D. (1977) - Fluorine-hydroxyl exchange in synthetic muscovite and its application to muscovite-biotite assemblages. Am. Mineralogist, 62, pp304-308.

Nakamura, N. (1974) - Determination of REE, Ba, Fe, Mg, Na and K in carbonaceous and ordinary chondrites. Geochim. cosmochim. Acta, 38, pp757-775.

Nielsen, H. (1979) - Sulfur isotopes. In Lectures in isotope geology, Jager, E. & Hunziker, Jour. C., eds. Springer-Verlag, Berlin, pp283-312.

Nordstrom, D.K. & Jenne, E.A. (1977) - Fluorite solubility equilibria in selected geothermal waters. Geochim. cosmochim. Acta, 41, pp175-188.

Norman, D.I. & Landis, G.P. (1983) - Source of the mineralizing components in hydrothermal ore fluids as evidenced by 87Sr/86Sr and stable isotope data from the Pasto Bueno deposit, Peru. Econ. Geol., 78, pp451-465.

Ohmoto, H. & Lasaga, A.C. (1982) - Kinetics of reactions between aqueous sulphates and sulphides in hydrothermal systems. Geochim. cosmoschim. Acta, 46, pp1727-1745.

Ohmoto, H. & Rye, R.O. (1979) - Isotopes of sulfur and carbon. In Geochemistry of hydrothermal ore deposits, Barnes, H.L. ed., Wiley, New York, pp509-567.

Parekh, P.P., Moller, P., Dulski, P. & Bausch, W.M. (1977) - Distribution of trace elements between carbonate and non-carbonate phases of limestone. Earth Planet. Sci. Letters, 34, pp39-50.

Pecsok, R.L., Shields, L.D., Cairns, T. & McWilliam, J.G. (1976) Modern methods of chemical analysis. Wiley, New York, 2nd ed.

Pering, K.L. (1973) - Bitumens associated with lead, zinc, and fluorite ore minerals in North Derbyshire, England. Geochim. cosmochim. Acta, 37, pp401-417.

Peterman, Z.E., Hedge, C.E. & Tourtelot, H.A. (1970) - Isotopic composition of seawater throughout Phanerozoic time. Geochim. cosmochim. Acta, 34, pp105-120.

Postgate, J.R. (1979) - The sulphate reducing bacteria. Cambridge University Press, 151p.

Potter, R.W. (1977) - Pressure corrections for fluid inclusion homogenization temperatures based on the volumetric properties of the system NaCl-H_2O. U.S. Geol. Survey. Jour. Res., 5, pp603-608.

Potter, R.W. & Brown, D.L. (1977) - The volumetric properties of the aqueous sodium chloride solutions from 0°C to 500°C and pressures up to 2000bars based on regression of available data in the literature. U.S. Geol. Survey. Bull., 1421-C, 36p.

Potter, R.W., Clyne, M.A. & Brown, D.L. (1978) - Freezing point depression of aqueous sodium chloride solutions. Econ. Geol., 73, pp284-285.

Ramsbottom, W.H.C. (1969) - The Namurian of Britain. G. R. 6me Cong. Int. Strat. Geol. Carb., Sheffield, 1967, 1, pp219-232.

Richardson, C.K. & Holland, H.D. (1979a) - The solubility of fluorite in hydrotheramal solutions, an experimental study. Geochim. cosmochim. Acta, 43, pp1313-1325.

Richardson, C.K. & Holland, H.D. (1979b) - Fluorite deposition in hydrothermal systems. Geochim. cosmochim. Acta, 43, pp1327-1335.

Roberson, C.E. (1966) - Solubility implications of apatite in sea water. U.S. Geol. Surv. Prof. Paper, 550-D, D178-D185.

Roberts, W.M.B. (1973) - Dolomitization and the genesis of the Woodcutters lead-zinc prospect, Northern Territory, Australia. Miner. Deposita, 8, pp35-56.

Robinson, B.W. & Ineson, P.R. (1979) - Sulphur, oxygen and carbon isotope investigations of lead-zinc-barite-calcite mineralization, Derbyshire, England. Trans. Instn Min. Metall. (Sect. B., Appl. earth sci.), 88, B107-B117.

Roedder, E. (1962) - Studies of fluid inclusions. I. Low temperature application of a dual purpose freezing and heating stage. Econ. Geol., 57, pp1045-1061.

Roedder, E. (1963) - Studies of fluid inclusions. II. Freezing data and their interpretation. Econ. Geol., 58, pp167-210.

Roedder, E. (1967) - Metastable superheated ice in liquid-water inclusions under high negative pressure. Science, 155, pp1413-1417.

Roedder, E. (1967) - Environment of deposition of stratiform (Mississippi Valley-type) ore deposits, from studies of fluid inclusions. Econ. Geol. Monograph, 3, pp349-362

Roedder, E. (1971) - Fluid inclusion evidence on the environment of formation of mineral deposits of the Southern Appalachian Valley. Econ. Geol., 66, pp777-791.

Roedder, E. (1979) - Fluid inclusions as samples of ore fluids. In Geochemistry of hydrothermal ore deposits, H.L. Barnes, ed., Wiley, New York, pp684-737.

Roedder, E., Ingram, B. & Hall, W.E. (1963) - Studies of fluid inclusions III: Extraction and quantitative analysis of inclusions in the milligram range. Econ. Geol., 58, pp353-374.

Roedder, E. & Skinner, B.J. (1968) - Experimental evidence that fluid inclusions do not leak. Econ. Geol., 63, pp715-730.

Rogers, P.J. (1977) - Fluid inclusion studies in fluorite from the Derbyshire orefield. Trans. Instn Min. Metall., (Sect. B., Appl. earth sci.), 86, B128-B132.

Rundle, C.C. (1981) - Discussion on the age of mineralization at the Parys Mountain, Anglesey. Jour. geol. Soc. London, 138, pp755-756.

Russel, W.L. (1933) - Subsurface concentration of chloride brines. Bull. Am. Assoc. Petrol. Geol., 17, pp1213-1228.

Sawkins, F.J. (1966) - Ore genesis in the North Pennine orefield, in the light of fluid inclusion studies. Econ. Geol., 61, pp385-401.

Schnellmann, G.A. & Willson, J.D. (1947) - Lead-zinc mineralization in North Derbyshire. Trans. Instn Min. Metall., 56, pp599-585.

Scott, S.D. & Barnes, H.L. (1971) - Sphalerite geothermometry and geobarometry. Econ. Geol., 66, pp653-669.

Shepherd, T.J. (1981) - Temperature-programmable, heating-freezing stage for microthermometric analysis of fluid inclusions. Econ. Geol., 76, pp1244-1247.

Shepherd, T.J. ,Beckinsale, R.D., Rundle, C.C. & Durham, J. (1976) - Genesis of Carrock Fell tungsten deposits, Cumbria: A fluid inclusion and isotopic study. Trans. Instn Min. Metall.,(Sect. B., Appl. earth sci.), 85, B63-B73.

Shepherd, T.J., Darbyshire, D.P.F., Moore, G.R. & Greenwood, D.A. (1982) - Rare earth element and isotopic geochemistry of the North Pennine deposits. Bull. du B.R.G.M. 2, pp371-377.

Shirley, J. & Horsfield, E.L. (1945) - The structure and ore deposits of the Carboniferous Limestone of the Eyam district, Derbyshire. Q. Jl. geol. Soc. London., 100, pp289-310.

Shirley, J. (1949) - The stratigraphical distribution of the lead-zinc ores of the Millclose Mine and the future propects of the area. 18th Internat. Geol. Congr., London, pt 7, pp351-353.

Sholkovitz, E.R. (1978) - The flocculation of dissolved Fe, Mn, Al, Cu, Ni, Co and Cd during estuarine mixing. Earth planet. Sci. Letters, 41, pp77-86.

Sibson, R.H., Moore, J.McM. & Rankin, A.H. (1975) - Seismic pumping- a hydrothermal fluid transport mechanism. Jour. Geol. Soc. London., 131, pp639-659.

Siegel, S. (1956) - Nonparametric statistics for the behavioural sciences. McGraw-Hill, New York, 312p.

Siever, R. (1962) - Silica solubility, 0-200 deg C and the diagenesis of siliceous sediments. Jour. Geol., 70, pp127-150.

Sillen, L.G. & Martell, A.E. (1964 & 1971) - Stability constants for metal ion complexes. Chem. Soc. London, Spec. Publ no. 17 (1964), 25 (1971).

Skinner, B.J. (1967) - Precipitation of Mississippi Valley-type ores: a possible mechanism. Econ. Geol. Monograph, 3, pp363-370.

Skinner, B.J. & Barton, P.B. (1967) - Precipitation of Mississippi Valley-type ores: A possible mechanism. Econ. Geol., Monograph, 3, pp363-370.

Smith, E.G., Rhys, G.H. & Eden, R.A. (1967) - Geology of the country around Chesterfield, Matlock and Mansfield. Mem. Geol. Surv. G.B., 430p.

Smith, F.W. (1973) - Fluid inclusion studies in fluorite from the North Wales Orefield. Trans. Instn Min. Metall. (Sect. B., Appl. earth sci.), 82, B174-B176.

Smith, F.W. (1974) - Factors governing the development of fluorspar orebodies in the Northern Pennine Orefield. PhD thesis, University of Durham.

Spears, D.A. & Amin, M.A. (1981) - Geochemistry and mineralogy of marine and non-marine Namurian black shales from the Tansley borehole, Derbyshire. Sedimentology, 28, pp407-418.

Spink, K. & Ford, T.D. (1968) - The Coal Measures. In The geology of the East Midlands, Sylvester-Bradley, P.C. & Ford, T.D., ed., Leicester University Press, pp95-111.

Spooner, E.T.C. (1981) - Fluid inclusion studies of hydrothermal ore deposits. In Fluid inclusions: applications to petrology. Hollister, L.S. & Crawford, M.L., eds, Mineralog. Assoc. Canada, Short course handbook, 6, pp209-240.

Stevenson, I.P. & Gaunt, G.D. (1971) - Geology of the country around Chapel-en-le-frith. Mem. Geol. Surv. G.B., 443p.

Stevenson, I.P., Harrison, R.K. & Snelling, N.J. (1970) - Potassium-argon age determinations of the Waterswallows Sill, Buxton, Derbyshire. Proc. Yorks. Geol. Soc., 37, pp445-447.

Stauffer, R.E. (1982) - Fluorapatite and fluorite stability controls on geothermal waters in the Yellowstone National Park. Geochim. cosmochim. Acta, 46, pp465-475.

Sunwall, M.T. & Pushkar, P. (1979) - The isotopic composition of strontium in brines from petroleum fields of south east Ohio. Chem. Geol., 24, pp189-197.

Susak, N.J. & Crerar, D.A. (1982) - Factors controlling mineral zoning in hydrothermal ore deposits. Econ. Geol., 77, pp476-482.

Sverjensky, D.A. (1981) - The origin of a Mississippi Valley-type deposit in the Viburnum Trend, Southeast Missouri. Econ. Geol., 76, pp1848-1872.

Taylor, H.P. (1979) - Oxygen and hydrogen isotope relationships in hydrothermal mineral deposits. In Geochemistry of hydrothermal ore deposits, Barnes, H.L., ed., Wiley, New York, pp236-277.

Till, R. (1974) - Statistical methods for the earth scientist. Macmillan, London, 154p.

Toulmin, P. & Barton, P.B. (1964) - A thermodynamic study of pyrite and pyrrhotite. Geochim. cosmochim. Acta, 28, pp641-671.

Traill, J.G. (1939) - The geology and the development of the Millclose Mine, Derbyshire. Econ. Geol., 34, pp851-889.

Truesdell, A.H. & Jones, B.F. (1974) - WATEQ: a computer program for calculating chemical equilibria of natural waters. U.S. Geol. Survey Jour. Res., 2, pp233-248.

Veizer, J. & Compston, W. (1974) - 87Sr/86Sr composition of sea water during the Phanerozoic. Geochim. cosmochim. Acta, 38, pp1461-1484.

Vogel, A.I. (1947) - A text book of qualitative chemical analysis including semimicro qualitative analysis. Longmans, Green & Co, London, 3rd ed, 578p.

Walsh, J.N., Buckley, F. & Barker, J. (1981) - The simultaneous determination of the REE in rocks using inductively coupled plasma source spectrometry. Chem. Geol., 33, pp141-153.

Weast, R.C. (1980) - C.R.C. handbook of chemistry and physics, 60th edition, C.R.C. Press, Inc, Boca Raton, Florida.

Wedd, C.B. & Drabble, G.C. (1908) - The fluorspar deposits of Derbyshire. Trans. Instn Min. Engrs., 35, pp501-535.

Wedepohl, K.H. (1969-1974) Handbook of geochemistry. Springer-Verlag, Berlin.

Whitcombe, D.N. & Maguire, P.K.H. (1981) - Seismic refraction evidence for a basement ridge between the Derbyshire Dome and W. of Charnwood Forest. J. Geol. Soc. London, 138, pp653-659.

White, D.E., Hem, J.D. & Warring, G.A. (1963) - Chemical composition of subsurface waters. U.S. Geol. Surv. Prof. Paper, 440-F.

Whittaker, E.J.W. & Muntus, R. (1970) - Ionic radii for use in geochemistry. Geochim. cosmochim. Acta, 34, pp945-956.

Wilkins, R.W.T. & Bird, J.R. (1980) - Characterization of healed fracture surfaces in fluorite by etching and proton irradiation. Lithos, 13, pp11-18.

Worley, N.E. (1978) - Mineralisation in Derbyshire. Ph.D. Thesis, University of Leicester.

Worley, N.E. & Ford, T.D. (1977) - Mississippi Valley-type orefields in Britain. Bull. Peak Distict Mines Histerical Soc., 6, pp201-208.

Ziegler, P.A. (1981) - Evolution of sedimentary basins in North West Europe. In, Illings, L.V. & Hobson, G.D. ed., Conference on petroleum geology of the continental shelf of North West Europe. 2nd ed., London, pp3-39.

Zimmermann, R.K. & Kesler, S.E. (1981) - Fluid inclusion evidence for solution mixing, Sweetwater (Mississippi Valley-type) district, Tennessee. Econ. Geol., 76, pp134-142.

Rankin, A.H. (1980) - Tritolyl phosphate - a suitable immersion oil for fluid inclusion freezing stage studies. Mineral. Mag., 43, pp315-316.

Roedder, E. (1976) - Fluid inclusion evidence on the genesis of ores in sedimentary and volcanic rocks. In Handbook of stratabound and stratiform ore deposits. Wolf, K.H. ed., Elsevier, Amsterdam, 2, pp67-110.

APPENDIX 1

FLUID INCLUSION THERMOMETRIC DATA

1.1: STATISTICAL TESTS

1.1.1: USE OF PARAMETRIC AND NON-PARAMETRIC TESTS

A parametric statistical test is a test whose model specifies certain conditions about the parameters of the populations (Siegel, 1956). These are: (1) the observations must be independent of each other; (2) the observations must be drawn from a normally distributed population; (3) the populations must have the same variance (4) the variables must have been measured on an interval scale. Unless all these conditions are met, non-parametric tests are required. The non-parametric tests are slightly less powerful than their parametric counterparts. For example a Mann-Whitney U-test has a power-efficiency approaching 95.5%. This means that an appropriate parametric test could be as effective with a sample that was 5% smaller. Since the difference is small, the Mann-Whitney U-test forms a useful alternative to the t-test. The f-test may be used to initially test for the similarity in variance of two populations before the t-test or the Mann-Whitney U-test is applied. If the f-test fails at a 5% level of significance, the Mann-Whitney U-test must be used. All the tests used have been described by Davis (1973), Till (1974) and Siegel (1956). Short notes on the tests used are given below.

1.1.2: COEFFICIENT OF SKEWNESS

This was estimated using the expression:

$$Sk = \frac{\sum_{i=1}^{N} (X_i - \bar{X}_i)^3}{(N - 1) \cdot \sigma}$$

where N is the number of values, X_i is the ith value, $\bar{X}_i$ is

the mean and σ is the standard deviation. The coefficient of skewness and other elementary statistical data were calculated using the NAG library subroutine G01AAA/F.

1.1.3: CHI-SQUARE TEST

This was evaluated using the method given by Davis (1973). The standard normal curve was divided into 4 segments using the limit $-\infty$to -0.67, -0.67 to 0.0, 0.0 to 0.67, 0.67 to∞. This gives the test one degree of freedom. At a 5% level of significance, the critical value is 3.84. If the test statistic exceeds the critical value, the null hypothesis, that the population is normally distributed, may be rejected at the appropriate level of significance.

1.1.4: STUDENT'S t-TEST

The t-test was used to compare two sample populations. The MINITAB interactive statistics package was used to carry out the tests. Two groups of unequal size may be used and both a t-statistic and a the level of significance of the test is provided by the program. The applicability of the t-test was first evaluated by using the f-test. Critical values for the test may be found in Davis (1973).

1.1.5: MANN-WHITNEY U-TEST

This is the most powerful non-parametric test and it forms a useful alternative to the t-test when the X-square test and the f-test showed the test populations to either have non-normal distributions or differing variances. Both the NAG library subroutine G08ADF and the MINITAB interactive package are able to compute the U-statistic and the significance of the test.

1.2: HEATING/FREEZING DATA: PRECISION AND ACCURACY

The maximum resolution of the Linkam TH600 heating-freezing stage is 0.1°C in the temperature range -100°C to 200°C. Macdondald and Spooner (1981) reported the precision to lie in the range 0.3% to 0.7% between -100°C and 200°C. A general value for precison ($\pm 2\sigma$) is $\pm$0.2°C. Accuracy has been evaluated by determining the melting points of compounds recommended by Mcdonald and Spooner (1981), and a calibration curve for the heating stage has been presented in figures 2.1 and 2.2. In the temperature ranges where true melting temperature deviated from measured melting temperature, appropriate corrections were applied to the thermometric data.

Normally, more than ten measurements were made in order to determine representative homogenization temperature and final ice melting temperature means for a single sample. Appendix 1.3 does, however, occasionally contain measurements from a smaller number of inclusions in a single sample where the results were of interest but fluid inclusions were scarce.

APPENDIX 1.3

FLUID INCLUSION DATA: PAIRED HOMOGENIZATION-FINAL ICE MELTING TEMPERATURE DATA

TYPE 1 FLUID INCLUSIONS

WATERGROVE MINE SK190 758
Purple fluorite lining a cavity in silicified limestone.

130.8	-.6	130.7	0.0	137.4	-1.1
119.4	-.8	120.3	-.3	121.1	-.7
129.7	-.5	130.5	-.9	138.3	-1.0
120.5	-1.2	123.2	-.7	125.7	-1.0
128.4	-1.0	130.7	-1.2		

HOMOGENIZATION TEMPERATURES
NUMBER = 14: MEAN = 127.6: ST. DEV = 6.1: SKEWNESS = .198: CHI-STATISTIC = 4.9:

FINAL ICE MELTING TEMPERATURES
MEAN = -.8: ST. DEV = .3: SKEWNESS = .776: CHI-STATISTIC = .9:

Note: Later fluorite encrusted on the purple fluorite contains no type 1 inclusions but abundant type 3 and 4 fluid inclusions.

TREAK CLIFF CAVERN SK136 832
Purple fluorite lining cavities in limestone

129.1	-.1	129.8	-.1	154.3	-.5
158.9	-.5	149.3	-.2	137.9	-.8
137.5	-.3	141.4	-.3	145.8	-.7
145.9	-.3				

HOMOGENIZATION TEMPERATURES
NUMBER = 10: MEAN = 143.0: ST. DEV = 9.8: SKEWNESS = .059: CHI-STATISTIC = .4:

FINAL ICE MELTING TEMPERATURES
MEAN = -.4: ST. DEV = .2: SKEWNESS = -.478: CHI-STATISTIC = .4:

Note: All these inclusions are negative crystal types and appear to be primary.

TREAK CLIFF CAVERN SK136 832
Purple fluorite lining cavities in limestone

135.2	-.8	129.0	-1.1	139.3	-1.3
144.1	-1.2	139.1	-1.3	142.4	-1.3
119.4	-.3	139.6	-1.1	143.1	-1.1

HOMOGENIZATION TEMPERATURES
NUMBER = 9: MEAN = 136.8: ST. DEV = 8.0: SKEWNESS = *****: CHI-STATISTIC = 1.2:

FINAL ICE MELTING TEMPERATURES
MEAN = -1.1: ST. DEV = .3: SKEWNESS = 1.467: CHI-STATISTIC = 3.9:

Note: Types 2, 3, 4 and 5 inclusions are present in the purple fluorite.

PINDALE QUARRY SK1610 8231
Purple fluorite associated with later calcite, filling cavities and joint faces in limestone.

122.6	-3.5	135.9	-2.3	139.4	-3.6
123.2	-4.0	132.7	-5.3	138.9	-3.6
100.1	-2.2	105.	-4.		

HOMOGENIZATION TEMPERATURES
NUMBER = 8: MEAN = 124.8: ST. DEV = 15.1: SKEWNESS = -.604: CHI-STATISTIC = 1.0:

FINAL ICE MELTING TEMPERATURES
MEAN = -3.6: ST. DEV = 1.0: SKEWNESS = -.162: CHI-STATISTIC = 3.0:

ODIN MINE SK 1344 8343
Purple fluorite filling cavities and replacing limestone.

140.2	-2.5	150.5	-3.1	139.3	-4.2
154.2	-2.3	145.9	-5.6	156.0	-4.4
147.5	-2.9	134.4	-4.2	142.2	-3.4
144.0	-4.5	120.5	-6.0	132.1	-3.3

HOMOGENIZATION TEMPERATURES
NUMBER = 12: MEAN = 142.2: ST. DEV = 10.0: SKEWNESS = -.617: CHI-STATISTIC = 0.0:

FINAL ICE MELTING TEMPERATURES
MEAN = -3.9: ST. DEV = 1.2: SKEWNESS = -.427: CHI-STATISTIC = .7:

MOSS RAKE SK 144 801
Fluoritized limestone.

169.9	-6.6	160.8	-6.3	156.6	-5.5
154.0	-6.3	149.0	-4.9	164.1	-6.2
142.4	-4.8	165.4	-5.7	152.9	-5.3
164.0	-5.7	151.2	-6.3		

HOMOGENIZATION TEMPERATURES
NUMBER = 11: MEAN = 157.3: ST. DEV = 8.3: SKEWNESS = -.183: CHI-STATISTIC = 1.7:

FINAL ICE MELTING TEMPERATURES
MEAN = -5.8: ST. DEV = .6: SKEWNESS = .322: CHI-STATISTIC = 4.6:

TOP OF TREAK CLIFF SK 135 831
Purple fluorite in limestone with a later generation of white calcite.

145.4	-1.1	132.2	-.4	146.3	-1.3
139.8	-.9	144.2	-.3	145.5	-1.5
141.4	-1.0	146.9	-.9	141.5	-1.2
146.2	-1.4	147.3	-1.1		

HOMOGENIZATION TEMPERATURES
NUMBER = 11: MEAN = 143.3: ST. DEV = 4.5: SKEWNESS = *****: CHI-STATISTIC = 2.5:

FINAL ICE MELTING TEMPERATURES
MEAN = -1.0: ST. DEV = .4: SKEWNESS = .692: CHI-STATISTIC = .3:

GATEHAM GRANGE SK1144 5713
Purple fluorite filling cavities and joint faces in limestone with later calcite

136.3	-3.6	123.1	-4.9	120.3	-4.6
125.1	-4.3	131.9	-5.0	118.7	-3.5
120.2	-4.1	123.8	-4.7	124.3	-4.8
131.8	-1.5	140.3	-1.2	118.3	-3.5
119.2	-3.4				

HOMOGENIZATION TEMPERATURES
NUMBER = 13: MEAN = 125.6: ST. DEV = 7.2: SKEWNESS = .789: CHI-STATISTIC = 4.5:

FINAL ICE MELTING TEMPERATURES
MEAN = -3.8: ST. DEV = 1.2: SKEWNESS = 1.064: CHI-STATISTIC = 2.1:

WINDY KNOLL SK 1261 8299
Purple fluorite filling cavities and joint faces in limestone with associated hydrocarbons.

143.4	-1.8	160.8	-2.4	143.3	-5.2
159.6	-1.7	148.2	-5.0	138.2	-3.5
146.5	-5.1	143.2	-5.8	166.3	-2.2
128.2	-3.4				

HOMOGENIZATION TEMPERATURES
NUMBER = 10: MEAN = 147.8: ST. DEV = 11.5: SKEWNESS = .116: CHI-STATISTIC = 2.0:

FINAL ICE MELTING TEMPERATURES
MEAN = -3.6: ST. DEV = 1.6: SKEWNESS = -.089: CHI-STATISTIC = 4.4:

DIRTLOW RAKE (CASTLETON) SK 154 821
Purple fluorite crystals on silicified limestone vein wall.

121.1	-2.7	119.5	-2.5	118.Ø	-4.1
113.9	-3.5	124.3	-3.Ø	118.4	-1.7
123.2	-2.1	117.8	-1.8	119.5	-2.9

HOMOGENIZATION TEMPERATURES
NUMBER = 9: MEAN = 119.5: ST. DEV = 3.1: SKEWNESS = -.1Ø5: CHI-STATISTIC = 4.8:

FINAL ICE MELTING TEMPERATURES
MEAN = -2.7: ST. DEV = .8: SKEWNESS = -.345: CHI-STATISTIC = 1.2:

TYPE 2 FLUID INCLUSIONS (HOMOGENIZATION-FINAL ANTARCTICITE MELTING TEMPERATURE PAIRS)

SALLET HOLE MINE (SUB-LEVEL 1) SK2194 7408
Yellow fluorite, south wall of Deep Rake.

62.4	5.Ø	74.5	4.4	71.5	3.8
76.1	5.5	81.5	5.8	79.9	6.4
71.9	6.6	74.2	5.2		

HOMOGENIZATION TEMPERATURES
NUMBER = 8: MEAN = 74.Ø: ST. DEV = 5.9: SKEWNESS = -.671: CHI-STATISTIC =1.Ø

FINAL ANTARCTICITE MELTING TEMPERATURES
MEAN = 5.3: ST. DEV = 1.Ø: SKEWNESS = -.196: CHI-STATISTIC = Ø.Ø:

HOPE QUARRY (SMALLDALE PIPE) SK 162 816
Pale mauve fluorite

75.6	3.9	74.3	2.6	75.8	3.8
74.5	3.8	75.3	3.3	75.3	3.7
71.7	5.6	7Ø.5	2.1	75.Ø	4.5

HOMOGENIZATION TEMPERATURES
NUMBER = 9: MEAN = 74.2: ST. DEV = 1.9: SKEWNESS = -.113: CHI-STATISTIC = 5.7:

FINAL ANTARCTICITE MELTING TEMPERATURES
MEAN = 3.7: ST. DEV = 1.Ø: SKEWNESS = .226: CHI-STATISTIC = 2.1:

SMALLDALE QUARRY SK 162 814
Pale mauve or yellow fluorite

73.5	2.1	75.3	3.1	75.2	2.1
75.2	2.2	74.2	2.4	75.8	3.Ø
77.5	1.8	76.2	3.2	76.4	4.1
76.2	3.2	73.9	3.5		

HOMOGENIZATION TEMPERATURES
NUMBER = 11: MEAN = 75.4: ST. DEV = 1.2: SKEWNESS = -.Ø371: CHI-STATISTIC = 1.7:

FINAL ANTARCTICITE MELTING TEMPERATURES
MEAN = 2.8: ST. DEV = .7: SKEWNESS = .239: CHI-STATISTIC = 2.5:

MOOR FARM (OPENCAST QUARRY) SK 249 593
Idiomorphic cubes of purple fluorite in silicified and dolomitized limestone

75.4	2.4	77.9	2.2	74.Ø	3.Ø
75.6	3.Ø				

HOMOGENIZATION TEMPERATURES
NUMBER = 4: MEAN = 75.7: ST. DEV = 1.6: SKEWNESS = .4Ø5: CHI-STATISTIC = 2.Ø:

FINAL ANTARCTICITE MELTING TEMPERATURES
MEAN = 2.7: ST. DEV = .4: SKEWNESS = -.1Ø: CHI-STATISTIC = 2.Ø:

MURPHY'S HOLE, TREAK CLIFF CAVERN SK 136 832
Purple fluorite, paragenetically post-dating purple fluorite containing type 1 and type 2 fluid inclusions.

79.5	72.4	75.1	81.2	76.3
77.8	76.3	78.2	75.2	71.3
77.1	77.1	71.3		

HOMOGENIZATION TEMPERATURES
NUMBER = 13: MEAN = 76.1: ST. DEV = 3.Ø: SKEWNESS = -.223: CHI-STATISTIC = 1.5:

TYPE 3 FLUID INCLUSIONS

EAKRING BOREHOLE NO. 146. SK 6807 5945
Colourless fluorite chippings form Dinantian strata at 80lm below o.d.

86.3	-22.2	97.9	-20.6	88.7	-23.5
93.7	-23.5	84.6	-22.4	87.0	-22.4
90.1	-22.0	88.1	-22.1	97.1	-22.6
95.1	-22.5	98.9	-25.0	94.1	-22.1
82.3	-21.5	83.4	-22.2	97.4	-20.2
95.6	-20.4				

HOMOGENIZATION TEMPERATURES
NUMBER = 16: MEAN = 91.3: ST. DEV = 5.6: SKEWNESS = -.159: CHI-STATISTIC = 2.5:

FINAL ICE MELTING TEMPERATURES
MEAN = -22.2: ST. DEV = 1.2: SKEWNESS = -.309: CHI-STATISTIC = 1.5:

Note: type 4 inclusions are also present.

BLACK OX SHAFT, MASSON HILL SK 288 588
Pale purple fluorite containing inclusions of doubly terminated quartz crystals.

91.3	-23.6	91.8	-23.4	88.8	-24.3
88.7	-23.7	92.1	-23.5	92.5	-23.4
91.6	-22.9	91.3	-22.7	92.1	-22.6
90.2	-25.0	97.0	-22.6		

HOMOGENIZATION TEMPERATURES
NUMBER = 11: MEAN = 91.6: ST. DEV = 2.2: SKEWNESS = 1.036: CHI-STATISTIC = 3.2:

FINAL ICE MELTING TEMPERATURES
MEAN = -23.4: ST. DEV = .7: SKEWNESS = -.711: CHI-STATISTIC = 1.0:

Note: type 4 inclusions are also present.

FAUCET RAKE SK 1373 8223
Yellow fluorite associated with baryte and containing inclusions of quartz and sulphides.

85.6	-21.9	84.2	-21.3	83.4	-21.4
83.6	-21.8	89.0	-21.1	84.6	-21.6
85.9	-21.9	77.7	-21.6		

HOMOGENIZATION TEMPERATURES
NUMBER = 8: MEAN = 84.3: ST. DEV = 3.2: SKEWNESS = -.737: CHI-STATISTIC = 2.0:

FINAL ICE MELTING TEMPERATURES
MEAN = -21.6: ST. DEV = .3: SKEWNESS = .307: CHI-STATISTIC = 1.0:

Note: type 4 inclusions abundant.

LEADMINES FARM, ELTON (OPENCAST SITE) SK 2260 6034
Yellow fluorite containing bravoite, chalcopyrite and pyrite inclusions.

79.3	-22.9	83.5	-23.5	89.5	-23.5
91.4	-24.9	76.4	-24.5	90.2	-24.7
95.4	-24.3	82.8	-24.8	85.8	-24.1
95.8	-25.3	97.5	-25.0		

HOMOGENIZATION TEMPERATURES
NUMBER = 11: MEAN = 88.0: ST. DEV = 7.0: SKEWNESS = -.182: CHI-STATISTIC = .3:

FINAL ICE MELTING TEMPERATURES
MEAN = -24.3: ST. DEV = .7: SKEWNESS = .558: CHI-STATISTIC = .3:

Note: a small number of type 4 inclusions were observed.

MOOR FARM, BLAKELOW HILL (OPENCAST SITE) SK 249 593
Early purple, idiomorphic crystals of fluorite replacing dolomitized and silicified wall rock

8Ø.5	-24.Ø	83.9	-24.Ø	86.3	-22.9
89.9	-23.2	83.Ø	-23.8	81.3	-22.1
77.8	-23.Ø	86.1	-23.4		

HOMOGENIZATION TEMPERATURES
NUMBER = 8: MEAN = 83.6: ST. DEV = 3.8: SKEWNESS = .149: CHI-STATISTIC = Ø.Ø:

FINAL ICE MELTING TEMPERATURES
MEAN = -23.3: ST. DEV = .6: SKEWNESS = .529: CHI-STATISTIC = 2.Ø:

Note: type 2 inclusions abundant but no type 4 inclusions observed.

BALL EYE QUARRY (OPENCAST SITE) SK 287 574
Clear fluorite containing quartz and sulphide inclusions.

81.2	-21.9	72.2	-21.3	72.3	-21.Ø
81.2	-23.1	83.3	-22.3	84.6	-22.7
81.4	-21.3	85.9	-21.9	9Ø.1	-21.2
78.3	-22.3	79.9	-23.1		

HOMOGENIZATION TEMPERATURES
NUMBER = 11: MEAN = 8Ø.9: ST. DEV = 5.4: SKEWNESS = -.25Ø: CHI-STATISTIC = 1.Ø:

FINAL ICE MELTING TEMPERATURES
MEAN = -22.Ø: ST. DEV = .8: SKEWNESS = -.162: CHI-STATISTIC = 1.Ø:

Note: type 4 inclusions abundant.

LADYWASH MINE (NORTH CROSSCUT) SK 219 776
Large fluorite cubes containing doubly terminated quartz crystals and bravoite inclusions.

84.5	-24.5	88.2	-24.3	8Ø.Ø	-23.7
81.7	-24.7	89.8	-25.6	85.5	-26.Ø
88.6	-25.9	88.1	-25.4	84.9	-25.3
88.2	-25.4				

HOMOGENIZATION TEMPERATURES
NUMBER = 1Ø: MEAN = 86.Ø: ST. DEV = 3.2: SKEWNESS = -.6Ø9: CHI-STATISTIC = 2.Ø:

FINAL ICE MELTING TEMPERATURES
MEAN = -25.1: ST. DEV = .7: SKEWNESS = .479: CHI-STATISTIC = 1.2:

Type 2 incluions present in fluorite close to the wall rock.

CRICH CLIFF QUARRY SK 3430 5544
Colourless fluorite in 4cm wide scrin, close to the Foresters' Monument.

84.7	-26.Ø	9Ø.2	-25.7	86.3	-25.Ø
82.2	-25.Ø	85.5	-23.5	97.4	-24.5
8Ø.6	-2Ø.Ø	79.5	-25.1	83.4	-24.7
96.2	-24.7	98.5	-22.7		

HOMOGENIZATION TEMPERATURES
NUMBER = 11: MEAN = 87.7: ST. DEV = 6.9: SKEWNESS = .5Ø4: CHI-STATISTIC = 1.7:

FINAL ICE MELTING TEMPERATURES
MEAN = -24.3: ST. DEV = 1.7: SKEWNESS = 1.496: CHI-STATISTIC = 5.4:

Note: type 4 inclusions present.

MIXON MINES, STAFFORDSHIRE SK Ø454 5734
Cubes of colourless fluorite on joint faces in limestone.

88.4	-25.2	88.7	-24.8	85.1	-25.Ø
88.4	-25.3	77.7	-2Ø.9	87.9	-24.5
74.6	-24.Ø	88.7	-23.8	88.Ø	-24.5

HOMOGENIZATION TEMPERATURES
NUMBER = 1Ø: MEAN = 85.8: ST. DEV = 5.3: SKEWNESS = *****: CHI-STATISTIC = 6.8:

FINAL ICE MELTING TEMPERATURES
MEAN = -24.3: ST. DEV = 1.3: SKEWNESS = 1.9Ø6: CHI-STATISTIC = 3.6:

TEMPLE MINE SK 2926 5806
Yellow fluorite cubes filling cavities in limestone.

81.8	-22.9	88.7	-22.8	84.0	-22.2
87.4	-21.9	90.8	-22.6	82.6	-22.9
87.6	-22.8	85.6	-22.7	80.4	-23.5
82.0	-22.2	85.2	-22.1		

HOMOGENIZATION TEMPERATURES
NUMBER = 11: MEAN = 85.1: ST. DEV = 3.3: SKEWNESS = .208: CHI-STATISTIC = 2.5:

FINAL ICE MELTING TEMPERATURES
MEAN = -22.6: ST. DEV = .5: SKEWNESS = -.206: CHI-STATISTIC = 4.6:
Note: type 4 inclusions abundant.

CHROME HILL (LONGNOR) SK 0710 6710
Pale purple fluorite cubes filling cavities in reef limestone.

71.0	-22.5	81.5	-23.0	72.2	-21.7
77.8	-21.6	79.8	-22.5	79.3	-22.5
79.5	-20.9	78.5	-21.9	83.1	-22.0
80.9	-23.0	74.7	-21.2	73.6	-22.3
75.4	-21.1				

HOMOGENIZATION TEMPERATURES
NUMBER = 13: MEAN = 77.5: ST. DEV = 3.8: SKEWNESS = -.312: CHI-STATISTIC = 2.7:

FINAL ICE MELTING TEMPERATURES
MEAN = -22.0: ST. DEV = .7: SKEWNESS = .132: CHI-STATISTIC = 2.7:

BLENDE VEIN, MAGPIE MINE SK 172 682
Pale purple fluorite filling cavities in silicified limestone.

78.8	-23.0	75.5	-22.9	81.1	-22.3
74.4	-23.6	79.0	-23.3	69.6	-21.9
82.9	-22.3	80.3	-22.8	75.3	-22.2
71.7	-21.9	77.2	-23.1	87.5	-22.1
69.6	-22.9				

HOMOGENIZATION TEMPERATURES
NUMBER = 13: MEAN = 76.8: ST. DEV = 5.4: SKEWNESS = .331: CHI-STATISTIC = .2:

FINAL ICE MELTING TEMPERATURES
MEAN = -22.6: ST. DEV = .6: SKEWNESS = -.119: CHI-STATISTIC = .8:

Note: a small number of type 4 inclusions observed.

TEARSALL QUARRY (OPENCAST SITE) SK 2630 5750
Yellow and colourless fluorite filling cavities and replacing silicified and dolomitized wall rocks. Abundant silica and sulphides present within the fluorite.

75.3	-22.7	80.6	-22.6	81.4	-22.4
79.0	-22.0	81.2	-22.1	68.6	-22.0
76.9	-22.7	80.2	-22.2	84.5	-23.7
84.6	-22.8	84.4	-22.5	84.1	-21.4
80.3	-21.4	87.2	-22.2		

HOMOGENIZATION TEMPERATURES
NUMBER = 14: MEAN = 80.5: ST. DEV = 4.6: SKEWNESS = *****: CHI-STATISTIC = .9:

FINAL ICE MELTING TEMPERATURES
MEAN = -22.3: ST. DEV = .6: SKEWNESS = -.386: CHI-STATISTIC = 2.6:

Note: type 3 inclusions tentatively identified as primary but type 4 inclusions abundant.

LADYWASH MINE (BROADLOW DECLINE) SK 219 776
Clear, glassy fluorite with inclusions of pyrite,bravoite and quartz.

90.7	-24.3	72.5	-25.0	78.3	-24.8
84.3	-24.5	87.1	-24.2	93.8	-24.3
72.2	-23.0	88.1	-24.0	84.3	-21.2
89.3	-22.4	92.6	-21.5	89.9	-22.0
83.3	-22.5				

HOMOGENIZATION TEMPERATURES
NUMBER = 13: MEAN = 85.1: ST. DEV = 7.0: SKEWNESS = -.721: CHI-STATISTIC = .2:

FINAL ICE MELTING TEMPERATURES
MEAN = -23.4: ST. DEV = 1.3: SKEWNESS = .342: CHI-STATISTIC = 2.1:

Note: a small number of type 4 inclusions observed.

GREAT RAKE (MILLTOWN QUARRY) SK 3528 6208
Colourless fluorite with inclusions of galena, bravoite, chalcopyrite and pyrite.

64.9	-24.8	67.0	-24.9	82.2	-24.7
85.2	-24.9	89.8	-24.9	81.3	-24.9
91.1	-20.4	93.4	-20.4	83.0	-24.1

HOMOGENIZATION TEMPERTURES
NUMBER = 9: MEAN = 82.0: ST. DEV = 10.0: SKEWNESS = -.697: CHI-STATISTIC = 1.2:

FINAL ICE MELTING TEMPERATURES
MEAN = -23.8: ST. DEV = 1.9: SKEWNESS = 1.206: CHI-STATISTIC = 14.6:

MILLDAM MINE, GREAT HUCKLOW SK 176 700
Yellow fluorite containing inclusions of galena.

84.5	-24.5	77.3	-20.7	85.7	-24.3
90.8	-24.3	80.2	-24.2	82.5	-24.3
77.0	-23.6	75.8	-22.8	89.0	-24.2
90.3	-25.0				

HOMOGENIZATION TEMPERATURES
NUMBER = 10: MEAN = 83.3: ST. DEV = 5.6: SKEWNESS = .024: CHI-STATISTIC = .4:

FINAL ICE MELTING TEMPERATURES
MEAN = -23.8: ST. DEV = 1.2: SKEWNESS = 1.655: CHI-STATISTIC = 6.8:

Note: a small number of type 4 inclusions observed.

MOOR FARM, BLAKELOW HILL (OPENCAST SITE) SK 2490 5930
Late, glassy yellow fluorite cubes filling cavities in dolomitized and silicified limestones.

89.6	-23.0	91.4	-21.7	89.8	-22.7
91.7	-23.1	85.8	-22.8	91.7	-21.7
92.9	-22.0	86.8	-22.0	88.0	-22.2
95.7	-22.8	84.0	-22.2	92.0	-22.3
94.1	-22.5	91.4	-23.3	86.1	-22.3
81.8	-21.2				

HOMOGENIZATION TEMPERATURES
NUMBER = 16: MEAN = 89.6: ST. DEV = 3.8: SKEWNESS = -.411: CHI-STATISTIC = 5.0:

FINAL ICE MELTING TEMPERATURES
MEAN = -22.4: ST. DEV = .6: SKEWNESS = .202: CHI-STATISTIC = 2.5:

Note: type 4 inclusions abundant.

WAPPING MINE SK 293 575
Pale purple fluorite, veined by later baryte and clearly pre-dating glassy yellow fluorite.

77.0	-22.2	72.3	-21.5	82.4	-21.6
80.5	-23.0	87.0	-22.1	84.2	-21.7
87.7	-22.8	81.5	-21.6	76.9	-22.2
77.9	-22.3	76.5	-22.0	78.3	-21.9
88.4	-22.3				

HOMOGENIZATION TEMPERATURES
NUMBER = 13: MEAN = 80.8: ST. DEV = 4.9: SKEWNESS = .130: CHI-STATISTIC = .8:

FINAL ICE MELTING TEMPERATURES
MEAN = -22.1: ST. DEV = .5: SKEWNESS = -.543: CHI-STATISTIC = 2.1:

Note: type 4 inclusions abundant.

WATERGROVE MINE, FOOLOW SK 190 758
Glassy cubes of pale purple fluorite paragenetically post-dating purple type 1 fluorite.

83.3	-22.8	83.5	-22.8	87.1	-21.9
78.3	-22.5	80.9	-23.5	75.2	-21.6
85.6	-24.0	86.2	-22.2	77.9	-20.4
80.5	-22.1				

HOMOGENIZATION TEMPERATURES
NUMBER = 10: MEAN = 81.9: ST. DEV = 4.0: SKEWNESS = -.210: CHI-STATISTIC = .4:

FINAL ICE MELTING TEMPERATURES
MEAN = -22.4: ST. DEV = 1.0: SKEWNESS = .280: CHI-STATISTIC = .4:

Note: type 4 inclusions abundant.

BACON CLOSE VEIN, YOULGREAVE SK 2175 6390
Yellow fluorite with sulphide inclusions.

73.5	-21.8	80.5	-23.0	67.2	-22.1
79.4	-21.9	83.1	-22.5	78.9	-22.4
81.8	-21.9	67.4	-21.1	74.6	-21.6
84.0	-21.7	81.8	-22.4		

HOMOGENIZATION TEMPERATURES
NUMBER = 11: MEAN = 77.5: ST. DEV = 6.0: SKEWNESS = -.718: CHI-STATISTIC = 1.7:

FINAL ICE MELTING TEMPERATURES
MEAN = -22.0: ST. DEV = .5: SKEWNESS = -.094: CHI-STATISTIC = 2.5:

TYPE 4 FLUID INCLUSIONS

BACON CLOSE VEIN, YOULGREAVE SK 2175 6390
Yellow fluorite.

77.5	-15.8	78.0	-15.7	79.0	-18.1
80.3	-15.9	79.6	-16.3	72.9	-16.3
80.7	-15.9	73.3	-16.2		

HOMOGENIZATION TEMPERATURES
NUMBER = 8: MEAN = 77.7: ST. DEV = 3.0: SKEWNESS = -.704: CHI-STATISTIC = 1.0:

FINAL ICE MELTING TEMPERATURES
MEAN = -17.1: ST. DEV = .7: SKEWNESS = -.060: CHI-STATISTIC = 3.3:

BALL EYE QUARRY SK 2882 5742
Yellow fluorite in scrin in dolomitized wall rock.

87.4	-18.2	86.0	-17.4	87.5	-16.3
76.0	-17.2	85.1	-17.3	82.6	-16.2

HOMOGENIZATION TEMPERATURES
NUMBER = 6: MEAN = 84.1: ST. DEV = 4.4: SKEWNESS = *****: CHI-STATISTIC = .7:

FINAL ICE MELTING TEMPERATURES
MEAN = -17.1: ST. DEV = .7: SKEWNESS = -.060: CHI-STATISTIC = 3.3:

CRICH CLIFF QUARRY SK 3430 5544
Colourless fluorite in 4cm wide scrin, close to the Foresters' monument.

93.8	-19.2	80.6	-19.8	84.3	-19.8
87.0	-19.7	88.9	-18.1	86.3	-18.5
81.8	-17.0	86.6	-18.8	87.4	-19.0

HOMOGENIZATION TEMPERATURES
NUMBER = 9: MEAN = 86.3: ST. DEV = 3.9: SKEWNESS = .331: CHI-STATISTIC = 2.1:

FINAL ICE MELTING TEMPERATURES
MEAN = -18.9: ST. DEV = .9: SKEWNESS = .800: CHI-STATISTIC = .3:

FALL HILL QUARRY SK 3538 6242
Massive colourless fluorite with solid inclusions of pyrite, chalcopyrite, and bravoite.

75.2	-17.9	85.8	-17.8	81.9	-18.9
74.4	-17.6	82.2	-17.3	77.1	-17.7
79.8	-17.5	83.8	-17.7	92.4	-17.2
87.3	-18.8	78.1	-18.1	79.5	-18.3
82.0	-17.9	85.8	-17.8		

HOMOGENIZATION TEMPERATURES
NUMBER = 14: MEAN = 81.8: ST. DEV = 5.0: SKEWNESS = .386: CHI-STATISTIC = .9:

FINAL ICE MELTING TEMPERATURES
MEAN = -17.9: ST. DEV = .5: SKEWNESS = -.754: CHI-STATISTIC = .9:

Note: type 3 inclusions also present.

EARL RAKE SK 1550 7983
Clear, colourless fluorite in cavities and metasomatically replacing limestone.

93.2	-19.5	84.8	-17.3	90.5	-17.9
79.5	-17.9	82.0	-18.1	75.2	-17.4
83.5	-17.2	82.8	-17.8	87.4	-18.3
79.4	-17.2				

HOMOGENIZATION TEMPERATURES
NUMBER = 10: MEAN = 83.8: ST. DEV = 5.4: SKEWNESS = .244: CHI-STATISTIC = .4:

FINAL ICE MELTING TEMPERATURES
MEAN = -17.9: ST. DEV = .7: SKEWNESS = *****: CHI-STATISTIC = 2.0:

RIBER MINE SK 2990 5875
Yellow fluorite filling cavities in silicified wall rocks. Inclusions of sphalerite and galena are incorporated into the fluorite.

84.6	-18.5	84.9	-18.4	85.5	-18.4
86.2	-18.2	91.1	-17.0	90.5	-16.5
83.3	-17.4	93.1	-18.3	86.7	-17.5
86.2	-18.7	85.4	-17.7	86.5	-17.9
84.2	-18.2				

HOMOGENIZATION TEMPERATURES
NUMBER = 13: MEAN = 86.8: ST. DEV = 2.9: SKEWNESS = .988: CHI-STATISTIC = 7.6:

FINAL ICE MELTING TEMPERATURES
MEAN = -17.9: ST. DEV = .6: SKEWNESS = .783: CHI-STATISTIC = .8:

MASSON HILL (OPENCAST SITE) SK 2860 5910
Yellow fluorite cubes with inclusions of chalcopyrite, pyrite and bravoite.

82.9	-16.9	84.1	-17.9	83.6	-17.0
83.3	-17.9	81.3	-17.5	81.4	-17.1
82.6	-17.5	82.9	-16.5	83.4	-16.0
85.1	-17.4	85.6	-17.7	84.5	-17.2
80.0	-15.5	86.3	-16.7		

HOMOGENIZATION TEMPERATURES
NUMBER = 14: MEAN = 83.4: ST. DEV = 1.7: SKEWNESS = -.158: CHI-STATISTIC = .3:

FINAL ICE MELTING TEMPERATURES
MEAN = -17.1: ST. DEV = .7: SKEWNESS = .784: CHI-STATISTIC = .9:

Note: 3 type 3 inclusions were tentatively identified as being primary in the sample.

WATERBANK MINE (ECTON) SK 1030 5735
Yellow glassy fluorite with inclusions of sphalerite and galena.

80.8	-16.6	82.3	-16.3	72.9	-16.1
74.2	-17.6	75.3	-16.6	77.0	-16.3
79.6	-17.6	79.7	-16.3	77.3	-17.0
78.2	-17.0	76.4	-16.9	79.1	-16.4
76.9	-16.4				

HOMOGENIZATION TEMPERATURES
NUMBER = 13: MEAN = 77.7: ST. DEV = 2.7: SKEWNESS = -.079: CHI-STATISTIC = .8:

FINAL ICE MELTING TEMPERATURES
MEAN = -16.7: ST. DEV = .5: SKEWNESS = -.748: CHI-STATISTIC = .8:

Note: type 3 inclusions observed in the sample.

LONGSTONE EDGE (OPENCAST SITE) SK 1858 7316
Pale yellow fluorite with sulphide inclusions.

83.2	-18.5	89.9	-17.5	83.2	-17.2
87.3	-17.2	80.4	-17.6	88.0	-18.9
80.6	-17.7	92.8	-17.3	82.7	-17.2
86.5	-17.2				

HOMOGENIZATION TEMPERATURES
NUMBER = 10: MEAN = 85.5: ST. DEV = 4.1: SKEWNESS = .351: CHI-STATISTIC = .4:

FINAL ICE MELTING TEMPERATURES
MEAN = -17.6: ST. DEV = .6: SKEWNESS = *****: CHI-STATISTIC = 2.0:

OLD MILLCLOSE MINE SK 258 618
Glassy yellow fluorite filling open cavities in silicified wall rocks.

83.6	-15.8	85.2	-16.6	84.0	-16.2
77.5	-15.4	80.0	-16.0	87.3	-16.4
77.9	-16.2	82.6	-17.1	85.0	-15.9
83.5	-15.4	84.2	-17.0	83.0	-16.9

HOMOGENIZATION TEMPERATURES
NUMBER = 12: MEAN = 82.9: ST. DEV = 3.0: SKEWNESS = -.563: CHI-STATISTIC = 2.7:

FINAL ICE MELTING TEMPERATURES
MEAN = -16.2: ST. DEV = .6: SKEWNESS = -.033: CHI-STATISTIC = .7:

ROYAL MINE SK 291 581
Glassy, colourless "bevel edged" fluorite filling cavities in limestone.

75.3	-18.2	85.8	-17.0	81.7	-18.5
86.1	-17.5	86.0	-17.4	91.3	-17.8
88.3	-17.5	87.7	-18.1	85.4	-17.4
80.4	-18.1	88.1	-17.7	83.0	-16.7

HOMOGENIZATION TEMPERATURES
NUMBER = 12: MEAN = 84.9: ST. DEV = 4.3: SKEWNESS = -.783: CHI-STATISTIC = 2.7:

FINAL ICE MELTING TEMPERATURES
MEAN = -17.7: ST. DEV = .5: SKEWNESS = .182: CHI-STATISTIC = 1.3:

Note: some type 3 inclusions were also observed.

JINGLER MINE (WAKEBRIDGE) SK 3398 5540
Colourless and purple fluorite with both sulphide and quartz inclusions.

82.0	-18.3	91.8	-18.2	92.9	-18.2
86.2	-18.5	93.6	-18.0	81.1	-18.4
82.6	-18.1	88.1	-18.7	81.5	-18.9
77.1	-17.9	81.3	-17.9		

HOMOGENIZATION TEMPERATURES
NUMBER = 11: MEAN = 85.3: ST. DEV = 5.6: SKEWNESS = .298: CHI-STATISTIC = 1.0:

FINAL ICE MELTING TEMPERATURES
MEAN = -18.3: ST. DEV = .3: SKEWNESS = -.541: CHI-STATISTIC = .3:

Note: type 4 inclusions tentatively identified as being primary.

TEMPLE MINE SK 2926 5806
Glassy, clear yellow fluorite lining cavities in limestone.

76.2	-17.1	87.8	-16.4	82.9	-15.9
82.6	-16.2	82.7	-18.8	92.1	-17.8
76.8	-16.8	86.2	-17.6	84.4	-17.4
92.9	-18.3				

HOMOGENIZATION TEMPERATURES
NUMBER = 10: MEAN = 84.5: ST. DEV = 5.6: SKEWNESS = .039: CHI-STATISTIC = 1.2:

FINAL ICE MELTING TEMPERATURES
MEAN = -17.2: ST. DEV = .9: SKEWNESS = -.170: CHI-STATISTIC = .4:

NEW ENGINE MINE SK 224 774
Clear glassy fluorite.

87.6	-17.6	87.4	-18.1	87.5	-17.3

HOMOGENIZATION TEMPERATURES
NUMBER = 3: MEAN = 87.5: ST. DEV = .1: SKEWNESS = 0.000: CHI-STATISTIC = 1.0:

FINAL ICE MELTING TEMPERATURES
MEAN = -17.7: ST. DEV = .4: SKEWNESS = -.241: CHI-STATISTIC = 1.0:

BROADLOW MINE SK 2069 7728
Yellow fluorite.

76.9	-15.9	74.7	-16.3	73.6	-16.6
77.2	-17.2				

HOMOGENIZATION TEMPERATURES
NUMBER = 4: MEAN = 75.6: ST. DEV = 1.7: SKEWNESS = -.155: CHI-STATISTIC = 2.0:

FINAL ICE MELTING TEMPERATURES
MEAN = -16.5: ST. DEV = .5: SKEWNESS = -.243: CHI-STATISTIC = 0.0:

PICTOR PIPE SK 1745 8011
Yellow fluorite cubes with sulphide inclusions.

90.7	-17.9	73.1	-18.9	88.4	-17.8
89.3	-17.9	85.9	-17.9	88.2	-18.0
81.7	-18.8	87.0	-18.2	93.1	-17.5
86.1	-17.5				

HOMOGENIZATION TEMPERATURES
NUMBER = 10: MEAN = 86.4: ST. DEV = 5.6: SKEWNESS = *****: CHI-STATISTIC = 1.2:

FINAL ICE MELTING TEMPERATURES
MEAN = -18.0: ST. DEV = .5: SKEWNESS = -.762: CHI-STATISTIC = 3.6:

EAKRING BOREHOLE (NO 146) SK 68075 59450
Chippings from 801m below ordnance datum level.

105.6	-17.0	98.2	-17.9	94.7	-18.9
95.2	-18.3	89.2	-17.0	106.2	-18.9
98.8	-17.9	85.1	-18.3	92.0	-18.0
91.8	-18.4	89.2	-17.9	91.3	-18.2
93.3	-17.6	90.8	-18.4		

HOMOGENIZATION TEMPERATURES
NUMBER = 14: MEAN = 94.4: ST. DEV = 6.1: SKEWNESS = .699: CHI-STATISTIC = .9:

FINAL ICE MELTING TEMPERATURES
MEAN = -18.1: ST. DEV = .6: SKEWNESS = .430: CHI-STATISTIC = 1.4:

FAUCET RAKE SK 1373 8223
Yellow fluorite with included sulphides and silica.

90.2	-18.5	91.2	-18.7	84.4	-17.4
88.6	-15.9	90.4	-17.8	83.2	-16.8
82.9	-16.5	84.3	-16.8	89.4	-16.3
81.8	-16.7	87.0	-16.7		

HOMOGENIZATION TEMPERATURES
NUMBER = 11: MEAN = 86.7: ST. DEV = 3.4: SKEWNESS = -.050: CHI-STATISTIC = 5.4:

FINAL ICE MELTING TEMPERATURES
MEAN = -17.1: ST. DEV = .9: SKEWNESS = -.634: CHI-STATISTIC = 3.2:

MOOR FARM (OPENCAST SITE) SK 249 593
Yellow fluorite filling cavities in dolomitized, fluoritized and silicified wall rocks.

78.2	-15.7	81.5	-15.6	82.1	-16.5
85.8	-18.0	82.3	-16.4	82.8	-16.3
81.5	-17.1	82.5	-17.1	84.4	-17.8
80.3	-17.4				

HOMOGENIZATION TEMPERATURES
NUMBER = 10: MEAN = 82.1: ST. DEV = 2.1: SKEWNESS = -.087: CHI-STATISTIC = .4:

FINAL ICE MELTING TEMPERATURES
MEAN = -16.8: ST. DEV = .8: SKEWNESS = .018: CHI-STATISTIC = .4:

WAPPING MINE SK 293 575
Pale purple fluorite, crosscut by narrow veins of pink baryte.

89.5	-16.4	87.1	-17.5	86.0	-18.6
85.7	-18.3	87.7	-17.9	82.4	-17.0

HOMOGENIZATION TEMPERATURES
NUMBER = 6: MEAN = 86.4: ST. DEV = 2.4: SKEWNESS = -.473: CHI-STATISTIC = .7:

FINAL ICE MELTING TEMPERATURES
MEAN = -17.6: ST. DEV = .8: SKEWNESS = .267: CHI-STATISTIC = .7:

WATERGROVE MINE SK 190 758
Purple fluorite crystals filling open cavity.

88.7	-16.0	90.5	-17.2	80.4	-18.0
90.2	-18.1	83.9	-16.5	87.6	-16.8
74.4	-18.4	83.3	-19.2	76.8	-17.0
77.8	-18.0				

HOMOGENIZATION TEMPERATURES
NUMBER = 10: MEAN = 83.4: ST. DEV = 5.8: SKEWNESS = -.160: CHI-STATISTIC = 2.0:

FINAL ICE MELTING TEMPERATURES
MEAN = -17.5: ST. DEV = 1.0: SKEWNESS = -.085: CHI-STATISTIC = .4:

OVERTON HALL MINE SK346 622
Clear, bevel edged fluorite covering an earlier generation of fluorite containing abundant bravoite inclusions.

91.8	-18.3	89.2	-17.8	91.3	-18.1
90.8	-18.3	93.	-18.		

HOMOGENIZATION TEMPERATURES
NUMBER = 5: MEAN = 91.3: ST. DEV = 1.5: SKEWNESS = -.055: CHI-STATISTIC = .6:

FINAL ICE MELTING TEMPERATURES
MEAN = -18.0: ST. DEV = .3: SKEWNESS = .469: CHI-STATISTIC = .6:

Note: the earlier material contains both type 3 and type 4 fluid inclusions.

THERMOMETRIC DATA FOR SALLET HOLE MINE

SALLET HOLE MINE SK 2194 7408 (ADIT ENTRANCE)
HIGH RAKE, NORTH WALL.

72.4	-23.8	80.3	-22.9	73.6	-22.4
73.4	-23.5	79.5	-23.3	80.6	-22.5
82.5	-22.2	77.7	-23.0	72.8	-22.9
82.0	-24.6				

HOMOGENIZATION TEMPERATURES
NUMBER = 11: MEAN = 78.1: ST. DEV. = 4.3: SKEWNESS = -.143: CHI-STATISTIC = 1.0:

FINAL ICE MELTING TEMPERATURES
MEAN = -23.1: ST. DEV = .7: SKEWNESS = .838: CHI-STATISTIC = 2.9:

HIGH RAKE, CENTRAL VEIN

86.3	-22.9	71.4	-22.3	78.5	-22.8
77.4	-23.0	84.0	-23.3	80.2	-22.9
72.5	-22.4	77.9	-23.3	84.4	-22.6
82.7	-24.2	75.2	-22.9	77.8	-22.9
85.5	-23.1	76.9	-23.2	74.5	-22.3

HOMOGENIZATION TEMPERATURES
NUMBER = 15: MEAN = 79.0: ST. DEV = 4.7: SKEWNESS = .076: CHI-STATISTIC = 2.9:

FINAL ICE MELTING TEMPERATURES
MEAN = -22.9: ST. DEV = 0.5: SKEWNESS = -.911: CHI-STATISTIC = 0.7:

HIGH RAKE, SOUTH WALL

72.5	-22.7	79.1	-22.4	75.2	-23.2
83.2	-23.3	76.5	-22.4		

HOMOGENIZATION TEMPERATURES
NUMBER = 5: MEAN = 77.3: ST. DEV = 4.1: SKEWNESS = .338: CHI-STATISTIC = 0.6:

FINAL ICE MELTING TEMPERATURES
MEAN = -22.8: ST. DEV = .4: SKEWNESS = -.189: CHI-STATISTIC = 2.2:

HIGH RAKE, SOUTH WALL

84.7	-18.4	79.4	-17.8	75.7	-17.6
85.2	-18.0	75.9	-17.7	82.8	-17.6
82.8	-16.8	79.3	-17.4	82.7	-17.2
77.5	-17.4	70.3	-17.3	81.7	-17.0

HOMOGENIZATION TEMPERATURES
NUMBER = 12: MEAN = 79.8: ST. DEV = 4.4: SKEWNESS = -.712: CHI-STATISTIC = .7:

FINAL ICE MELTING TEMPERATURES
MEAN = -17.5: ST. DEV = .4: SKEWNESS = -.307: CHI-STATISTIC = .7:

DEEP RAKE, SUB-LEVEL 2, SOUTH WALL

87.2	-18.2	81.3	-18.0	82.3	-18.4
88.5	-18.6	83.4	-17.9	83.6	-17.2
82.3	-17.7	83.6	-17.6	85.1	-17.8
88.4	-17.5	82.7	-17.4	87.8	-17.5

HOMOGENIZATION TEMPERATURES
NUMBER = 12: MEAN = 84.7: ST. DEV = 2.6: SKEWNESS = .380: CHI-STATISTIC = 2.0:

FINAL ICE MELTING TEMPERATURES
MEAN = -17.8: ST. DEV = .4: SKEWNESS = -.436: CHI-STATISTIC = .7:

DEEP RAKE,SUB-LEVEL 2, 2M FROM THE SOUTH WALL

70.0	-23.0	84.1	-22.2	71.0	-22.6
85.1	-22.6	85.1	-23.9	89.7	-22.9
84.3	-22.9	81.7	-22.9		

HOMOGENIZATION TEMPERATURES
NUMBER = 8: MEAN = 81.4: ST. DEV = 7.1: SKEWNESS = -.752: CHI-STATISTIC = 7.0:

FINAL ICE MELTING TEMPERATURES
MEAN = -22.9: ST. DEV = .5: SKEWNESS = -.891: CHI-STATISTIC = 3.0:

DEEP RAKE, SUB-LEVEL 2, 2M FROM THE SOUTH WALL

81.6	-17.8	73.7	-17.4	78.0	-17.9
69.8	-18.8	69.3	-18.3		

HOMOGENIZATION TEMPERATURES
NUMBER = 5: MEAN = 74.5: ST. DEV = 5.3: SKEWNESS = .273: CHI-STATISTIC = .6:

FINAL ICE MELTING TEMPERATURES
MEAN = -18.0: ST. DEV = .5: SKEWNESS = -.295: CHI-STATISTIC = .6:

DEEP RAKE, SUB-LEVEL 2, 2.2M FROM THE SOUTH WALL

85.4	-17.5	73.4	-19.2	88.7	-17.4
85.3	-18.0	87.2	-18.0		

HOMOGENIZATION TEMPERATURES
NUMBER = 5: MEAN = 84.0: ST. DEV = 6.1: SKEWNESS = *****: CHI-STATISTIC = 3.8:

FINAL ICE MELTING TEMPERATURES
MEAN = -18.0: ST. DEV = .7: SKEWNESS = -.863: CHI-STATISTIC = 2.2:

DEEP RAKE, SUB-LEVEL 2, 1M FROM THE NORTH WALL

83.5	-17.7	84.4	-18.5	85.0	-18.1
90.3	-19.3	84.5	-18.3	84.5	-18.1
81.7	-17.0	74.2	-18.8	85.7	-17.6
75.0	-18.6				

HOMOGENIZATION TEMPERATURES
NUMBER = 10: MEAN = 82.9: ST. DEV = 4.9: SKEWNESS = -.662: CHI-STATISTIC = 6.8:

FINAL ICE MELTING TEMPERATURES
MEAN = -18.2: ST. DEV = .7: SKEWNESS = .168: CHI-STATISTIC = .4:

DEEP RAKE, SUBLEVEL 2, 0.5M FROM THE NORTH WALL

67.6	-19.7	75.5	-18.8	84.5	-17.6
71.2	-18.3	76.7	-18.1	83.9	-17.5
82.7	-18.4	82.9	-17.7	81.4	-18.7

HOMOGENIZATION TEMPERATURES
NUMBER = 9: MEAN = 78.5: ST. DEV = 6.1: SKEWNESS = -.642: CHI-STATISTIC = 2.1:

FINAL ICE MELTING TEMPERATURES
MEAN = -18.3: ST. DEV = .7: SKEWNESS = -.631: CHI-STATISTIC = .3:

DEEP RAKE, SUB-LEVEL 2, 2.5M FROM THE NORTH WALL

81.5	-17.1	77.4	-17.5	84.1	-17.3
85.9	-17.2	85.4	-17.9	63.4	-17.3
85.8	-18.0	81.1	-17.7	81.2	-17.3
82.4	-17.2				

HOMOGENIZATION TEMPERATURES
NUMBER = 10: MEAN = 80.8: ST. DEV = 6.7: SKEWNESS = *****: CHI-STATISTIC = 4.4:

FINAL ICE MELTING TEMPERATURES
MEAN = -17.5: ST. DEV = .3: SKEWNESS = -.681: CHI-STATISTIC = 1.2:

DEEP RAKE, SUB-LEVEL 1, SOUTH WALL

62.4	5.0	81.5	5.8	74.5	4.4
79.9	6.4	71.5	3.8	71.9	6.6
76.1	5.5	74.2	5.2		

HOMOGENIZATION TEMPERATURES
NUMBER = 8: MEAN = 74.0: ST. DEV = 5.9: SKEWNESS = -.671: CHI-STATISTIC = 1.0:

FINAL ICE MELTING TEMPERATURES
MEAN = 5.3: ST. DEV = 1.0: SKEWNESS = -.196: CHI-STATISTIC = 0.0:

DEEP RAKE, SUB-LEVEL 1, 0.5-1M FROM THE SOUTH WALL

83.8	-17.1	80.8	-17.3	83.4	-17.1
83.0	-18.3	84.0	-16.2	83.5	-18.2
85.6	-18.0	81.5	-17.6	81.4	-17.9
83.0	-17.5	82.7	-17.2		

HOMOGENIZATION TEMPERATURES
NUMBER = 11: MEAN = 83.0: ST. DEV = 1.4: SKEWNESS = .105: CHI-STATISTIC = 3.2:

FINAL ICE MELTING TEMPERATURES
MEAN = -17.5: ST. DEV = .6: SKEWNESS = .542: CHI-STATISTIC = 2.5:

DEEP RAKE, SUB-LEVEL 1, 1-3M FROM THE SOUTH WALL

83.8	-16.7	81.3	-17.6	84.6	-17.9
81.4	-17.8	85.9	-16.7	83.9	-17.5
70.4	-19.9	84.5	-17.5	83.2	-17.6
81.8	-17.6	86.0	-17.6	82.2	-17.3
87.4	-17.9	87.6	-16.8		

HOMOGENIZATION TEMPERATURES
NUMBER = 14: MEAN = 83.1: ST. DEV = 4.2: SKEWNESS = *****: CHI-STATISTIC = 3.7:

FINAL ICE MELTING TEMPERATURES
MEAN = -17.6: ST. DEV = .8: SKEWNESS = *****: CHI-STATISTIC = 5.4:

APPENDIX 2

ANALYSIS OF FLUID INCLUSIONS

2.1: FLUID INCLUSION LEACHING PROCEEDURE

A standard method of leaching has been outlined by Roedder et al., 1963, but the proceedure they suggested has been modified for this study. Samples used for analysis had been examined for their fluid inclusion type content, although few samples were found which contained only one fluid inclusion type. Clean, fresh samples were used which appeared to contain little included material. They were crushed in a pestle and mortar until all the fragments passed through a 5mm sieve but were contained wihin a 1mm sieve. The sample (40g) was then washed in distilled and then distilled and deionized water. The final washing (30ml) was taken to represent a blank sample for the leaching proceedure, and was stored within an acid cleaned polythene container. Cleaning in acid was used for some runs but the acid was found to move into fractures within the fluorite and produce erroneously high calcium concentrations in the leachates, despite prolonged washing of the sample in deionized water. Electrolytic cleaning of the sample was considered unnecessary.

The sample was then dried at 100°C in a PTFE dish and then crushed using a mechanical agate pestle and mortar. The powder so produced was placed in 100ml PTFE beaker and magnetically stirred for 60 minutes with 40ml of distilled and deionized water. The vessel was covered to avoid loss of calcium through precipitation by atmospheric carbon dioxide. The solution was allowed to settle and the leachate was decanted into a pyrex centrifuge tube. The fluid was centrifuged (4000rpm) for 10-15 minutes, and then decanted into another centrifuge tube. Any residue was washed back into the leaching vessel. The leachate was centrifuged a second time and then placed in a acid cleaned polythene sample bottle. This process was repeated four times, using

deionized water (30ml) for leaching. As a result of the removal of some water in wetting the powder on the fisrt run, all the samples contained approximately 30ml of leachate. Rubber gloves were warn to prevent sodium contamination and all containers were washed with hydrochloric acid and deionized water.

2.2: CHEMICAL ANALYSIS OF FLUID INCLUSION LEACHATES

Sodium and potassium concentrations were determined using a flame photometer and calcium and magnesium concentrations were analysed by atomic absorption.

2.2.1: ATOMIC ABSORPTION SPECTROSCOPY

The instrument used was a Perkin Elmer 360 atomic absorption spectrophotometer. A hollow cathode calcium-magnesium lamp provided the radiation source. Atomization was effected by an air-acetylene flame. A slit width of 0.7nm was used for both elements and the wavelengths used to measure absorption were 422.7nm (calcium) and 285.2nm (magnesium). The detection limits are 0.001ppm and 0.0003ppm for the two elements respectively (Pecsok et al., 1976). Distilled and deionized water was used as a blank. Fresh standards were prepared for each run from 1000ppm standard solutions. The linear range for calcium is 0-10ppm and for magnesium, 0-5ppm. If the concentration of calcium in the fluid fell in the range 10-100ppm, the true concentrations were calculated directly by the instrument using Beer's law. If the concentration exceeded 100ppm, the leachates were diluted

and re-analysed. Concentrations were measured over an integration period of five seconds.

2.2.2: FLAME PHOTOMETRY

The instrument used was an Evans Electroselenium, Model A, flame photometer. Atomization was effected by an air-methane flame. Appropriate filters were selected for sodium and potassim analysis. The detection limit was found to be Ø.Ø6ppm for potassium and Ø.Ø5ppm for sodium. A mixed 5ppm sodium and 6ppm potassium standard produced a full galvanometer deflection for both elements. This corresponds to their linear ranges. Leachate concentrations in excess of these were diluted and re-analysed. More than $1cm^3$ of fluid was volatized to produce a constant reading. The effect of calcium interfering with the measured concentrations of potassium and sodium was investigated, but no significant interference was detected.

2.3: ESTIMATION OF CATION RATIOS

On analysis of the leachates it was found that potassium and sodium move into solution with greater ease than calcium and magnesium (figure A.1). Therefore, any sodium/calcium ratio for a specific leachate will not represent the true ratio. To overcome this problem leachates were taken until the calcium concentration had reached or fallen below the saturation value for fluorite (14ppm). This usually occurred after five runs. The values were then corrected for the blank, and the sum of the leachate concentrations calculated. The cation ratios produced from the summed concentrations appeared to give reasonably reproducable analyses, given the limited sample control. The sums of the leachate analyses are shown for samples containing types 2, 3 and 4 fluid inclusions (table A.1).

Figure A.1

The diagram illustrates the relative retardation of the alkaline earth chlorides with respect to the alkali metal chlorides during the fluid inclusion leaching process.

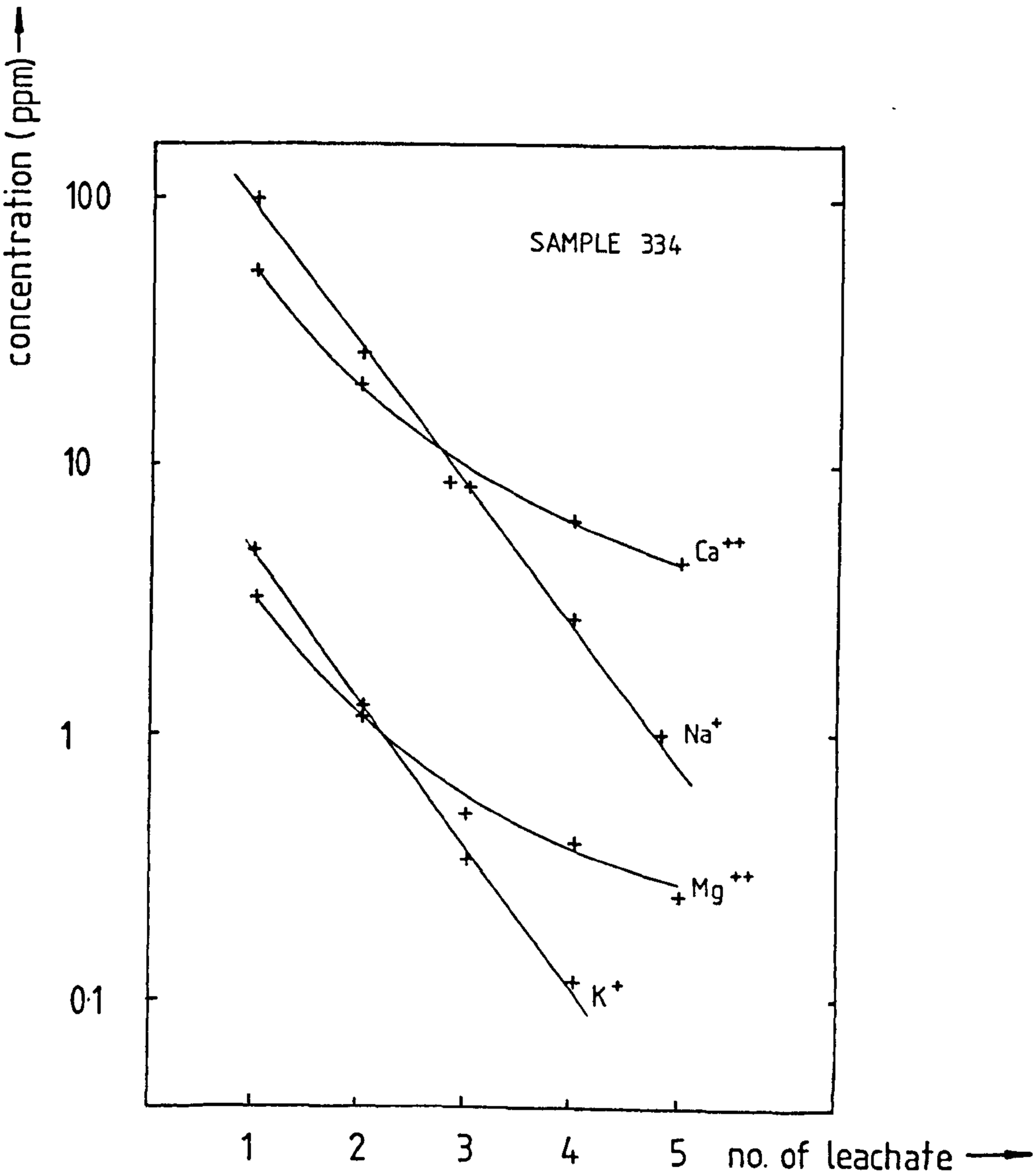

TABLE A.1

LEACHATE ANALYSES (TOTALS IN PPM)

Type	No.	Na	Mg	Ca	K	Na/K	Ca/Na	Na/Mg
2	346a	2.79	Ø.Ø22	14Ø.5	Ø.Ø98	28.5	5Ø.	127.
2	346b	4.72	Ø.Ø27	25Ø.2	Ø.143	33.	53.	175
2	56a	1Ø.15	Ø.185	66.4	Ø.555	18.	6.5	55.
2	3Ø3	7.34	Ø.Ø25	62.5	Ø.1Ø9	64.	8.5	294.
3	236	18.35	Ø.268	3Ø.1	Ø.378	48.5	1.64	68.5
3	236b	18.72	Ø.26Ø	22.7	Ø.24Ø	48.7	1.21	72.
3	92	15.2	Ø.216	3Ø.2	Ø.24	63.6	2.Ø	71.
3	341	22.1	Ø.44Ø	1Ø.3	Ø.57	39.	Ø.45	5Ø.
3	112	17.92	Ø.248	17.3	Ø.24	75.	Ø.78	72.
3	334	28.54	1.142	18.5	1.368	21.	Ø.65	25.
4	17Øa	11.83	Ø.1Ø2	74.6	Ø.289	4Ø.	6.5	112.
4	17Øb	11.84	Ø.Ø77	93.4	Ø.252	47.	7.9	154.
4	265	Ø.64	Ø.498	6.98	Ø.Ø96	6.7	1Ø.9	1.3?
4	34Ø	9.2Ø	Ø.142	3Ø.3	Ø.46Ø	2Ø.	3.3	65.
4	56b	8.45	Ø.154	25.8	Ø.693	12.2	3.1	55.

KEY TO SAMLE NUMBERS

SAMPLE NUMBER	LOCALITY
346a&b	Treak Cliff Cavern (Murphy's Hole)
56a&b&3Ø3	Smalldale Quarry (West)
236	White Rake
341&34Ø	Hope Quarry
112	Earl Rake
334	Deep Rake (Black Dale Wood)
17Ø	Fall Hill Quarry
265	Royal Mine
9Ø	Ladywash Mine

APPENDIX 3

ELECTRON PROBE MICROANALYSIS

3.1 CONCENTRATIONS OF IRON AND CADMIUM IN SPHALERITE

Analyses of iron and cadmium in sphalerite were performed using a Cambridge Microscan 5 electron probe microanalyser. The machine was operated using an accelerating potential of 15kV with a constant specimen current. The analyses were performed using the wavelength dispersive system. Counting time for peaks and backgrounds were 60 seconds each. Counts from the two spectrometers were directly fed into an on line Link computer where the data was processed using the Magic IV program. Concentrations were calculated assuming a stoichiometric formula for sphalerite. Pure metal cadmium and iron standards were used.

3.2: PRECISION OF IRON AND CADMIUM ANALYSES

Precison for iron (2σ) fell in the range 170-200ppm and for cadmium 300-500ppm. The analyses are shown in table A.2.

TABLE A.2

Sphalerite in... calcite (Ecton)		calcite (Blende Vein)		calcite (Earl Rake)	
Fe (ppm)	Cd (ppm)	Fe (ppm)	Cd (ppm)	Fe (ppm)	Cd (ppm)
480.0	5900.0	410.0	11600.0	600.0	5600.0
470.0	8200.0	8400.0	630.0	630.0	11300.0
570.0	7800.0	380.0	7600.0	930.0	6200.0
590.0	12300.0	770.0	6700.0	1500.0	9600.0
450.0	10300.0	430.0	6400.0	730.0	10400.0
370.0	5100.0	600.0	5400.0	1200.0	9400.0
300.0	6100.0	420.0	7700.0	550.0	7400.0
430.0	4200.0	500.0	11400.0	380.0	5800.0
450.0	4800.0	430.0	9900.0	910.0	1120.0

Sphalerite inclusions in..... fluorite (Ladywash Mine)		fluorite (Riber Mine)	
Fe (ppm)	Cd (ppm)	Fe (ppm)	Cd (ppm)
940.0	7000.0	300.0	7500.0
900.0	13100.0	400.0	11700.0
680.0	2400.0	590.0	6900.0
640.0	3100.0	470.0	7800.0
560.0	3300.0	400.0	10200.0
750.0	5700.0	700.0	8300.0
930.0	2500.0	720.0	12600.0
750.0	11800.0	570.0	8900.0
760.0	7200.0	510.0	8900.0
870.0	8000.0	770.0	8600.0

APPENDIX 4

ANALYSIS OF YTTRIUM, ZIRCONIUM, AND STRONTIUM IN FLUORITE BY X-RAY FLUORESCENCE SPECTROMETRY

4.1 ANALYTICAL METHODS

Clean, glassy fluorite samples (100g) were coarsely crushed in a pestle and mortar and then reduced to a fine powder in an agate tema disc mill. Fifteen grams of the powder was used to produce a pressed disc, suitable for analysis. Y, Zr and Sr were analyzed using a rhodium anode X-ray tube on a Philips PW 1400 automatic spectrometer. The count data was processed by an on-line Philips P851 computer. Analysis was carried out at 70kV and 40mA. K_α lines were used with a Zr K_α count corrected for Sr K_β overlap. A lithium fluoride crystal (220) with a fine collimator and a scintillation detector was used with a pulse weight window of 25%-70%. First order corrections and differences in mass adsorption coefficients were corrected using the rhodium-compton scatter peak.

The standard addition method of calibration was used. An accurately weighed blank fluorite sample was spiked with known quantities of $SrCO_3$, Y_2O_3 and ZrO_2. The sample was mixed in a ball mill and a powder pellet made with part of the standard. Another part was weighed diluted with more of the blank fluorite and a second standard was produced. Three standards and a blank in all were used for calibration.

Concentrations are based on the average of two counts. Concentrations of Sr, Y and Zr in ppm are shown in table A.3 Precison (2o) for Sr at 100ppm (4%), Y at 10ppm (35%) and Zr at 10ppm (30%).

The analyses were made in order to attempt to use trace element geochemistry to distinguish fluorite formed in

the four mineralizing events. A plot of strontium against yttrium (figure A.2) shows the type 1 fluorite to contain generally higher concentrations of both trace elements than the other fluorite types. Similarly a plot of zirconium against yttrium (figure A.2) shows zirconium to be present at higher concentrations in the type 1 fluorite when compared to the other fluorite types.

TABLE A.3

LOCALITY	INCLUSION TYPE	SR	Y	ZR
Treak Cliff	1	92	38	4
Treak Cliff	1	105	27	6
Ladywash Mine	3	142	11	4
Royal Mine	4	56	12	3
Masson opencast	3	67	11	1
Treak Cliff	2	48	7	4
Smalldale Quarry	2?	113	5	5
Hope Quarry	2?	88	-	6
Earl Rake	-	53	-	4
Ladywash Mine	3	237	-	12
Winnats Pass(SK134828)	1	69	19	4
Moor Farm (opencast)	-	45	6	4
New Engine Mine	-	27	-	34
Moss Rake (SK13838026)	-	183	8	3
Moss Rake (SK144801)	-	42	4	2
Tearsall Quarry	-	-	-	27
Tideslow Rake	-	134	13	6
Dirtlow Rake(Sheldon)	-	249	-	11
Nestus Mine	3	53	7	2
Ricklow Quarry	1?	100	22	10
Treak Cliff	1	72	16	17
Ball Eye Quarry	3	55	17	3
Deep Rake	3	168	-	43
Deep Rake	3	90	6	6
Riber Mine	4?	34	-	35
Overton Hall Mine	4	60	-	3
Ladywash Mine (Hucklow Edge Vein)		130	8	6
Pindale Quarry	3?	50	-	4
Crich Cliff Vein		67	8	4
Jingler Mine	4?	54	13	2
Winnats (Fibrous)	1	106	17	6
Deep Rake, 3rd sublevel		124	14	4
Smalldale Quarry	2?	291	10	5
Fall Hill Quarry	4?	86	-	7
Fall Hill Quarry	4?	283	8	14

Figure A.2

PLOT OF ZIRCONIUM AGAINST YTTRIUM IN FLUORITE

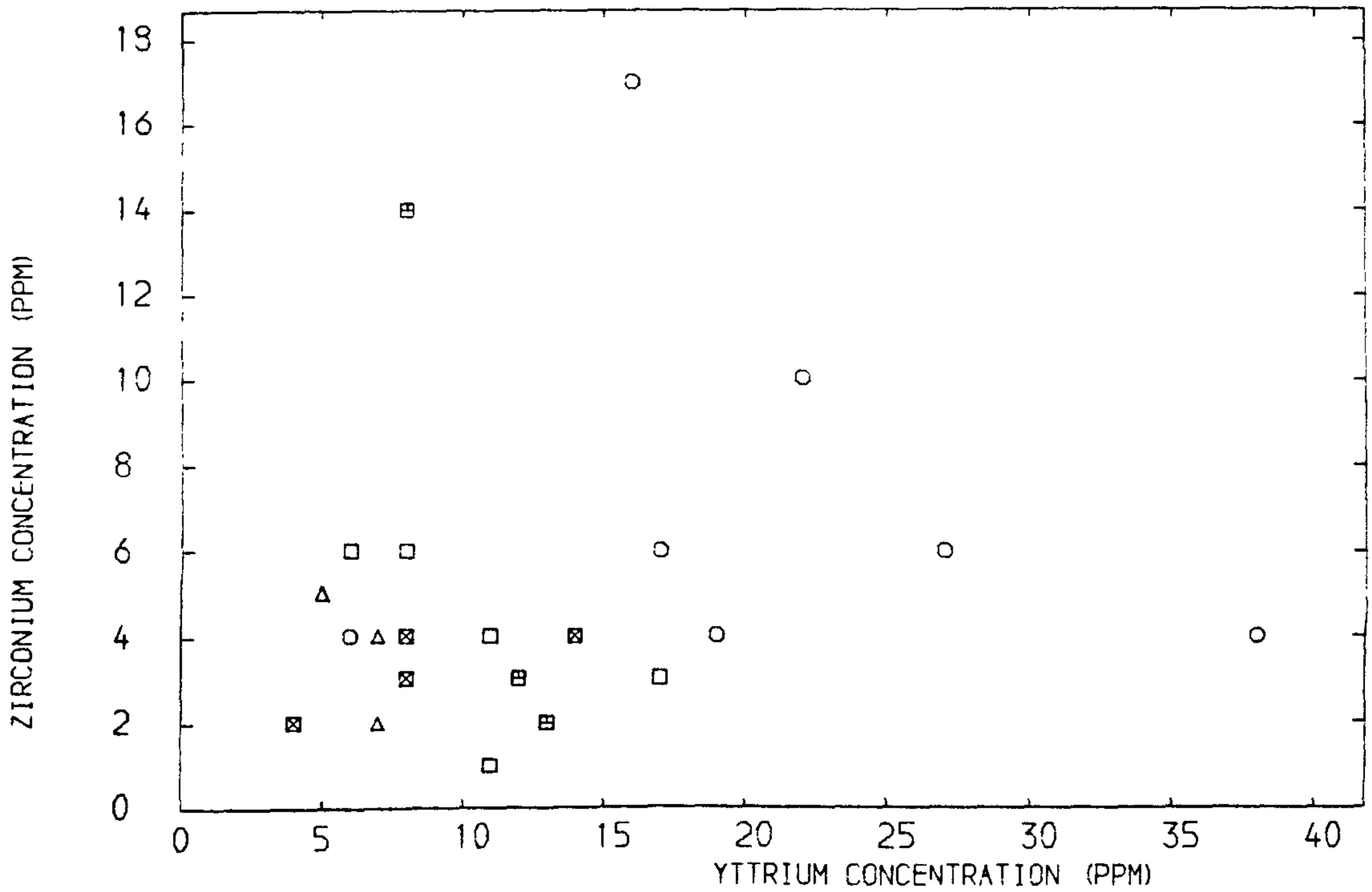

FLUID INCLUSION TYPES

TYPE 1 o. TYPE 2 Δ. TYPE 3 □
TYPE 4 ⊞. UNDEFINED ⊠

PLOT OF STRONTIUM AGAINST YTTRIUM

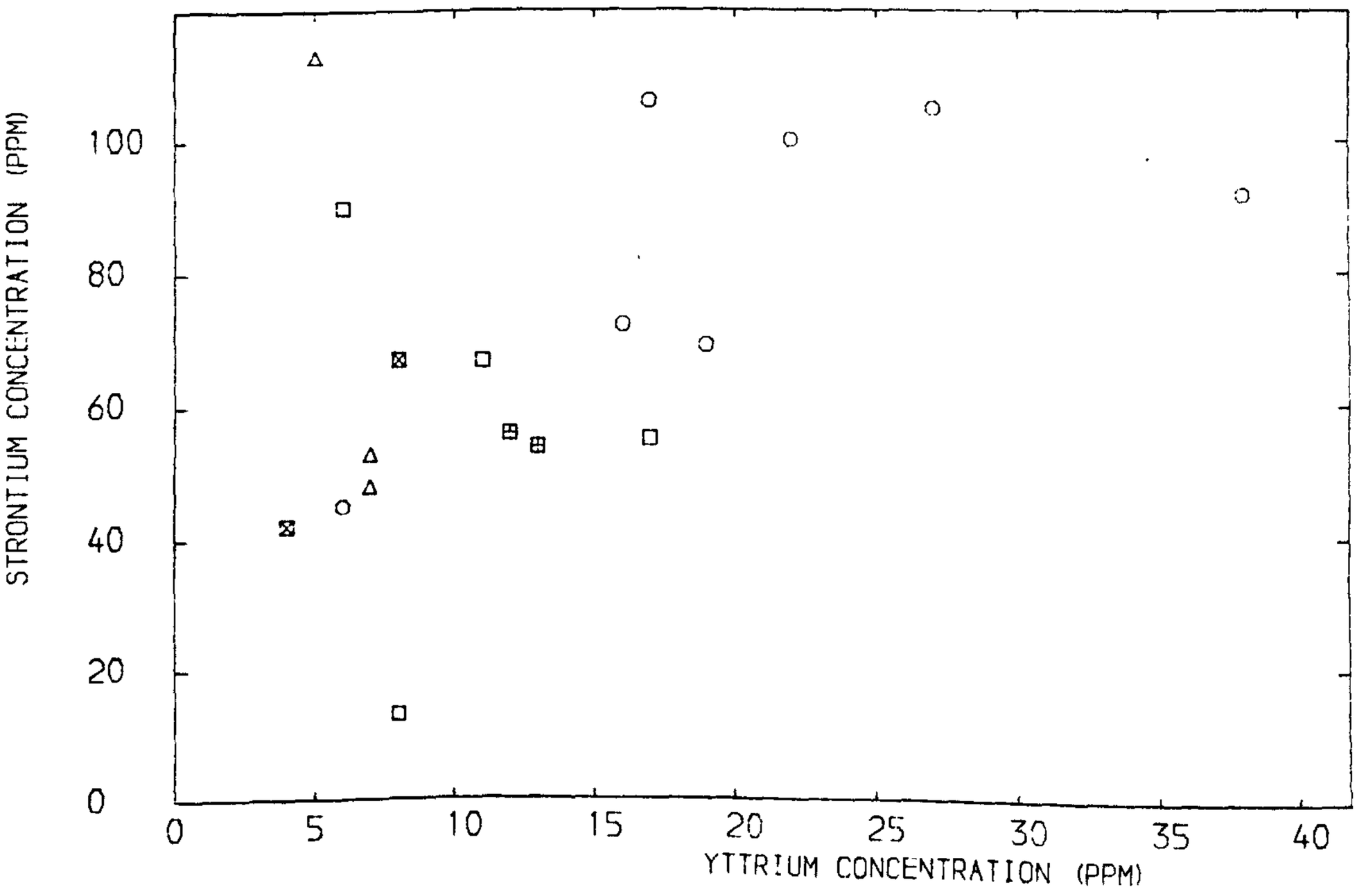

FLUID INCLUSION TYPES

TYPE 1 o. TYPE 2 Δ. TYPE 3 □
TYPE 4 ⊞. UNDEFINED ⊠

APPENDIX 5

CALCULATING ACTIVITY COEFFICIENTS

5.1: ACTIVITY COEFFICIENTS FOR THE TYPE 3 FLUID

Individual ion activity coeficients calculated by Sverjensky (1981) for an ore fluid similar in composition to the phase 3 ore fluid (2.8m NaCl, 0.64m $CaCl_2$) were used for calculations involving the phase 3 brines. Activity coefficients used for the type 3 fluid are shown below.

ION	INDIVIDUAL ION ACTIVITY COEFFICIENT		
Temperature	50°C	100°C	150°C
CO_3^{--} , Pb^{++}	0.14	0.05	0.02
Ca^{++} , Zn^{++}	0.23	0.07	0.02
K^+ Cl^-	0.88	0.80	0.65
Na^+ , HCO_3^-	0.90	0.82	0.67

Stoichiometric ionic strength = 4.7.

5.2: ACTIVITY COEFFICIENTS FOR THE TYPE 4 FLUID

For the phase 4 fluids, the equation of Helgeson (1969) was used. The size parameters ($\mathring{a}$) were taken from Garrels and Christ (1965). Activity coefficients used in calculations involving the type 4 fluid are shown below.

INDIVIDUAL ION ACTIVITY COEFFICIENTS

Temp	25°C	50°C	100°C	150°C
K^+, Cl^-	Ø.63	Ø.61	Ø.58	Ø.52
F^-	Ø.67	Ø.62	Ø.63	Ø.57
Na^+, HCO_3^-	Ø.71-Ø.75Ø	Ø.66-Ø.7Ø	Ø.67-Ø.7Ø	Ø.64
SO_4^{--}	Ø.1-Ø.14	Ø.1-Ø.12	Ø.Ø8-Ø.1	Ø.Ø7
Pb^{++}, CO_3^{--}	Ø.16	Ø.13	Ø.1	Ø.Ø7
Ca^{++}, Zn^{++}	Ø.21	Ø.2Ø	Ø.17	Ø.13
Mg^{++}	Ø.31	Ø.3Ø	Ø.26	Ø.21

Stoiciometric ionic strength = 3.Ø

Although the calculated values are not good enough to calculate mineral solubilities, they do provide a guide to the relationship between activity and molality. Neutral species (Helgeson et al., 1981) were considered to have an activity coefficient of one.

APPENDIX 6

THERMODYNAMIC CALCULATIONS AND DATA

6.1: FORMATION OF THE COMPLEX $CaCl^+$

Sodium chloride is completely dissociated at 100°C but calcium will undergo some complexing by the reaction:

$$Ca^{++} + Cl^- = CaCl^+ \qquad (1)$$

where K_1 is the association constant for the complex. Two simplified mass balance equations were used to calculate the concentration of complexed and uncomplexed calcium and chloride ions in solution:

$$\Sigma Cl^- = m_{Cl^-} + m_{CaCl^+}$$
$$\Sigma Ca^{++} = m_{Ca^{++}} + m_{CaCl^+}$$

where ΣCl^- and ΣCa^{++} are the total molal concentrations.
A second equation can be written which relates the free ion concentrations to the complexed concentration of calcium

$$\Sigma m_{Ca^{++}} = m_{Ca^{++}} (1 + K'_{CaCl^+} m_{Cl^-})$$

K'_1 is the equilibrium constant with an added activity coefficient correction. The change in the activity coefficients as a result of decreasing true ionic strength was estimated from a trial calculation. The activity coefficient of $CaCl_+$ was taken as the same as for the chloride ion:

$$\Sigma m_{Ca^{++}} = m_{Ca^{++}} .(1 + K'_{CaCl^+}.(\Sigma m_{Cl^-} - \Sigma m_{Ca^{++}} + m_{Ca^{++}})$$

A quadratic equation results:

$$K_1' (m_{Ca}{}^{++})^2 + m_{Ca}{}^{++} (1 + K_1' \Sigma m_{Cl}{}^{-} - K_1' \Sigma m_{Ca}{}^{++}) - \Sigma m_{Ca}{}^{++} = 0$$

Free calcium ion molality may be found by using a standard solution for a quadratic equation.

6.2: FORMATION OF SULPHATE COMPLEXES

The total complexed sulphate (ΣSO_4^{--}) in the system may be estimated from:

$$\Sigma m_{SO_4^{2-}} = m_{SO_4^{2-}} + m_{NaSO_4^-} + m_{CaSO_4^o} + m_{MgSO_4^o} + m_{KSO_4^-}$$

Since concentrations of potassium and magnesium are small, their corresponding complexes may be ignored. Using the association constants for the following reactions:

$$Ca^{2+} + SO_4^{2-} = CaSO_4^o \quad (2)$$

$$Na^{+} + SO_4^{2-} = NaSO_4^- \quad (3)$$

Total sulphate ΣSO_4^{--}

$$\Sigma m_{SO_4^{2-}} = m_{SO_4^{2-}} (1 + K_2' m_{Ca}{}^{++} + K_3' m_{Na}{}^{+})$$

Where K'_2 and K'_3 are association constants corrected by activity coefficients. Using this equation the degree of sulphate complexing was estimated.

If a total sulphate concentration of $3x10^{-6}$ is assumed, the calculated free ion molal sulphate concentration for phase 3 is $8x10^{-7}$ and for phase 4 , $6x10^{-7}$.

6.3: ACTIVITY RATIO DIAGRAMS

Methods of construction have been given by Helgeson (1967) and Krauskopf (1979). All equilibria in hydrothermal systems can be represented in terms of the ratios of activity of cations in the aqueous phase to that of the hydrogen ion (Helgeson, 1970). They have the advantage over the fugacity diagrams that both the ordinate and the abscissa may be interpreted in terms of analytical concentrations of the actual thermodynamic components.

6.3.1: THE FLUORITE-CALCITE STABILITY BOUNDARY

The reaction used was:

$$H^+ + CaCO_3 + 2F^- = CaF_2 + CO_3^{2-} + H^+ \quad (4)$$

which was derived from:

$$CaCO_3 = Ca^{++} + CO_3^{2-} \quad (5)$$

$$CaF_2 = Ca^{++} + 2F^- \quad (6)$$

Taking logs of the activities and the equilibrium constant K_4, the stability boundary may be calculated from the equation:

$$\log a_{F^-}^2 / a_{H^+} = \log a_{CO3^{2-}} / a_{H^+} - \log K_4$$

6.3.2: WITHERITE-CALCITE STABILITY

The equation used was:

$$H^+ + CaCO_3 + Ba^{++} = H^+ + BaCO_3 + Ca^{++} \quad (7)$$

which was derived from:

$$BaCO_3 = Ba^{++} + CO_3^{2-} \quad (8)$$

and equation 5.

6.3.3: BARYTE-ANHYDRITE STABILITY

The equation used was:

$$H^+ + CaSO_4 = H^+ + BaSO_4 + Ca^{++} \quad (9)$$

which was derived from:

$$BaSO_4 = Ba^{++} + SO_4^{2-} \quad (10)$$
$$CaSO_4 = Ca^{++} + SO_4^{2-} \quad (11)$$

6.4: CALCITE STABILITY DIAGRAM

The equation used was:

$$CaCO_3 + 2H^+ = Ca^{++} + H_2O + CO_2(g) \quad (12)$$

and the stability boundary defined by:

$$-\log fCO_2 = \log a_{Ca}{}^{++} + 2pH$$

The upper limit to CO_2 fugacity was estimated from the maximum gas pressures determined from crushing fluid inclusions in oil. Fugacities may be related to partial pressures by a fugacity coefficient (Houghton et al., 1957). At pressures less than one atmosphere the fugacity coefficients are close to unity, and therefore fugacities approximate to partial pressures.

6.5: CONSTRUCTION OF LOGfO_2-pH DIAGRAMS

The diagram is similar to an Eh-pH diagram, but geologically more meaningful. The method of construction has been detailed by Barnes and Kullerud (1961), Barnes and Czamanske (1967) showed that the important aqueous sulphur species in an ore-forming environment are HSO_4^-, SO_4^{--}, HS^-, H_2S and solid sulphur. Boundaries between these species may be dependant on oxygen fugacity and/or pH. Equations used to construct the boundaries were:

$$H^+ + HS^- = H_2S \quad (13)$$

$$H_2S + 2O_2 = SO_4^{2-} + 2H^+ \quad (14)$$

$$HS^- + 2O_2 = SO_4^{2-} + H^+ \quad (15)$$

The boundaries were calculated in the following way.

At the HS^--H_2S boundary, $a_{H2S} = a_{HS^-}$

Taking the log of the equilibrium constant of equation (13)

$$\log K_{13} = \log a_{H_2S} - \log a_{HS^-} - \log a_{H^+}$$

which was simplified to:

$$\log K_{13} = -\log a_{H^+} = pH$$

The other boundaries were calculated in the same way.

6.6: CALCULATION OF REDUCED SULPHUR CONTOURS

Reduced sulphur contours in the sulphate stability field were calculated from equation (14). The total sulphur

activity (ΣS) of the system is known and, therefore, at the H_2S-SO_4^{--} boundary:

$$\Sigma a_S = a_{H_2S} + a_{SO_4^{2-}}$$

If a $a_{H_2S} = 10^{-7}$ contour is required, then:

$$\log K_{14} = 2\log a_{H^+} - 2\log fO_2 + \log(\Sigma S - 10^{-7}) - \log a_{H_2S}$$

since a_{H_2S} is small compared with ΣS, $\log(\Sigma S)$ may be substituted for $\log(\Sigma S - a_{H_2S})$:

6.7: PYRITE-PYRRHOTITE STABILITY BOUNDARY

The equations used were:

$$FeS + \tfrac{1}{2}O_2 + HS^- + H^+ = FeS_2 + H_2C \quad (16)$$

$$FeS + \tfrac{1}{2}O_2 + H_2S = FeS_2 + H_2O \quad (17)$$

Equations containing the correct aqueous sulphur species are required for the corresponding stability field.

6.8: PYRITE-HAEMATITE STABILITY BOUNDARY

The equations used were:

$$2O_2 + H_2S = SO_4^{--} + 2H^+ \quad (14)$$

$$Fe_2O_3 + \tfrac{1}{2}O_2 + 4H_2S = 2FeS_2 + 4H_2O \quad (18)$$

The law of mass action for equation (14) gives:

$$K_{14} = (a_{H^+}^2 \cdot a_{SO_4^{2-}}) / (a_{H_2S} \cdot f_{O_2}^2)$$

therefore:

$$a_{H_2S} = (a_{H^+} \cdot \Sigma S) / (K_{14} \cdot f_{O_2}^2) \quad (A)$$

and:

$$K_{18} = 1/(a_{H_2S}^4 \cdot f_{O_2}^{\frac{1}{2}})$$

substituting A into K_{18}:

$$K_{18} = (K_{14}^4 \cdot f_{O_2}^8)/(f_{O_2}^{\frac{1}{2}} \cdot a_{H^+}^8 \cdot a_{\Sigma S}^4)$$

and taking logarithms:

$$-8pH = 4\log K_{14} + 7.5\log fO_2 - \log K_{18} - 4\log a_{\Sigma S}$$

6.9: CHALCOPYRITE-BORNITE+PYRITE STABILITY FIELD

The equations used were:

$$5CuFeS_2 + O_2 + 2HS^- + 2H^+ = Cu_5FeS_4 + 4FeS_2 + 2H_2O \quad (19)$$

$$5CuFeS_2 + 4H^+ + 2SO_4^{2-} = Cu_5FeS_4 + 4FeS_2 + 2H_2O + 3O_2 \quad (20)$$

6.10: GALENA STABILITY

A useful upper limit to oxygen fugacity is the galena-anglesite stability boundary.

The reaction used was:

$$PbS + 2O_2 = PbSO_4 \quad (21)$$

and therefore: $\log K_{21} = -2\log fO_2$

6.11: CARBON DIOXIDE-METHANE STABILITY

The reaction used was:

$$CO_2 + 2H_2O = CH_4 + 2O_2 \qquad (22)$$

At the CO_2/CH_4 stability boundary:

$$\log K_{22} = 2\log fO_2$$

TABLE A.4 EQUILIBRIUM CONSTANTS FOR EQUATIONS 1 TO 22

Equation	50°C	100°C	150°C	Source
1	0.22	0.61	1.03	G&B
2	2.17	2.50	2.91	G&B
3	1.1	1.4	1.7	G&B
4	0.36	0.13	0.62	
5	-8.65	-9.33	-10.28	G&B
6	-10.66	-10.41	-	R&H
6	-9.01	-9.20	-9.66	HE
7	-0.37	-0.70	-1.03	
8	-8.28	-8.63	-9.25	H
9	4.42	3.66	3.27	
10	-9.41	-9.29	-9.62	G&B
11	-4.99	-5.63	-6.35	HE
12	9.48	9.25	9.04	HE
13	6.7	6.49	6.63	G&B
14	113.3	94.44	79.40	G&B
15	120.0	100.93	86.03	G&B
16	49.42	42.27	36.97	G&B
17	42.72	35.78	30.34	G&B
18	92.8	80.6	72.24	G&B
19	91.2	77.74	67.64	G&B
20	-148.8	-124.46	-104.42	G&B
21	-26.67	-23.96	-21.93	M
22	-131.14	-113.03	-100.41	M

6.12: STABILITY OF EUROPIUM COMPLEXES

The following equations were used to calculate the stabilities:

$$Eu^{3+} + e^{-} = Eu^{++} \qquad (23)$$

$$\Delta H = 19.6 \text{ kcal mol}^{-1}$$

$$\tfrac{1}{4}O_2 + H^{+} + e^{-} = \tfrac{1}{2}H_2O \qquad (24)$$

$$Eu^{3+} + F^{-} = EuF^{++} \qquad (25)$$

$$Eu^{++} + F^{-} = EuF^{+} \qquad (26)$$

$$Eu^{++} + SO_4^{--} = EuSO_4^{o} \qquad (27)$$

The association constant for the complex CaF^{+} used in place of EuF^{+}, with data from Richardson and Holland (1979a). The association constant for $CaSO_4^{o}$ was used instead of $EuSO_4^{o}$.

The equations used in constructing the stability boundaries were:

$$Eu^{3+} + \tfrac{1}{2}H_2O = Eu^{++} + \tfrac{1}{4}O_2 + H^{+} \qquad (28)$$

$$EuF^{++} + \tfrac{1}{2}H_2O = EuF^{+} + \tfrac{1}{4}O_2 + H^{+} \qquad (29)$$

$$EuF^{++} + \tfrac{1}{2}H_2O + SO_4^{--} = \tfrac{1}{4}O_2 + H^{+} + EuSO_4^{o} + F^{-} \qquad (30)$$

6.13: FLUORIDE-HYDROXIDE ION EXCHANGE

6.13.1 BIOTITE (ANNITE)

Munoz and Luddington (1974) measured the equilibrium

constant for the reaction, which can be calculated from the equation:

$$\log K = 2552./T - 0.31 \qquad T^{\circ}K$$

The reaction used was:

$$\tfrac{1}{2}\ \text{biotite (OH)} + HF^{\circ} = \tfrac{1}{2}\ \text{biotite (F)} + H_2O \quad (31)$$

Using the association constant for HF

$$H^+ + F^- = HF^{\circ} \quad (32)$$

An equation relating the activity of aqueous fluoride in equilibrium with biotite at a given pH is given below:

$$0.5\ \text{Biotite (OH)} + H^+ + F^- = 0.5\ \text{Biotite (F)} + H_2O$$

The boundaries on the diagram were constructed from the relation:

$$\log K_{33} = pH - \log a_{F^-}$$

6.13.2 FLUORAPATITE

The reaction given by Roberson (1966) was used:

$$Ca_{10}(PO_4)_6(OH)_2 + 2F^- = Ca_{10}(PO_4)_6(F)_2 + 2OH^- \quad (34)$$

Equilibrium constants were extrapolated using the equilibrium constant at $298^{\circ}K$ ($\log K = 6.6$) and the enthalpy of the reaction ($\Delta H = 9.58\ kcal mol^{-1}$).

Taking the association constant for water:

$$H^+ + OH^- = H_2O \quad (35)$$

An equation relating the stabilities of fluor- and hydroxy-apatite in equilibrium with a fluid at a set pH and temperature is:

$$Ca_{10}(PO_4)_6(OH)_2 + 2F^- + 2H^+ = Ca_{10}(PO_4)_6F_2 + 2H_2O \quad (36)$$

Concentrations of the various components may be calculated from the relation:

$$\log K_{36} = 2pH - 2\log a_F-$$

6.14: MINERAL DISSOLUTION/ALTERATION

6.14.1: STABILITY OF MUSCOVITE, K-FELDSPAR AND KAOLINITE

The stability boundaries for these silicates, plotted on to figure 7.2, were calculated from the data of Helgeson (1969), using the method given by Krauskopf (1979). The three boundaries may be calculated from the following equations:

$$\text{K-feldspar} + 4H^+ + 4H_2O = K^+ + Al^{3+} + 3H_4SiO_4 \quad (37)$$

$$\text{kaolinite} + 6H^+ = 2Al^{3+} + H_2O + 2H_4SiO_4 \quad (38)$$

$$\text{muscovite} + 1OH^+ = 3Al^{3+} + K^+ + 3H_4SiO_4 \quad (39)$$

Quartz solubility, at elevated temperatures, in pure water may be calculated from the expression given by Siever (1962).

$$\log c_o = 4.829 - 1.132 \times 10^3 / T \quad (T^oK)$$

(where c_o is the concentration in ppm)

Amorphous silica solubility in pure water at temperatures up to 350°C has been measured by Chen and Marshall (1982), and they calculated a regression relating molal solubility (s_m) to temperature.

$$\log s_m = -0.1185 - 1.126 \times 10^3/T + 2.3305 \times 10^5/T$$

At low temperatures, the presence of dissolved salts has a relatively minor effect on quartz and amorphous silica solubility.

6.14.2 SOLUBILITY OF FLUORAPATITE

Roberson (1966) gave an expression for the dissolution of fluorapatite. The equation was:

$$Ca_5(PO_4)_3F + 6H_2O = 5Ca^{++} + 3H_2PO_4^- + F^- + 6OH^- \quad (40)$$

Using the association constant for water (equation 35), the equation may be written as a function of pH, fluoride and calcium activity at elevated temperatures. Equation (40) was extrapolated to higher temperatures using the equilibrium constant (logK = -85.8) and enthalpy ($\Delta H = 54.23 kcal mol^{-1}$) at 298°K.

The new equation is:

$$Ca_5(PO_4)_3F + 6H^+ = 5Ca^{++} + 3H_2PO_4^- + F^- \quad (41)$$

Taking logs:

$$\log K_{41} = 5\log a_{F^-} + 3\log a_{H_2PO_4^-} + \log a_{F^-} + 6pH$$

TABLE A.6

LOG OF EQUILIBRIUM CONSTANTS FOR REACTIONS 23 to 41

Equation no.	Temperature					Source
	25°C	50°C	60°C	100°C	150°C	
23	-9.3	-8.19		-6.42	-5.08	S&M
24	-	19.16		16.62	-	H
25	3.07	3.19		3.25	3.32	B&K
26	-	1.36		1.76	-	
27	2.17	2.50		2.91	-	
28	-	-27.35		-22.94	-	
29	-	-29.18		-24.43	-	
30	-	-28.37		-23.69	-	
31	-	7.59		6.53	5.72	M&L
32	-	3.4		3.86	4.34	H
33	-	10.99		10.20	10.07	
34	-	7.14		8.00	8.66	HE
35	-	13.27		12.26	11.64	HE
36	-	33.53		22.52	31.94	HE
37	-		0.42	-0.32	-1.14	HE
38	-	-	4.75	2.27	-0.12	HE
39	-	-	12.21	7.97	3.8	HE
40	-	-82.7		-77.85	-74.12	R
41	-	-162.32		-151.41	-143.96	

KEY TO SOURCES OF THERMODYNAMIC DATA

B&K	Bilial & Koss (1980)
G&B	Giordano & Barnes (1981)
HE	Helgeson (1969)
H	Hogfeldt (1982)
M	Moore (1980)
M&L	Munoz and Luddington (1974)
R&H	Richardson and Holland (1979a)
R	Roberson (1966)
S&M	Sillen and Martell (1971)

6.15: ESTIMATION OF A MAXIMUM GAS PRESSURE WITHIN A FLUID INCLUSION

On crushing fluid inclusion types 1,2,3 and 4, the vapour bubble invariably expands. The ratio of vapour to liquid may be estimated from the homogenization temperature of the fluid inclusion (Potter and Brown, 1977), if the fluid composition is known. On opening the inclusion, the new filling density may be estimated from the ratio of the size of the vapour bubble to fluid inclusion (Hollister et al., (1981). The pressure in the inclusion is assumed to be atmospheric when it is opened. Therefore the increase in the volume of the vapour bubble may be used to estimate the gas pressure in the inclusion at room temperature. The pressure at elevated temperatures may be estimated using the general gas law. The calculation does, however, assume that all the gas is present in the vapour bubble and therefore gives an overestimate of total gas pressure. Upper limits on total gas pressure are given below.

FLUID INCLUSION TYPE	DEGREE OF FILLING	TH (^{o}C)	PRESSURE (atm)
1	Ø.Ø-Ø.2	14Ø	21-32atm.
2,3,4	Ø.46-Ø.21	1ØØ	7-16atm.